LIBRARY SYNTHESIS OF PIPERIDINONE SULFONAMIDES, TRANSITION METAL-FREE C–H TRIFLUOROMETHYLATION OF CYCLIC ENAMINONES, AND ELUCIDATING THE BINDING SITE OF EPOTHILONES ON BETA-TUBULIN WITH EPOTHILONE PHOTOAFFINITY PROBES

A DISSERTATION
SUBMITTED TO THE FACULTY OF THE
UNIVERSITY OF MINNESOTA
BY

ADWAIT R. RANADE

IN PARTIAL FULFILLMENT OF THE REQUIREMENTS
FOR THE DEGREE OF
DOCTOR OF PHILOSOPHY

ADVISER: DR. GUNDA I. GEORG

JULY 2014

Acknowledgements

This thesis is a fruit of the research work that I carried out in Professor Gunda Georg's laboratory over the last six years. I couldn't have accomplished this without cordial support from my mentors, coworkers, friends and family. I want to take this opportunity to express my heartfelt gratitude to all of them who have assisted me during my graduate career.

First and foremost, I wish to thank my adviser Professor Dr. Gunda Georg for providing me a wonderful opportunity to work in her lab and learn from her scientific expertise. She has always been a constant source of support, guidance and encouragement throughout my graduate career in her laboratory. I will forever be obliged to her. I am very thankful to Drs. Georg, Johnson, Fecik and Douglas for graciously serving on my dissertation committee.

I need to specially thank Dr. LeeAnn Higgins (Center for Mass Spectrometry and Proteomics) for her guidance and support for mass spectrometry work, proteomics studies and invaluable discussions. I want to sincerely thank Dr. Gerhard Höfle (Germany) for his valuable advice and guidance concerning the epothilone project, and for graciously providing us with ample amounts of starting materials including the natural product, epothilone. I also want to thank Dr. Earnest Hamel (NCI) for carrying out the biological work for my epothilone project and for informative discussions. I have been very lucky to have, and greatly benefited from the support of the faculty and coworkers in the Department of Medicinal Chemistry, Institute for Therapeutics Discovery and Development (ITDD), Department of Chemistry. I want to sincerely thank Dr. Peter

Dosa, Dr. Michael Walters and Dr. Shameem Sultana Syeda for their guidance and very useful discussions from time to time. I want to thank Dr. Thomas Hoye and Dr. Christopher Douglas again for valuable discussions and their help in the epothilone project.

I also want to thank Dr. Alicia Regueiro-Ren (BMS Pharma), Dr. Robert Grubbs, Myles Herbert (CalTech) and Dr. Herbert Plenio (Germany) for their help in the epothilone project.

This research was supported by grants from the NIH and the College of Pharmacy. Support was also provided for this project through the Robert Vince Endowed Chair and the McKnight Presidential Chair.

I have been very fortunate to have close friends like Dr. Satish Patil, Dr. Rahul Lad, Dr. Srikant Kotapati and Dr. Amit Gangar who were there with me in my time of need. My heartfelt thanks to them for everything! I would like to thank my colleagues Dr. Micah Niphakis, Dr. Bryant Gay, Dr. Kwon Ho Hong and Dr. Kathy Nelson for their help and support over the years. Special thanks to Dr. Yiyun Yu for his tremendous help in the trifluoromethylation project and his camaraderie throughout my time here at UMN. Also, I am thankful to Andrea Knickerbocker, Mary Crosson, and Sarah Sexton for their crucial administrative help.

I would like to thank the faculty and staff of the Department of Medicinal Chemistry at UMN for providing the opportunity to study and research in the one of the world's top program.

Last, but certainly not the least, I need to thank my parents, sister and wife Aditee whose love, patience and support have been fundamental during my graduate work.

Abstract

Library Synthesis of Piperidinone Sulfonamides, Transition Metal-Free C–H Trifluoromethylation of Cyclic Enaminones, and Elucidating the Binding Site of Epothilones on Beta-Tubulin with Epothilone Photoaffinity Probes

Chapter 1 focuses on synthesizing a library of piperidinone sulfonamides. The piperidinones serve as valuables intermediates for the synthesis of nitrogen-containing bioactive molecules, various alkaloids, and drug candidates. Amongst the myriads of highly derivatized *N*-heterocyclic compounds, molecules possessing the piperidinone sulfonamide moiety in their structures show interesting biological activities. A library of 18 piperidinone sulfonamides was prepared under a Pilot Scale Library grant and submitted to NIH for testing in various biological assays. Two compounds from the library were identified as active hits. One of the compounds showed prion protein 5' UTR inhibition while the other showed inhibition of human platelet-activating factor acetylhydrolase 1b, catalytic subunit 2.

Chapter 2 focuses on direct C–H trifluoromethylation of cyclic enaminones. Cyclic enaminones are of interest in natural product synthesis and are regarded as valuable synthons due to unique structural and chemical properties. They serve as versatile precursors for synthesizing piperidine-containing alkaloids and drug molecules. In this project, transition metal free, direct C–H trifluoromethylation of cyclic enaminones was developed with trimethyl(trifluoromethyl)silane ($TMSCF_3$). This method proceeds under mild conditions at room temperature and possibly involves a radical mechanism. The C–H functionalization was successful with both electron-rich

and electron-deficient cyclic enaminones. This methodology circumvents substrate prefunctionalization and transition metal catalysis, and allows a convenient and direct access to a variety of medicinally significant 3-trifluoromethylpiperidine derivatives. This chemistry also presents a rare example of a direct trifluoromethylation of an internal olefinic C–H bond.

Chapter 3 focuses on efforts toward elucidating the binding site of epothilones on β-tubulin. Epothilones are potent cytotoxic tubulin-binding polyketide-derived macrolides. Even though the binding sites for epothilones and paclitaxel on β-tubulin overlap, epothilones show efficacy against paclitaxel-resistant cancer cell lines. This implies a significantly different binding mode for epothilones. To date, two epothilone binding models have been proposed based on NMR and electron-crystallography data. In order to differentiate the proposed binding modes, four epothilone A photoaffinity analogues were designed. Three of those analogues were successfully synthesized and showed excellent cytotoxicity as well as the required tubulin assembly. It was hypothesized that the protein region labeled by these photoprobes is dependent on the epothilone conformation at the binding site. For one of the analogues, the probe-labeled peptide fragment 'TARGSQQY' (residues 274 to 281) in the β-tubulin isoform TBB3 was identified by MS analysis. Our experimental results corroborated the consensus of both the models that Thr 274 and Arg 276 are necessary for binding of epothilones to β-tubulin. However, based on the photoaffinity labeling studies results and molecular modeling studies, an orientation of the epothilone in the binding site is proposed that is significantly different from those previously proposed.

Table of Contents

Chapter 2

Transition Metal-Free C–H Trifluoromethylation of Cyclic Enaminones

List of Tables

Chapter 1

Chapter 2

Chapter 3

List of Figures

Chapter 1

Chapter 2

Chapter 3

List of Schemes

Chapter 1

Chapter 2

Chapter 3

List of Compounds

Abbreviations

Aβ	Amyloid Beta
AcOH	Acetic Acid
AD	Alzheimer's Disease
Ala	Alanine
anh	Anhydrous
APP	Amyloid Precursor Protein
aq.	Aqueous
Ar	Aromatic
Arg	Arginine
Asp	Aspartate
BACE	Beta-site Amyloid Precursor Protein Cleaving Enzyme
BHT	Butylated Hydroxytoluene
BINAP	2,2'-Bis(diphenylphosphino)-1,1'-binaphthyl
bmim	1-Butyl-3-methylimidazolium
Bn	Benzyl
Boc	*tert*-Butyloxycarbonyl
BOP	(Benzotriazol-1-yloxy)tris(dimethylamino)phosphonium Hexafluorophosphate
br	Broad
brsm	Based on Recovered Starting Material
Bu	Butyl
Bzl	Benzoyl

Cbz	Benzyloxycarbonyl
CCR1	Chemokine Receptor 1
CDS	Chemical Diversity Space
CE	Chicken Erythrocyte
$Cu(OTf)_2$	Copper (II) Trifluoromethanesulfonate
d	Day(s)
dd	Doublet of Doublet
Da	Dalton(s)
DCE	Dichloroethane
DCM	Dichloromethane
DDA	Data Dependent Acquisition
DEAD	Diethyl Azodicarboxylate
DIPEA	Diisopropylethylamine
DMAP	4-Dimethylaminopyridine
DMF	*N*,*N*-Dimethylformamide
DMSO	Dimethylsulfoxide
DNA	Deoxyribonucleic Acid
DOS	Diversity Oriented Synthesis
EC	Electron Crystallography
EC_{50}	50% Effective Concentration
EDG	Electron-Donating Group
ee	Enantiomeric Excess
ERK	Extracellular Regulated Kinases

Epo	Epothilone
eq	Equation
equiv	Equivalent(s)
ESI	Electro-Spray Ionization
Et	Ethyl
EtOAc	Ethyl Acetate
EtOH	Ethanol
EWG	Electron-Withdrawing Group
FDA	Food and Drug Administration
Fppy	2-(2,4-difluorophenyl)pyridine
FT	Fourier Transform
GDP	Guanosine Diphosphate
gen	Generation
GFP	Green Fluorescent Protein
Gl	Glacial
Gln	Glutamine
Glu	Glutamate
Gly	Glycine
GPCR	G-Protein Coupled Receptors
GTP	Guanosine-5’-triphosphate
h	Hour(s)
Het	Heterocycle
His	Histidine

HRMS	High Resolution Mass Spectrometry
IC_{50}	Half Maximal (50%) Inhibitory Concentration
IL-1b	Interleukin-1 Beta
i-Pr	Isopropyl
IR	Infrared
JNK	c-Jun N-terminal Kinase
KDa	Kilodalton
L	Ligand
LC	Liquid Chromatography
Leu	Leucine
liq	Liquid
M	Molar
m	Multiplet
μM	Micromolar
mM	Millimolar
MAP	Mitogen-Activated Protein
m-CPBA	*meta*-Chloroperoxybenzoic Acid
Me	Methyl
MeCN	Acetonitrile
MeOH	Methanol
Mes	(Morpholino)ethanesulfonate
$MeSiCl_3$	Trichloromethylsilane
mg	Milligram(s)

min	Minute(s)
MLPCN	Molecular Libraries Probe Production Centers Network
MLSMR	Molecular Libraries Small Molecular Repository
mPGES-1	Microsomal Prostaglandin E Synthase 1
MS	Mass Spectrometry
Ms	Mesyl (Methanesulfonyl)
NaOH	Sodium Hydroxide
NCI	National Cancer Institute
NHC	N-Heterocyclic Carbene
NIH	National Institute of Health
nm	Nanometer(s)
nM	Nanomolar
NMP	*N*-Methyl-2-pyrrolidinone
NMR	Nuclear Magnetic Resonance
NOE	Nuclear Overhauser Effect
Nu	Nucleophile
OAc	Acetate
OTf	Trifluoromethanesulfonate
OX_1	Orexin Receptor 1
p	Pentet
PAF	Platelet-Activating Factor
PAFAH1B2	Platelet-Activating Factor Acetylhydrolase 1b, Catalytic Subunit 2

PCA	Principal Component Analysis
PGP	P-Glycoprotein
Ph	Phenyl
Phe	Phenylalanine
phen	Phenanthroline
PIDA	Phenyliodine Diacetate
PIFA	Phenyliodine Bis(trifluoroacetate)
Pim1	Proto-Oncogene Serine/Threonine-Protein Kinase 1
Piv	Pivaloyl
PLA2	Phospholipase 2
PMP	*para*-Methoxyphenyl
ppm	Parts Per Million
Pro	Proline
PrP	Prion Protein
PrP^{Sc}	Prion Protein in the Scrapie Form
PSL	Pilot Scale Libraries
PTFE	Polytetrafluoroethylene
q	Quartet
Ra Ni	Raney Nickel
rpm	Revolutions Per Minute
rt	Rt
RTIL	Rt Ionic Liquid
s	Singlet

SAR	Structure-Activity Relationship
Sat	Saturated
SD	Standard Deviation
SET	Single Electron Transfer
t	Triplet
TBAF	Tetrabutylammonium Fluoride
TBPA	Tris(4-bromophenyl)-aminium Hexachloroantimonate
TBS	*tert*-Butyl Dimethylsilyl
t-Bu	*tert*-Butyl
TEMPO	2,2,6,6-Tetramethylpiperidine 1-oxyl
TES	Triethylsilyl
TFA	Trifluoroacetic Acid
THF	Tetrahydrofuran
Thr	Threonine
TLC	Thin Layer Chromatography
TMS	Trimethylsilyl
TNF	Tumor Necrosis Factors
TOF	Time of Flight
Ts or tosyl	*para*-Toluenesulfonyl
UTR	Untranslated Region
UV	Ultraviolet

Chapter 1

Library Synthesis of Piperidinone Sulfonamides

1.1 Rationale for Library Synthesis

"Chemical Space" is a term used in place of multi-dimensional descriptor space. It is a region defined by a particular choice of descriptors with limits placed on them. This region is comprised of all energetically stable chemical compounds. About 10^{60} small molecules with molecular weights of less than 500 exist[1] in this "Chemical Diversity Space (CDS)" out of which only 10^{8} have been synthesized or isolated so far. This means that large areas of the diversity space are either not yet explored or under-explored. These sparsely populated areas, however, are believed to offer unprecedented opportunities to find new molecules that can be developed as probes and drug leads. However, one of the problems with new types of organic compounds that are now being explored is that they may show remarkable potency when tested against isolated targets in the laboratory environment, but within the complex cellular environment they might interact with other cellular components and fail to show similar potency.[2] "Natural products" are relatively robust having passed through evolutionary development, and they are possibly less likely to interact with common components of living systems, such as membranes or DNA in a harmful manner. Indeed, around 30% of all the drugs approved over the past 20 years are natural products or derivatives of them.[3] A comparison of the properties of combinatorial chemistry libraries, natural products, and drugs shows that combinatorial compounds by and large cover a significantly smaller area of chemical space than either natural products or drugs (Fig. 1.1).[4]

A large database that contained compounds from combinatorial chemistry (**a**), natural products (**b**) and drugs (**c**) was analyzed on the basis of a variety of molecular properties such as molecular mass, lipophilicity, and topological factors.[4] To visualize the

diversity of these compounds on the basis of these properties, a statistical approach known as principal component analysis (PCA) was used. PCA is a mathematical procedure that uses an orthogonal transformation to convert a set of observations of possibly correlated variables into a set of values of uncorrelated variables called principal components.[4] Figure 1.1 is a plot of the first two principal components obtained from a database.

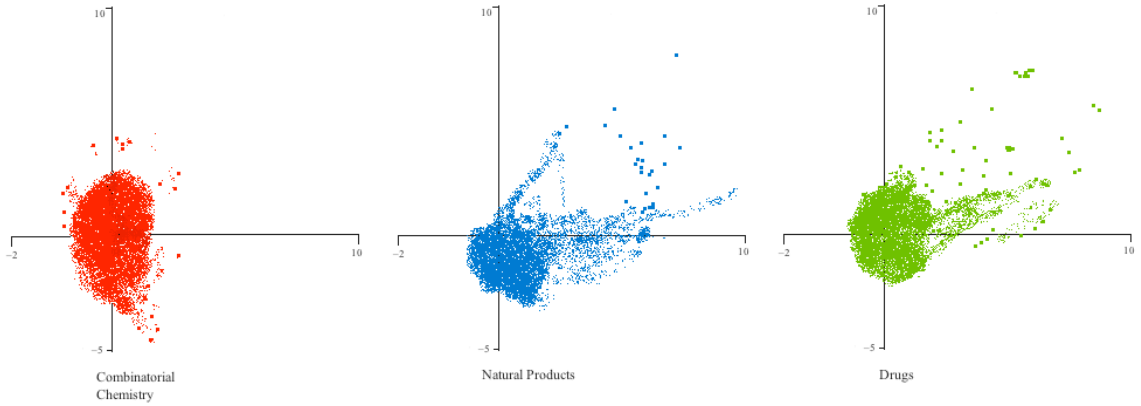

Figure 1.1. Comparison of Properties of Combinatorial Chemistry Libraries, Natural Products and Drugs. (Figure adapted with permission from the literature reference[4]. Copyright 2014 American Chemical Society).

As seen in Figure 1.1, combinatorial compounds cover a well-defined region in diversity space according to the principal components analysis. Natural products and drugs together cover not only the same space, but also additional regions of space. Interestingly, there is a significant overlap of the plots of natural products and successful drug molecules.[4] This suggests that by aiming to mimic some properties of natural products and drug molecules, new combinatorial compounds could be made that are substantially more diverse and have greater biological relevance[4] than those currently

known.

Based on those considerations, the NIH launched a national effort and provided research grants to investigators to prepare Pilot Scale Libraries (PSL) that contain compounds covering novel or underexplored regions of the chemical space and that are hypothesized to possess bioactivity. The aim of the PSL projects was to synthesize compounds residing in sparsely populated CDS by a variety of novel synthetic chemistry strategies. Compounds prepared under the PSL grants were submitted to the Molecular Libraries Small Molecular Repository (MLSMR). About 500,000 compounds have been collected to date and are mainly comprised of diversity sets. In addition, specialty sets of pharmacologically active compounds, targeted libraries for proteases, kinases, GPCRs, ion channels, nuclear receptor targets and natural products were collected from various sources. It is anticipated that expanding the "chemical space" through these efforts will ultimately serve to provide chemical probes for new targets and starting compounds for the development of a new classes of therapeutic agents.

The MLSMR compound collections were provided by investigators from across the country to the Molecular Libraries Probe Production Centers Network (MLPCN) and used for screening of novel targets. The screening results were subsequently deposited into the PubChem database, thus making this information freely available on the Internet. As a part of this national effort, the Georg group received a PSL grant to prepare libraries with nitrogen-containing cyclic scaffolds, and for the design and synthesis of factorial libraries from privileged structures, novel medium-sized ring combinatorial libraries, diversity-oriented library synthesis and natural product-derived libraries. It was my task to synthesize a piperidinone sulfonamide library as part of the PSL subproject "synthesis

of libraries with nitrogen-containing cyclic scaffolds." The Georg group and others have extensively investigated the chemistry of 2,3-dihydropyridin-4(1*H*)-ones (Figure 1.2). Studies have included the development of general and asymmetric synthetic methods, chemoselective functionalizations,[5-10] and their conversion to piperidones, piperidines, and piperidine-containing natural products and bioactive molecules.

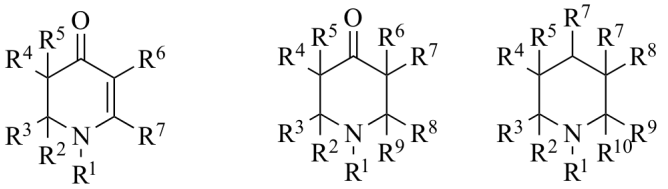

Figure 1.2. Structures of 2,3-Dihydropyridones, 4-Pyridones and Piperidines.

Among several possibilities to prepare piperidine-containing pilot scale libraries, a literature review revealed that highly derivatized *N*-heterocyclic sulfonamides had shown interesting biological activities. Some of the structures are shown in Figure 1.3. Compounds of structure types **1.1**[11,12] and **1.2**[13] showed very good γ–secretase inhibitory activity (100-1000 nM). Aggregation/deposition of amyloid beta peptide (Aβ) in the brain of Alzheimer's disease (AD) patients is thought to contribute to the disease pathology. AD is a degenerative brain disorder characterized by progressive loss of memory, cognition, reasoning, judgment and emotional stability that gradually leads to profound mental deterioration and ultimately death.[13] It is the fourth most common medical cause of death in the United States. Beta amyloid peptide is formed by sequential cleavage of amyloid precursor protein (APP) by two aspartyl proteases, β-secretase (BACE) and γ-secretase respectively.[13] Thus, inhibiting γ-secretase could prove to be

useful in preventing Alzheimer's disease. Compounds of structure type **1.3** showed good JNK-2 and JNK-3 inhibitory activity (inhibition of more than 20% of the JNK activity at 10 μM).[14] JNK or c-Jun N-terminal kinases are kinases that bind and phosphorylate c-Jun proteins. They belong to the mitogen-activated protein (MAP) kinase family. MAP kinases are serine/threonine kinases that are activated by dual phosphorylation on threonine and tyrosine residues. In mammalian cells there are at least three separate, but parallel pathways that convey information gathered by extra-cellular stimuli to the MAP kinases. These pathways include kinase cascades leading to activation of ERKs (extracellular regulated kinases), the JNKs and the p38/CSBP kinases. The JNK cascades are activated by different external stimuli such as cellular stress, DNA damage following UV irradiation, heat shock, osmotic shock, TNF-α, IL-1β, ceramide, and reactive oxygen species. They also play a role in the cellular apoptosis pathway.[14] It has been shown that inhibition of JNK could be sufficient for blocking apoptosis.[15] It has also been reported that the JNK signaling pathway is implicated in cell proliferation and could play an important role in autoimmune diseases that are mediated by T-cell activation and proliferation.[16] Therefore, compounds inhibiting the JNK pathway could be helpful in prevention of diseases, which are preferably mediated by the JNK function. Structures **1.4**[17] were found to be very good metalloprotease inhibitors effective for several conditions in humans including: reduction in inflammation in rheumatoid arthritis, inhibition of further erosion of articular cartilage in osteoarthritis, rapid healing in corneal abrasion, substantial reduction in scars due to chemical burns, diminishing asthma symptoms, reduction in premetastatic tumor size, prevention of oral degeneration, prevention in loosening of an implant in the maxilla, prevention in the loosening of the

dentures, and prevention of colitis flare ups.

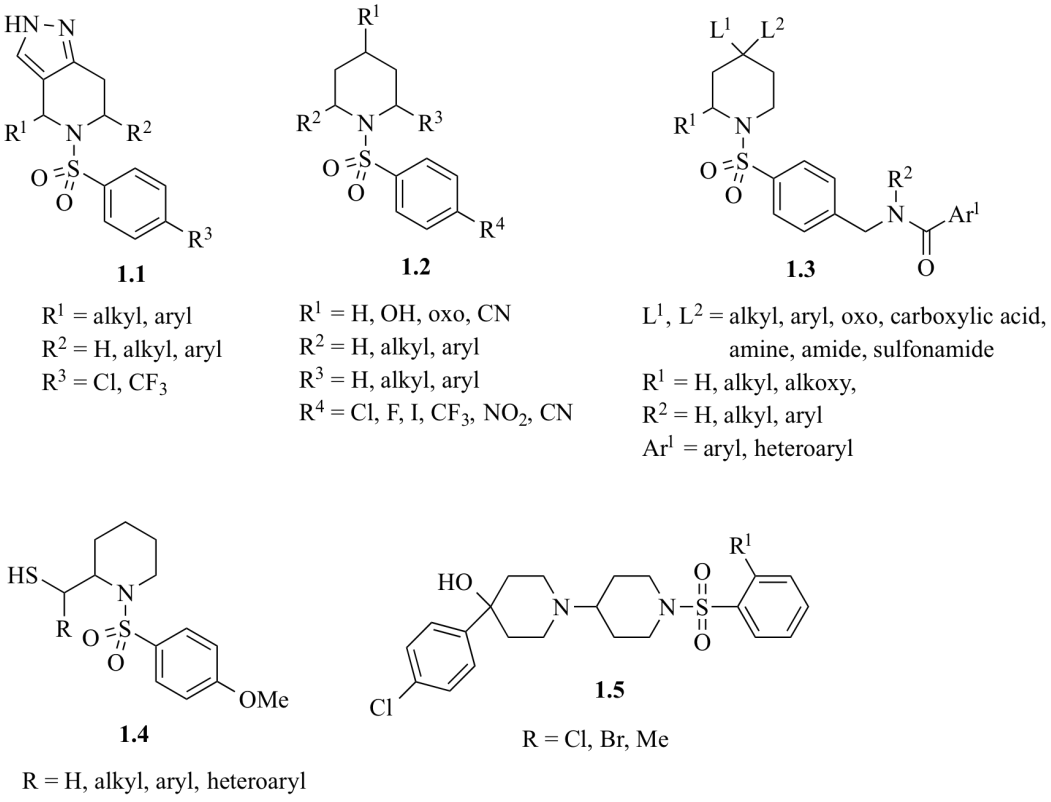

Figure 1.3. Literature Examples of Biologically Active Piperidine Sulfonamides.

Compounds **1.5** showed potent CCR1 (chemokine receptor) antagonistic activity (CCR1 binding IC_{50} 90-500 nM).[18] Chemokines are a growing family of proteins that play an important role in leukocyte activation and migration.[19] Chemokines bind to receptor CCR1, which is expressed on a number of cell types including monocytes, macrophages, dendritic cells, and T cells. A substantial body of evidence has linked the chemokine receptor CCR1 and its major ligands to the pathogenesis of rheumatoid arthritis.[20,21] A small molecule CCR1 antagonist showed marked decrease in synovial inflammation and a trend toward a decrease in clinical disease activity after 2 weeks of treatment without severe side effects.[22] Therefore, CCR1 antagonists are currently being explored as anti-

inflammatory compounds, especially for rheumatoid arthritis. Encouraged by the various reported biological activities of the piperidine sulfonamides type scaffolds, it was decided to prepare a library of sulfonamide derivatives of cyclic enaminones and 4-piperidinones.

1.2 Introduction to Piperidones

The piperidones are a family of organic chemicals characterized by a 6-membered heterocycle possessing a nitrogen atom in the ring and a ketone functional group. Particularly, the piperidin-4-ones play a vital role in heterocyclic chemistry, driven by their importance in biology and medicinal chemistry.[23,24] They are found in the skeletons of many biologically active natural products.[25-31] Systems having a piperidine-4-one core have stimulated great interest in past and in recent years due to the fact that this moiety is a part of molecules with a variety of biological properties such as antiviral,[32] antitumor,[32,33] central nervous system,[34-37] local anesthetic,[35-38] anticancer,[39] antithrombogenic,[40] blood cholesterol lowering,[41] and antiarrythmic activities.[42]

Importantly since the carbonyl group can be easily converted into various functional groups, piperidin-4-ones serve as valuable advanced intermediates to piperidines,[24,43-47] some of which are found in many drugs and drug candidates (Figure 1.4).[48-50] Piperidone-derived piperidines are biologically important and are part of many bioactive compounds such as neurobinin receptor antagonists,[51] analgesic and antihypertensive agents.[52] Because the piperidin-4-ones have seen extensive use as intermediates in the synthesis of physiologically active compounds,[53-58] many of the chemical studies undertaken in the past with 4-piperidones are related to the synthesis of drugs.[59,60] Heterocyclic compounds bearing a piperidine skeleton are interesting targets of

organic synthesis owing to their pharmacological activity and their wide presence in nature.[61-63] The piperidine scaffold is undoubtedly one of the most common and important structures in natural products and pharmaceutically active molecules.[64-66] Piperdine-containing alkaloids occur in both the plant and the animal kingdom.[30,67] Piperidine derivatives are useful as anti-osteoporotic (raloxifene),[68] vasodilator (minoxidil),[69,70] analgesic (fentanyl),[71,72] and the anti-Pakinsonian agent (biperiden).[73,74]

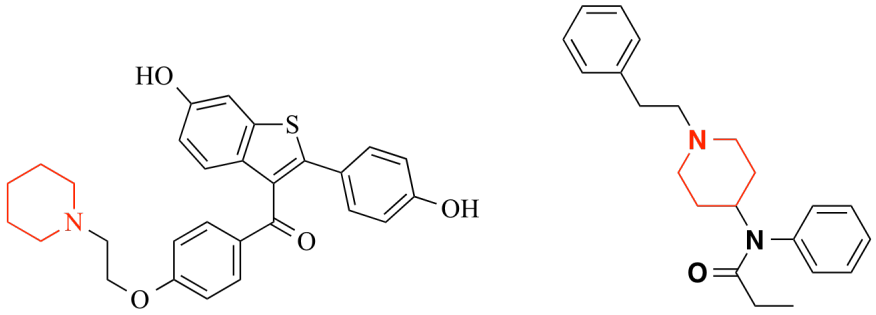

Raloxifene
(Anti-osteoporotic)

Fentanyl
(Opioid Analgesic)

Figure 1.4. Structures of Representative Piperidine-Containing Drugs.

1.3 Syntheses of Piperidones

Due to their utility, numerous methods have been devised for the synthesis of 4-piperidones.[75] As will be shown below, many methods exist for their preparation including asymmetric syntheses, which is a distinct advantage for structure-activity studies once initial chemical hits have been discovered in high throughput screening campaigns.

1.3.1 Mannich Condensation

1.3.1.1 Reactions with Ammonia or Ammonium Salts

Among the several methods to synthesize piperidones, the Mannich condensation remains the most widely used. In 1912, Petrenko-Kritschenko synthesized a 2,3,5,6-tetrasubstituted piperidone by combining diethyl-α-ketoglutarate with benzaldehyde and ammonia (or ammonium salt).[76] In a similar manner, Noller and Baliah synthesized 2,3,5,6-tetrasubstituted piperidones by boiling a mixture of NH_4OAc or an amine, an aldehyde, and a ketone in glacial acetic acid (Scheme 1.1, eq 1).[77] Edwards *et al*. developed a one-step protocol for the synthesis of 2,6-disubstituted piperidin-4-ones by reacting an α,β-unsaturated ketone, an aldehyde and NH_4OAc at room temperature (Scheme 1.1, eq 2).[78] This reaction presumably involves both a Michael and a Mannich condensation. Rastogi *et al.* developed a microwave procedure for synthesizing 2,5,6-trisubstituted piperidones by subjecting a mixture of a 4-substituted benzaldehyde, 2-butanone, benzaldehyde and NH_4OAc to microwave conditions.[79] Compared to the conventional approach, the reaction time in the microwave protocol was notably reduced from several hours to a few minutes while the yield almost doubled. The Xu group developed an efficient route for the construction of 2-substituted-6,6-dimethyl-4-piperidones via a tandem Mannich reaction of aldehydes, acetone, and ammonia in the presence of L-proline as a catalyst at room temperature in ionic liquid (RTIL) [bmim][PF_6] (Scheme 1.1, eq 3).[80] The use of L-proline dramatically enhanced the chemoselectivity and gave high yields. The advantages of this process were easily available and low-cost starting materials, easy operation, recyclability of catalyst and mild reaction conditions. The Soundarrajan group developed a "green" approach by substituting ammonium acetate with ethyl aspartate, a naturally occurring amino acid for synthesizing 2,6-disubstituted piperidones.[81]

Scheme 1.1. Mannich Condensation Using Ammonia

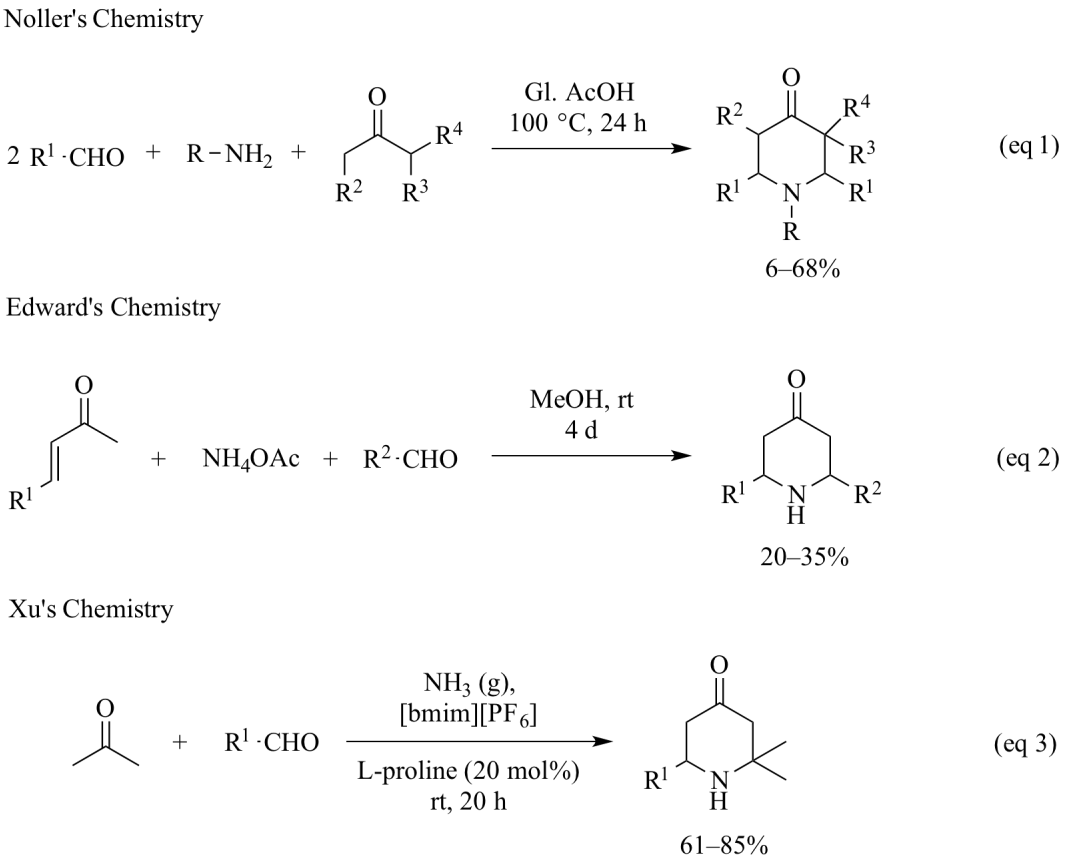

1.3.1.2 Reactions without Ammonia or Ammonium Salts

The Barker group established a double Mannich reaction protocol of bisaminol ethers and substituted β–keto esters using trichloromethylsilane as a Lewis acid, as a quick and efficient method to obtain 3,5-substituted 4-piperidones (Scheme 1.2, eq. 1).[82] Jia and Wang developed a novel approach involving a Mannich reaction of imines and ketones, induced by persistent radical cation salts to form β–aminoketones (Mannich bases) (Scheme 1.2, eq 2).[83] Thus, a novel cyclization to form the 4-piperidone skeleton was achieved in a tandem process. In this radical cation process, the ketone served as a carbocation trapping agent to form 4-piperidone derivatives under tris(4-bromophenyl)-

aminium hexachloroantimonate ($TBPA^{+}\cdot$) induced condition. The same group later developed an I_2-induced stereospecific synthesis of 1,2,6-triaryl-4-piperidones through a double Mannich reaction and tandem cyclization.[84] In this efficient protocol, unactivated ketones served as Mannich donors in the reaction with various imines to produce the corresponding 4-piperidone derivatives. Again, in a similar way, the same group developed an indium (III) chloride tetrahydrate catalyzed stereoselective synthesis of 1,2,6-triaryl-4-piperidones.[85]

Scheme 1.2. Mannich Condensation without Using Ammonia

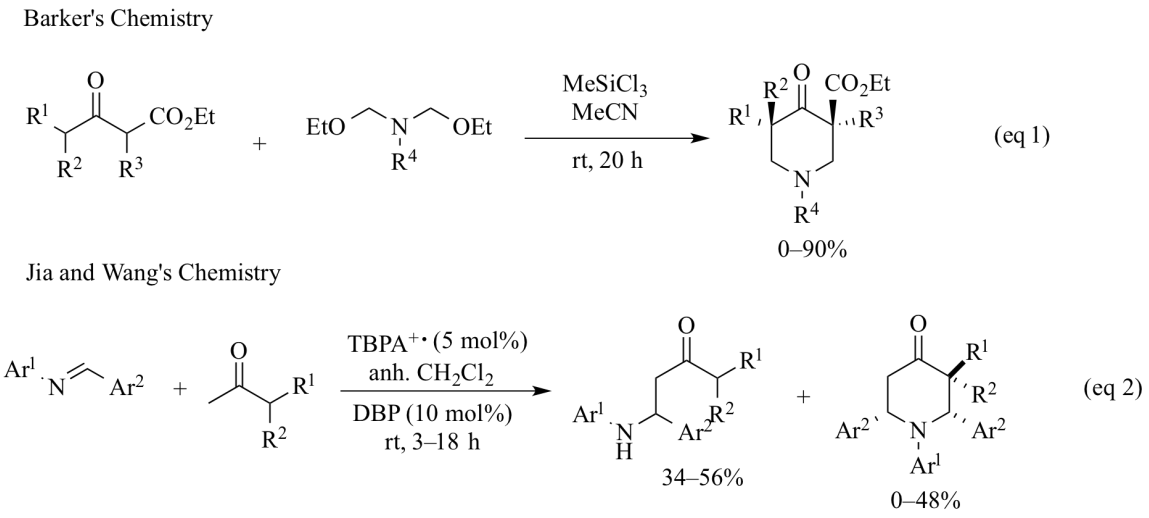

1.3.2 Addition of Nucleophiles to Cyclic Enaminones

A frequently used method for the synthesis of 2-substituted-4-piperidones is the addition of nucleophiles to cyclic enaminones or 2,3-dihydropyridin-4(1*H*)-ones. The asymmetric versions involve chiral ligands and metal catalysts. 2,3-Dihydropyridin-4(1*H*)-ones are a well known class of molecules that have been extensively studied. Their versatility and unique chemical properties continue to spark interest in novel and more efficient methods

for their enantiospecific synthesis[86] and are of interest in natural product and diversity-oriented synthesis (DOS).[87] 2,3-dihydropyridin-4(1*H*)-ones are versatile structures that have utility for the synthesis of piperidine-containing natural products, such as indolizidine and quinolizidine alkaloids[88,89] and piperidine-containing bioactive molecules.[24,47,90-93]

Comins reported reduction of *N*-acyl-2,3-dihydro-4-pyridones using zinc/acetic acid to prepare *N*-acyl-4-piperidones (Scheme 1.3, eq 1),[94] while the Hayashi group reported the asymmetric addition of arylzinc reagents to 2,3-dihydropyridin-4(1*H*)-ones in a rhodium-catalyzed reaction to obtain 2-aryl-4-piperidones in up to 99% ee (Scheme 1.3, eq 2).[95] Several other groups also developed similar protocols using either alkyl- or arylzinc reagents.[96-98] Feringa and Minnard developed enantioselective syntheses of 2-aryl-4-piperidones in up to 99% ee by conjugate addition of arylboroxines in a rhodium/phosphoramidite catalyzed reaction.[99] The Shi group synthesized 2-aryl-4-piperidones by axially chiral NHC–Pd(II) complexes catalyzed asymmetric 1,4-addition of arylboronic acids to 2,3-dihydropyridin-4(1*H*)-ones.[93] In a similar manner, the Knochel group prepared 2-aryl-4-piperidones by 1,4-addition of arylboronic acids to 2,3-dihydropyridin-4(1*H*)-ones catalyzed by rhodium-sulfoxide-alkene hybrids as chiral ligands.[100] The Liao group employed (*R,R*)-1,2-bis(tert-butylsulfinyl)benzene as a chiral ligand in rhodium-catalyzed enantioselective conjugate additions of sodium tetra-arylborates to 2,3-dihydro-4-pyridones to prepare 2-aryl-4-piperidones (Scheme 1.3, eq 3).[101]

Scheme 1.3. Addition of Nucleophiles to Cyclic Enaminones

Comin's Chemistry

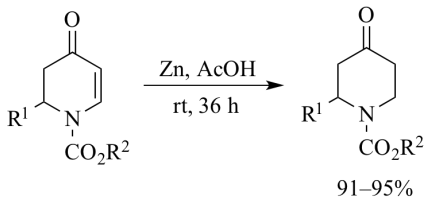

(eq 1)

Hayashi's Chemistry

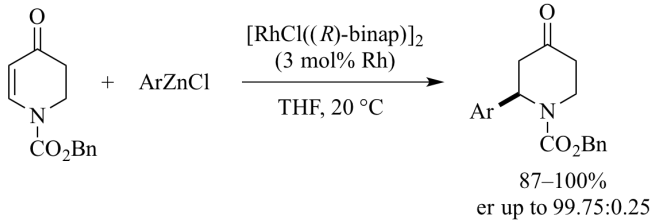

(eq 2)

Liao's Chemistry

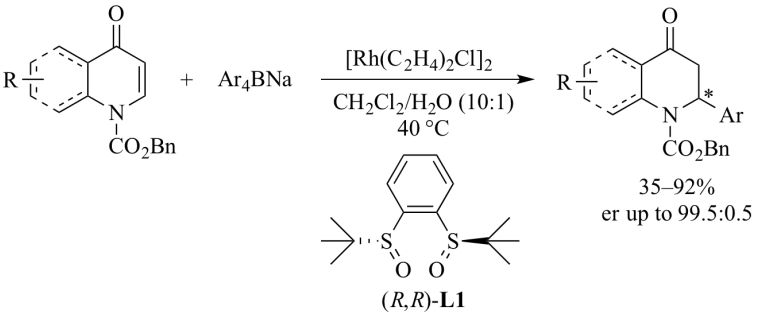

(eq 3)

Nakao, Hiyama and Hayashi's Chemistry

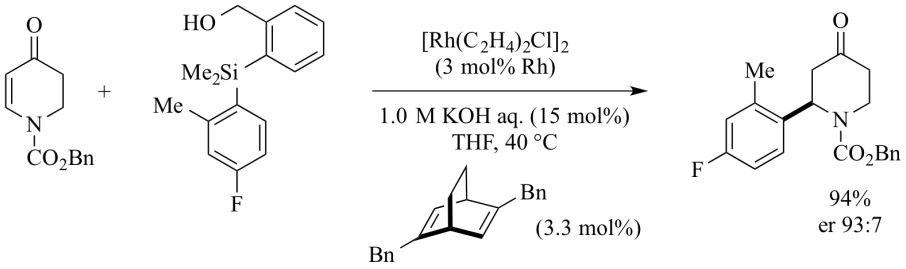

(eq 4)

Alexakis's Chemistry

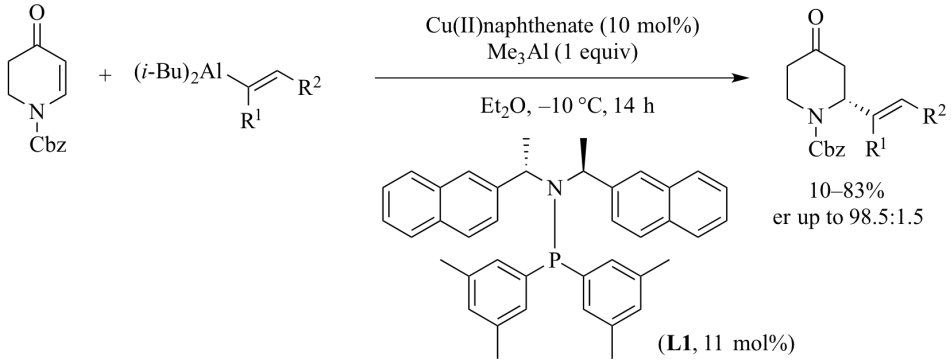

(eq 5)

Nakao, Hiyama, and Hayashi synthesized 2-(4-fluoro-2-methyl)phenyl-4-piperidone by utilizing 4-fluoro-2-methyl)phenyl [2'-(hydroxymethyl)phenyl]dimethylsilane as a mild and reproducible agent for the rhodium-catalyzed 1,4-addition reaction on a cyclic enaminone (Scheme 1.3, eq 4).[102] The Feringa group obtained 2-methyl-4-piperidone by 1,4-addition of trimethylaluminum to 2,3-dihydro-4-pyridone.[103] The chiral catalyst needed for this transformation was formed from $Cu(OTf)_2$ and a chiral phosphoramidite ligand. A highly enantioselective synthesis of chiral 2-alkenyl-4-piperidones in up to 97% ee was realized by the Alexakis group via asymmetric addition of alkenyl alanes to 2,3-dihydro-4-pyridones with the aid of Cu(II) catalyst and a chiral ligand L1 (Scheme 1.3, eq 5).[104]

1.3.3 Other Approaches

1.3.3.1 Imino-Diels-Alder Reaction

Ishimaru and co-workers developed a [4+2] cycloaddition of *N*-benzylaldimines with 2-silyloxybuta-1,3-dienes in the presence of TMSOTf to synthesize *trans*-2,6-disubstituted-4-piperidones. Increases in the diastereoselectivities of the products was attempted with greater bulkiness of the α-substituent of the aldimine.[105] However, high diastereoselectivities could not be achieved with benzaldimine because of the moderate bulkiness of the aromatic ring at the α-position of the aldimines. The same group later reported a protocol with more effective diastereocontrol (Scheme 1.4, eq 1). In this route, the benzaldimine derivatives were attached to a planar chiral tricarbonyl(1,2- or 1,3-disubstituted arene)chromium complex for enhancing the diastereoselectivities of the reaction.[31]

Scheme 1.4. Imino-Diels-Alder Chemistry

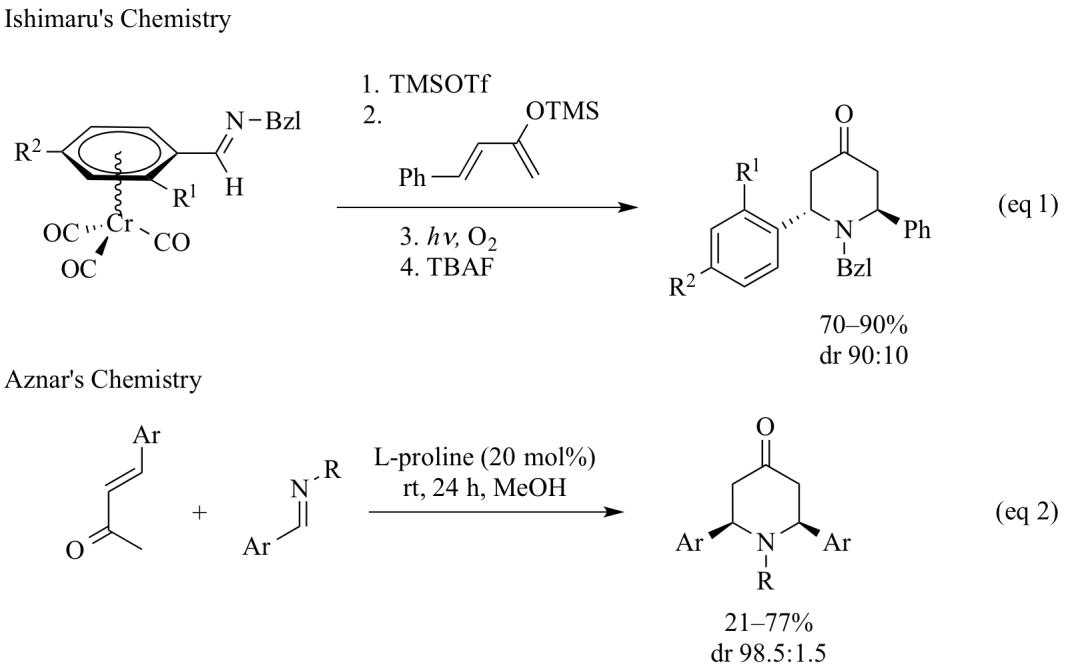

Aznar and co-workers established a synthesis of *meso*-2,6-diaryl-4-piperidones (both *N*-substituted and *N*-unsubstituted) by an L-proline catalyzed imino-Diels-Alder reaction between acyclic α,β-unsaturated ketones and aldimines at room temperature (Scheme 1.4, eq 2).[106]

1.3.3.2 Reductive Cleavage of Cycloadducts

The Padwa group synthesized substituted 4-piperidones by subjecting 7-oxa-1-azanorbornane cycloadducts to reductive cleavage (H_2, Pd/C) of the *N*-*O* bond (Scheme 1.5).[107] These isoxazolidine cycloadducts were in turn synthesized by reacting oximes with 2,3-bis(phenylsulfonyl)-1,3-butadiene.[108,109]

Scheme 1.5. Reductive Cleavage of Cycloadducts

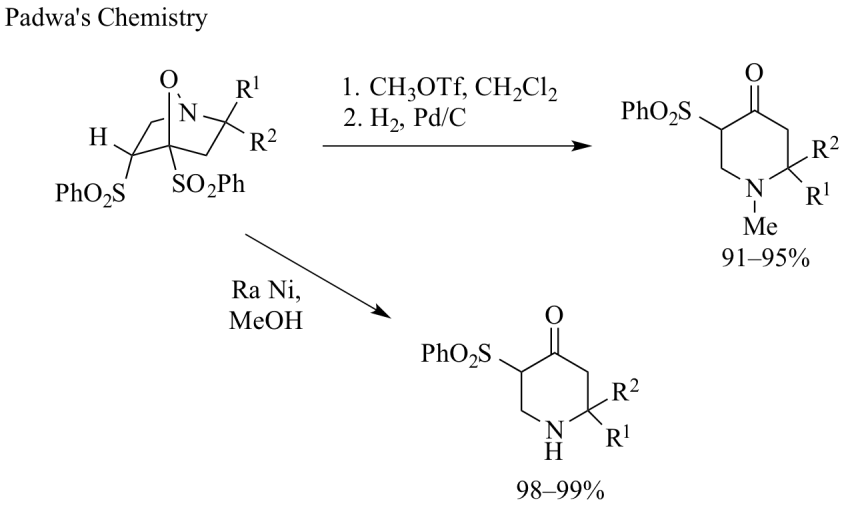

1.3.3.3 Double Aza-Michael Addition

Selvaraj *et al.* first synthesized *meso*-*N*-methyl-2,6-diaryl-4-piperidones by reacting 2-methyl-1,5-diaryl-1,4-pentadien-3-ones with aqueous methylamine solution at room temperature.[110] Padmavathi and co-workers extended this protocol to synthesize *N*-methyl-2-phenyl-3-methyl-6-arylpiperidin-4-ones by using 2-methyl-1-phenyl-5-aryl-1,4-pentadien-3-ones as the starting ketones (Scheme 1.6, eq 1).[111] Dörrenbächer *et al.* developed a one-pot domino Stille coupling/Michael addition protocol starting from easily available vinyl stannanes to synthesize 2,5-disubstituted-4-piperidones (Scheme 1.6, eq 2).[112] In this straightforward method, a vinyl stannane was coupled with an α,β-unsaturated acid chloride using a Stille coupling in the presence of Pd(II) and triphenylphosphine to generate the 2,5-disubstituted-1,4-pentadien-3-ones *in situ* to which an alkylamine was added. The amine reacted in a double 1,4-addition generating the desired products. Owing to its significant Lewis acid activity, the Pd(II) not only

greatly helped the Michael addition, but also enabled the entire process to be conducted in one-pot.

Scheme 1.6. Double Aza-Michael Addition

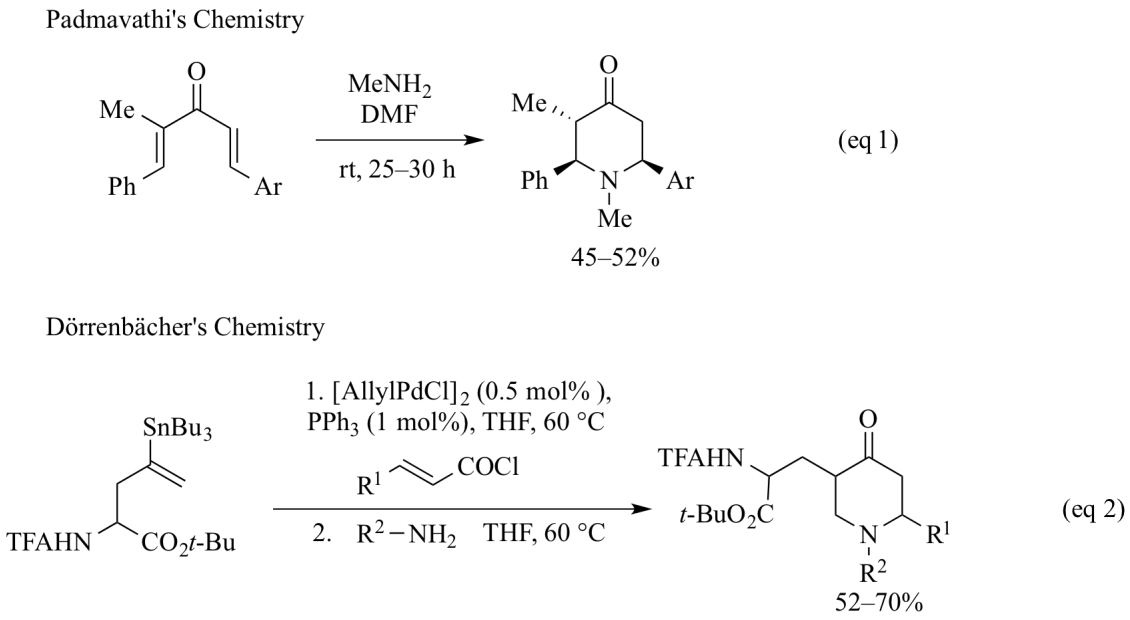

1.3.3.4 Carbanion Cyclization

Sun and co-workers synthesized *N*-substituted-4-piperidones employing a Dieckmann condensation followed by decarboxylation. Refluxing *N*,*N*-bis[2(methoxycarbonyl)ethyl] substituted amines with sodium methoxide followed by extraction with HCl, refluxing again, and finally treating with NaOH (Scheme 1.7, eq 1) furnished the desired piperidones.[113] The *N*,*N*-bis [2(methoxycarbonyl)ethyl] substituted amines were in turn obtained by a Michael addition of substituted amines, methyl acrylate and acetic acid. Bing and Guo-Qiang developed a protocol to access chiral 2-aryl/alkyl-4-piperdiones (Scheme 1.7, eq 2).[114] The key ring-formation reaction relied on the competitive intramolecular attack of the carbanion generated by the lithium-iodine exchange at the

ester moiety. This method can also generate 2-aryl or 2-alkyl-4-piperidones.

Scheme 1.7. Carbanion Cyclization

Sun's Chemistry

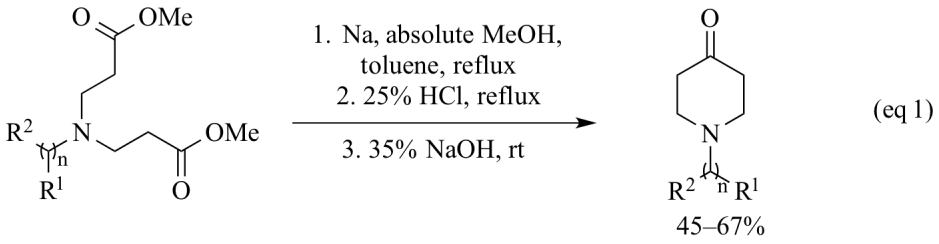

(eq 1)

Bing and Guo-Qiang's Chemistry

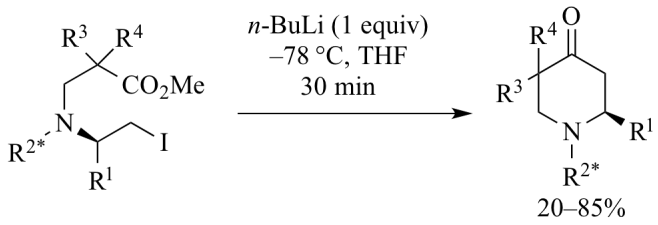

(eq 2)

The above review showcases that a variety of methods exist for the synthesis of piperidones including asymmetric methods that could be used for structure-activity studies if the piperidone skeleton was identified in a high throughput screening campaign.

1.4 Synthesis of Piperidinone Sulfonamides Library

The piperidinone sulfonamide library was prepared as shown in Scheme 1.8. In order to synthesize the required cyclic enaminones **1.7-1.11**, we decided to take advantage of the well-established Comin's chemistry.[115,116]

Scheme 1.8. Synthesis of Piperidinone Library

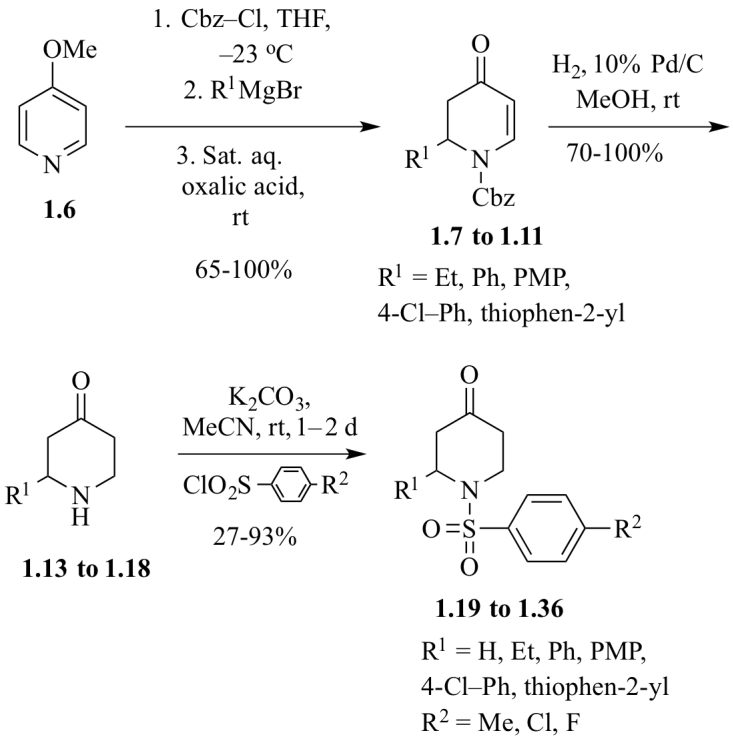

1.4.1 Synthesis of Cyclic Enaminones

4-Methoxypyridine (**1.6**) was treated with Cbz-chloride followed by addition of an appropriate Grignard reagent. Next, the reaction mixture was treated with saturated aqueous oxalic acid solution. After column chromatography, the cyclic enaminones **1.7** to **1.11** were furnished smoothly in 65-100% yields.

Table 1.1. Synthesis of Cyclic Enaminones

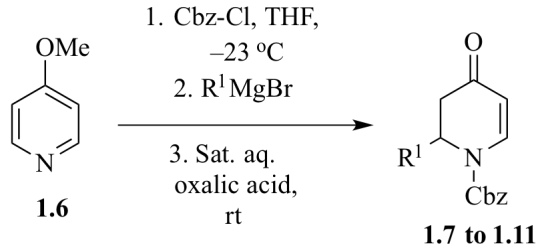

Entry	R^1	Product	Yield (%)
1	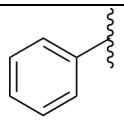	**1.7**	100
2	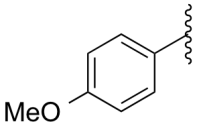	**1.8**	75
3	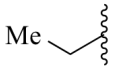	**1.9**	65
4	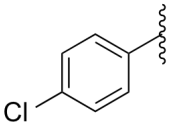	**1.10**	66
5	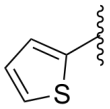	**1.11**	67

1.4.2 Synthesis of 2-Substituted Piperidinones

In order to get the piperidinones, it was necessary to reduce the double bond as well as remove the Cbz group off of nitrogen. Initially, we followed literature precedent[117] and used L-selectride to reduce the double bond (Scheme 1.9), and obtained 52% yield of benzyl 4-oxo-2-phenylpiperidine-1-carboxylate (**1.12**). Then, the Cbz group was deprotected using hydrogen gas and 10% Pd/C catalyst. This protocol provided a quantitative yield of the 2-phenylpiperidin-4-one (**1.13**).

Scheme 1.9. Two-step Synthesis of Piperidinone from Cyclic Enaminone

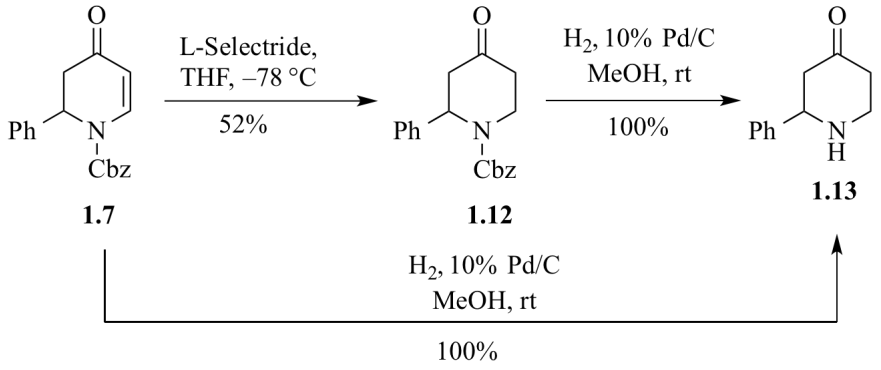

However, we had observed a low yield in the double bond reduction reaction. Based on literature precedent[118,119], we surmised that this two-step process could be shortened by directly subjecting the cyclic enaminones **1.7** to **1.11** to hydrogenolysis. Hydrogenolysis of **1.7** not only removed the Cbz group, but also saturated the C5-C6 double bond to generate the 2-phenylpiperidin-4-one (**1.13**) in quantitative yield (crude). We therefore subjected all enaminones to hydrogenolysis to get the 2-substituted piperidinones **1.13** to **1.17** in good yields (45-100%) (Table 1.2). Reduction of compound **1.11** under these conditions furnished the Cbz-deprotected compound 2-(thiophen-2-yl)-2,3-dihydropyridin-4(1*H*)-one (**1.17**), because the C5-C6 double bond could not be reduced with this strategy. However, it was decided to carry forward the crude product **1.17** to next step. The piperidones **1.13-1.17** were used in the next step without purification. Piperidin-4-one (**1.18**) was commercially available as a monohydrochloride monohydrate salt and was used directly without any purification in the next step.

Table 1.2. Synthesis of Piperidinones

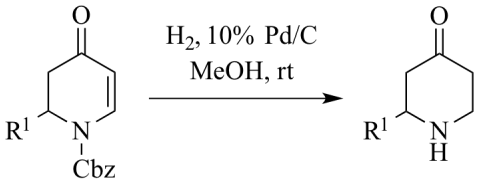

1.7 to 1.11 **1.13 to 1.18**

Entry	Product	Yield (%)
1	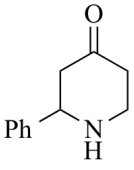 **1.13**	100
2	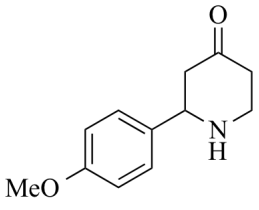 **1.14**	70
3	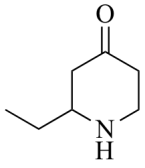 **1.15**	100
4	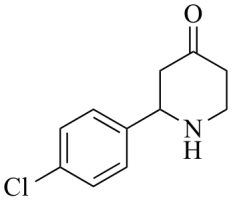 **1.16**	45
5	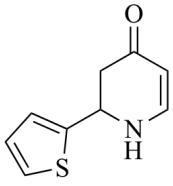 **1.17**	45% (62% brsm)
6	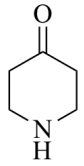 **1.18**	Commercially available

1.4.3 Synthesis of Piperidinone Sulfonamides

Piperidinones **1.13** to **1.18** were then converted to sulfonamide with commercially available 4-substituted benzenesulfonyl chlorides. Initial attempts of stirring piperidinone **1.14** with tosyl chloride in pyridine as a solvent and base did not furnish the required product **1.22** (Scheme 1.10).[120,121] Subjecting a THF solution of piperidinone **1.14** to sodium hydride followed by addition of tosyl chloride also did not lead to product formation **1.22**.[122] In another attempt, adding tosyl chloride to a slurry of a piperidinone **1.14** in a biphasic mixture of 1:1 water/chloroform and potassium carbonate did not yield any product **1.22**.[123]

Scheme 1.10. Failed Attempts at Synthesizing Piperidinone Sulfonamides

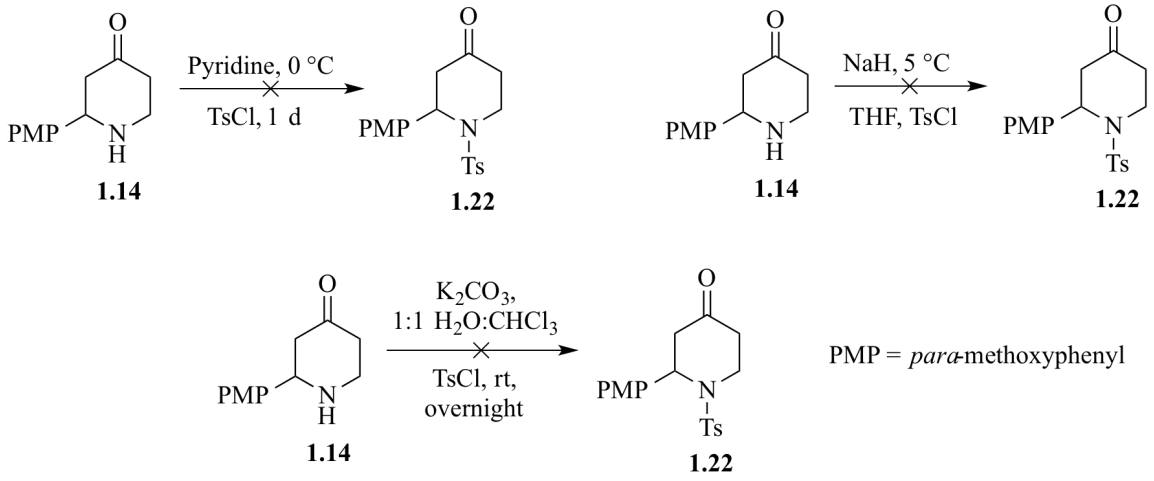

At last, piperidinone **1.14** was dissolved in acetonitrile, and potassium carbonate and tosyl chloride were added sequentially.[124] The reaction mixture was stirred for 1 day at room temperature to yield the required piperidinone sulfonamide **1.22** in 48% yield. Encouraged by this result, all piperidinones **1.13**–**1.18** were subjected to the above sulfonylation conditions to provide the targeted piperidinone sulfonamides **1.19** to **1.36** in

27-93% yield (Table 1.3).

Table 1.3. Synthesis of Piperidinone Sulfonamides

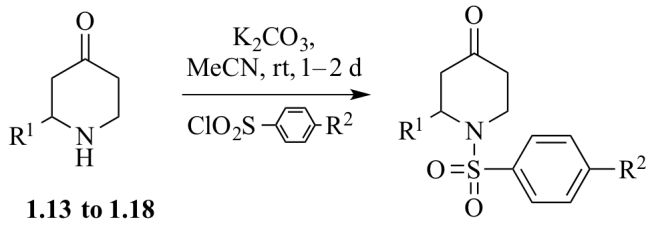

1.13 to 1.18 **1.19 to 1.36**

Entry	R^1	R^2	Product	Yield[a] (%)
1	Ph	Me	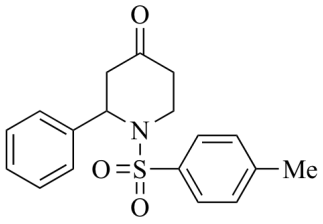 **1.19**	64
2	Ph	F	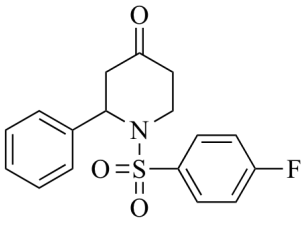 **1.20**	38
3	Ph	Cl	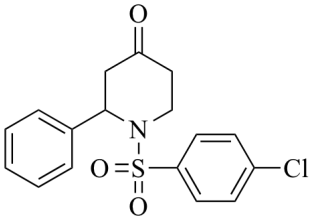 **1.21**	34
4	PMP	Me	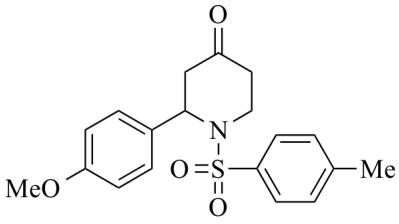 **1.22**	48
5	PMP	F	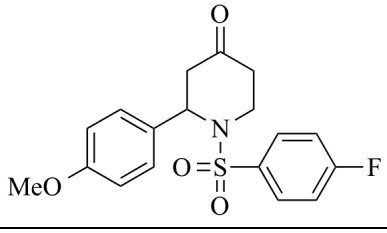 **1.23**	27

6	PMP	Cl	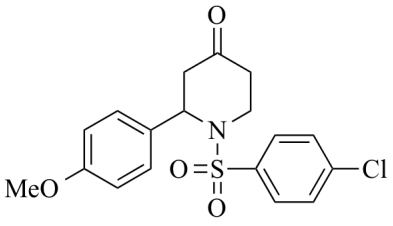 **1.24**	30
7	Et	Me	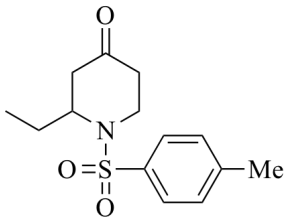 **1.25**	44
8	Et	F	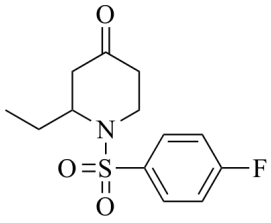 **1.26**	51
9	Et	Cl	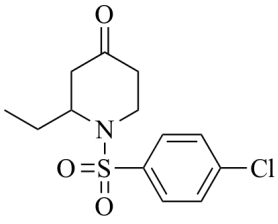 **1.27**	50
10	4-Cl-C_6H_4	Me	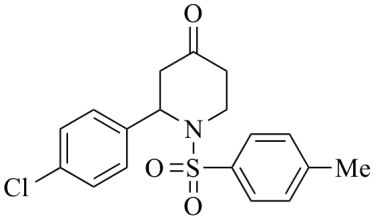 **1.28**	80
11	4-Cl-C_6H_4	F	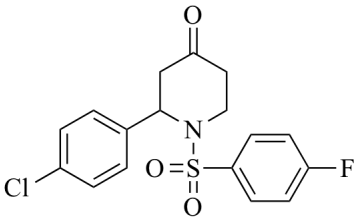 **1.29**	80
12	4-Cl-C_6H_4	Cl	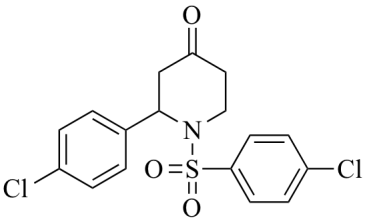 **1.30**	78

13	H	Me	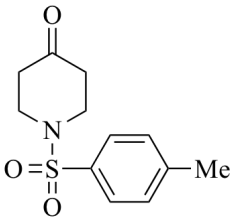 **1.31**	91
14	H	F	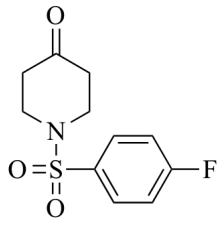 **1.32**	93
15	H	Cl	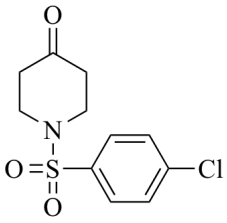 **1.33**	85
16	Thiophen-2-yl	Me	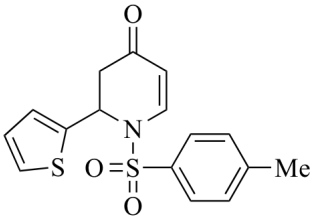 **1.34**	52
17	Thiophen-2-yl	F	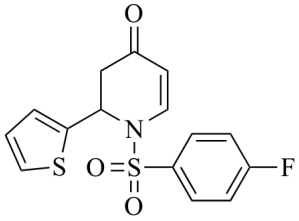 **1.35**	43
18	Thiophen-2-yl	Cl	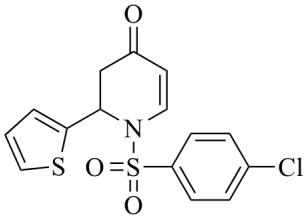 **1.36**	55

[a]All the yields are unoptimized. PMP = *para*-methoxyphenyl.

1.5 Results of HTS Assays at NIH

The piperidinone sulfonamides (25 mg of each compound) were placed into pre-tared,

bar-coded vials and submitted to NIH for testing in various biological assays. From the 18 submitted library members, 2 compounds, **1.19** and **1.31**, (Figure 1.5) were identified as primary hits in high throughput screening campaigns.

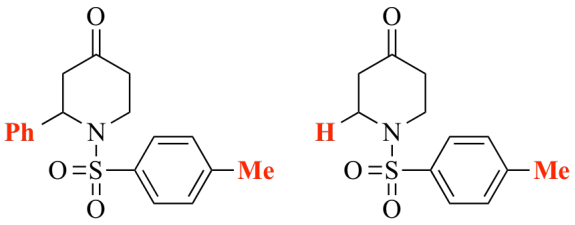

Figure 1.5. Structures of Biologically Active Hits.

Compound **1.19** was identified as an inhibitor of prion protein (PrP) 5' UTR in the primary *in vitro* screening. The build-up of prion proteins with the disease causing conformation (PrP^{Sc}) in neuronal cells is associated with cell death and encephalopathy. One possible way to alleviate the succession of prion-based diseases is to decrease the overall levels of PrP in the nerve cells. This can be achieved by inhibiting the expression of PrP at the message translation level. In order to identify compounds that might reduce translation of the PrP message, the compounds were assayed against H4 neuroblastoma cells transfected with a plasmid reporter construct. The reporter consisted of a stem-loop sequence from the human Prion protein variant 2 (PrP) 5'UTR fused to a luciferase gene as well as a viral internal ribosome entry site driving Green Fluorescent Protein (GFP). This screening looked for compounds which interact with the PrP 5' UTR and reduce the protein expression by observing luciferase activity.[125] The other compound **1.31** was found to be inhibiting the human platelet-activating factor acetylhydrolase 1b, catalytic subunit 2 (PAFAH1B2). Human platelet activating factor acetylhydrolase (pPAFAH) is a

Ca^{2+} independent phospholipase A2 (PLA2) identified in human plasma as the enzyme responsible for the hydrolysis/inactivation of platelet activating factor (PAF),[126] a potent pro-inflammatory phospholipid signaling molecule.[127] In this assay, recombinant PAFAH1B2 protein was incubated with test compounds for a defined period followed by addition of the FP-rhodamine probe and measurement of fluorescence polarization at a specific time point. As per the assay design, test compounds that act as PAFAH1B2 inhibitors will prevent PAFAH1B2-probe interactions, thereby increasing the proportion of free (unbound) fluorescent probe in the well, leading to low fluorescence polarization.[128] Development of selective inhibitors of PAFAH would help in the investigation of its involvement in the dysregulated biochemical pathways that support tumorigenesis. As a result, identifying such inhibitors would also elucidate the physiological role of this enzyme and its contribution to atherosclerosis, cancer and other inflammatory pathologies.

1.6 Summary

In summary, a small library of 18 piperidinone sulfonamides was synthesized in three steps in good yields. All compounds were submitted to NIH for high throughput screening assays. Piperidinone sulfonamides **1.19** and **1.31** were identified as primary hits. Compound **1.19** showed prion protein (PrP) 5' UTR inhibitory activity, and compound **1.31** displayed human platelet-activating factor acetylhydrolase 1b, catalytic subunit 2 (PAFAH1B2) inhibitory activity.

Chapter 2

Transition-Metal-Free C–H Trifluoromethylation of Cyclic Enaminones

2.1 Introduction

Although inorganic fluorides are plentiful on earth, nature does not produce more than a dozen of compounds containing a fluorine atom,[129] while on the other hand, almost 30–40% of all commercial agrochemicals and 20–30% of all pharmaceuticals have at least one fluorine atom in their structures.[130] Among all the fluorinated compounds, molecules possessing a trifluoromethyl (CF_3) group comprise an important class of compounds. These compounds have generated a lot of interest due to their unique properties such as increased electronegativity, hydrophobicity, and metabolic stability.[130,131] Structural modification via trifluoromethylation is a common practice in both the pharmaceutical and agrochemical industries.[130,132] Classic methods to synthesize trifluoromethylated compounds largely employ Lewis acid-promoted exchange of chloride by fluoride *via* the Swarts-type reaction (Scheme 2.1).[133] These harsh conditions limit their synthetic application. Newer synthetic methods are urgently needed due to the increasing significance of fluorinated compounds.

Scheme 2.1. Traditional Trifluoromethylation Protocol

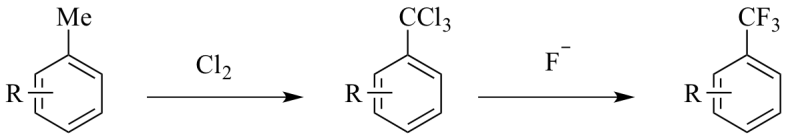

In the past decade, Pd– and Cu–catalyzed trifluoromethylation cross-coupling reactions have been developed that show high regioselectivity, good functional group tolerance, and reaction efficiency.[134-140] However, most of these coupling methods required substrate prefunctionalization resulting in low atom-economy, thereby, limiting their

usefulness for industrial applications. A more sustainable approach is through direct C–H activation. However, innate C–H trifluoromethylation is very challenging largely because until very recently, mild and robust methods had not been available.[141-143]

2.2 Recent Advances in Trifluoromethylation Chemistry

2.2.1 Direct Trifluoromethylation of *sp* C–H Bonds

There is a very limited number of examples of direct C–H trifluoromethylation on *sp* carbon centers due to the dimerization of alkynes. In 2010, Qing and co-workers reported the first example of a Cu-mediated oxidative trifluoromethylation of terminal alkynes with $TMSCF_3$ (Scheme 2.2).[144] The reaction required stoichiometric amounts of CuI in order to proceed efficiently. The same group later published a modified version of the above reaction employing catalytic amounts of Cu(I), which was achieved by slow addition of reagents through a syringe pump.[145] Following this, the Qing group reported an improved protocol for trifluoromethylation of terminal alkynes using *in situ* generated (phen)Cu(CF_3) at room temperature with a small amount of $TMSCF_3$.[146]

Scheme 2.2. First Example of *sp* C–H Trifluoromethylation

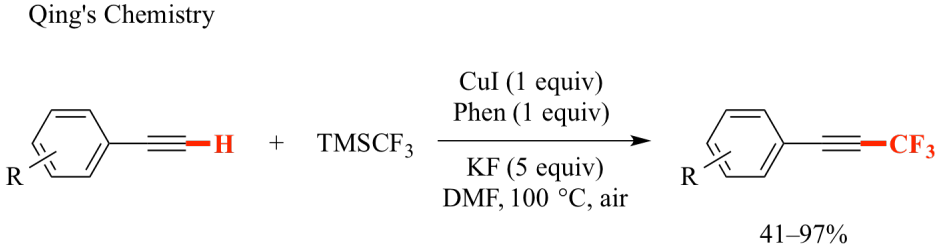

2.2.2 Direct Trifluoromethylation of sp^2 C–H Bonds

Trifluoromethylated (hetero)arenes are present in agrochemicals, pharmaceuticals, and

advanced materials. Direct trifluoromethylations of sp^2 C–H bonds are currently therefore a popular topic, because they are the most effective methods to synthesize (hetero)arenes containing CF_3 in their structures.[134,137,139,142,143] These established protocols can be categorized into three classes based on the three CF_3 sources used: CF_3^+, CF_3^-, and $CF_3\bullet$.[147]

2.2.2.1 Trifluoromethylation with CF_3^+ Reagents

An electrophilic *ortho*-trifluoromethylation reaction of arenes tethered with directing groups using Umemoto's reagent (Scheme 2.3, eq. 1) was first reported by Yu *et al.*[148] A variety of *N*-heterocyclic directing groups such as pyridine, pyrimidine, imidazole, and thiazole, could be used. This revolutionary chemistry was catalyzed *via* a proposed Pd(II)/Pd(IV) catalytic cycle necessitating a stoichiometric amount of $Cu(OAc)_2$ as the oxidant. Subsequently, the same group also developed a similar electrophilic trifluoromethylation reaction using an amide as the directing group.[149] In particular, *N*-methylformamide as an additive was crucial for the coupling process. In a similar manner, Shi and co-workers successfully developed regioselective *ortho*-trifluoromethylations of arenes using the acetamino group as an alternative directing group (Scheme 2.3, eq. 2).[150] Later, the Sanford group reported that the oxidation of the cyclometalated Pd(II) dimer with CF_3^+ reagents produces a monomeric CF_3–Pd(IV) intermediate, which undergoes selective reductive elimination to form a C–CF_3 bond.[151] Very recently, the Besset group developed Cu(I)-mediated β-trifluoromethylation of α,β-substituted *N,N*-diethylacrylamides with TFA and *N*-methylformamide as additives (Scheme 2.3, eq. 3).[152]

Scheme 2.3. Directed Electrophilic *ortho*-Trifluoromethylation Using Umemoto's Reagent

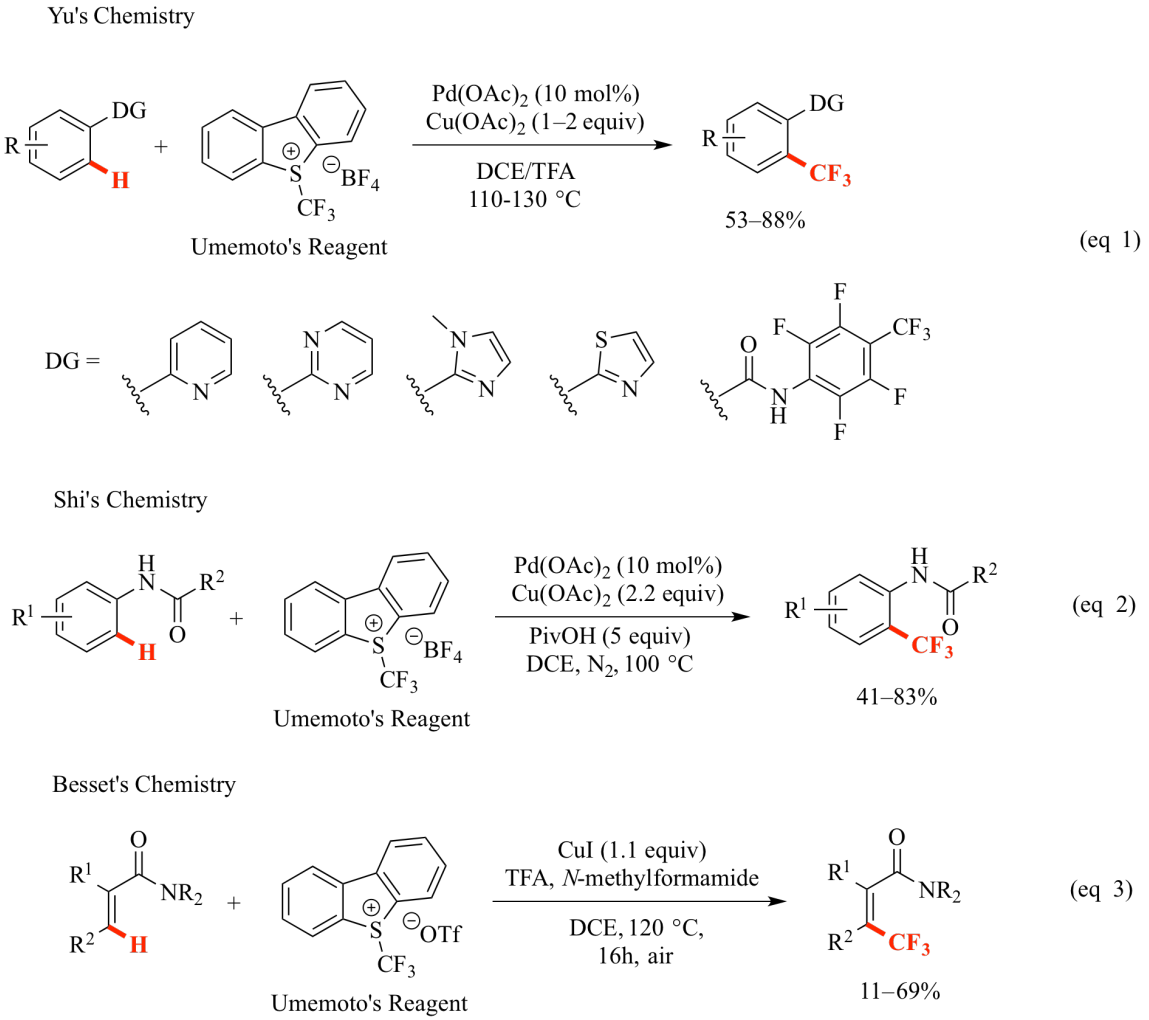

Togni's reagent is another remarkable CF_3^+ source (Scheme 2.4). Togni and co-workers had initially reported that no catalysts were needed for electrophilic aromatic trifluoromethylation on a broad range of arenes and *N*-heteroarenes, although Togni's reagent had shown increased electrophilicity in the presence of a Lewis acid.[153] Next, Sodeoka and co-workers developed a $Cu(OAc)_2$-catalyzed regioselective trifluoromethylation of indole derivatives using Togni's reagent under very mild

conditions (Scheme 2.4, eq 1).[154] Recently, the same group reported a difunctionalization-type trifluoromethylation reaction of activated alkenes bearing allylic protons using Togni's reagent.[155] This Cu(I)-catalyzed protocol provides trifluoromethylated carbocycles and heterocycles in good to excellent yields. Loh and co-workers reported the first example of C–H trifluoromethylation of alkenes (Scheme 2.4, eq 2).[156] In this Cu(I)-catalyzed methodology, a series of enamides were β-trifluoromethylated with Togni's reagent in good to excellent yields.

Scheme 2.4. Electrophilic Trifluoromethylation Using Togni's Reagent

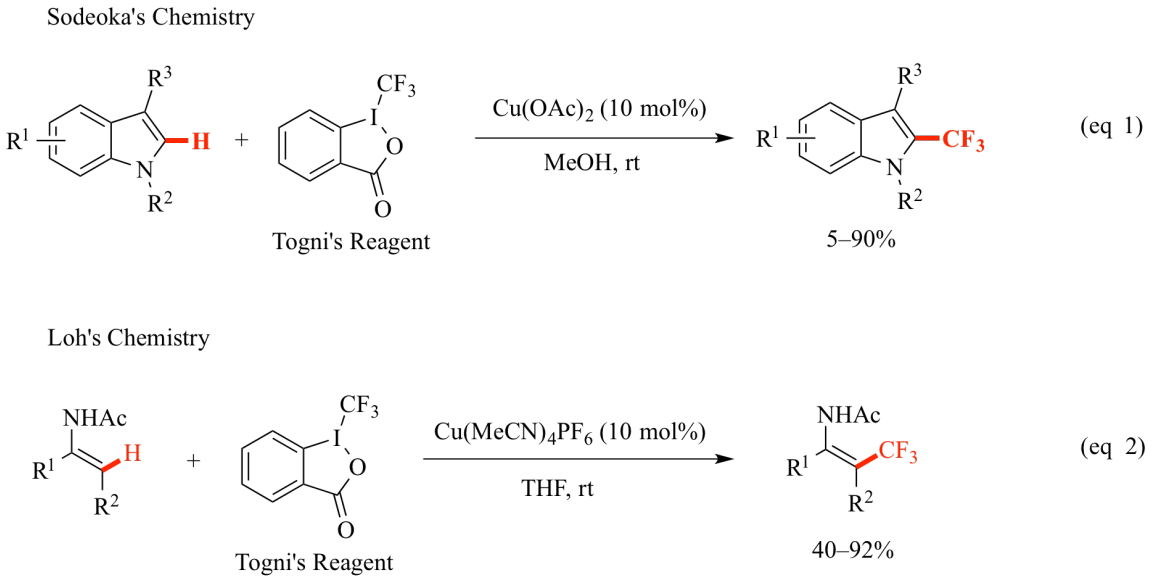

2.2.2.2 Trifluoromethylation With CF_3^- Reagents

$TMSCF_3$ (Ruppert-Prakash reagent) is the most commonly used CF_3^- reagent. Liu and co-workers developed a Pd-catalyzed oxidative trifluoromethylation of indoles using $TMSCF_3$ (Scheme 2.5, eq 1)[157] in which $PhI(OAc)_2$ (PIDA) was employed as an oxidant and the proposed mechanism of the reaction was thought to involve a Pd(II)/Pd(IV) species. The same group next developed a tandem oxidative aryl trifluoromethylation of

activated alkenes using analogous conditions;[158] a bifunctionalization reaction that offered a variety of CF_3-containing oxindoles in good yields. More recently, Qing and co-workers reported a Cu-catalyzed C–H trifluoromethylation reaction of heteroarenes and electron-deficient arenes with $TMSCF_3$ (Scheme 2.5, eq 2).[159] The key to this regioselective transformation was the acidity of the targeted C–H proton. Under optimized conditions a wide range of aromatic compounds including benzoxazoles, oxadiazoles, benzothiazoles, benzoimidazoles, indoles, and perfluoroarenes were compatible.

Scheme 2.5. Nucleophilic Trifluoromethylation Using the Ruppert-Prakash Reagent

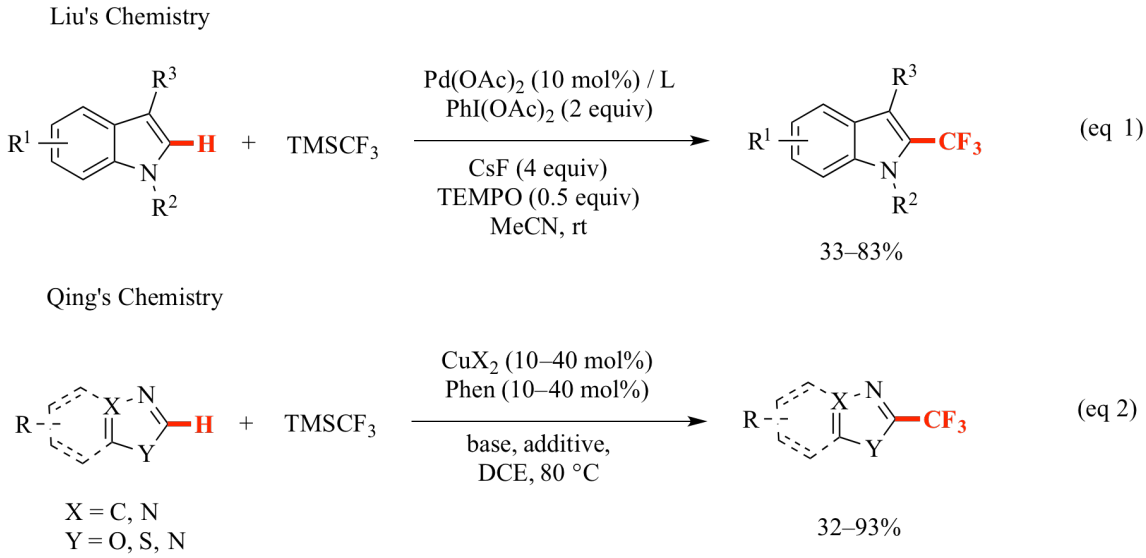

2.2.2.3 Trifluoromethylation Involving CF_3• Reagents

Trifluoromethylation of various (hetero)aromatic compounds using CF_3I in the presence of a Fe(II) catalyst, H_2O_2, and DMSO was demonstrated by the Yamakawa group.[160] Mainly the general trend of aromatic electrophilic substitution directed the regioselectivity. Later, the Sanford group reported a silver-mediated direct

trifluoromethylation of arenes with $TMSCF_3$ (Scheme 2.6, eq 1).[161] The key intermediate to produce the CF_3• radical was proposed to be a Ag–CF_3 species. Even though a wide scope of substrates was generally tolerated, this methodology had a few drawbacks including the need for using stoichiometric amounts of silver salts and problematic regioselectivity. An extension of this Ag-mediated protocol to aryl triazene substrates with good *ortho*-selectivity was achieved by Bräse and co-workers (Scheme 2.6, eq 2).[162]

Scheme 2.6. Ag(I)-Mediated C–H Trifluoromethylation

Sanford's Chemistry

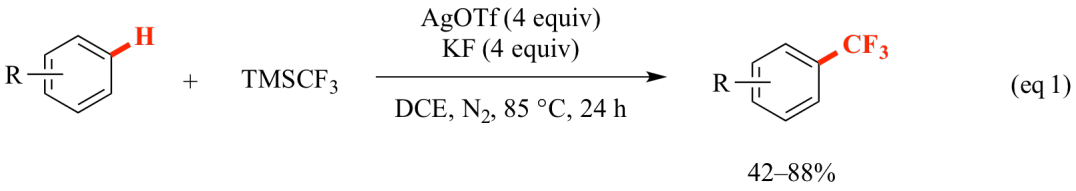

Bräse's Chemistry

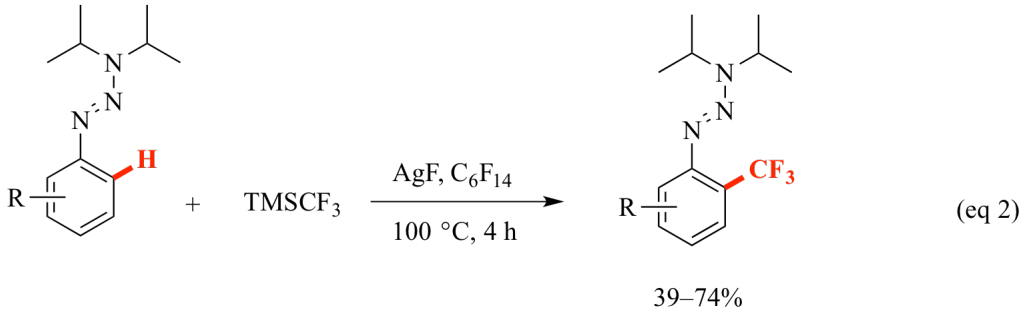

Recently there have been a few breakthroughs in radical direct C–H trifluoromethylation using inexpensive reagents that proceed under mild conditions.[135,163] The MacMillan group invented a novel photoredox protocol involving Ru(II)-catalyzed direct C–H trifluoromethylation on a wide variety of arenes and heteroarenes (Scheme 2.7).[164] In this methodology, CF_3SO_2Cl (*i.e.* TfCl) was employed as a CF_3• source. The low cost of TfCl and the mild conditions used in this protocol made it a very promising procedure. Since

then, a series of successive developments based on this photoredox protocol have been accomplished. For example, the Cho group achieved direct trifluoromethylation of a wide range of heteroarenes with good to excellent yields using CF_3I as a CF_3• source.[165]

Scheme 2.7. MacMillan's Photoredox Trifluoromethylation Protocol

MacMillan's Chemistry

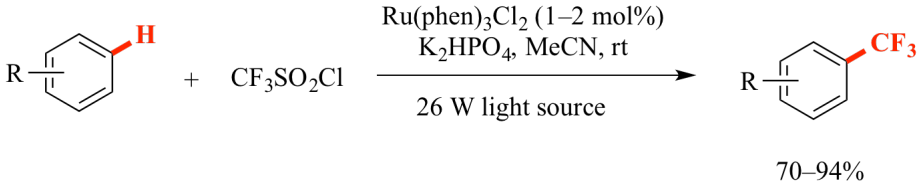

At the same time, Baran's group developed a metal-free trifluoromethylation reaction with peroxides as radical initiators using CF_3SO_2Na (Langlois' reagent); a benchtop-stable and inexpensive solid (Scheme 2.8).[166]

Scheme 2.8. Baran's Radical-based Trifluoromethylation Protocol

Baran's Chemistry

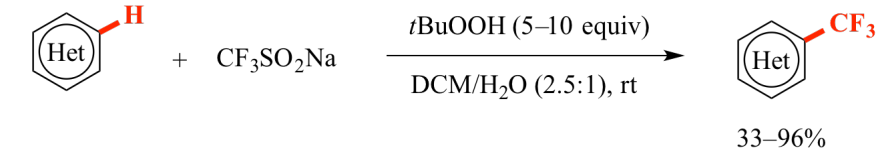

The versatility of this reaction lies in the fact that both electron-rich and electron-deficient heteroarenes can be efficiently used with high functional group tolerance. Although, the regioselectivity was modest, the choice of solvent sometimes could help modify the innate substrate reactivity. Very recently, Fu and co-workers developed a domino synthesis of 3-(trifluoromethyl)-indolin-2-one derivatives in good to excellent

yields using Langlois' reagent with *N*-alkyl-*N*-phenylacrylamides as starting materials.[167] These two methods, developed by MacMillan and Baran, are very beneficial for medicinal chemistry, because of their robust conditions and broad functional group tolerance allowing one to achieve late stage trifluoromethylation to prepare diversified drug analogs.[163]

2.2.3 Direct Trifluoromethylation of sp^3 C–H Bonds

Direct trifluoromethylation of sp^3 C–H bonds is as challenging as those for *sp* C–H bonds. Currently available approaches are applicable to only a few substrate examples, for example, allylic C–H bonds and α–carbonyl C–H bonds.[168-177] Liu and co-workers first reported a rare Cu(I)-catalyzed C–H trifluoromethylation of terminal alkenes *via* allylic C–H activation/functionalization using Umemoto's reagent (Scheme 2.9, eq 1).[171] Both the experimental and theoretical analyses indicated that the reaction may proceed via a Heck-like four-membered-ring transition state. This method worked with an array of terminal alkenes without 2-substitutents, however 2-substituted terminal alkenes or internal and cyclic alkenes were not compatible. Followed by this, Buchwald[172] and Wang[173] also independently reported Cu(I)-catalyzed allylic C–H trifluoromethylation reactions using Togni's reagent (Scheme 2.9, eq 2 and eq 3). Both of these methods tolerated a wide range of functional groups and gave good yields. Interestingly, branched terminal alkenes and cyclic alkenes were not compatible in Buchwald's method, but worked well in Wang's method at higher temperature.

Scheme 2.9. Allylic C–H Trifluoromethylation

Liu's Chemistry

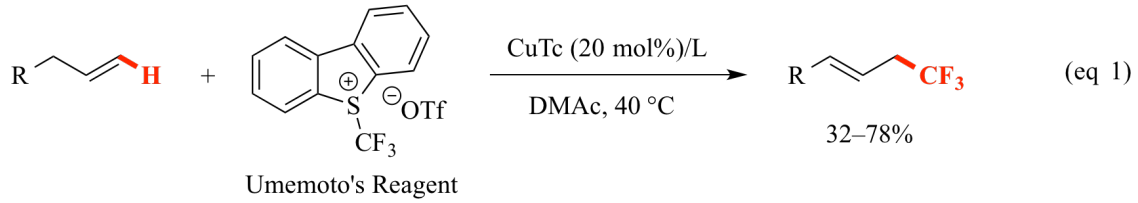

Umemoto's Reagent

Buchwald's Chemistry

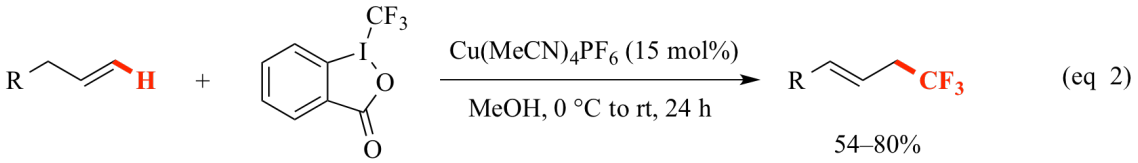

Togni's Reagent

Wang's Chemistry

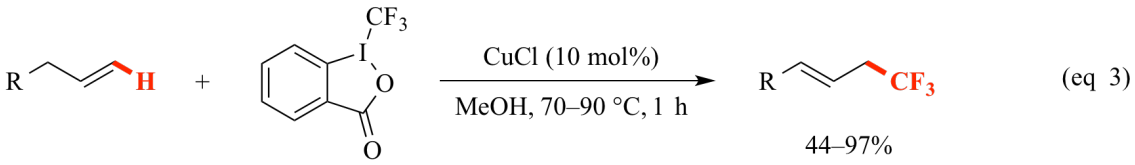

Togni's Reagent

Qing's Chemistry

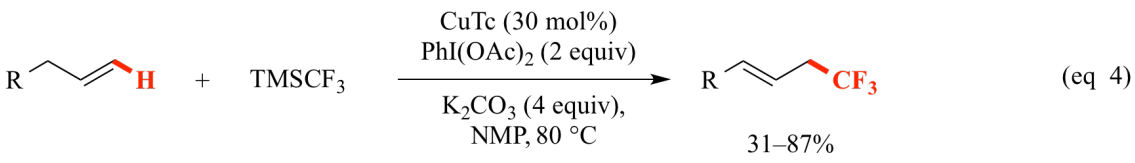

Later, Qing and co-workers developed a Cu-catalyzed oxidative trifluoromethylation of terminal alkenes using $TMSCF_3$ (Ruppert-Prakash reagent) (Scheme 2.9, eq 4).[174] This method provided a complementary pathway for direct allylic trifluoromethylations without using Umemoto's reagent or Togni's reagent. The MacMillan group pioneered

the direct trifluoromethylation of α-carbonyl C–H bonds using their above mentioned photoredox chemistry. Previously they had reported a highly enantioselective α-trifluoromethylation of a series of aldehydes using CF_3I as a CF_3• source (Scheme 2.10).[175] Shortly after this, they expanded the scope of substrates from aldehydes to ketones, esters, and amides by first converting the carbonyl compounds to enolsilanes. This strategy further enhanced the utility of this novel protocol and also gave very good yields.[177] Concurrently, the same group had reported a non-photolytic enantioselective α-trifluoromethylation of aldehydes using Togni's reagents instead of CF_3I.[176]

Scheme 2.10. Enantioselective α–Trifluoromethylation of Aldehydes

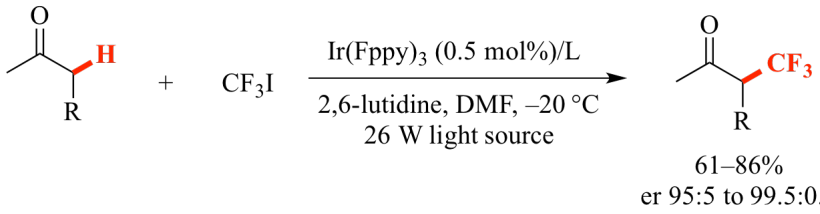

Although the trifluoromethylation chemistry is currently a popular topic and there have been rapid advances in this field, the existing methods and substrates are still nevertheless not sufficient. Of particular interest, the direct trifluoromethylation of alkenyl C–H bonds is especially uncommon; only three such methods have been reported to date. First, the Loh group developed trifluoromethylation of enamides using Togni's reagent (Scheme 2.4, eq 2).[156] Second, very recently the Besset group developed a Cu(I)-mediated β-trifluoromethylation of α,β-substituted *N,N*-diethylacrylamides with TFA and *N*-methylformamide as additives (Scheme 2.3, eq. 3).[152] Third, at almost the same time, Yu and co-workers achieved Cu(II)-catalyzed trifluoromethylation of α-oxo-ketene dithioacetals (internal olefins) using $TMSCF_3$ as a trifluoromethylating agent.[178] Other

than these findings, the trifluoromethylation of internal or cyclic alkenes has remained elusive.

2.3 Rationale for Development of Direct Trifluoromethylation of Cyclic Enaminones

Amongst the trifluoromethylated compounds particularly the trifluoromethylated piperidine derivatives have been widely applied as common moieties in medicinal structure-activity relationship (SAR) studies.[179-185]

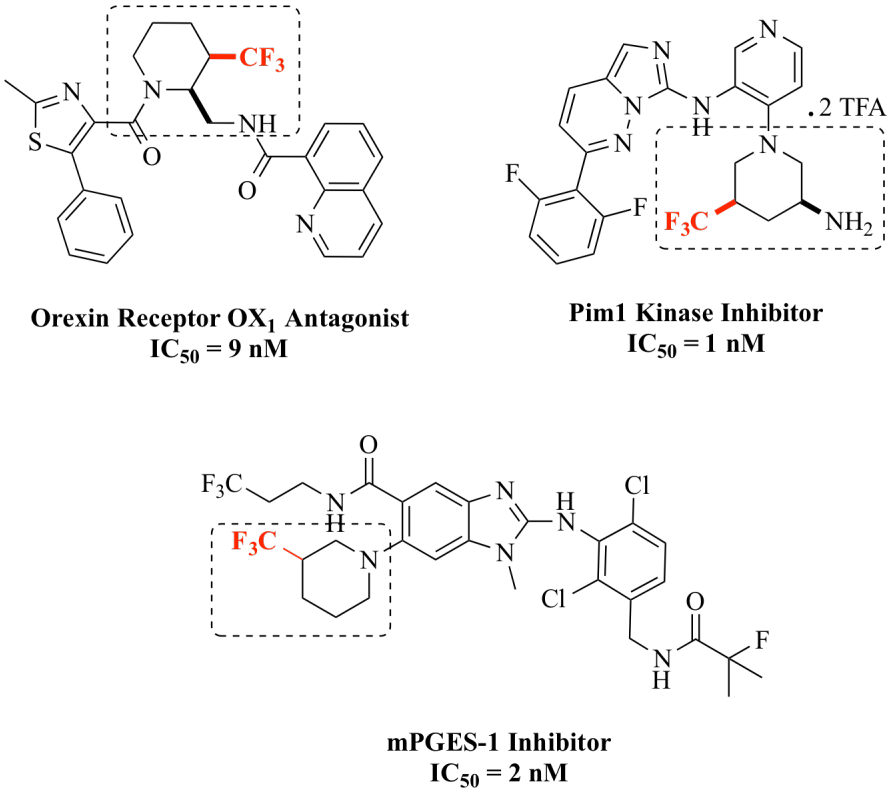

Figure 2.1. Recent Examples of Potent Bioactive 3-Trifluoromethylpiperidine Derivatives.

The trifluoromethylated piperidines are found in compounds with a variety of biological activities, such as orexin receptor OX_1 antagonists (for sleep disorders),[180] Pim1 kinase

inhibitors (for cancers),[181] and mPGES-1 inhibitors (for inflammatory diseases)[182] (Figure 2.1). Conventional syntheses usually entail the expensive commercially available 3-trifluoromethylpiperidine as a precursor,[179,182,185] while substituted piperidines often stem from prefunctionalized 3-trifluoromethylated pyridines and lack the versatility for late-stage functionalization.[180,181] The high cost, long reaction sequences, and inflexibility limit the practicality for industrial applications. A more sustainable and flexible trifluoromethylation approach is much desired.[141,142,186]

Scheme 2.11. Distinct Cyclic Enaminone Chemistry– Functionalizations of Olefinic C–H Bonds and Their Applications

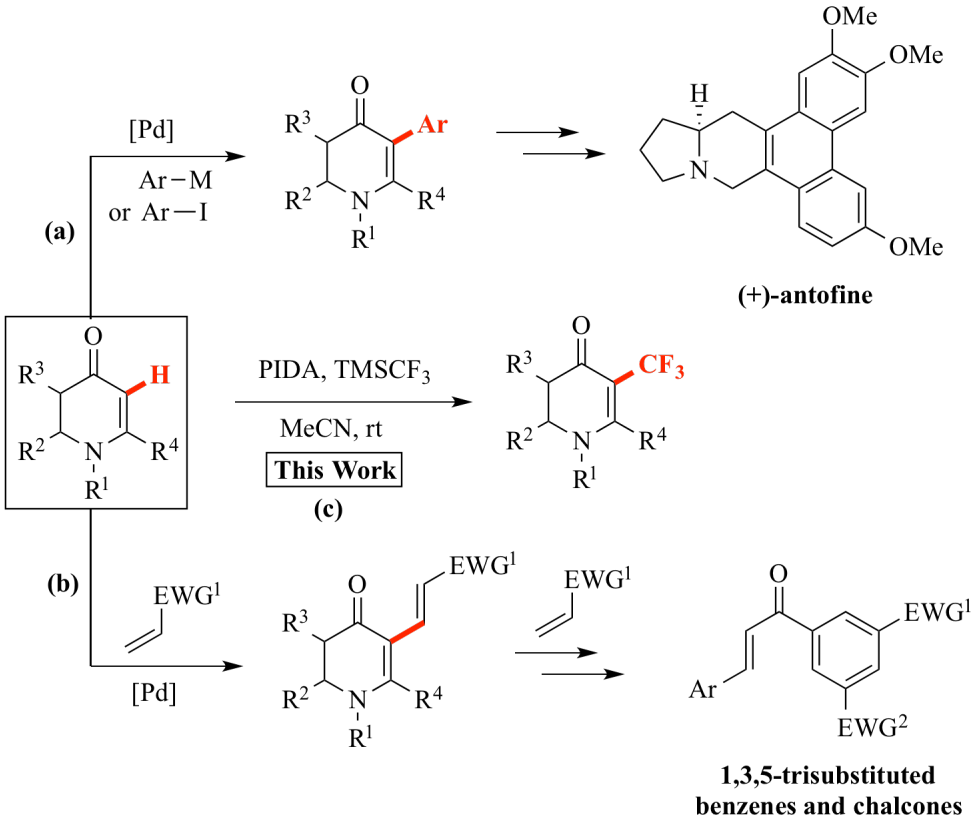

Cyclic enaminones, namely 2,3-dihydropyrid-4(1*H*)-ones, are regarded as excellent

piperidine surrogates (Scheme 2.11). These non-aromatic substrates have been extensively employed as synthetic intermediates in a plethora of alkaloid syntheses,[187-189] including recent reports from the Georg group of (+)-antofine and (*R*)-tylocrebrine and related analogues with potent antiproliferative properties.[190] Key to the versatile application is the distinctive reactivity profile of cyclic enaminones.[191] In order to further increase their synthetic utility, the Georg group has developed a number of efficient, regioselective C–H functionalization reactions based on enaminone olefin moiety.[6-10,192,193] These atom-economical transformations have already improved the syntheses of phenanthropiperidine alkaloids[194,195] (Scheme 2.11a) and 1,3,5-trisubstituted chalcones[193] (Scheme 2.11b). Inspired by this earlier success, we proposed that combining C–H trifluoromethylation with the divergent enaminone chemistry could be more advantageous (Scheme 2.11c).

With the above mentioned intrinsic reactivities and inherent nucleophilicity at the α-position, *non-aromatic* cyclic enaminones offer a promising platform to assess the feasibility of innate trifluoromethylation of alkenyl C–H bonds, which would potentially furnish a direct route to access 3-trifluoromethylpiperidine derivatives. Not only do cyclic enaminones offer an excellent platform as *cyclic alkenes* for C–H trifluoromethylation, but achieving this transformation would in addition furnish a straightforward pathway to synthesize 3-trifluoromethylpiperidine derivatives, which are important structural motifs in structure-activity relationship (SAR) studies.[179,180] Despite the rapid advance in the field of C–H trifluoromethylation,[141,142,186] direct construction of the intended olefinic C–CF_3 bond from an olefinic C–H bond is surprisingly sparse compared to numerous (hetero)arene counterparts.[148,153,154,157,159,161,162,164,166] The lack of methods is partly

because the migration of the double bond could form an allylic substrate when α-hydrogens are present,[171-174] or the high reactivity of olefins could easily lead to difunctionalizations.[158,196,197] To date, the reported examples of C–H trifluoromethylation of olefins have largely relied on terminal olefins and required transition-metal catalysis.[198-200] On the other hand, C–H trifluoromethylation of less reactive internal/cyclic olefins remains less accessible.[201-203] Hence, more olefin substrates and green, mild methods are still needed. Cyclic enaminones offer an excellent platform as internal/cyclic olefins with well-tuned reactivities.

2.4 Reaction Optimization

2.4.1 Screening of Existing Protocols

We first subjected cyclic enaminone **2.1** to the existing methods in order to determine the most effective protocol. Dr. Yiyun Yu from our lab carried out the initial screening of existing trifluoromethylation methods (Scheme 2.12) and observed that electrophilic trifluoromethylation using Umemoto's reagent with and without the use of transition metals failed to give any desired product **2.2**.

Scheme 2.12. Screening of Various Conditions

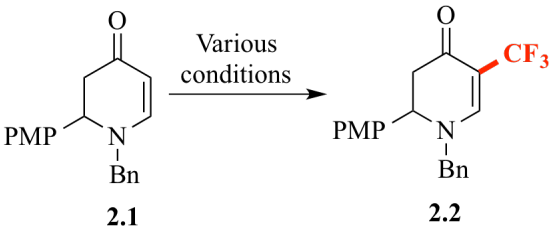

2.1 **2.2**

Using Togni's reagent with and without transition metals only gave yields from 11–25%.

Dr. Yiyun Yu also screened for radical-based protocols. MacMillan's photoredox chemistry showed discrete results. Electron-rich enaminones only produced 12% of the desired product, whereas in sharp contrast electron-deficient enaminone afforded a much better 62% yield. Baran's radical protocol also gave varied results. The reported solvent mixture (DCM/H_2O) only generated a trace amount of product **2.2** over an extended period of time (48 h). Replacing DCM with a more polar solvent DMSO increased the yield to 40%. A few $TMSCF_3$-based protocols were also tested. Unfortunately, Cu-catalyzed trifluoromethylation failed to furnish any desired product. Attempts to adopt Sanford's protocol involving stoichiometric amounts of AgOTf also did not yield any desired product. Lastly, a Pd-catalyzed, PIDA-mediated protocol developed by Liu and coworkers was tried. This protocol gave 32% of the product **2.2**. Adding TEMPO (0.5 equiv) to the reaction increased the yield to 41%. In all, two existing protocols afforded satisfactory yields after the preliminary investigation: 1) Baran's *t*BuOOH-mediated radical trifluoromethylation and 2) Liu's PIDA-mediated nucleophilic trifluoromethylation. Although both methods use operationally easy procedures and readily available reagents, Liu's protocol offers more variables for optimization. Therefore, he proceeded with Liu's conditions[157] for subsequent optimization. Compound **2.1** was used as the starting material with $TMSCF_3$, $PhI(OAc)_2$, CsF, and $Pd(OAc)_2$ as the catalyst in EtOAc at room temperature. It became evident that only PIDA was effective as the oxidant and the desired C–H trifluoromethylation proceeded almost as well in the absence of a Pd(II) catalyst. It is worth noting that metal-free $PhI(OAc)_2$-mediated C–H trifluoromethylation of arenes has been reported very recently by Qing and co-workers[204] and the effective trifluoromethylating agent was proposed to be an acyclic hypervalent

$[PhICF_3]^+$ species.[201] Its strong electrophilicity seemingly coincides with the C5-nucleophilicity of cyclic enaminones. This finding encouraged us to pursue a "greener" transition-metal-free protocol for C–H trifluoromethylation of cyclic enaminones.

2.4.2 Further Optimization

2.4.2.1 Solvent Screening

Using the modified conditions of Liu *et al.*[157] as a starting point, we optimized various parameters of the reaction. Table 2.1 shows the survey results with nine solvents. More polar solvents, such as DMSO, NMP, DMF, dioxane (entries 3–6) only furnished a trace amount of **2.2**. THF and acetone were detrimental to the reaction (entries 7, 9). Less-polar solvents such DCM failed to deliver a better yield (entry 8). MeCN (entry 2) turned out to be more effective than EtOAc (entry 1) making it the best solvent.

Table 2.1. Screening of Solvents[a]

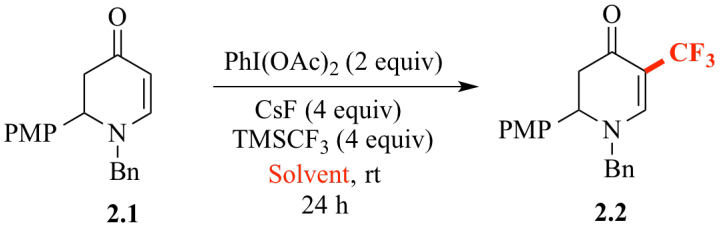

Entry	Solvent	% Yield[b]
1	EtOAc	46
2	**MeCN**	**50**
3	DMSO	trace
4	NMP	trace
5	DMF	trace
6	Dioxane	trace
7	THF	1
8	DCM	41
9	Acetone	13

[a] Conditions: enaminone **2.1** (0.1 mmol), $TMSCF_3$ (4.0 equiv), $PhI(OAc)_2$ (2.0 equiv), CsF (4.0 equiv), in solvent (1 mL) at rt for 24 h. [b] ^1H NMR yields with Ph_3SiMe (1.0 equiv) as the internal standard.

2.4.2.2 Base Screening

After optimizing the solvent, we next focused on the efficacy of F^- sources (bases) in generating the CF_3^- species. Table 2.2 shows the survey results of seven bases. When CsF (entry 1) was replaced with KF or AgF, the reaction afforded nearly the same yield (entries 3, 4). NaF and ZnF_2 gave lower yields (entries 2, 5). NiF_2 and CuF_2 failed to provide any desired product (entries 6, 7). Ultimately, KF was chosen over AgF because of its lower cost and because it does not generate heavy metal waste.

Table 2.2. Screening of Bases[a]

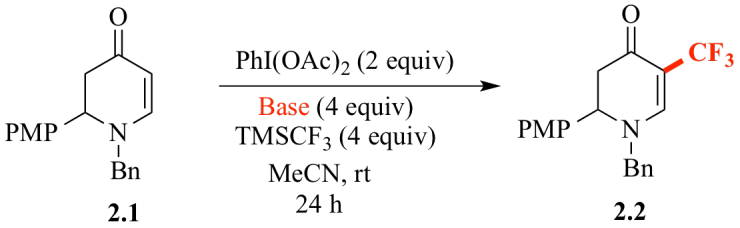

Entry	Base	% Yield[b]
1	CsF	50
2	NaF	29
3	**KF**	**59**
4	AgF	58
5	ZnF_2	23
6	NiF_2	0
7	CuF_2	0

[a] Conditions: enaminone **2.1** (0.1 mmol), $TMSCF_3$ (4.0 equiv), $PhI(OAc)_2$ (2.0 equiv), base (4.0 equiv), in MeCN (1 mL) at rt for 24 h. [b] ^1H NMR yields with Ph_3SiMe (1.0 equiv) as the internal standard.

2.4.2.3 Oxidant Screening

After optimizing the base, we next focused on the oxidants. Table 2.3 shows the survey results with three oxidants. We evaluated other hypervalent iodine reagents such as $PhI(TFA)_2$ (PIFA) and $PhI(OPiv)_2$ (entries 2, 3) along with PIDA (entry 1). Interestingly, the PIFA-mediated conditions could not install the CF_3 group possibly due to its strong oxidizing property, while $PhI(OPiv)_2$ furnished a modest yield (16%, entry 3), but was nearly four times less effective than PIDA (59%, entry 1). Therefore, PIDA was chosen as the best oxidant.

Table 2.3. Screening of Oxidants[a]

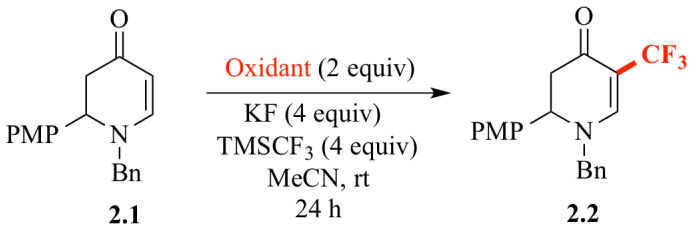

Entry	Oxidant	% Yield[b]
1	**$PhI(OAc)_2$**	**59**
2	$PhI(TFA)_2$	trace
3	$PhI(OPiv)_2$	16

[a] Conditions: enaminone **2.1** (0.1 mmol), $TMSCF_3$ (4.0 equiv), oxidant (2.0 equiv), KF (4.0 equiv), in MeCN (1 mL) at rt for 24 h. [b] ^1H NMR yields with Ph_3SiMe (1.0 equiv) as the internal standard.

2.4.2.4 Temperature Screening

In order to further improve the yield, we screened various reaction temperatures from 0 °C up to 80 ºC. Table 2.4 shows the survey results for five temperatures. Carrying out the reaction at 0 °C gave a good yield of 40% (entry 1). Temperatures higher than the ambient temperature only resulted in lower yields and more side reactions (entries 3–5). Based on the screening, room temperature was chosen as the optimum temperature for the course of the reaction.

Table 2.4. Screening of Temperatures[a]

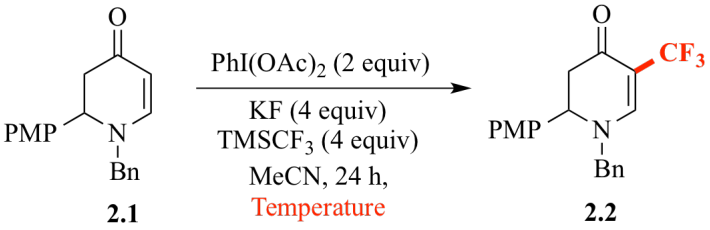

Entry	Temperature (°C)	% Yield[b]
1	0	40
2	**rt**	**59**
3	40	38
4	60	37
5	80	32

[a] Conditions: enaminone **2.1** (0.1 mmol), $TMSCF_3$ (4.0 equiv), $PhI(OAc)_2$ (2.0 equiv), KF (4.0 equiv), in MeCN (1 mL) for 24 h. [b] ^1H NMR yields with Ph_3SiMe (1.0 equiv) as the internal standard.

2.4.2.5 Stoichiometry Screening

We also screened the effects of stoichiometry on the outcome of the reaction. Table 2.5 shows the survey results of six stoichiometries. Using only 1 equivalent of PIDA while using 4 equivalents each of the KF and $TMSCF_3$ was unfavorable for the reaction

resulting in only 10% yield (entry 1). Increasing the PIDA equivalents to 3 gave a similar yield (entry 3, 58%) to that using 2 equivalents (entry 2, 59%). Using 4 equivalents of PIDA actually slightly decreased the yield to 52% (entry 4). Decreasing or increasing the equivalents of both KF and $TMSCF_3$ while simultaneously keeping the PIDA at 2 equivalents did not increase the yield (entries 5, 6). We concluded, thereby, that using 2 equivalents of PIDA and 4 equivalents of both KF and $TMSCF_3$ was the best stoichiometric combination for the reaction.

Table 2.5. Screening of Stoichiometry[a]

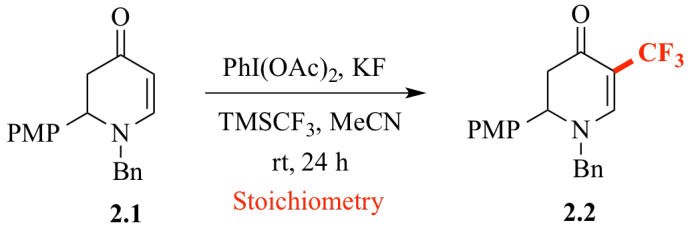

Entry	$PhI(OAc)_2$ (equiv)	$TMSCF_3$ (equiv)	KF (equiv)	% Yield[b]
1	1	4	4	10
2	**2**	**4**	**4**	**59**
3	3	4	4	58
4	4	4	4	52
5	2	2	2	46
6	2	6	6	51

[a] Conditions: enaminone **2.1** (0.1 mmol), $TMSCF_3$, $PhI(OAc)_2$, KF, in MeCN (1 mL) at rt for 24 h. [b] ^1H NMR yields with Ph_3SiMe (1.0 equiv) as the internal standard.

2.4.2.6 Concentration Screening

We screened various concentrations in efforts to further improve the yield of the reaction. Table 2.6 shows the survey results for five concentrations. Diluting the reaction concentration to 0.01 M had negative effects on the reaction (entry 1). Keeping the

concentration at 0.05 M increased the yield to 36% (entry 2), but was lower than the starting condition of 0.1 M (entry 3, 59%). Further concentrating the reaction mixture resulted in decreasing the product yield (entries 4, 5). Therefore, 0.1 M was chosen as an optimum concentration for the reaction.

Table 2.6. Screening of Concentrations[a]

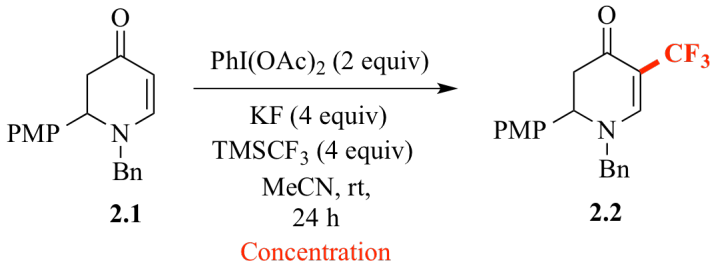

Entry	Concentration (M)	% Yield[b]
1	0.01	4
2	0.05	36
3	**0.1**	**59**
4	0.25	40
5	0.5	34

[a] Conditions: enaminone **2.1**, $TMSCF_3$ (4.0 equiv), $PhI(OAc)_2$ (2.0 equiv), KF (4.0 equiv), in MeCN at rt for 24 h. [b] ^1H NMR yields with Ph_3SiMe (1.0 equiv) as the internal standard.

2.4.2.7 Reaction Time Screening

Table 2.7 shows the survey results of various times that were screened. Stirring the reaction for 2 h resulted in a 38% yield (entry 1). Successively increasing the time to 4, 8, 12 and 48 h did not change the yields much (entries 2–4, 6). It was ultimately found that 24 h is the optimum time for the reaction.

Table 2.7. Screening of Reaction Time[a]

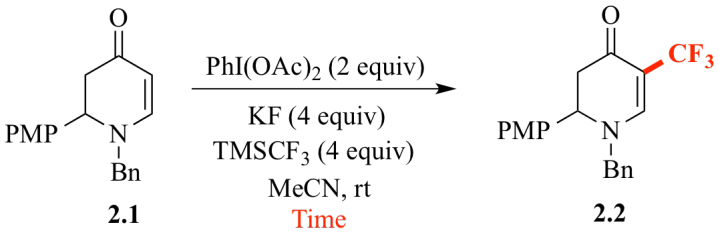

Entry	Time (h)	% Yield[b]
1	2	38
2	4	42
3	8	36
4	12	42
5	**24**	**59**
6	48	43

[a] Conditions: enaminone **2.1** (0.1 mmol), $TMSCF_3$ (4.0 equiv), $PhI(OAc)_2$ (2.0 equiv), KF (4.0 equiv), in MeCN at rt for 24 h. [b] ^1H NMR yields with Ph_3SiMe (1.0 equiv) as the internal standard.

2.4.2.8 Additives Screening

Next, a series of additives was introduced to the reaction conditions (Table 2.8). $Yb(OTf)_3$ completely inhibited the trifluoromethylation (entry 2). Weak carboxylic acids, like benzoic acid and pivalic acid, did not increase the yields (entries 3–4). We also tested a few radical scavengers, such as 2,6-di-*t*-butyl-4-methylphenol and TEMPO (entries 5–6), yet interestingly, both of them failed to improve the yield. Therefore, having no additive was found to be the best condition for the reaction (entry 1).

Table 2.8. Screening of Additives[a]

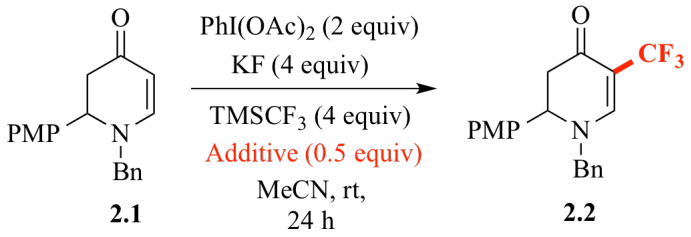

Entry	Additive (equiv)	% Yield[b]
1	**–**	**59**
2	$Yb(OTf)_3$ (0.5)	0
3	Benzoic Acid (0.5)	38
4	Pivalic Acid (0.5)	37
5	2,6-Di-*t*Bu-4-methylphenol (0.5)	7
6	TEMPO (0.5)	16

[a] Conditions: enaminone **2.1** (0.1 mmol), $TMSCF_3$ (4.0 equiv), $PhI(OAc)_2$ (2.0 equiv), additive (0.5 equiv), KF (4.0 equiv), in MeCN at rt for 24 h. [b] ^1H NMR yields with Ph_3SiMe (1.0 equiv) as the internal standard.

After optimizing 8 parameters, we confirmed that reacting enaminone **2.1** (0.1 M) with $TMSCF_3$ (4.0 equiv), $PhI(OAc)_2$ (2.0 equiv), and KF (4.0 equiv) in MeCN (1 mL) over 24 h at rt were the best reaction conditions to regiospecifically introduce the CF_3 group to the cyclic enaminone scaffold **2.2**.

2.5 Investigation of Scope of Cyclic Enaminones

With the optimized conditions determined, we next examined the reaction scope of cyclic enaminones (Table 2.9). In general, the reaction tolerated a number of diversified cyclic enaminones with moderate to excellent yields. It is noteworthy that in previous studies, the *N*- and C6-substituents were critical to the C5-nucleophilicity/reactivity, which could

only be preserved when *N*-electron-donating-groups (EDGs) and sterically less-demanding C6-substituents were present.[6-10] In the present case, substitution abiding by these rules was tolerated as anticipated.

Table 2.9. Scope of Cyclic Enaminones for Direct C-H Trifluoromethylation

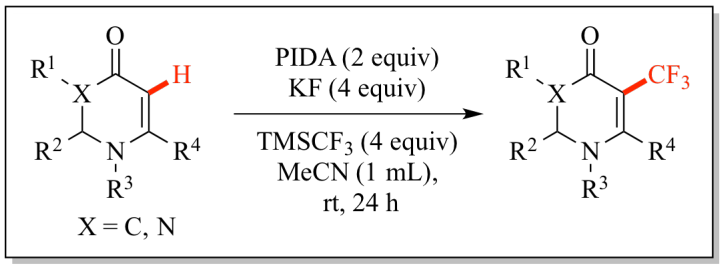

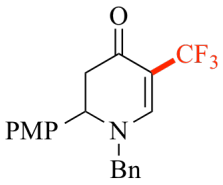

2.2, 59%[a]

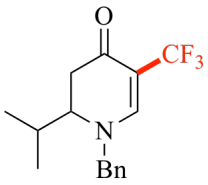

2.3, 78%

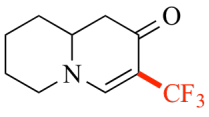

2.4, 66%

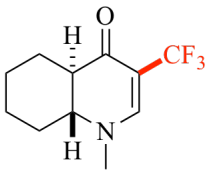

2.5, 61%

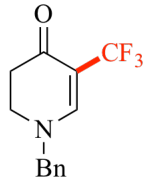

2.6, 67%

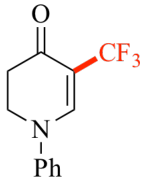

2.7, 81%

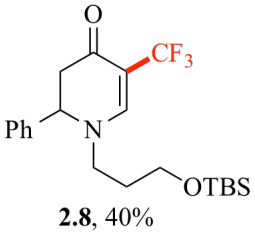

2.8, 40%

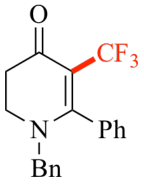

2.9, 75%

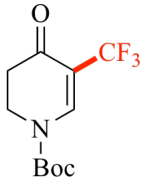

2.10, 66%

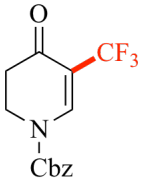

2.11, 61%

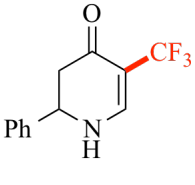

2.12, 23%

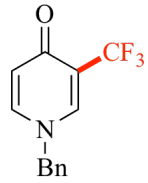

2.13, 45%

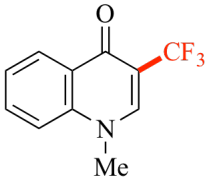

2.14, 44%

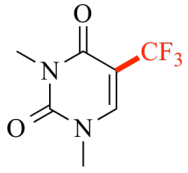

2.15, 46% (61%[b])

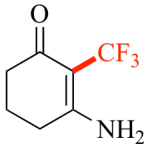

2.16, 26%

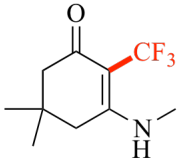

2.17, 26%

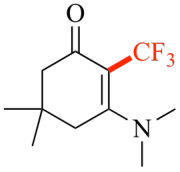

2.18, 36%

[a] Isolated yield, [b] Yield based on recovered starting material.

For instance, cyclic enaminones with an aryl (*e.g.* PMP) or alkyl (*e.g. i*-Pr) group on the C2-position afforded the desired products in good yields (**2.2**, **2.3**). Bicyclic enaminones also furnished good yields (**2.4**, **2.5**). Those with *N*-EDGs offered yields up to 81% (**2.6**–**2.8**). On the other hand, we were surprised to observe an increased yield when employing an enaminone bearing a bulky C6-phenyl group (75%, **2.9** *vs.* 67%, **2.6**), which had completely inhibited C–H arylation in the past.[8] In addition, previously nonreactive[6-10] enaminones due to *N*-electron-withdrawing-groups (EWGs, *e.g.* Boc and Cbz) were also enabled toward C–H functionalization *for the first time*. The corresponding products **2.10** and **2.11** were generated in similar yields as those carrying *N*-EDGs. The unsubstituted *N*-H enaminone provided only a low yield of **2.12** (23%), indicating that *N*-substituents play a key role in the reaction. We also tested a few structurally analogous scaffolds. *N*-Benzyl-4-pyridone, a synthetic precursor for cyclic enaminones,[10] notably only furnished the mono-trifluoromethylated product **2.13**. Similarly, *N*-methyl-4-quinolone, an important substrate for antimicrobial and anticancer agents,[205-207] was converted smoothly to **2.14** in moderate yield. Moreover, because uracil's C5-position is of interest for the labeling and the preparation of bioactive uracil derivatives,[208-210] we were pleased to see the amenability of 1,3-dimethyluracil (**2.15**) to our protocol. Lastly, *E*-enaminones were considered. The yields of the corresponding products **2.16**–**2.18**, albeit low, demonstrate the potential of these substrates to be utilized for direct C–H functionalization.

2.6 Investigation of Reaction Mechanism

In light of the unexpected compatibility for both electron-rich and electron-deficient enaminones in this reaction, it is likely that the trifluoromethylation takes place *via* a

mechanism that is different from previously observed electrophilic substitution.[6-10] We reasoned that if the electrophilic trifluoromethylation were in play, electron-deficient cyclic enaminones would suffer from reduced nucleophilicity and afford lower yields than their electron-rich counterparts. However, in fact, an opposite relationship was observed. For example, less nucleophilic *N*-phenylenaminone delivered a higher yield (**2.7**, 81%) than *N*-benzylenaminone (**2.6**, 67%).

Scheme 2.13. Radical Trapping Experiments

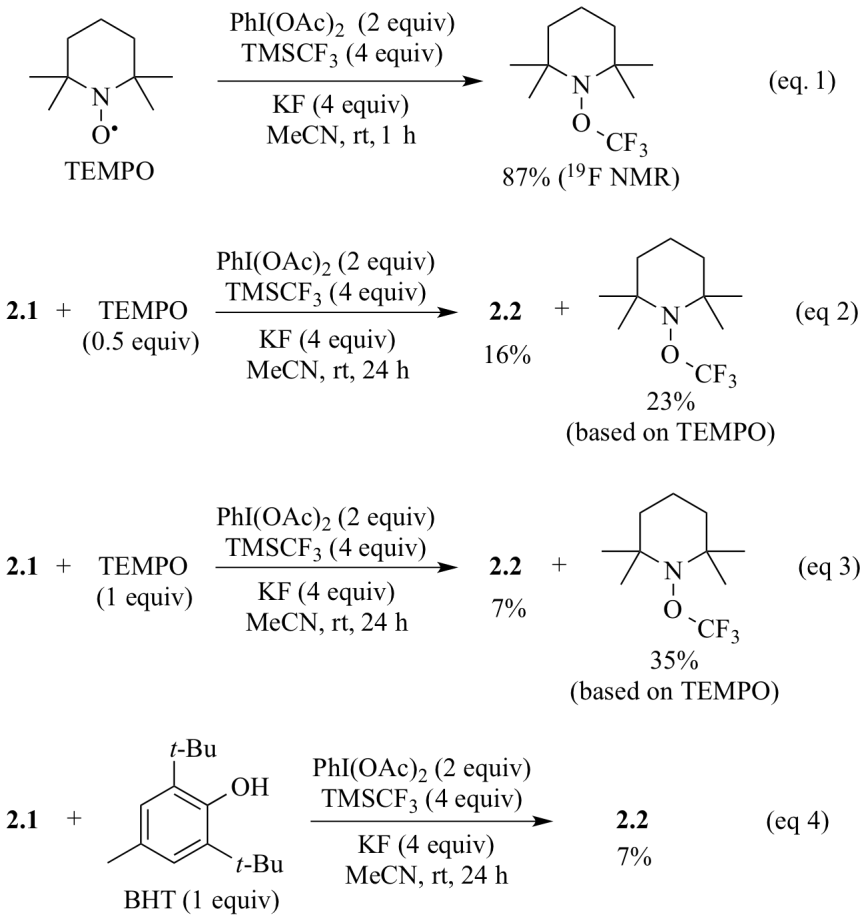

Under acidic conditions, TEMPO will undergo disproportionation to form an oxoammonium ion, which then can react with $TMSCF_3$ to generate TEMPO–CF_3 via an

ionic pathway.[211] Indeed, AcOH is formed as a by-product of the trifluoromethylation reaction. Therefore, in order to test this possibility, we subjected TEMPO to the reaction conditions without the presence of cyclic enaminones (Scheme 2.13, eq 1). TEMPO (15.6 mg, 0.1 mmol), $PhI(OAc)_2$ (64.4 mg, 0.2 mmol) and KF (23.5 mg, 0.4 mmol) were added into a 2-dram PTFE sealed glass vial, followed by $TMSCF_3$ (59.7 μL, 0.4 mmol) and anhydrous MeCN (1.0 mL) through syringes. The reaction mixture was stirred at room temperature for 1 hour. An internal standard α,α,α-trifluorotoluene (0.1 mmol) was then added. If the ionic pathway was indeed in action, there shouldn't be any formation of TEMPO–CF_3. However, we still detected the formation of the byproduct TEMPO–CF_3. This clearly implies the intermediacy of the CF_3 radical (Scheme 2.13, eq 1).

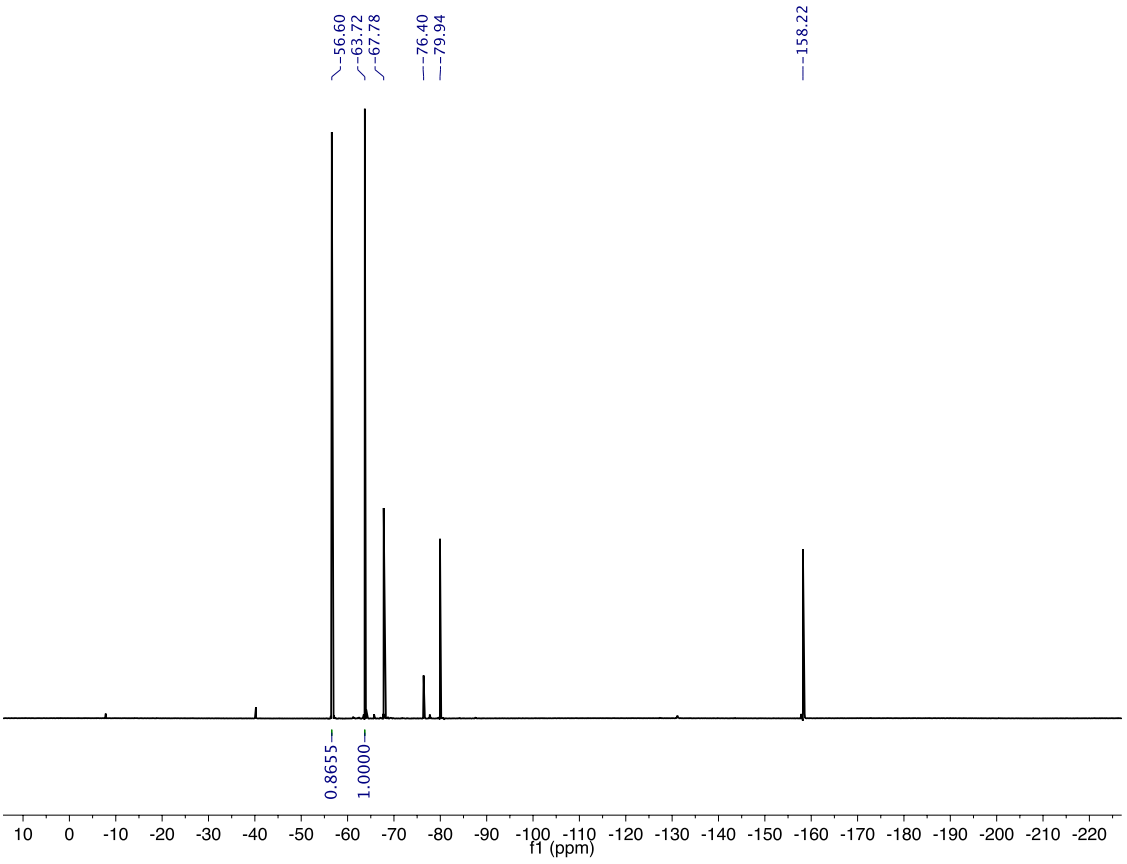

Figure 2.2. ^{19}F NMR of the Crude Mixture. (Scheme 2.13, eq 1).

^{19}F NMR of the crude product (Figure 2.2) showed that TEMPO–CF_3 was formed (peak at –56.6 ppm) in 87% yield (based on α,α,α-trifluorotoluene as an internal standard, peak at –63.72 ppm). It is worth noting that $PhI(OAc)_2$ does not oxidize TEMPO to form an oxoammonium cation, nor does TEMPO undergo disproportionation under non-acidic conditions as in Scheme 2.13, eq 1.[211] Hence, the formation of TEMPO–CF_3 by the reaction of the oxoammonium cation with $TMSCF_3$ via an ionic pathway might be excluded. In order to gain more insight into the mechanism, we introduced radical scavengers (*i.e.* TEMPO and BHT) into the reaction (Scheme 2.13) and found that the yields decreased to 7% in the presence of these additives (Scheme 2.13, eq 2–4). This inhibition effect suggests that the reaction involved radical species. In order to further corroborate the involvement of the trifluoromethyl radical under our reaction conditions, we tested diethyl diallylmalonate as a radical clock (Scheme 2.14). Two cyclopentane derivatives **2.19**[212] and **2.20** were isolated as the major products. They should stem from a radical 5-*exo*-trig cyclization after addition of a CF_3 radical to the double bond. These observations are consistent with a mechanism involving a CF_3 radical.

Scheme 2.14. Radical Clock Experiment

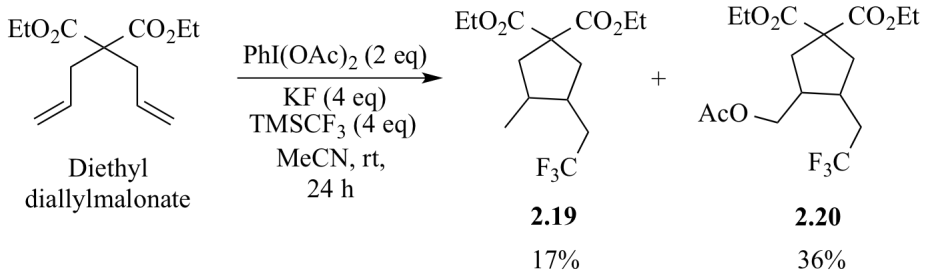

Given the experimental facts and recent reports on PIDA-mediated trifluoromethylations,[204,213,214] a radical mechanism is postulated (Scheme 2.15). First, a

ligand exchange between PIDA and $TMSCF_3$ in the presence of KF forms hypervalent iodine(III) **2.21**,[201,213] which was detected by mass spectrometry. For the mass detection of the intermediate $PhI(OAc)CF_3$.(**2.21**) we carried out an experiment in which, $PhI(OAc)_2$ (64.4 mg, 0.2 mmol) and KF (23.5 mg, 0.4 mmol) were added into a 2-dram TFE sealed glass vial, followed by $TMSCF_3$ (59.7 μL, 0.4 mmol) and anhydrous MeCN (1.0 mL) through syringes. The reaction mixture was then stirred at room temperature. Samples were taken after 15 minutes of stirring and diluted with MeCN prior to injection into the mass spectrometer. The results are shown in Figure 2.3. We found that the majority of $PhI(OAc)_2$ (at m/z = 361.0) had been consumed. The proposed intermediate $PhI(OAc)CF_3$ (**2.21**) (at m/z = 333.0) was also detected, but quickly underwent dissociation to form $[PhICF_3]^+$ (at m/z = 273.0). This finding is consistent with previous MS studies by other groups.[201,213] Therefore, the possibility of the formation of the $PhI(OAc)CF_3$ (**2.21**) was confirmed experimentally.

Scheme 2.15. Proposed Radical Mechanism for C–H Trifluoromethylation of Cyclic Enaminones

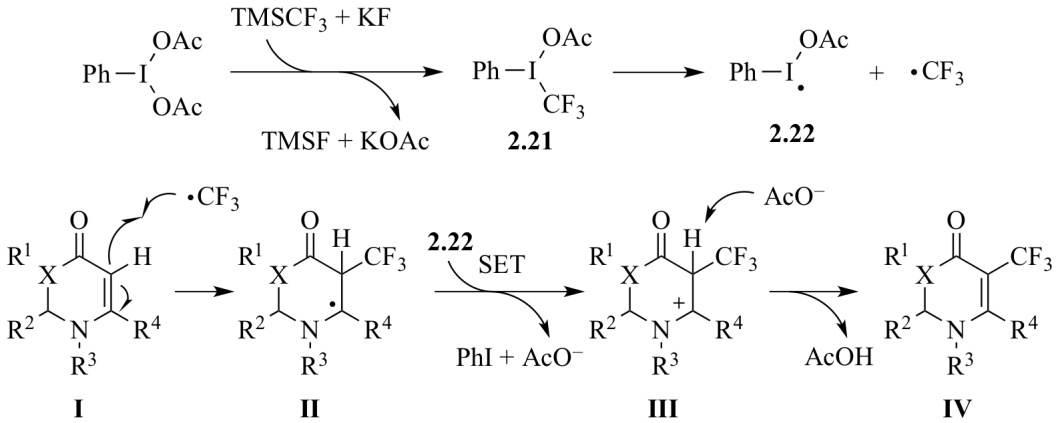

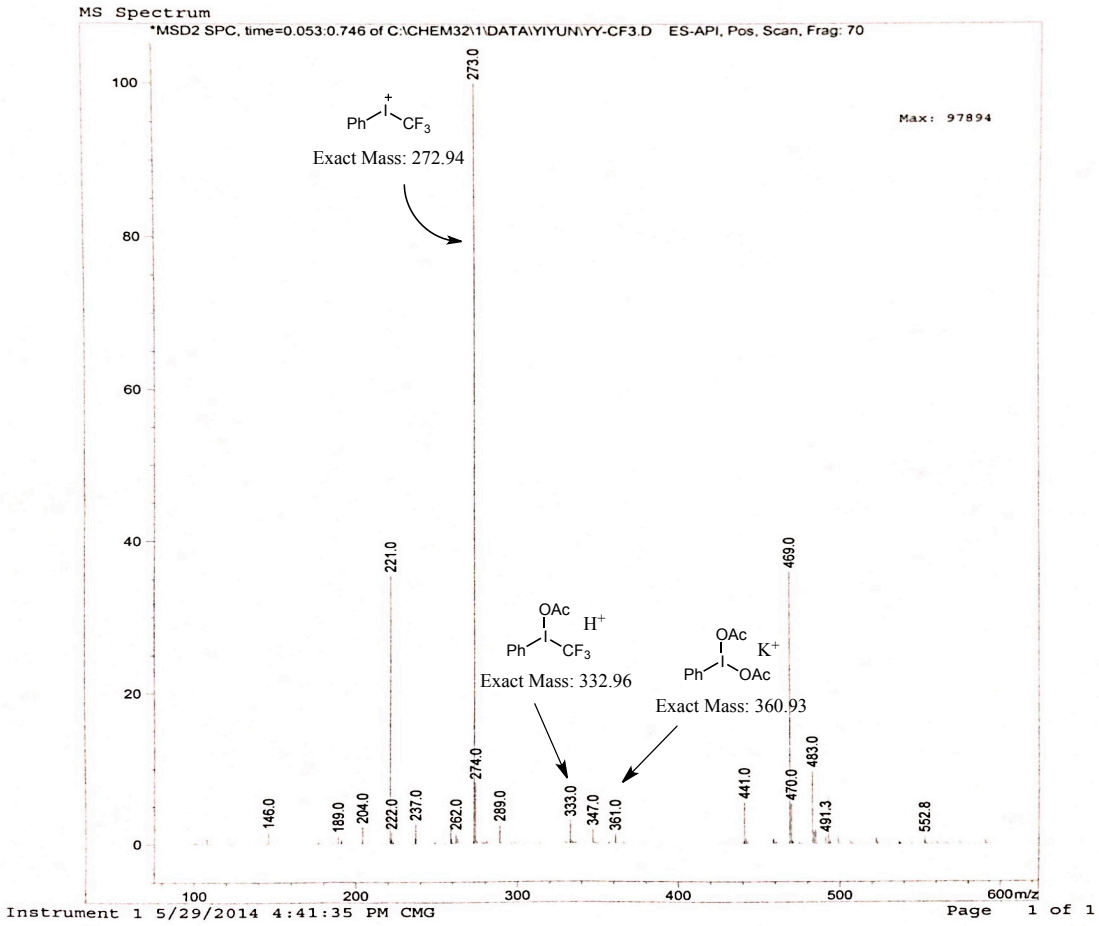

Figure 2.3. Mass Spectrum for the Detection of the Intermediate **2.21**.

The second step of the postulated mechanism involves homolysis of the $PhI(OAc)CF_3$ (**2.21**) generating two radicals (**2.22** and $\bullet CF_3$).[213,214] The CF_3 radical attacks enaminone **I** to afford the intermediate **II**, which is subsequently converted to a cationic species **III** through a single electron transfer (SET) oxidation by the iodine radical **2.22**.[213,215] Lastly, deprotonation by the acetate anion furnishes the final product **IV**. Although other mechanisms including the above mentioned electrophilic trifluoromethylation cannot be completely ruled out, the proposed mechanism is more likely, because it could account for the tolerance of previously unreactive enaminones. For example, we presume that *N*-

substituents (as R^3 in Scheme 2.15) that are capable of stabilizing the intermediate **II** through conjugation should facilitate the CF_3 radical attack. Indeed, we observed good yields for the formation of C5–trifluoromethyl enaminones **2.7**, **2.10**, and **2.11** with EWGs such as *N*-Boc and *N*-Cbz, which had been detrimental to C–H functionalizations before. In a similar vein, adding a C6-phenyl group (Scheme 2.15, R^4 = Ph) would also stabilize intermediates **II** and **III**. Despite its steric bulk, we speculate that the stabilizing effect of the phenyl group overcomes its steric repulsion against the relatively small CF_3 radical, generating a high yield in the reaction (75%, **2.9**).

2.7 Utility of the Newly Synthesized Trifluoromethyl Cyclic Enaminones

After synthesizing the trifluoromethylated cyclic enaminones, their elaboration was also briefly explored (Scheme 2.16). The unique structural core of cyclic enaminones offers four nucleophilic sites and two electrophilic sites for modification from which a plethora of chemoselective transformations have already been well established,[191] such as the enolate chemistry,[216] 1,2-addition,[217] and [2+2] cycloaddition.[218] In addition, we chose to chemoselectively deconjugate the cyclic enaminones (such as **2.6)** with L-Selectride (Eq. 1). The resultant isolation of the carbonyl and amine moieties leads to a γ-piperidone core (as in **2.21**), which is both synthetically versatile and pharmaceutically important.[75,219] Meanwhile, we also considered the preparation of "ready-to-install" trifluoromethylated enaminone precursors. Since the yield of enaminone **2.12** was less satisfactory, *N*-deprotection of enaminone **2.11** was achieved smoothly under H_2 with good functional group tolerance (Eq. 2). Product **2.22** should be easily engrafted onto desired lead molecules.[220,221]

Scheme 2.16. Partial reduction and *N*–Deprotection of Selected 5-Trifluoromethylated Cyclic Enaminones

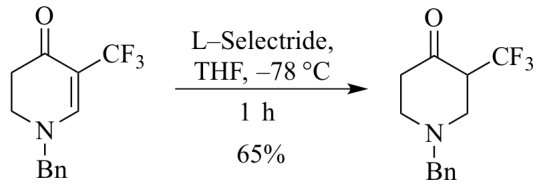

2.6 **2.23** (eq. 1)

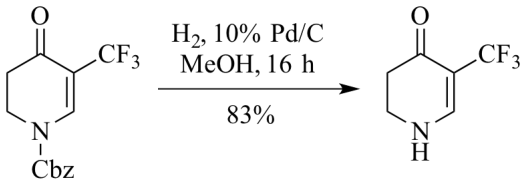

2.11 **2.24** (eq 2)

2.8 Summary

In summary, we have developed a transition-metal-free C–H trifluoromethylation protocol for a variety of cyclic enaminones. This method proceeds smoothly at room temperature and it tolerates a broad scope of functionalities including both electron-rich and electron-deficient cyclic enaminones. A radical mechanism is proposed for this transformation. While this method is not specific for piperidine synthesis, the combination of the efficient C–H trifluoromethylation and the broad synthetic utilities of cyclic enaminones provide an unprecedented and easy route to access a multitude of 3-trifluoromethylpiperidine derivatives, and therefore should serve as an additional method to benefit medicinal chemistry SAR studies.

Chapter 3

Elucidating the Binding Site of Epothilones on Beta-Tubulin with Epothilone Photoaffinity Probes

3.1 Introduction

The epothilones are a family of potent cytotoxic polyketide macrolide natural products.[222] They are metabolites that are produced by the soil-dwelling myxobacterium *Sorangium cellulosum* and were first isolated in 1992 by Höfle and collaborators.[222,223] Six major epothilones (epothilone A to F) from 37 variants have been identified and characterized. As shown in Figure 3.1, the epothilones have a characteristic lactone functional group in their structures. They carry hydroxyl groups at C3 and C7 and a ketone functional group at C5.

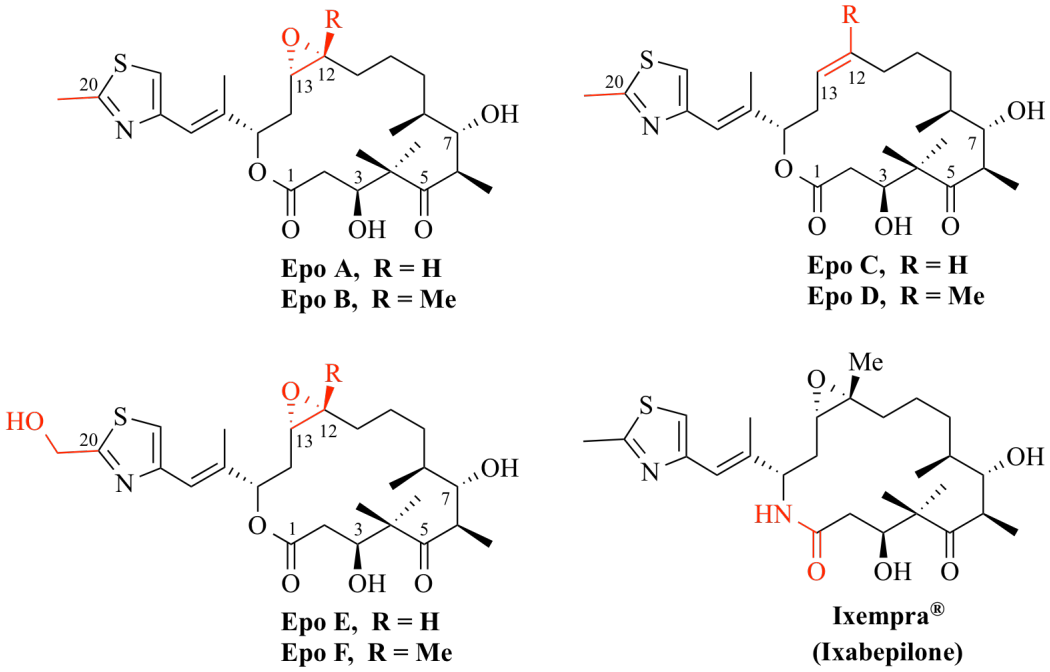

Figure 3.1. Structures of Epothilones A to F and Ixabepilone.

Epothilones A and B possess a C12–C13 epoxide moiety, a C20 methyl group on the thiazole ring and either a proton (epothilone A) or a methyl group on C12 (epothilone B). Epothilones C and D lack the C12-C13 epoxide moiety and instead have an olefinic bond

at C12–C13. Epothilones E and F are metabolized forms of epothilones A and B with a hydroxymethyl substituent at the C20 position on the thiazole ring. The FDA approved epothilone B analogue Ixempra® (Figure 3.1) in 2007 for the treatment of metastatic or locally advanced breast cancer. In addition, epothilone D is currently in clinical trials for the treatment of Alzheimer's disease.[224] This treatment is based on Trojanowski and Lee's theory, which surmised that tubulin-stabilizing agents could be used for the treatment of Alzheimer's disease.[225] The pathological characteristics of Alzheimer's disease are the deposition of β-amyloid proteins and neurofibrillary tangles (primarily tau proteins) in the brain. Tau, a microtubule-associated protein, stabilizes the intraneuronal microtubular structure that is necessary for the transport of neurotransmitters and essential nutrients. In Alzheimer's disease, tau proteins are abnormally hyperphosphorylated and can no longer stabilize the microtubular structure inside nerve cells resulting in death of neurons. Since taxol and the epothilones induce tubulin polymerization and stabilize microtubules, they were proposed as possible Alzheimer's disease therapeutics assuming they could preserve the integrity of the microtubular structure.[225,226] The epothilones were shown to have a neuroprotective effect on nerve cells, which are non-dividing and post-mitotic. Unlike taxol, the epothilones cross the blood-brain barrier and thus, epothilone D (Figure 3.1) eventually entered clinical trials.[224]

3.2 Biological Activity and Mechanism of Action of Epothilones

Epothilones were originally identified as natural product fungicidal and cytotoxic macrolides.[222] After noticing the taxol-like activity of the epothilones in 1995,[227] they

became the subject of thorough investigations, including semisyntheses, total syntheses, SAR studies, pharmacological, and clinical studies.[228] Studies point out that the principle mechanism of action of epothilones is similar to taxanes. Epothilones trigger microtubule bundling, formation of multipolar spindles and mitotic arrest.[227,229] The mechanism by which epothilones induce the microtubule polymerization seems to be similar to that of paclitaxel, in that epothilones compete with paclitaxel for binding to microtubules and repress microtubule dynamics in a manner similar to that of paclitaxel.[227,230,231] The epothilones have a number of advantages compared to taxol. They can be produced in large quantities by fermentation, are highly active against taxol-resistant and multi-drug resistant cancers, they cross the blood-brain barrier, and they are more water-soluble than taxol.[228] By 2010, five natural, synthetic, and semisynthetic epothilone derivatives had entered advanced cancer clinical trials.[228]

3.2.1 Microtubules

3.2.1.1 Structure

Tubulin is a member of a small family of globular proteins. The tubulin superfamily comprises five discrete families: α-, β-, γ-, δ-, and ε-tubulins. Out of these, the α- and β-tubulin family of proteins weighing approximately 55 KDa each, are the most common and make up the microtubules.[232] Microtubules are a component of the cytoskeleton and are found throughout the cytoplasm. They are important in a number of cellular processes such as the maintenance of cell structure, protein trafficking, providing a platform for intracellular transport, chromosomal segregation, and cell division (mitosis and meosis) including mitotic spindle formation.[233] Although they serve as the robust cytoskeleton of

the cell, the microtubules are not static, but very dynamic polymers. The α- and β-tubulin dimers polymerize end-to-end in protofilaments forming long, hollow cylindrical microtubules.[234] Microtubules display polarity that is critical for their biological function. For the end-to-end tubulin polymerization, the α-subunits of one tubulin dimer contacts the β-subunits of the next. Therefore, in a protofilament, one end will have the α-subunits exposed while the other end will have the β-subunits exposed. These ends are designated as the (−) and (+) ends, respectively. The protofilaments bundle parallel to one another. Thus, in a microtubule in one end, the (+) end, only the β-subunits are exposed, while the other end, the (−) end, only α-subunits are exposed. Elongation of microtubules typically only occurs from the (+) end.[235]

3.2.1.2 Dynamic Instability of Microtubules

The coexistence of assembly and disassembly at the (+) end of a microtubule is referred to as the dynamic instability (Figure 3.2). The microtubule can dynamically change between growing and shrinking stages in this region.[236] During polymerization, both the α- and β-subunits of the tubulin dimer are bound to a GTP molecule.[234] The GTP bound to the α-tubulin is stable and has a structural function. The GTP bound to the β-tubulin may be hydrolyzed to GDP shortly after assembly, which results in the addition of new dimers. The kinetics of the GDP-bound tubulin is different from that of the GTP-bound tubulin in that the GDP-bound tubulin is prone to depolymerization.[237] The GDP-bound tubulin subunit at the tip of a microtubule can fall off. However, the GDP-bound tubulin in the middle of a microtubule cannot spontaneously leave. Since tubulin appends onto the end of the microtubule only in the GTP-bound state, there is a cap of GTP-bound

tubulin at the tip of the microtubule, protecting it from disassembly. When hydrolysis reaches up to the tip of the microtubule, it begins a rapid depolymerization and shrinkage. This switch from growth to shrinking is defined as a "catastrophe". The GTP-bound tubulin can begin adding to the tip of the microtubule again, affording a new cap and protecting the microtubule from shrinking. This is termed as "rescue".[238]

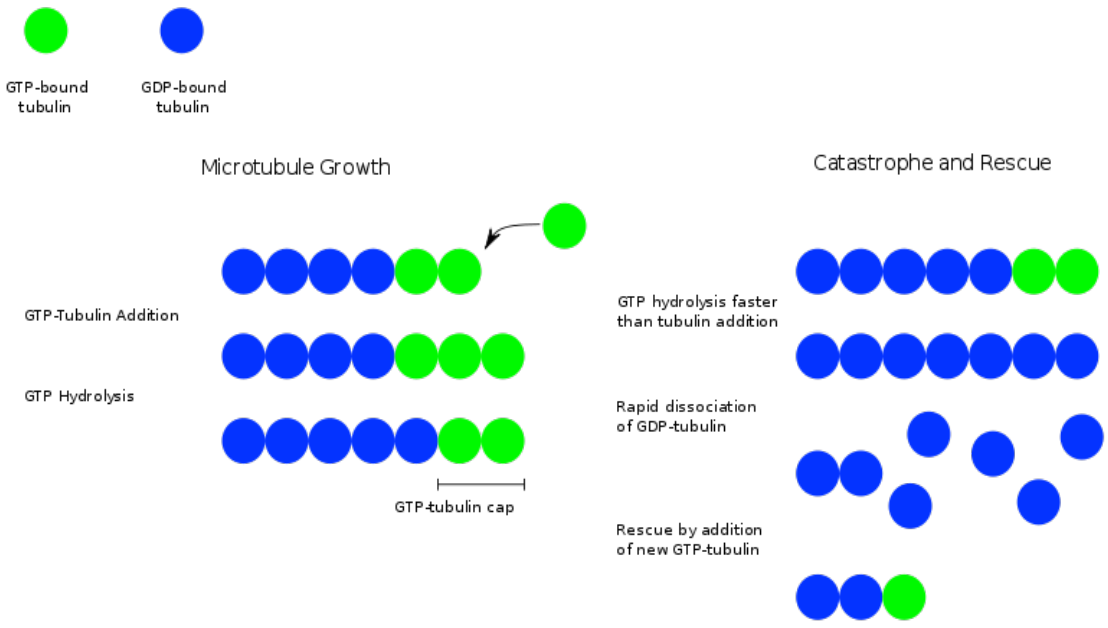

Figure 3.2. Dynamic Instability of Microtubules.

A large number of drug molecules can bind to tubulin and modify its activation state. This results in disturbing the microtubule dynamics. This interference with microtubule dynamics can in turn arrest the cell cycle and ultimately lead to apoptosis. The epothilones and the taxanes block the dynamic instability by stabilizing GDP-bound tubulin in the microtubule. When the hydrolysis of GTP reaches the tip of the microtubule, depolymerization stops and the microtubule is prevented from shrinking back. In contrast, the Vinca alkaloids (*e.g.* vincristine) block the polymerization of

tubulin into microtubules.

3.2.2 Mechanism of Action

The principle mechanism of action of epothilones is similar to taxanes. It was experimentally found that the epothilones competitively bind at the taxol-binding site on β-tubulin, suggesting that the binding site for the epothilones and the taxanes must be overlapping.[227,230,231] Two groups suggested that the epothilones and the taxanes possess a common pharmacophore for microtubule binding.[239,240] However, epothilones have shown impressive efficacy against paclitaxel-resistant cancer cell lines, suggesting a significantly different mode of binding.[241] There are three reasons for resistance to paclitaxel: Overexpression of P-glycoprotein (Pgp) (thus lowering the intracellular concentration of drug), overexpression β-tubulin isotype β-III, and tubulin point mutations in key amino acid residues essential for taxane binding.[241] Epothilones evade Pgp efflux, and are active against the paclitaxel-resistant cancer cell lines due to the tubulin point mutations of key amino acid residues. The Himes group identified differences in the interaction between these drugs and yeast microtubules.[242] Epothilones were found to promote the assembly of yeast tubulin while paclitaxel was not. The difference in the behavior of these drugs was rationalized based on the models of paclitaxel and epothilone binding to mammalian microtubules[239,240,243] available at that time. Data from several different experimental approaches[244-246] denoted that the 1–31, 217–231, 270–289, 358–372 amino acid regions of β-tubulin interact or form hydrophobic sites for paclitaxel; whereas a model for epothilone binding[240] suggested that epothilones make contacts with the residues in the 217–231 and 270–282 regions.

With the exception of a few crucial differences, most of the residues in the four regions that have been proposed to be involved in paclitaxel binding are the same in brain and yeast β-tubulin. These differences are at positions 19, 23, 26, 227, 231, and 270.

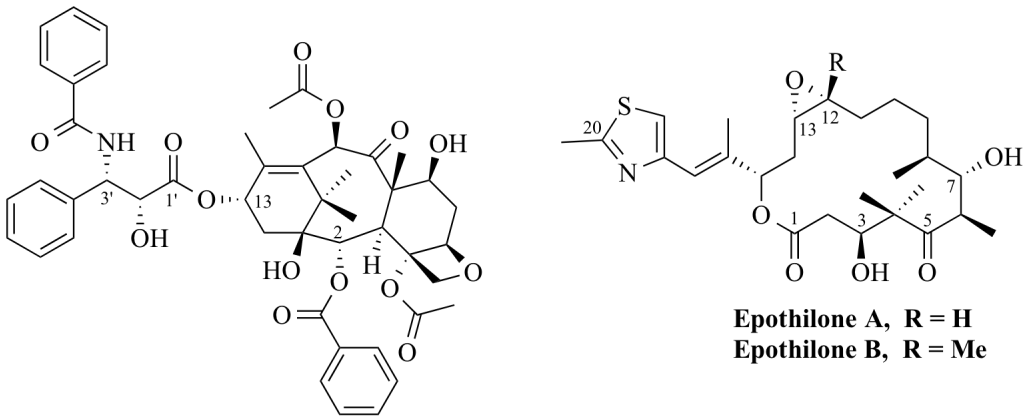

Figure 3.3. Structures of Paclitaxel and Epothilones.

Based on one of the models illustrating paclitaxel binding to brain tubulin,[243] the isopropyl group of Val23 is adjacent to the C3'-benzamidophenyl ring (Figure 3.3). A threonine residue is present at this position in yeast tubulin, increasing the polarity and thus possibly affecting paclitaxel binding. The same model predicts that the methylene groups of Lys19, Glu22, Asp26 will make short contacts with the C3'-benzamidophenyl ring.[243] Yeast tubulin contains alanine at the 19 position instead of lysine and glycine at the 26 position instead of aspartate, thus causing substantial reduction in the number of methylene groups. The residues Lys19, Val23, and Asp26 were identified in a peptide that was found to cross-link to a photoaffinity analog of paclitaxel.[245] The epothilone binding model,[240] did not associate these residues with epothilone binding, and thus the changes in these residues do not disrupt epothilone binding to yeast tubulin. Another

important site for paclitaxel binding is the position 227 in β-tubulin. In brain β-tubulin, this position is occupied by histidine. The paclitaxel binding model[240] predicts that His227 lies in between the C2 phenyl and the C13 side chain and forms π-stacking interactions with the C2 phenyl and C3' benzamidophenyl rings. Yeast tubulin has asparagine residue at the 227 position, which eliminates the possibility of π-stacking, thereby, weakening the binding of paclitaxel.

3.3 Structure–Activity Relationships and Binding on β-Tubulin of Epothilones

3.3.1 Structure–Activity Relationships

The structure-activity data currently available, presents some insight into the interaction between epothilones and microtubules. A variety of epothilone analogs have been synthesized and evaluated for their activity in microtubule assembly and cytotoxicity assays. Increasing microtubule-stabilizing activity does not always result in increased cytotoxicity, most likely because of the importance of other variables such as cellular accumulation and metabolic stability.[247] Naturally occurring epothilones have been isolated in two variants: those with a C12–hydrogen (epothilone A-like) or with a C12 methyl (epothilone B-like). Irrespective of the structure, epothilone B-like epothilones are five to 20 times more active in cytotoxicity and tubulin polymerization assays. Particularly, epothilone B is approximately twice as potent as epothilone A or paclitaxel in inducing tubulin polymerization *in vitro*.[230,248] Not surprisingly, therefore most *in vivo* studies and clinical trials have been performed with epothilone B-like epothilones. Various structural modifications that affect the activity of epothilones are shown in Figure 3.4a and 3.4b. For manifesting the required biological activity, a 16-membered

macrocycle and the configuration of all the seven stereocenters are absolutely needed.[249] Moderate activity was seen with a few 18-membered epothilones. However, 14-, 15- and 17-membered analogs were very weakly active or inactive.[249-251] Replacing the lactone moiety of epothilone B with a lactam (i.e., ixabepilone) reduces cytotoxicity and tubulin binding only slightly, but improves other properties such as resistance to esterase cleavage, protein binding, and therapeutic window.[229,252] No other bioisosteric replacement of the lactone group with a ketone or an ether has been reported yet. Removing the C3 OH and the presence of a C2–C3 (*E*)-olefinic bond yields epothilones that are moderately active. This observation indicates that the C3 OH does not act as a hydrogen bond donor or a hydrogen bond acceptor when the epothilones are bound to β-tubulin. However, the stereochemistry at the C3 position is crucial for maintaining the activity. 3β-Nitrile analogs with the natural configuration are highly active whereas the 3α-nitrile analogs are inactive.[253] This observation suggests that there are considerable steric restraints. For the same reason, most likely the ester and ether analogs of C3 and C7 hydroxyl groups are also inactive. Oxidizing the C3 and C7 alcohols to ketones or reducing the C5 ketone to epimeric alcohols results in a complete loss of activity. Both epimeric C4–monomethylepothilones are highly active,[254] but linking both C4 methyl groups and forming a cyclopropane results in an analog with significantly reduced activity.[255,256] Replacing the C8 methyl with hydrogen also reduces the activity.[255,256] The reason behind this could be a result of the absence of the C6 methyl/C8 methyl *syn* interaction and a change of C3–C4–C5 bond angles altering the conformation. Substituting the C6 methyl group with an ethyl group causes the activity to increase four times, but placing an allyl or propyl substituent on C6 results in slightly less active

compounds compared to the parent compounds.[257]

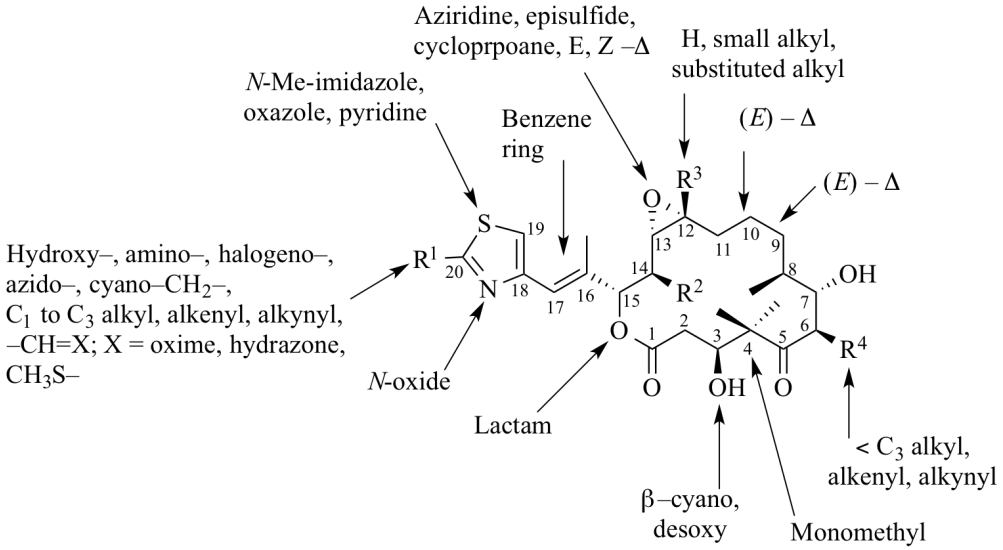

a) Modifications on epothilones rendering moderate to high activity

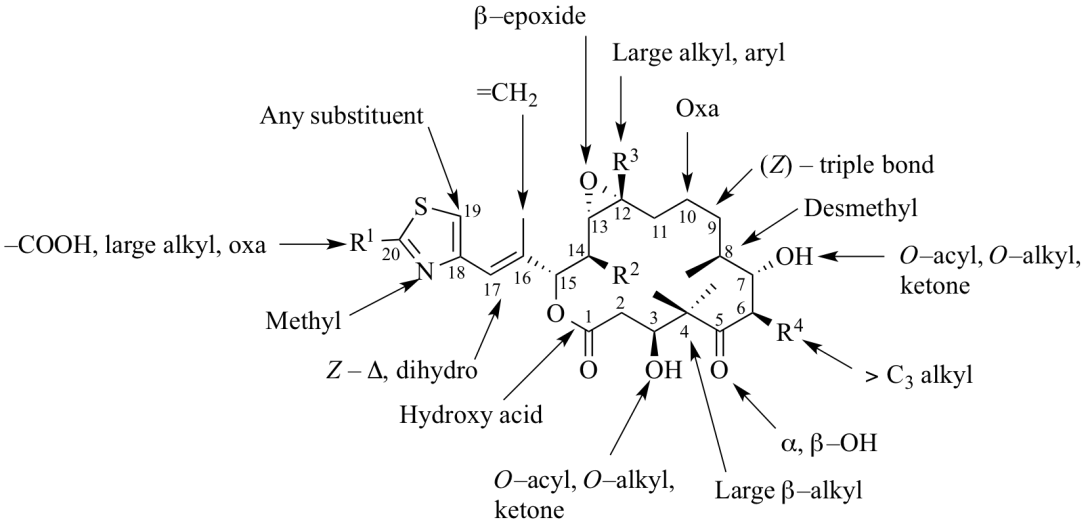

b) Modifications on epothilones rendering low activity or inactivity

Figure 3.4a and **3.4b.** SAR Studies on Epothilones.

Based on the crystal structure[258] and NMR in solution (D_2O)[259], it is known that the carbon backbone C8–C12 assumes a anti-periplanar conformation and thus, the C9–

C10[260-263] and C10–C11 *trans* olefinic analogs are highly active[254,264,265], while the C9–C10 *cis* isomer[266] and the C9–C10 alkyne derivative[266] are inactive. The C10-oxa derivative is also inactive for unknown reasons.[267] The C12–C13 epoxide and olefin have been extensively modified. Replacing the epoxide with a cyclopropane[268-270], cyclobutane[270], oxazoline[271], aziridine, *N*-acyl and *N*-alkyl aziridine[272] maintains or improves the cytotoxicity. This observation disproves the initial hypothesis that epothilones covalently bind to tubulins via epoxide opening. However, the acetonides of C12, C13–diols are less active[273] and the C12–C13 benzo analog is completely inactive.[274] C12–C13 epoxides and other related analogs in the unnatural β-configuration are inactive. Epothilones C and D, which lack the C12–C13 epoxide and instead have a double bond, are equally active or even more active in the tubulin polymerization assay compared to the epoxide containing analogs, however, significantly less cytotoxic.[275-278] Interestingly, the desoxyepothilones with an unnatural C12–C13 (*E*)-double bond are also similarly highly active.[279] The C12 methyl group is vital for high *in vitro* and *in vivo* activity of epothilone B-like epothilones. Replacing this methyl group with small alkyl, alkenyl or alkynyl groups or modifying the C12 methyl group by introduction of a halogen or oxygen substituents retains the activity. A fluorescent epothilone D analog with a large *m*-dimethylaminobenzoyloxy substituent at the C12 methyl group is as active as paclitaxel.[280] Adding an extra methyl group at C14 in the α-configuration slightly reduces the activity while a C14β-methyl group results in complete loss of activity.[281] The C16–C17 vinyl spacer in the side chain and the (*E*)-configuration are crucial for the biological activity.[275,282] However, the C16 methyl is not that important.[254,283] Epothilone derivatives which lack the C16–C17 spacer,[275,284] or have a single atom extension,[285] or

contain an alkyne spacer,[282] or have a C16–C17 epoxide,[277] or have conformationally flexible spacers with a C16–C17 single bond are not active.[286]

The thiazole ring can be replaced with an oxazole ring or an α–pyridyl ring with no observed loss in the activity. The β–pyridyl and the γ-pyridyl derivatives are moderately active or inactive.[254-256,287,288] Based on these observations, it was deduced that the position where the nitrogen atom is naturally situated in the epothilone molecule is very important for acting as a hydrogen bond acceptor in the tubulin bound state. This inference is supported by the fact that *N*-methylthiazolium epothilone B is inactive whereas the thiazole *N*-oxides are still active due to hydrogen bond acceptor like behavior of the *N*-oxide.[289] C19-substituted thiazole analogs[290] or accordingly substituted pyridyl analogs[287,288] result in complete loss activity due to a possibility that the conformational restraints may place the nitrogen atom out of its ideal orientation. Condensing the heterocycle with a benzene ring probably locks the nitrogen in its most favorable position thus rendering highly active analogs such as benzothiazoles, benzoxazoles, benzimidazoles and benzoquinolines.[257,291,292] Surprisingly though, the quinoline analog of epothilone D with the nitrogen in the *para* position is 100 times less active while the regioisomers of the quinoline analogs of epothilone B show high activity.[293-295] Highly active analogs can be prepared by replacing the C20 methyl of the epothilone thiazole side chain with hydrogen, small alkyl, alkenyl, or alkynyl groups.[289] The C20 methyl group can also be modified by an array of substituents like halogens, oxygen, nitrogen, and sulfur, or oxidized to an aldehyde and further functionalized while retaining the activity as long as the length of the residue does not exceed three to four atoms.[289] However, the thiazole C20 carboxylic acid analog is still inactive.[289]

3.3.2 Epothilone Binding

Competitive binding studies revealed that epothilones can displace taxol from microtubules, which suggested that they have the same or overlapping binding sites.[227] However, epothilones occupy only half of the taxol binding site on β-tubulin.[296] Although the binding sites for the epothilones and taxol on β-tubulin overlap, epothilones show impressive efficacy against taxol-resistant cancer cell lines, suggesting a significantly different binding mode.[241] Comparison of the crystal structures of both taxol and epothilones, their NMR solution structures, cross-resistance to β–tubulin mutations,[240,297-299] and computationally derived overlays of their structures, led to several proposed common pharmacophore models.[239,258,296,300-303]

In 2004, a model of the conformation and binding mode of epothilone A, based on electron crystallography of Zn^{2+}-induced tubulin sheets, was reported (Figure 3.5b).[258] A similar structure determination had been reported earlier for the taxol/α,β-tubulin complex (Figure 3.5a).[243] However, due to the relatively low resolution, the structures could only be solved with the help of additional NMR studies and molecular modeling.[258] As shown in Figure 3.5b, the C3 and C7 hydroxyl groups and the C5 carbonyl of epothilone A form hydrogen bonds with Arg282 and Thr274, the C1 lactone carbonyl with Arg276, and the thiazole nitrogen with His227 in the H7 helix. The C12-C13 epoxide is folded inwards towards a protein pocket and explains the observations that additional substituents can be attached at that site without loss of binding. In this model, Gln292 and Ala231 are needed to maintain the correct conformation of the M-loop and H7 helix respectively, although they are remote from the actual binding site. This conformation and binding mode is very different from that derived from NMR

measurements in the presence of tubulin (Figure 3.6), but supported by SAR studies,[291] and explains the requirements of a nitrogen *anti*-periplanar to C15 for biological activity.

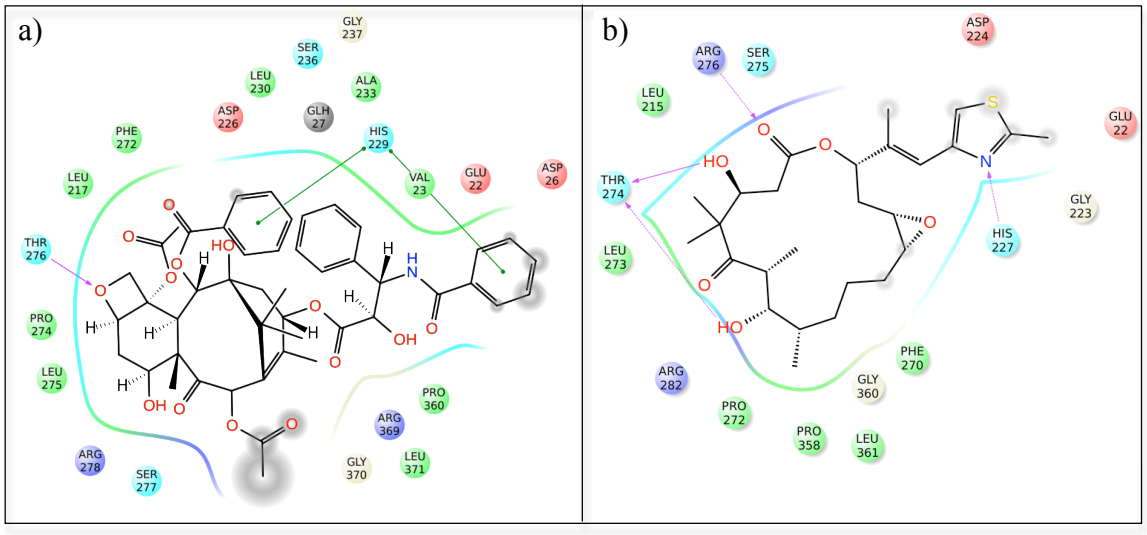

Green = Hydrophobic amino acids
Red = Negatively charged amino acids
Blue = Positively charged amino acids
Cyan = Amino acids with Coulombic interactions
Gray = Solvent exposed

Figure 3.5a and **3.5b.** Electron Crystallography-Derived 2D Models of (a) Taxol and (b) Epothilone A Bound to Zinc-Stabilized α,β-Tubulin Sheets. (Images generated in PyMol).

The competing model was obtained from NMR NOE-transfer studies of epothilone A bound to unpolymerized α,β-tubulin dimers in solution (Figure 3.6).[259] A significant difference in this model is that the C3 hydroxy group is not involved in hydrogen bonding with the protein, a result that is supported by SAR studies at that site.[292,304] Another difference is that the C7 hydroxyl group has electrostatic interactions with Arg282 (rather than with Thr274), which in turn induces electrostatic interactions between Arg282 and Thr274. It also locks Arg276 in such a position so that it forms a

salt bridge with Asp224. The thiazole and His227 engage in a π-π interaction instead of hydrogen bonding with His227 as seen in the electron-crystallography model. The NMR model shows involvement of a hydrophobic pocket hosting Phe270, which is important for taxol activity and also binds the C12 methyl group of epothilone B, thus accounting for its 10-fold increase in activity over epothilone A.

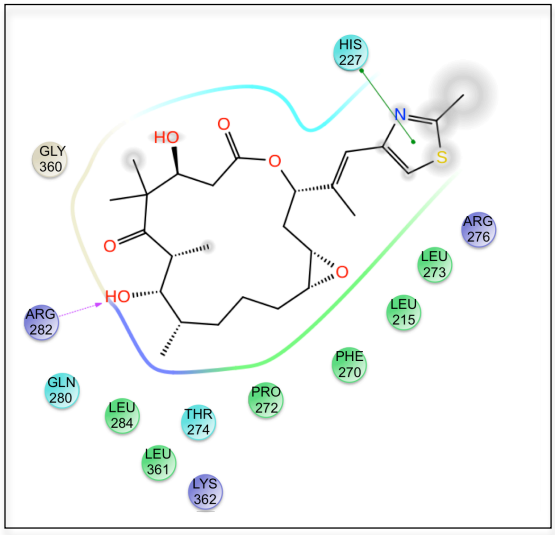

Green = Hydrophobic amino acids
Red = Negatively charged amino acids
Blue = Positively charged amino acids
Cyan = Amino acids with Coulombic interactions
Gray = Solvent exposed

Figure 3.6. NMR-Derived 2D Model of Epothilone A Bound to Monomeric Tubulin. (Images generated in PyMol).

In both models epothilones cause rigidification and alignment of the M-loop and the H7 helix leading to conformational change in the α,β-tubulin dimer. However both of them are models and the exact conformation of epothilone A required for binding and activity is still not known. One of the problems is that the electron crystallography-derived structure consists of antiparallel protofilaments instead of parallel ones as seen in natural

microtubules, which may distort the binding site as well as the epothilone conformations. The relevance of the NMR/modeling results are also subject to concerns because the soluble monomers, oligomers, or microtubule protofilaments are not well defined in the NMR studies and binding to the various tubulin species could be different. A second low-affinity binding site for Taxol[305] may also be involved in the ligand exchange,[306] which is not considered in the NMR model. As a result, it is not clear which of the two proposed binding models is correct or whether others need to be considered. Figure 3.7 shows four three-dimensional structures of epothilone conformers that have been observed or proposed: (3.7a) epothilone A bound to zinc-stabilized α, β-tubulin; (3.7b) epothilone A in aqueous medium in the presence of α, β-tubulin monomers; (3.7c) epothilone A X-ray structure crystallized from dichloromethane, and the conformation (3.7d) derived from the crystal structure of epothilone B bound to cytochrome P450. While there is some similarity among the structures with regard to the conformation of the macrocycles that are shown in Figure 3.7, it is also clear that the orientations of the epoxide and the thiazole group at C15 are quite different. In the tubulin-bound electron crystallography structure (3.7a) the epoxide is pointing inward, whereas the epoxide is pointing outward in the three other structures. The orientation of the presumably highly flexible thiazole group in structure 3.7b, derived from NMR studies and structure 3.6c, derived from X-ray are similar in that C16 and C19 are in a syn orientation, whereas that is not the case in structures (3.7a) and (3.7c) that were derived crystallographically.

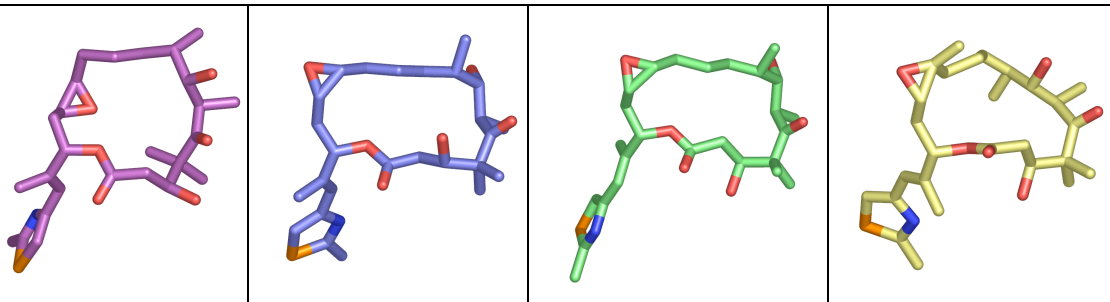

(a) Tubulin-bound electron crystallography	(b) Tubulin-bound NMR	(c) X-ray structure	(d) Cytochrome P450-bound X-ray crystallography

Figure 3.7. Structures of 3-D Epothilone A and B Conformers Obtained by Different Methods. (Images reproduced from the literature reference[296] with permission).

3.4 Photoaffinity Probes

Additional evidence is needed to decide which of the two models (electron crystallography or NMR) for the structure of the epothilone-tubulin complex is correct. One solution to resolve this ambiguity is to carry out photoaffinity labeling studies with epothilone derivatives having photolabile substituents at the C21 methyl group of the thiazole side chain or on the aziridine nitrogen atom in case of the C12–C13 aziridine analogs. Both of these positions can be modified without having an impact on the binding of epothilones to tubulin.[272,289]

3.4.1 Background

Photoaffinity reagents are compounds that are attached to a molecule that binds to a biological target with a photolabile moiety that remains dormant until photoactivated. This concept was established in the 1960's by Westheimer's group.[307,308] The photolabeling strategy has been newly rejuvenated by proteomic methods for identifying labeled targets. This method has conventionally been employed in identifying probe

labeled proteins but is now being increasingly applied to locating specific sites within proteins.[309] In a typical photoaffinity labeling study, the probe containing a photolabile moiety is added to the biological environment containing its target. The probe is assumed to bind its target at equilibrium. Upon photolysis, the inert photolabile moiety becomes activated and generates a reactive radical, carbene or nitrene intermediate depending upon its structure, and reacts covalently with a functional group on the target in its vicinity. Unlike for a chemical affinity probe, there is no need for a chemical complementarity between the probe and the target in case of the photoaffinity probe. Even though binding to a target is biospecific, probe–target coupling is comparatively arbitrary.[310]

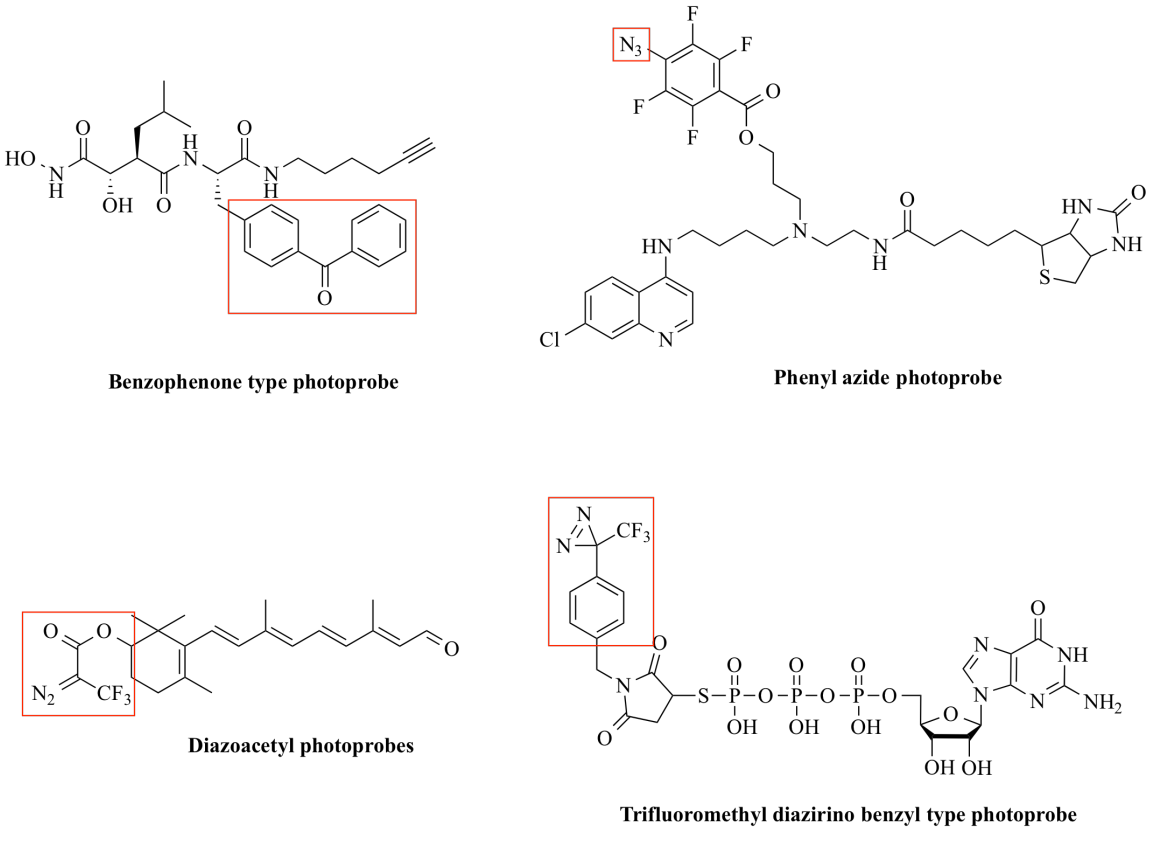

Figure 3.8. Structures of Some Common Photoaffinity Probes.

As seen in the Figure 3.8, the most commonly used photoaffinity probes have a benzophenone, an aryl azide, a diazoacetyl or a trifluoromethyldiazirino-type of photolabile group in their structures. Galardy and co-workers were the first to introduce benzophenones for photoaffinity labeling.[311] The benzophenone photolabel gives rise to radical formation upon photoactivation. In most of the cases, a triplet excited state is formed, which abstracts a hydrogen atom from a donor producing two radicals that subsequently couple.[311] Unreacted excited species relax to the ground state and may be excited over and over again until they react. A typical mechanism of benzophenone activation is shown in Scheme 3.1.

Scheme 3.1. Activation of Benzophenone Photolabel to Generate Radical Species

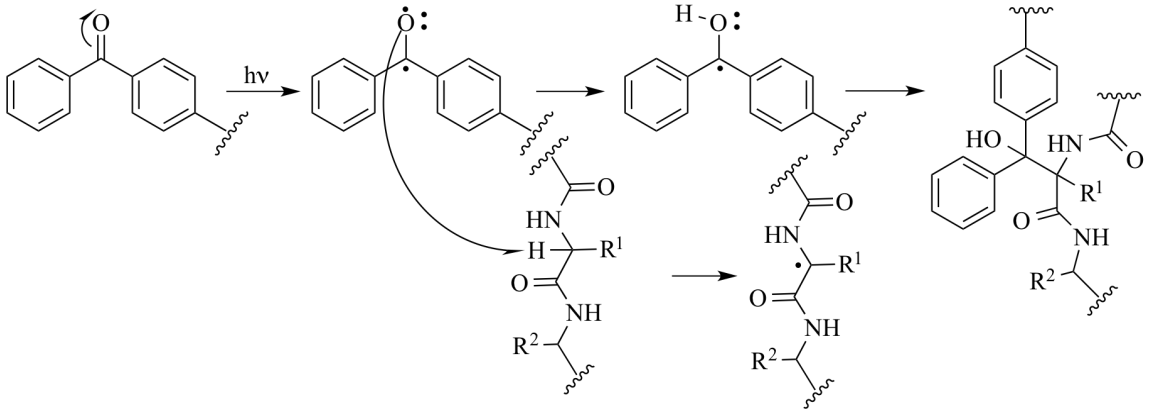

The aryl azides were introduced as photoaffinity reagents by Fleet et al.[312] They are generally stable at room temperature. However, aryl azides require photoactivation at shorter wavelengths (λ_{max} 250–290 nm) that can be damaging to proteins. Upon photolysis the aryl azide-containing photoprobes generate nitrenes. Nitrenes are molecules that have monovalent nitrogen in their structures and are relatively less reactive compared to carbenes. The reactive aryl nitrenes can efficiently insert into N–H,

O–H, and S–H bonds but are generally not very proficient at inserting into C–H bonds. Aryl nitrenes can rearrange from singlet state to less reactive and long-lived species such as azacycloheptatetraenes or benzaziridines that can also react with nucleophiles (Scheme 3.2).[313-317]

Scheme 3.2. Reactions of Aryl Nitrenes

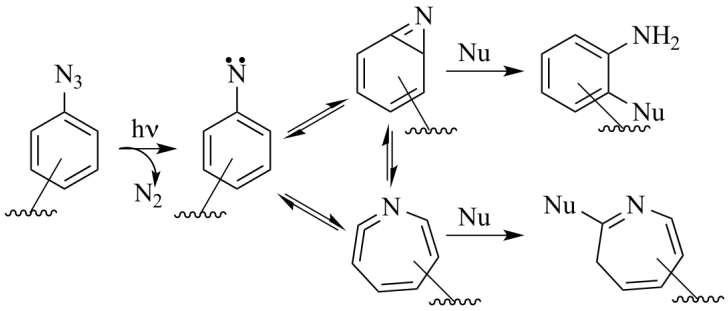

Diazocarbonyl-containing photoprobes were first synthesized by the Westheimer group in their original photoaffinity labeling experiment.[308] The diazo compounds possess a strong absorption band in the UV region (λ_{max} 240–280 nm) and a very weak band at longer wavelengths (~ 340 nm). Their photolysis gives rise to formation of carbene intermediates (Scheme 3.3, Path A). In order to achieve complete photolysis, prolonged irradiation at >300 nm with the usual lamps is needed. Such prolonged periods damage the proteins. Therefore, the photolysis properties of the diazo compounds are not the best for photoaffinity labeling. One of the major disadvantages of the diazoacetyl group is that it is unstable at low pH and is reactive in the dark towards protein functional groups. To partially overcome the challenges faced by the diazoacyl compounds, the Westheimer group synthesized improved and more stable 2-diazo-3,3,3-trifluoropropionyl[318] and tosyl diazoacetyl[319] containing photoprobes. These are much more stable at lower pH and

possess improved absorption properties. However, all of the diazoacyl photoprobes not only generate carbene species upon photolysis but these carbenes further undergo Wolff rearrangement and give rise to ketene intermediates (Scheme 3.3, Path B), which are highly reactive and can result in formation of unwanted side products.

Scheme 3.3. Reactions of Diazoacyl Photoprobes

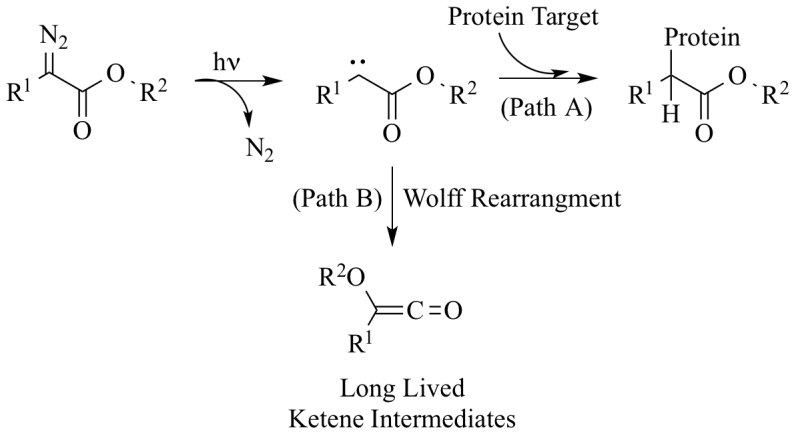

Diazirine containing photoaffinity probes were first synthesized by Smith and Knowles.[320,321] The three-membered ring has exceptionally high chemical and thermal stability.[322,323] The 3*H*-3-phenyldiaziridine was reported to be unstable on storage as a neat liquid, but its stability was improved in hexanes solution at –20 °C.[321] Higher molecular weight derivatives of this compound have been stored for months in solution at –80 °C without decomposition. The diazirines possess characteristic absorption bands in the near UV region (λ_{max} 350–380 nm). Among the diazirine containing photoaffinity probes, the trifluoromethyl-3-*H*-diazirine is an important class. They undergo efficient photolysis giving rise to formation of a carbene, which do not rearrange. A typical mechanism of photoactivation is shown in Scheme 3.4. These carbenes can form stable

covalent cross-links with the receptor and are capable of inserting into C–H, N–H, O–H or S–H bonds. None of the naturally occurring 20 amino acid side chains are immune to attack from the carbenes. The carbenes are therefore not only useful for labeling enzyme active sites, which are anticipated to contain nucleophiles, but also other receptors, which might predominantly contain hydrocarbon residues in their binding sites. They have better photostability compared to nitrenes or radicals and are easily and efficiently activated. Another advantage of the diazirines is that they only require short irradiation times to form carbenes, which assures that the integrity of the protein is maintained under the irradiation conditions.

Scheme 3.4. Photoactivation of A Trifluoromethyl-3-*H*-diazirine Probe

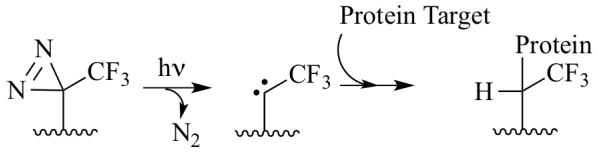

3.4.2 Epothilone Photoaffinity Labels

Although mammalian brain tubulin has been studied extensively, it is highly heterogeneous largely because of posttranslational modifications and therefore, significant advances in understanding of microtubule stabilizing agents have yet to be made.[228] Photoaffinity labeling studies to characterize the taxol and discodermolide binding sites have been reported, but so far photolabeling of tubulin with epothilones has remained elusive. Earlier photoaffinity labels designed and tested in the Georg laboratory (Figure 3.9) resulted only in non-specific labeling.[324-326] The analog A, a C25 benzyloxy substituted epothilone C, was prepared to probe whether an ether-linked benzyl group

was tolerated at this site for the planned introduction of a benzyl azide or benzyl aziridine. Yet, this analog displayed drastically reduced biological activity in cytotoxicity and microtubule assembly assays. Molecular modeling simulations suggested that excessive steric demand at the C25 position might disrupt the key hydrogen-bonding interactions ultimately resulting in weaker ligand binding and reduced activity.[326]

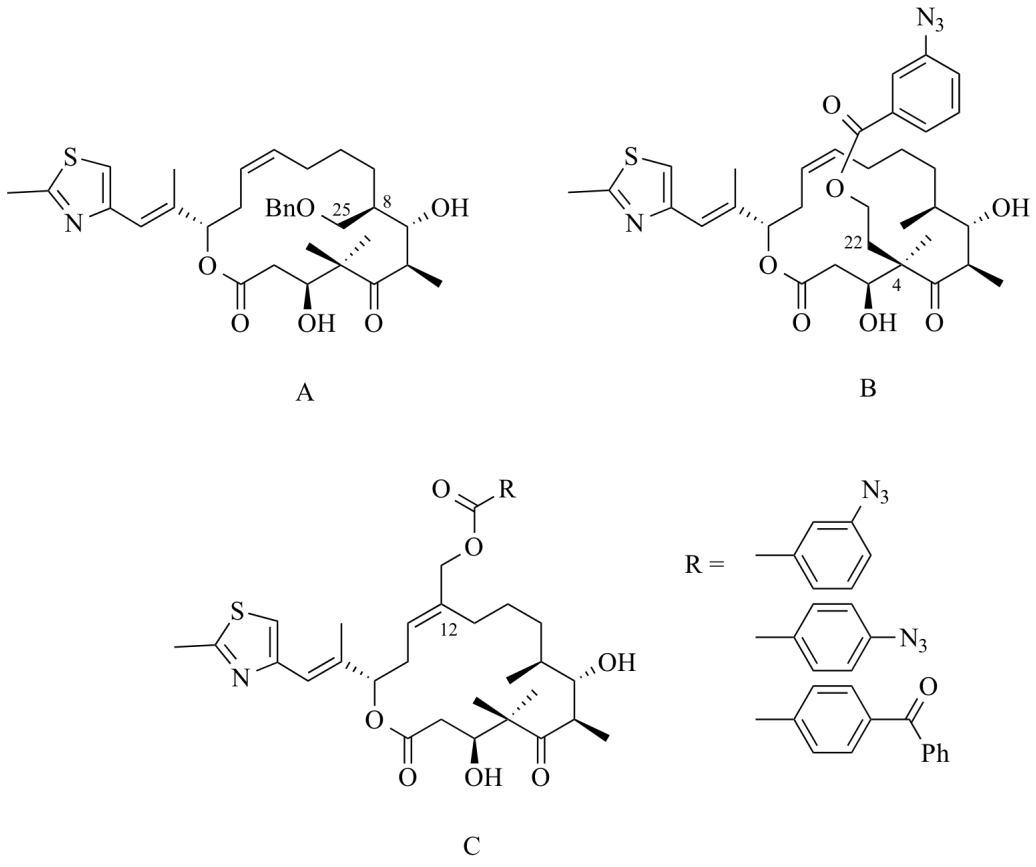

Figure 3.9. Structures of Earlier Synthesized Epothilone Photoaffinity Probes.

Analog B, a C22–functionalized epothilone C, showed good activity in microtubule assembly assays, but suffered from reduced cytotoxicity. Molecular modeling studies indicated that steric bulk at C22 could be accommodated by the hydrophobic binding pocket.[324] However the photoaffinity labeling studies were inconclusive. The covalent

labeling was non-specific. In case of the analogs C, only the azidobenzoyl derivatives were actively cytotoxic and promoted microtubule assembly.[325] Docking studies suggested that the azidobenzoyl derivatives could bind to the epothilone-binding site. Photolabeling studies with the 3-azidobenzoyl analog could not identify covalently labeled peptide fragments. This result suggested that the phenylazido side chain was predominantly solvent-exposed in the bound conformation and therefore was unable to make a covalent bond to the tubulin protein. The benzophenone derivative was inactive in both the assays. Docking studies suggested that the benzophenone derivative underwent a sterically driven ligand arrangement interrupting all hydrogen bonding and hence the protein binding.

Taking into account these results and the extensive SAR studies data, new epothilone A photoaffinity probes were designed (Figure 3.10) that should allow differentiation between the proposed binding modes. We hypothesized that the protein region, which will be labeled, is dependent on the epothilone conformation at the binding site. Thus, affinity labels were placed at the thiazole and aziridine moieties, which occupy distinctly different positions in the two proposed binding models. Compound **3.1**, carrying a diazo/triazolo moiety, and compounds **3.2**, **3.3**, and **3.4**, carrying trifluoromethyldiazirine groups, would generate highly reactive carbenes when subjected to photolysis. Additionally, we presumed that having a variety of photoaffinity probes with photoreactive groups at the different positions in their structures would more likely label different amino acid residues once bound to β-tubulin, thus giving a complete picture of the optimum conformation for binding.

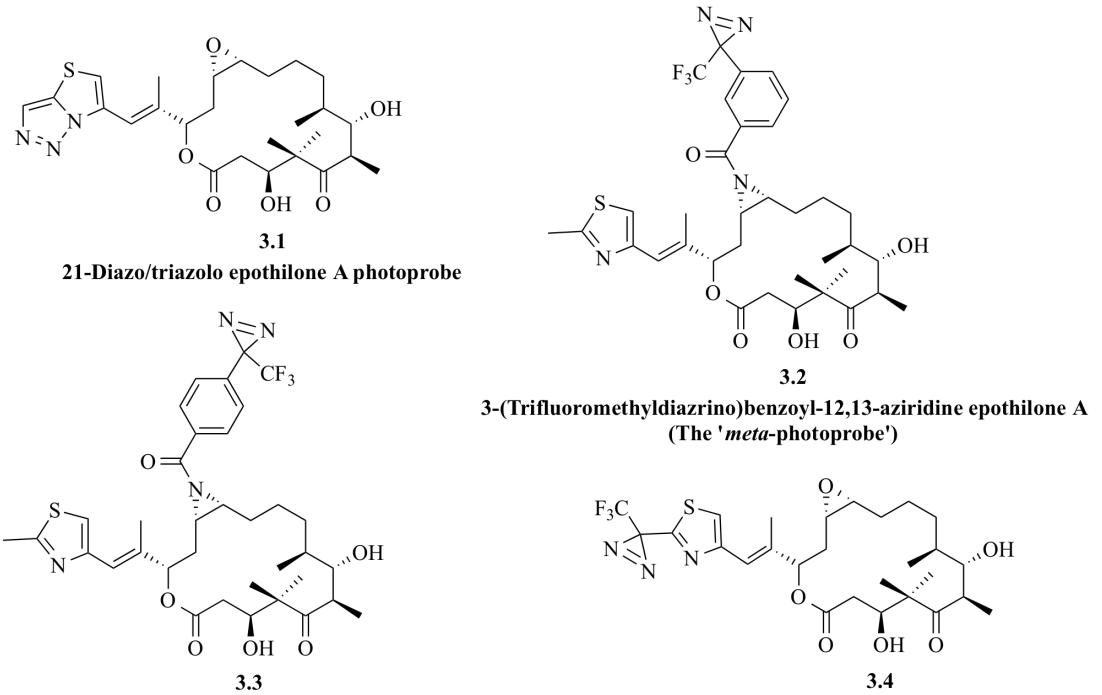

Figure 3.10. Structures of Newly Designed Epothilone A Photoaffinity Probes.

3.5 Synthesis of Newly Designed Epothilone A Photoaffinity Probes

3.5.1 Synthesis of 21-Diazo/triazolo Epothilone A Photoprobe 3.1

Synthesis of the 21-diazo/triazolo epothilone A photoprobe is shown in Scheme 3.5.[289] Epothilone A was oxidized with *m*-CPBA to provide thiazole *N*-oxide **3.6**. The *N*-oxide was then subjected to a Polonovski rearrangement by treating *N*-oxide **3.6** with trifluoroacetic anhydride and 2,6-lutidine to furnish the trifluoroacetate intermediate **3.7** in 40% overall yield over 2 steps. This intermediate was then dissolved in THF and saponified with ammonia to obtain 20-(hydroxymethyl) epothilone A (epothilone E, **3.8**) in 90% yield.

Scheme 3.5. Synthesis of 21-Diazo/triazolo Epothilone A Photoprobe **3.1**

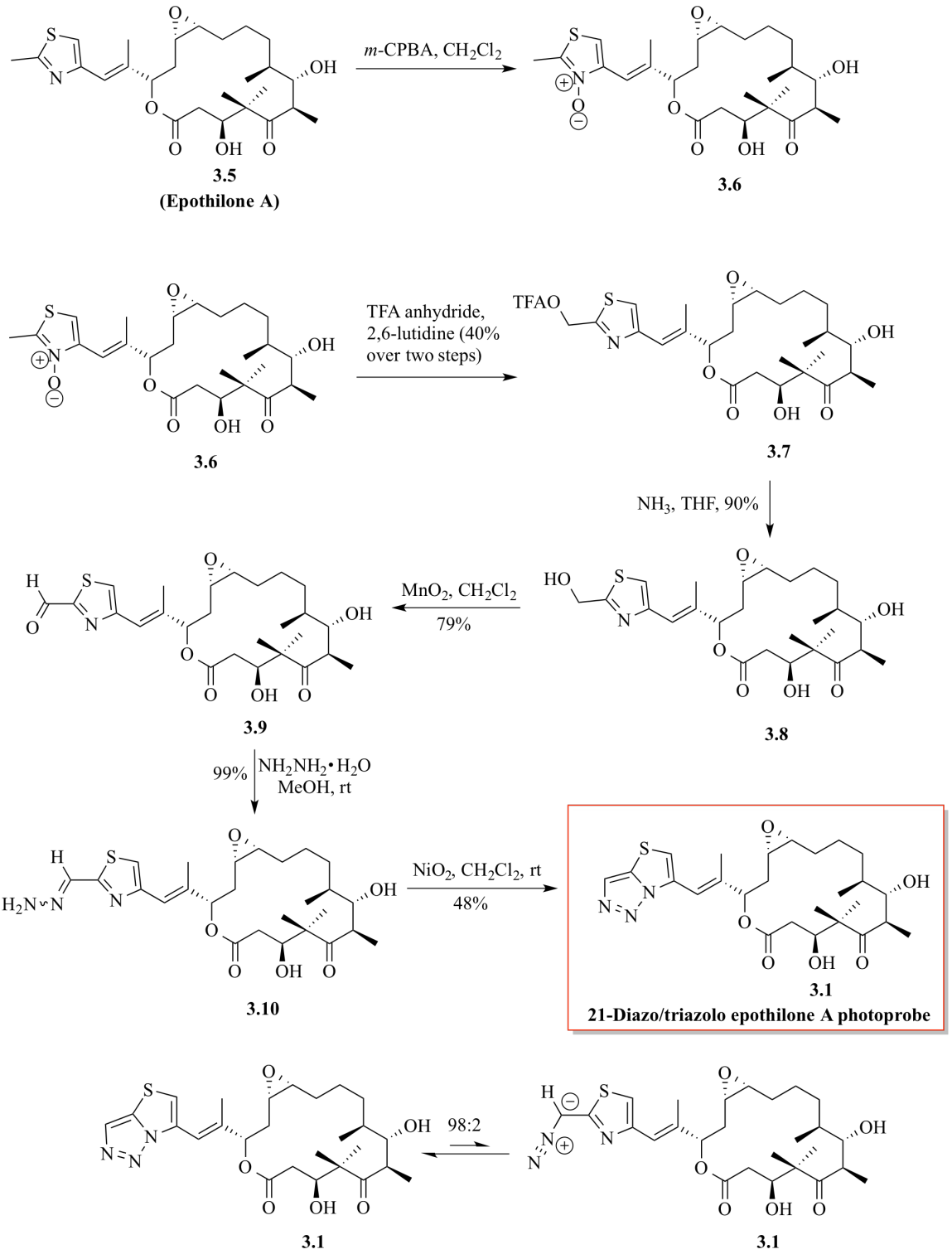

The allylic (C21-) alcohol of epothilone E **3.8** was oxidized to C21 aldehyde **3.9** in 79%

yield using manganese dioxide. Aldehyde **3.9** was converted to a mixture of *E*- and *Z*-hydrazones **3.10** in 99% yield by treatment with hydrazine hydrate. The next step was to oxidize the hydrazones **3.10**. Attempts with PIDA (diaceto(phenyl)iodide) oxidation of **3.10** did not succeed. The mixture of hydrazones **3.10** was then subjected to nickel peroxide oxidation at room temperature to furnish the required 21–diazo/triazolo epothilone A photoprobe **3.1** in 48% yield.

21–Diazo/triazolo epothilone A **3.1** had been synthesized earlier by Nicole Glaser and shown to exist in two tautomeric forms in equilibrium,[289] the most predominant tautomer being the triazolo derivative (98%). The diazo derivative is a minor tautomer and exists only as 2% of the total compound.[289] Only the diazo tautomer is photocleavable and therefore the tautomerization is a rate-determining step in the photolabeling studies. The ratio of the tautomers was determined based on the intensity of the IR band at 2078 cm^{-1}.[289] Moreover, the diazo/triazolo epothilone A **3.1** was shown to convert to pyrrolothiazole epothilone A (Scheme 3.6) by cycloaddition with dimethyl acetylenedicarboxylate.[289] Also, it was shown that, the diazo/triazolo epothilone A **3.1** is stable as a neat compound or in solution but underwent decomposition on irradiation in methanol to give epothilone E 21–methyl ether (Scheme 3.6).[289] These reactions prove the presence of the diazo tautomer in equilibrium with the triazolo tautomer.

Scheme 3.6. Reactions of 21–Diazo/triazolo Epothilone A Photoprobe **3.1**

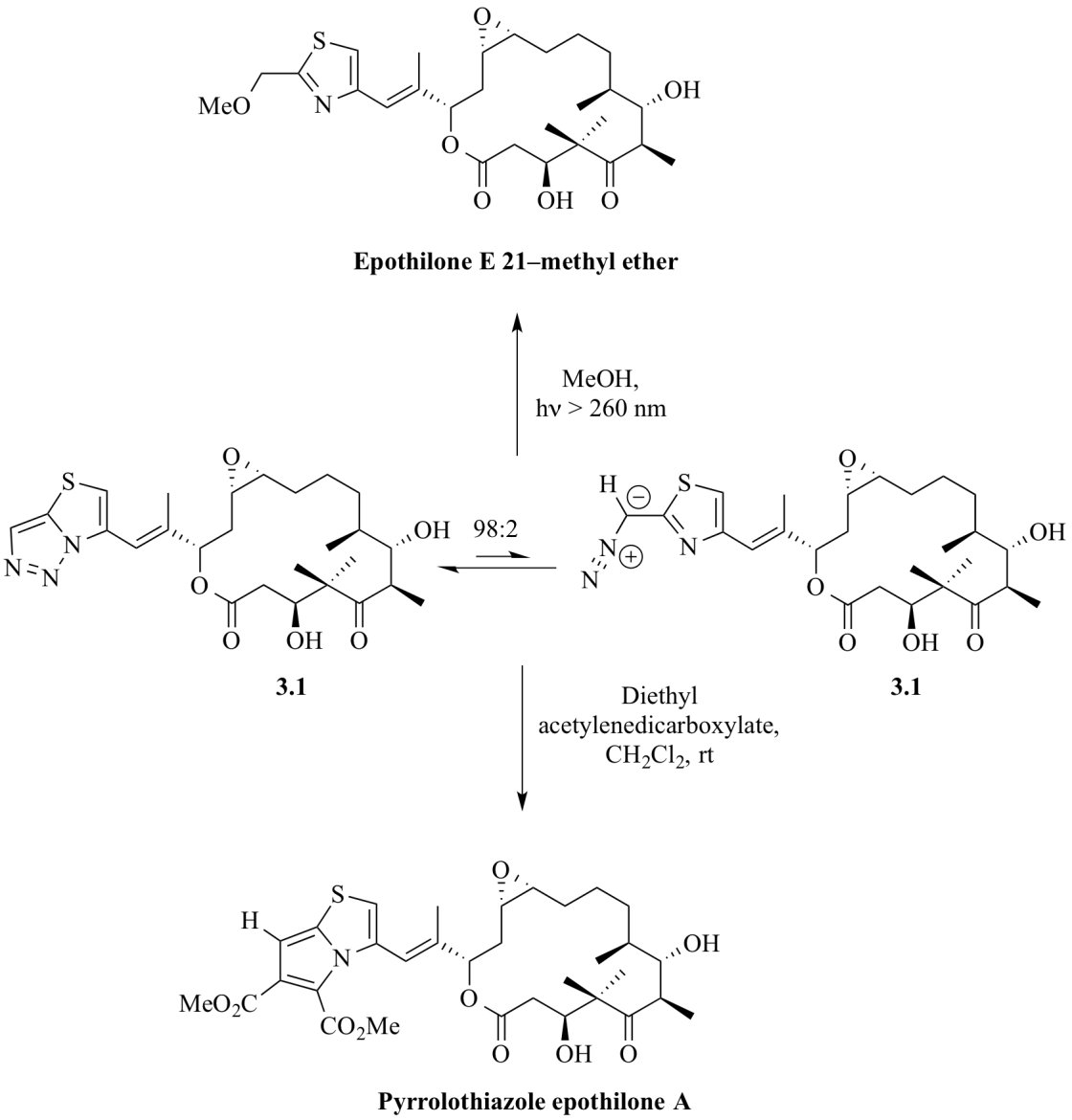

Pyrrolothiazole epothilone A

3.5.2 Synthesis of 3-(Trifluoromethyldiazrino)benzoyl-12,13-Aziridine Epothilone A or the '*meta*-Photoprobe' 3.2 and 4-(Trifluoromethyldiazrino)benzoyl-12,13-Aziridine Epothilone A or the '*para*-Photoprobe' 3.3

The retrosynthetic scheme for the photoprobes **3.2** and **3.3** (Scheme 3.7) shows that the probes could be synthesized by acylation of epothilone A aziridine **23** with *meta*- or

para-(trifluoromethyldiazirino)benzoic acids.

Scheme 3.7. Retrosynthetic Analysis for *meta*-Photoprobe **3.2** and *para*-Photoprobe **3.3**

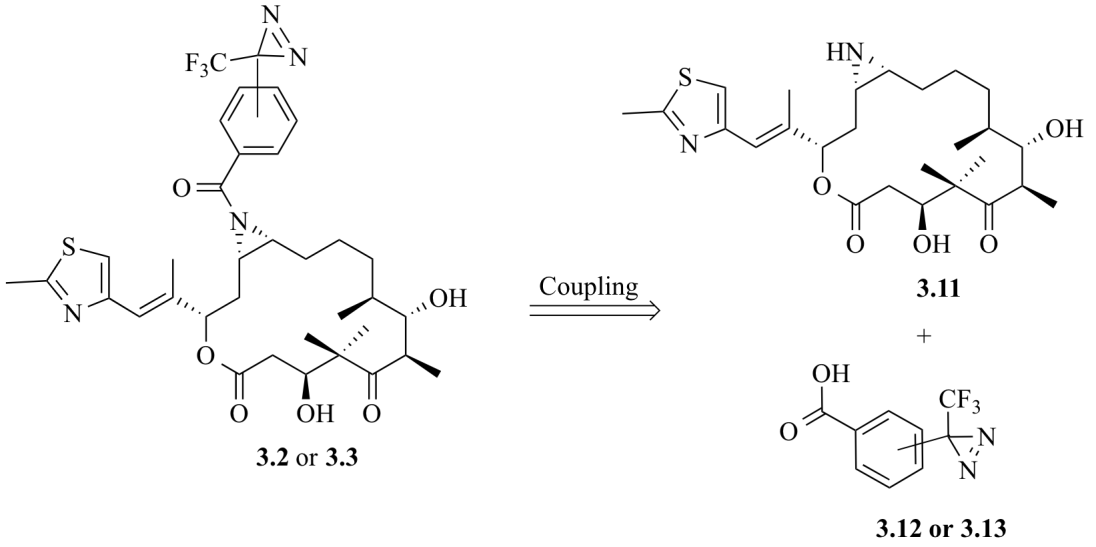

In a forward sense, epothilone A aziridine **3.11** was synthesized as shown in Scheme 3.8 using a literature protocol.[272] Protection of both the C3 and C7 hydroxyl groups of epothilone A by reaction with TES-chloride in the presence of *N*,*N*-diisopropylethylamine (DIPEA or Hünig's base) generated the bis-triethylsilyl ether **3.14** in 92% yield. The bis-triethylsilyl ether **3.14** was treated with magnesium bromide etherate at low temperature (–20 °C) to open the epoxide and form the corresponding regioselective C12α–OH/C13β–Br bromohydrin **3.15** in 63% yield. Nucleophilic substitution of the bromide of bromohydrin **3.15** was carried out with sodium azide to produce the *cis*-azido alcohol **3.16** in 62% yield. The *cis*-azido alcohol **3.16** was converted to *trans*-azido alcohol **3.18** in 77% yield (over 2 steps) by Mitsunobu inversion at the C12 position using *p*-nitrobenzoic acid. The *p*-nitrobenzoate ester **3.17** was obtained from **3.16** in 77% yield, which was subjected to ester hydrolysis conditions

using 2.0 M liquid ammonia solution in methanol to furnish the *trans*-azido alcohol **3.18** in quantitative yield. The C12β–OH of the *trans*-azido alcohol **3.18** was activated by reaction with mesyl chloride to form the azido mesylate intermediate, which without isolation, was subjected to reduction with trimethylphosphine and *in situ* cyclization to obtain bis-TES epothilone A 12α, 13α-aziridine **3.19** in 85% yield. Removal of both the TES groups from the alcohols of **3.19** furnished the required epothilone A 12α, 13α-aziridine **3.11** in 91% yield.

Scheme 3.8. Synthesis of Epothilone A Aziridine **3.11**

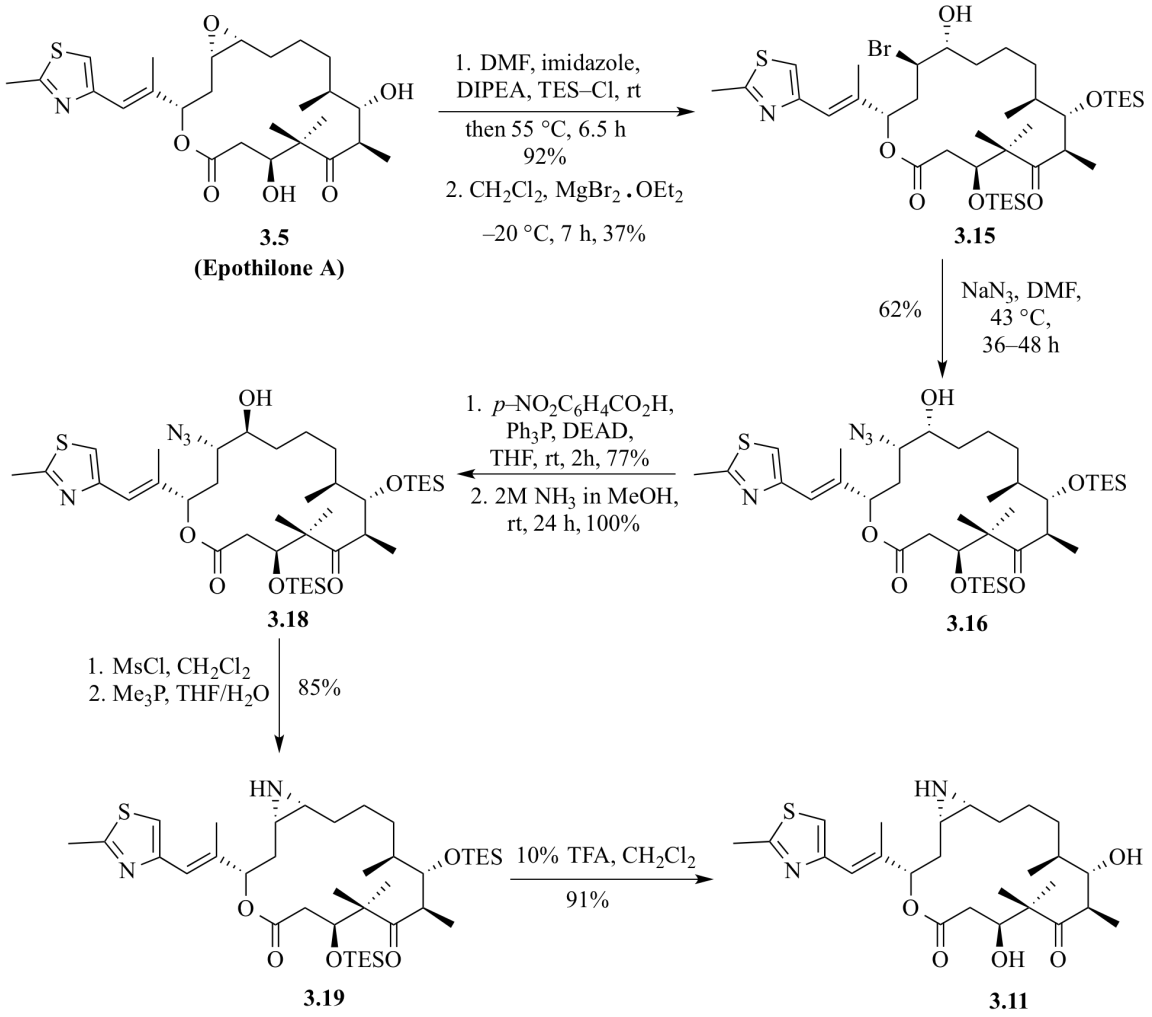

meta-(Trifluoromethyldiazirino)benzoic acid (**3.12**) was provided to us by our collaborator Dr. Gerhard Höfle and was prepared as shown in Scheme 3.9. The hydroxyl group of the bromobenzyl alcohol (**3.20**) was first protected as TBS ether **3.21** and then subjected to lithium-halogen exchange with *n*-butyl lithium followed by addition of *N*,*N*-diethyl trifluoroacetamide to provide trifluoromethyl ketone **3.22**.

Scheme 3.9. Synthesis of *m*-Trifluoromethyldiazirino Benzoic Acid **3.12**

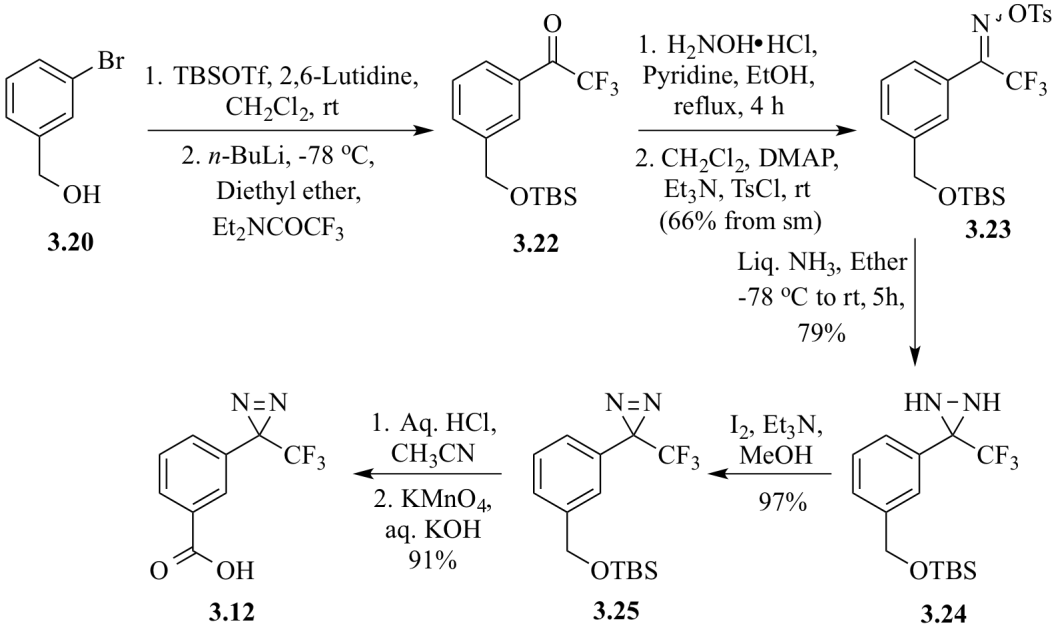

Ketone **3.22** was reacted with hydroxylamine hydrochloride to generate a mixture of *E*- and *Z*-oximes, which were treated with tosyl chloride to provide a mixture of tosyloximes **3.23** in 66% yield starting from bromobenzyl alcohol (**3.20**). Tosyloximes **3.23** were treated with condensed liquid ammonia to diaziridine **3.24** in 79% yield, which was oxidized with molecular iodine to the diazirine **3.25** in 97% yield. Deprotection of the silyl group of diazirine **3.25** with aqueous hydrochloric acid, followed by basic potassium

permanganate oxidation converted the alcohol to the carboxylic acid, producing the required *m*-(trifluoromethyldiazirino)benzoic acid (**3.12**) in 91% yield. The corresponding *p*-(trifluoromethyldiazirino)benzoic acid (**3.13**) is commercially available.

Scheme 3.10. Synthesis of Photoprobes **3.2** and **3.3**

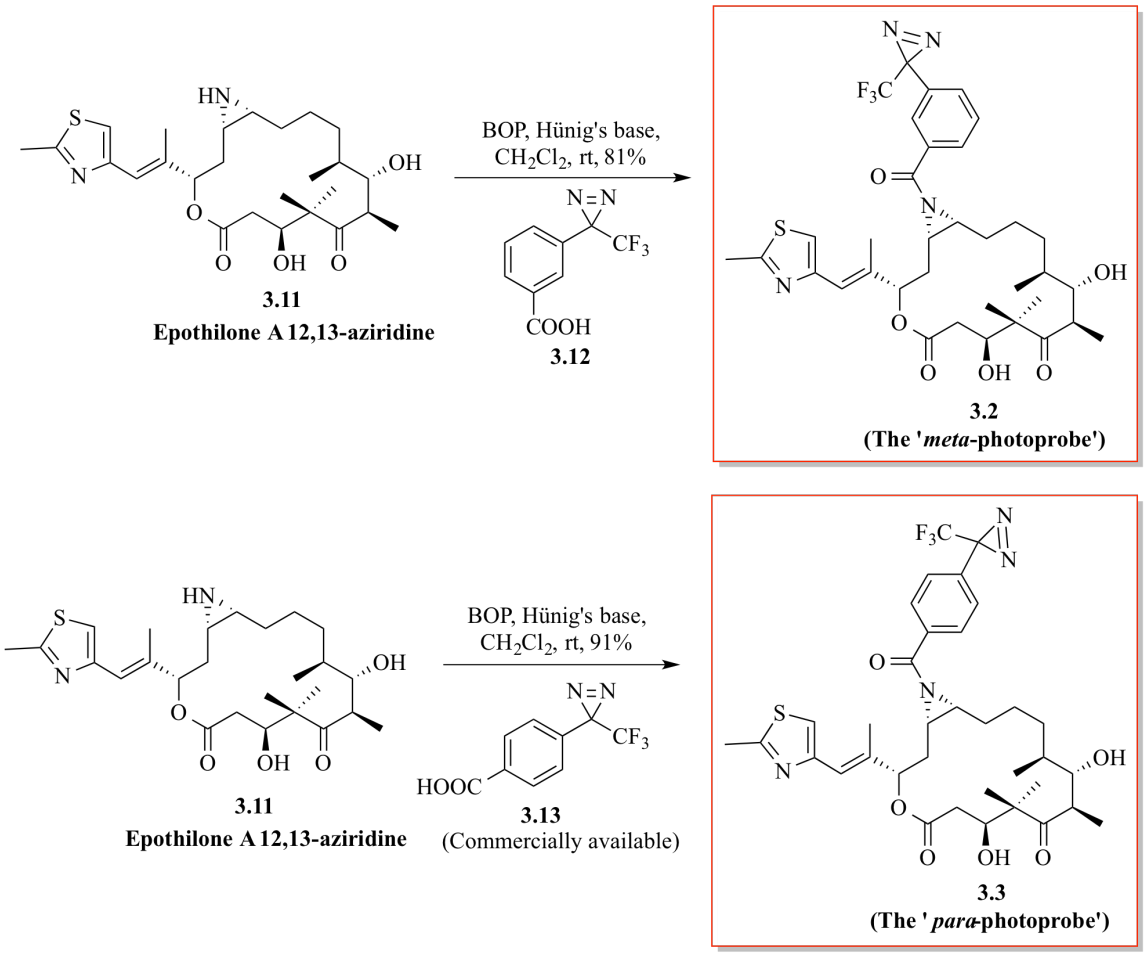

The epothilone A photoprobes **3.2** and **3.3** were prepared by acylation of aziridine **3.11** with acids **3.12** and **3.13** (Scheme 3.10). Epothilone A aziridine **3.11** and the *m*-(trifluoromethyldiazirino)benzoic acid (**3.12**) were reacted in the dark using benzotriazol-1-yloxy)tris(dimethylamino)phosphonium hexafluorophosphate (BOP) as a coupling

agent and Hünig's base to furnish the *meta*-photoprobe **3.2** in 81% yield. In a similar manner, the *para*-photoprobe **3.3** was synthesized by acylating epothilone A aziridine **3.11** with *p*-(trifluoromethyldiazirino)benzoic acid (**3.13**) in 91% yield.

3.5.3 Attempts Towards the Synthesis of the 20-Trifluoromethyldiazirino Epothilone A Photoprobe 3.4

3.5.3.1 Suzuki Coupling

A retrosynthetic analysis for photoprobe **3.4** is shown in Scheme 3.11, suggesting that a Suzuki coupling of fragments **3.26** and **3.27** could be employed to prepare the designed photoprobe.

Scheme 3.11. Retrosynthetic Analysis for 20-Trifluoromethyldiazirino Epothilone A **3.4**

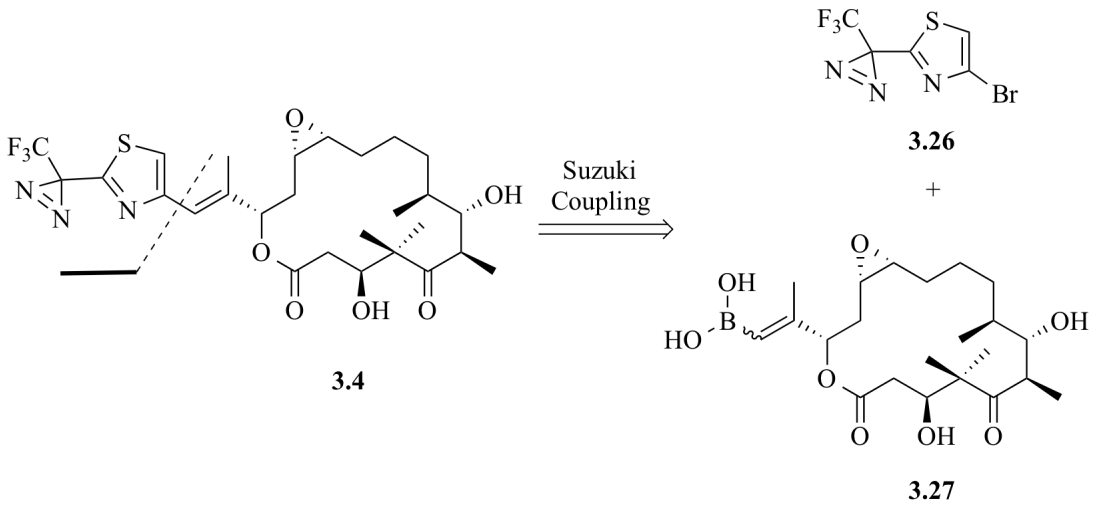

The synthesis of fragment **3.26** (Scheme 3.12) started with lithium halogen exchange at the C2 position of 2,4-dibromothiazole (**3.28**) using *n*-butyllithium at –78 °C, followed by addition of *N*,*N*-diethyl trifluoroacetamide to furnish the trifluoromethyl ketone **3.29**. The crude trifluoromethyl ketone **3.29** was refluxed in pyridine with hydroxylamine

hydrochloride to obtain a mixture of *E*- and *Z*-oximes, which was further treated with tosyl chloride to generate a mixture of tosyloximes **3.30** in 50% yield starting from 2,4-dibromothiazole (**3.28**) over 3 steps. The mixture of tosyloximes **3.30** was dissolved in ether and treated with condensed liquid ammonia at –78 °C to furnish trifluoromethyl diaziridine **3.31** in 79% yield. Finally, the trifluoromethyl diaziridine **3.31** was oxidized with silver (I) oxide to obtain the volatile 2-(trifluoromethyldiazirino)-4-bromothiazole (**3.26**) in 70% yield.

Scheme 3.12. Synthesis of 2-(Trifluoromethyldiazirino)-4-Bromothiazole **3.26**

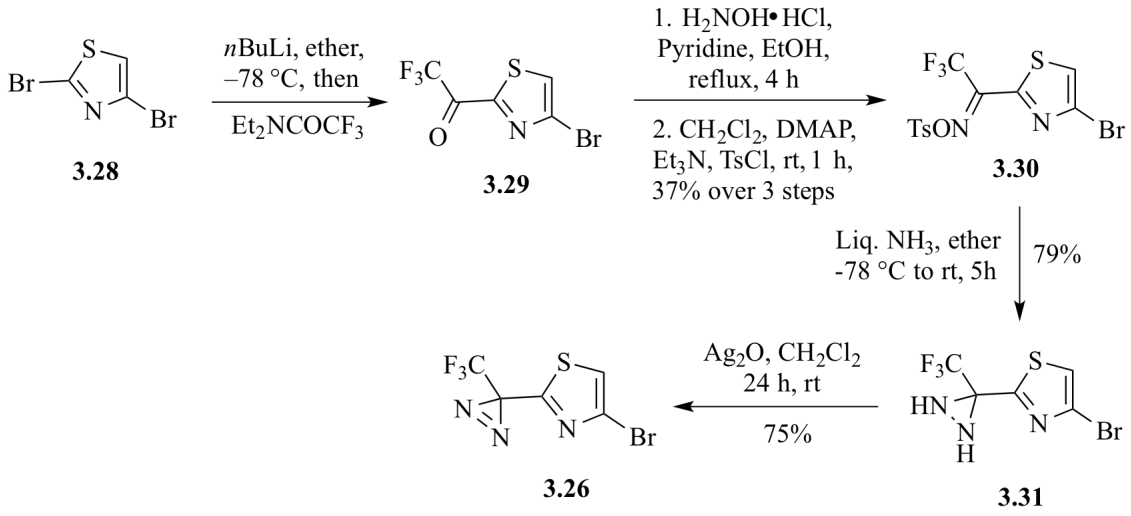

Next, we focused on preparing the boronic acid fragment **3.27**. The proposed synthesis route is shown in Scheme 3.13. The C15 ketone epothilone A **3.32**, which was provided to us by our collaborator Dr. Höfle, was prepared by subjecting epothilone A (**3.5**) to ozonolysis at –70 °C. The hydroxyl groups of the crude C15 methyl ketone were protected as trimethylsilyl ethers to furnish the bistrimethylsilyl epothilone A ketone **3.32**. In order to convert the ketone **3.32** into the corresponding vinylogous boronic acid

we needed to prepare a special boronic ester reagent, tris(ethylenedioxyboryl)methane (**3.33**, Scheme 3.14).

Scheme 3.13. Synthesis of Epothilone A Boronic Acid Fragment **3.27**

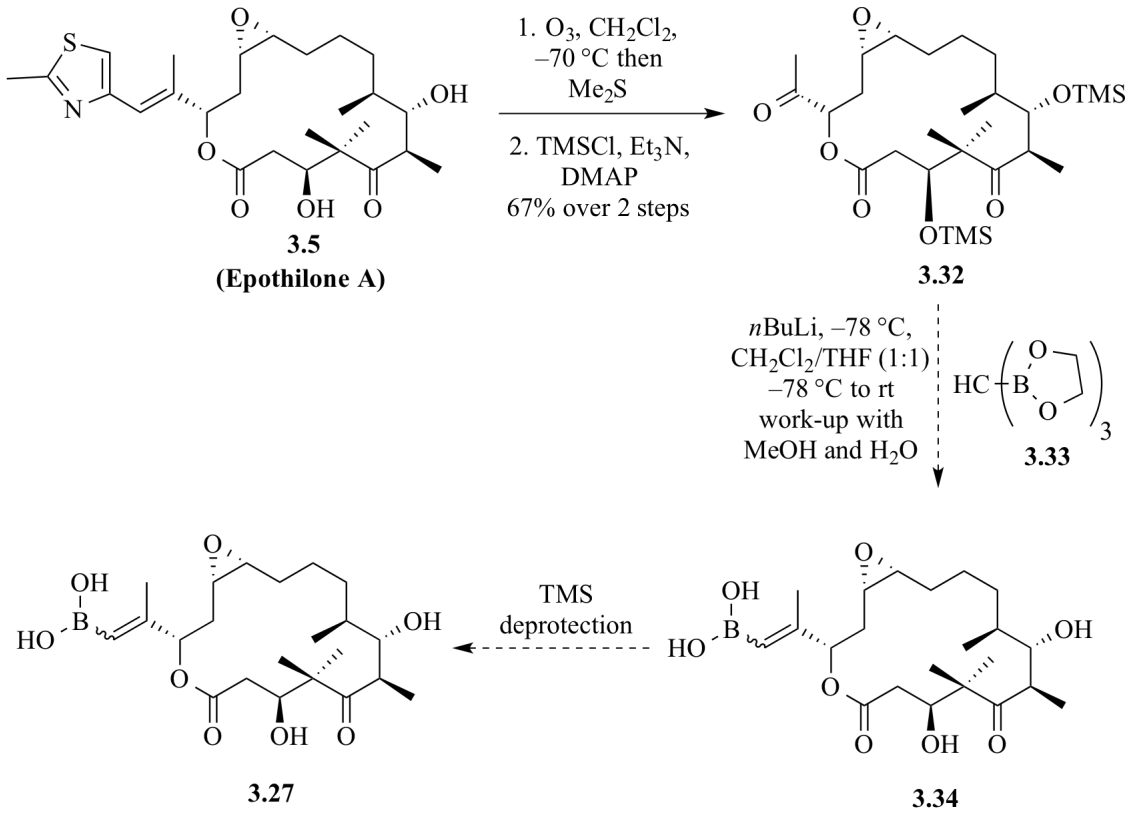

Tris(ethylenedioxyboryl)methane (**3.33**) was synthesized as shown in Scheme 3.14 following a literature procedure[327] with some modifications. Instead of condensing the boron chloride gas into a reaction flask at low temperature, we mixed a 1.0 M solution of boron trichloride (**3.35**) with a trimethoxyborane (**3.36**) solution at –50 °C. To this solution, chloroform was added to obtain 'mixture A', which contained dimethoxyboron chloride (**3.37**). Mixture A was then added to lithium metal at –40 °C to obtain tris(dimethoxyboryl)methane (**3.39**). Reacting **3.39** with ethylene glycol followed by

recrystallization furnished the required tris(ethylenedioxyboryl)methane (**3.33**) in 16% overall yield.

Scheme 3.14. Synthesis of Tris(ethylenedioxyboryl)methane (**3.33**)

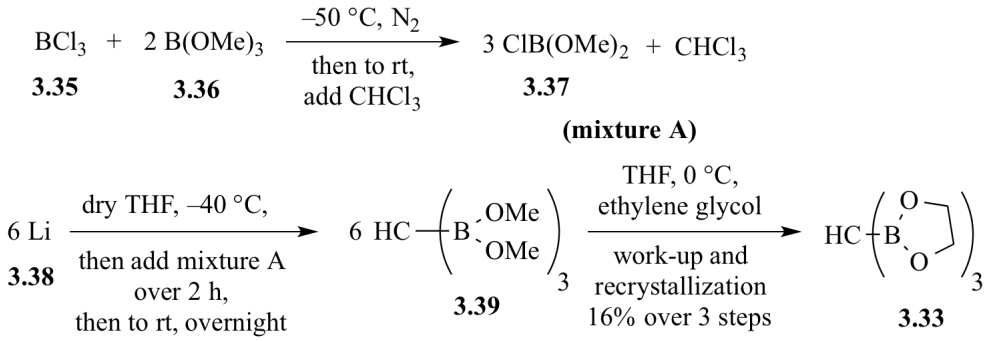

In order to synthesize the epothilone A boronic acid fragment **3.27**, tris(ethylenedioxyboryl)methane (**3.33**) was dissolved in a 1:1 mixture of THF/DCM, cooled to –78 °C and *n*-BuLi was slowly added. To the above solution, a 1:1 THF/DCM solution of bistrimethylsilyl epothilone A ketone **3.32** was added slowly and allowed to react. Unfortunately, the TLC analysis revealed that most of the bistrimethylsilyl epothilone A ketone **3.32** had decomposed, while some of it remained unreacted. The sequence of addition was altered but unfortunately it did not result in the formation of the product. These failed attempts forced us to abandon this route. Therefore, another route to synthesize the 20-trifluoromethyldiazirino epothilone A photoprobe **3.4** was needed.

3.5.3.2 Cross Metathesis

It was envisioned that photoprobe **3.4** could be obtained by cross metathesis of fragments **3.40** and **3.41** as shown in Scheme 3.15.

Scheme 3.15. Retrosynthetic Analysis for Photoprobe **3.4**

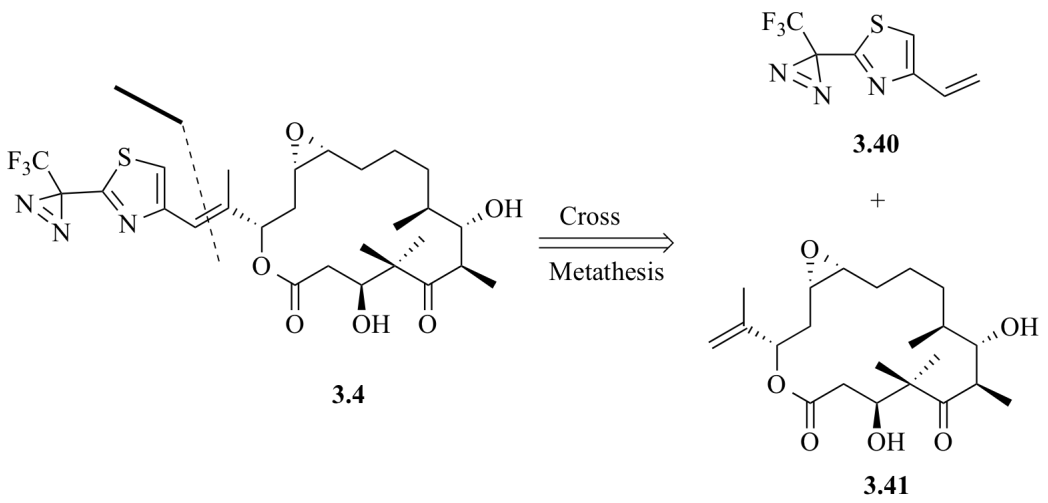

For the synthesis of the vinyl thiazole fragment **3.40** we started with 4-formyl-2-bromothiazole (**3.42**, Scheme 3.16). Subjecting **3.42** to Wittig reaction conditions furnished the 2-bromo-4-vinylthiazole (**3.43**) in 79% yield. Lithium-halogen exchange at the C2 position of 2-bromo-4-vinylthiazole (**3.43**) using *n*-butyllithium at –78 °C followed by addition of *N*,*N*-diethyl trifluoroacetamide yielded the corresponding trifluoromethyl ketone. The crude trifluoromethyl ketone was refluxed in pyridine with hydroxylamine hydrochloride to get a mixture of *E*- and *Z*-oximes, which was further treated with tosyl chloride to get a mixture of tosyloximes **3.44** in 62% yield starting from the 2-bromo-4-vinylthiazole **3.43**. The mixture of tosyloximes **3.44** was dissolved in ether and treated with condensed liquid ammonia at –78 °C to furnish trifluoromethyl diaziridine **3.45** in 93% yield. Finally, the trifluoromethyl diaziridine **3.45** was oxidized with silver (I) oxide to produce the volatile 2-(trifluoromethyldiazirino)-4-vinylthiazole (**3.40**) in 84% yield.

Scheme 3.16. Synthesis of Vinyl (Trifluoromethyldiazirino)-thiazole **3.40**

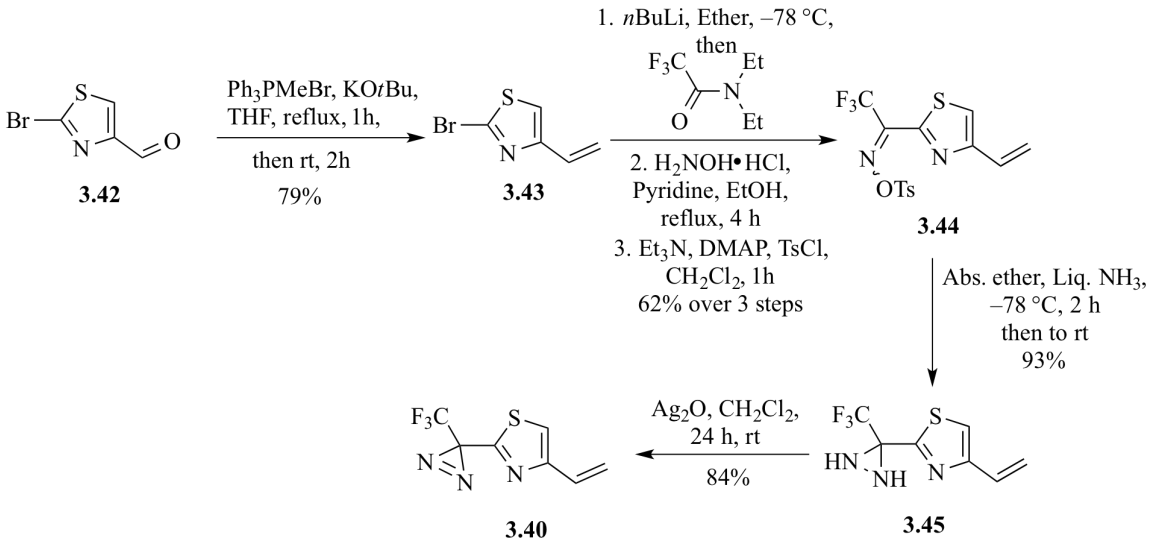

Next, we focused our attention on the synthesis of the epothilone A alkene fragment **3.46** (Scheme 3.17). We first synthesized bistrimethylsilyl epothilone A ketone **3.32** from epothilone A (**3.5**) as described earlier in Scheme 3.13.

Scheme 3.17. Conversion of Epothilone A Ketone **3.32** to Epothilone A Alkene **3.46**

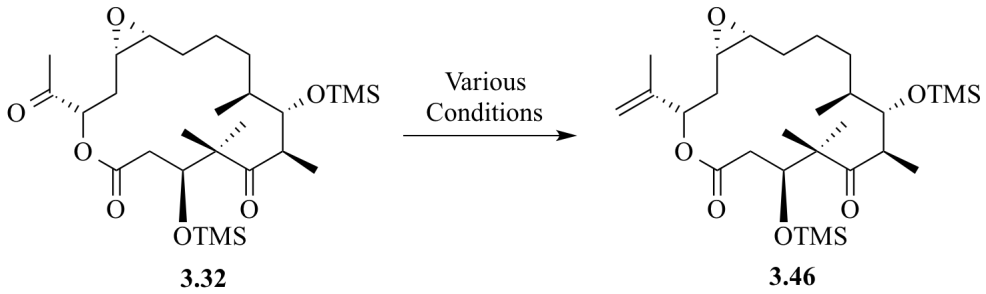

We subjected ketone **3.32** to Wittig reaction conditions wherein 1.5 equiv. of solid potassium *tert*-butoxide were dissolved in THF and cooled to 0 °C. Then 2 equivalents of methyl triphenylphosphonium bromide were added to the above solution and the mixture

was refluxed for 1 hour and then cooled to room temperature. Ketone **3.32** was dissolved in THF, added to the above mixture upon cooling and then stirred. This reaction resulted in the formation of 20% of the required product along with the C2-C3 dehydrated product **3.47**, the structure of which is shown in Scheme 3.18.

Scheme 3.18. Wittig Reaction on Epothilone A Ketone **3.32**

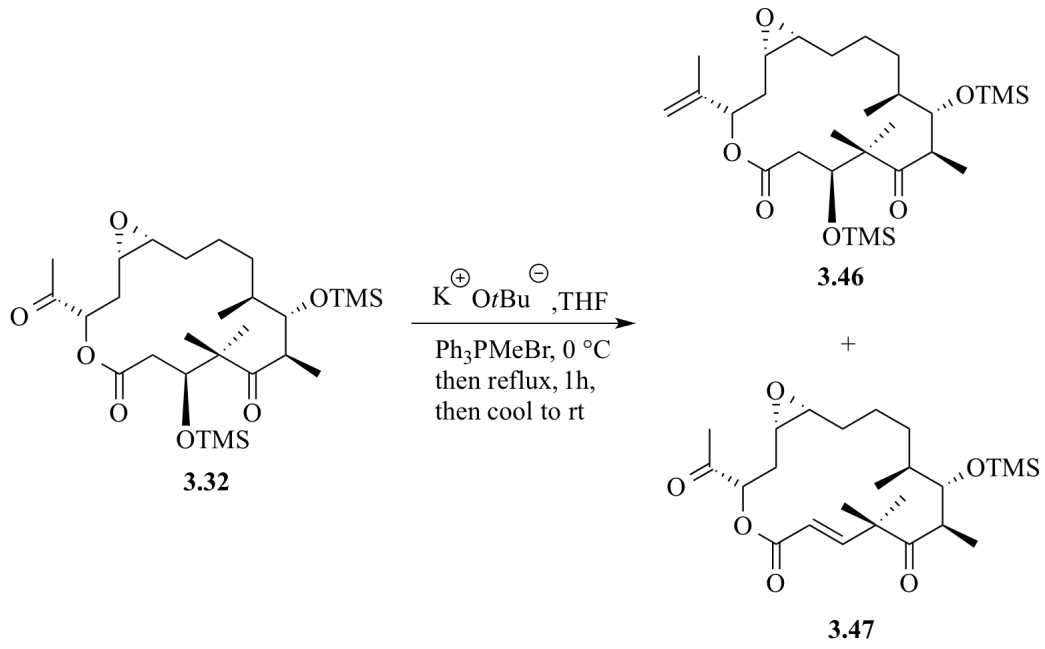

3.32 **3.46** **3.47**

Optimization attempts for the Wittig reaction are shown in Table 3.1. In spite of using different equivalents of the Wittig salt and the base or using a THF solution of the base, changing solvents or changing the order of addition of reagents the yield of the desired product could not be improved.

Table 3.1. Wittig Reaction Optimization Studies

Form of Base	Solvent	Equiv. of Salt	Equiv. of Base	Product Yield (%)	Comments and Results
Solid	THF	2	1.5	11	Dehydrated Product + Required Product
1.0 M in THF	THF	2.5	1.3	0	Dehydrated Product
1.0 M in THF	THF	1	0.95	0	Dehydrated Product
1.0 M in THF	THF	1.4	1.05	0	Complex Mixture
1.0 M in THF	Toluene	1.1	1	9	Unreacted SM
1.0 M in THF	Ether	1.1	1	0	Decomposition
1.0 M in THF	THF	1.1	1	0	At 0 °C, 1 d No reaction
1.0 M in THF	THF	1.1	1	0	At 0 °C, reverse addition No reaction

Since the formation of the dehydrated product **3.47** can be traced to the inherent basicity of the Wittig ylide, we turned to the less basic Tebbe reagent in efforts to increase the yield of the olefin **3.46** and reduce the amount of the undesired elimination product **3.47**. When ketone **3.32** was subjected to Tebbe olefination condition using 1 equivalent of the Tebbe reagent 45% of the desired epothilone A alkene **3.36** was obtained and no other side products were formed. After optimizing the reaction, we found that using 1.6 equiv. of the Tebbe reagent provides a 53% yield of product **3.36** (Scheme 3.19). Based on the TLC analysis, some starting material was identified, although this was not isolated and quantified. Increasing or decreasing the equivalents of the Tebbe reagent reduced the

yield of product **3.36**.

Scheme 3.19. Tebbe Olefination of Epothilone A Ketone **3.32** to Epothilone A Alkene **3.46**

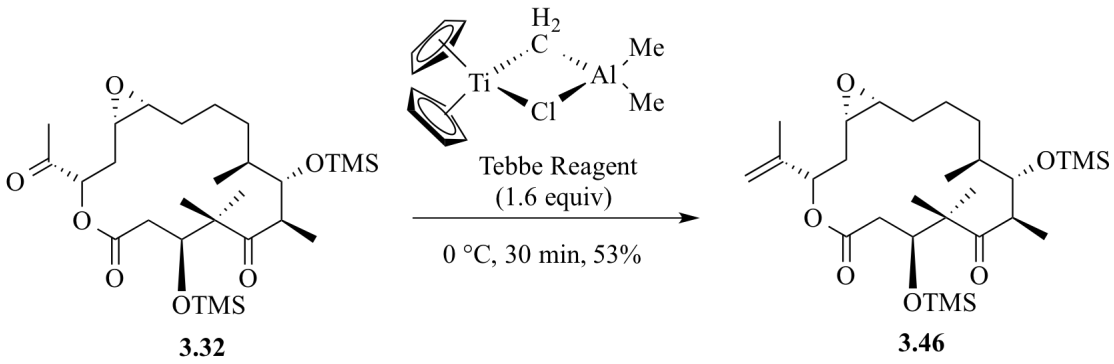

Next cross metathesis reactions were attempted between vinyl (trifluoromethyldiazirino)-thiazole **3.40** and epothilone A ketone **3.46**. We first employed the Hoveyda-Grubbs 2nd generation catalyst in this reaction (Scheme 3.20) but the desired product was not formed. TLC analysis showed that the starting materials remained unreacted. Increasing the reaction time to more than 96 hours also did not yield any product.

Scheme 3.20. Cross Metathesis of Fragments **3.46** and **3.40**

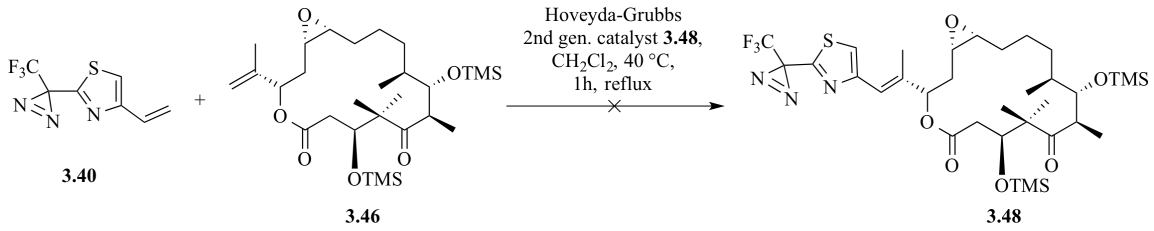

Attempts with higher temperatures in higher boiling point solvents and longer reaction times did not lead to product formation. Changing the metathesis catalysts was also tried. The structures of the catalysts used are shown in Figure 3.11.

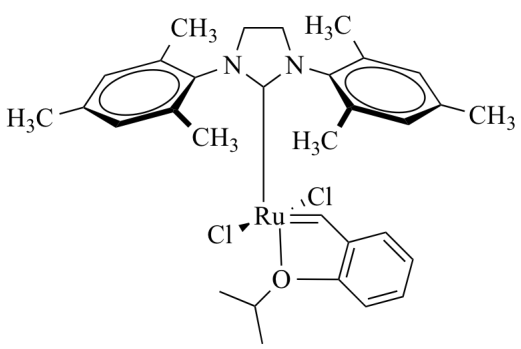

3.48

Hoveyda-Grubbs 2nd Generation Catalyst

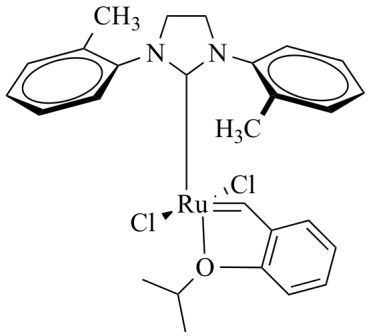

3.49

Stewart-Grubbs Catalyst

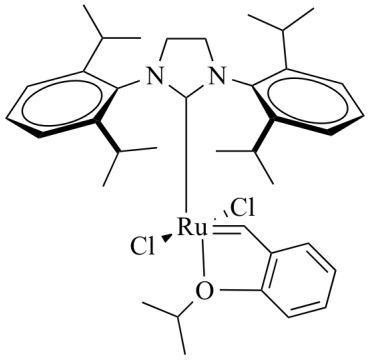

3.50

Dichloro[1,3-bis(2,6-isopropylphenyl)-2-imidazolidinylidene] (2-isopropoxyphenylmethylene)ruthenium(II)

Figure 3.11. Structures of Cross Metathesis Catalysts.

1,1-Disubstituted double bonds are very unreactive to cross metathesis conditions and only a single examples of such a transformation can be found in the literature.[328] Stewart *et al.* reported using catalyst **3.50** (Figure 3.11) to cross metathesize 1,1-disubstituted double bonds with a simple terminal alkene. Employing this catalyst in our system did not furnish any product. Various cross metathesis conditions that were tried are summarized in Table 3.2. None of these conditions gave any product. Based on these results we discontinued our attempts to synthesize photoprobe **3.4**.

Table 3.2. Summary of Cross Metathesis Conditions Explored

Catalyst	Solvent	Temperature (°C)	Time (h)	Product Yield (%)
Hoveyda-Grubbs 2nd gen.	DCM	40	1, 12, 24, 48, 96	0
Hoveyda-Grubbs 2nd gen.	Toluene	111	24, 48, 96	0
Hoveyda-Grubbs 2nd gen.	DCE	85	24, 48, 96	0
Stewart-Grubbs	DCM	40	24, 48, 96	0
Stewart-Grubbs	DCE	85	24, 48, 96	0
Stewart-Grubbs	Toluene	111	24, 48, 96	0

3.6 Biological Studies

3.6.1 Biological Assays

The photoprobes **3.1**, **3.2**, and **3.3** were examined for cytotoxicity, in a tubulin-assembly assay, and for inhibition of [^{3}H]paclitaxel binding (Table 3.3, Table 3.4 and Table 3.5). These studies were conducted in the laboratories of our collaborators, Dr. Hamel, at the NCI and Dr. Höfle, at the HZI, Germany.

Table 3.3. Cytotoxicity Studies of Photoprobes **3.1**, **3.2**, and **3.3**

Entry*	Compound	OVCAR-8[a] $IC_{50} \pm SD$ (nM)	NCI/ADR-RES[b] $IC_{50} \pm SD$ (nM)
1	Paclitaxel	5.3 ± 2	800 ± 200
2	Docetaxel	7.0 ± 2	290 ± 10
3	Epothilone A (**3.5**)	7.0 ± 1	140 ± 20
4	Epothilone B	4.0 ± 0	15 ± 0
5	Diazo-probe **3.1**	8.0 ± 1	160 ± 40
6	*Meta*-probe **3.2**	5.0 ± 1	130 ± 40
7	*Para*-probe **3.3**	7.0 ± 2	150 ± 70

* Studies carried out by Dr. Ruoli Bai at NCI, NIH, USA
[a]OVCAR-8 = Ovarian cancer lines
[b]ADR-RES = Multi-drug resistant cancer cell lines

Table 3.4. Cytotoxicity Studies of the '*meta*-Probe' **3.2** and the '*para*-Probe' **3.3**

Entry*	Compound	L929[a] IC_{50} (ng/mL)	PtK2[b] IC_{50} (ng/mL)
1	Epothilone A (**3.5**)	4	-
2	Epothilone A aziridine **3.11**	1.9	2
3	*Meta*-probe **3.2**	20	7
4	*Para*-probe **3.3**	14	2

*Studies carried out by Dr. Florenz Sasse at Helmholtz Centre for Infection Research, Braunschweig, Germany
[a]L929 cells = murine fibrosarcoma cell line
[b]PtK2 Cells = Male rat kangaroo kidney epithelial cell line

Table 3.5. Inhibition of [^{3}H]Paclitaxel Binding Assay

Entry	Compound	% Inhibition[a]
1	Epothilone A (**3.5**)	67
2	Epothilone B	82
3	Diazo-probe **3.1**	64
4	*Meta*-probe **3.2**	17
5	*Para*-probe **3.3**	2.3

Studies carried out by Dr. Ruoli Bai at NCI, NIH, USA
[a]Concentrations used: tubulin = 2 μM, [^{3}H]paclitaxel = 4 μM, compounds = 20 μM

As seen from the above tables, the newly synthesized photoprobes exhibited excellent cytotoxicity. In addition, photoprobe **3.1** showed a 64% [^{3}H]paclitaxel inhibition, which is comparable to epothilone A (82% inhibition), thereby demonstrating that the probe binds in the taxol-binding cavity on β-tubulin. Photoprobes **3.2** and **3.3** showed 17 and 2.3% inhibition respectively in this assay. Next, the photoprobes were examined for their ability to promote tubulin assembly. For this assay, the photoprobes and epothilone A and epothilone B were treated at room temperature for 15 minutes with purified tubulin in 0.4 M monosodium glutamate + 0.5 mM $MgCl_2$, followed by centrifugation at 14000 rpm.

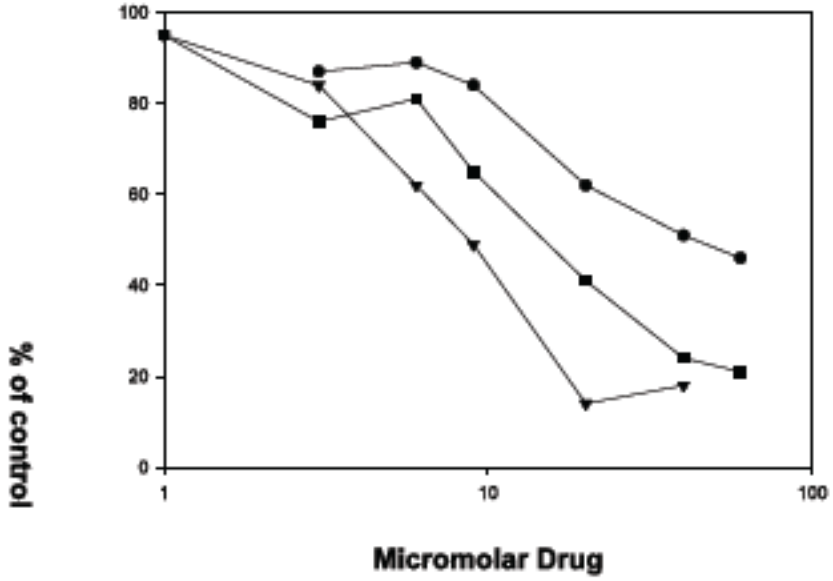

Triangles = Epothilone B (EC_{50} = 9.8 μM)
Squares = Photoprobe **3.1** (EC_{50} = 15 μM)
Circles = Epothilone A (EC_{50} = 45 μM)

Figure 3.12. Tubulin Assembly Assay for Photoprobe **3.1**.

The supernatant containing unpolymerized tubulin was assayed by the Lowry method [329] for protein content. The EC_{50} for this assay is defined as the concentration of the drug that reduces the protein content of the supernatant by 50% vs. the drug-free control. The

curves can be shifted to either the left (by increasing the glutamate concentration) or to the right (by decreasing the glutamate concentration) to allow one to measure either active or relatively inactive compounds. It was shown that photoprobe **3.1** was more active (EC_{50} = 15 μM) (Figure 3.12) than epothilone A (EC_{50} = 45 μM) and was therefore considered a viable photoaffinity probe. Photoprobes **3.2** and **3.3** failed to show the required tubulin assembly in this assay as well as in a medium sensitivity assembly assay. Therefore, a low sensitivity tubulin assembly assay (turbidimetry assay) was carried out with photoprobes **3.2** and **3.3**, in which both the analogs showed good activity (Figure 3.13).

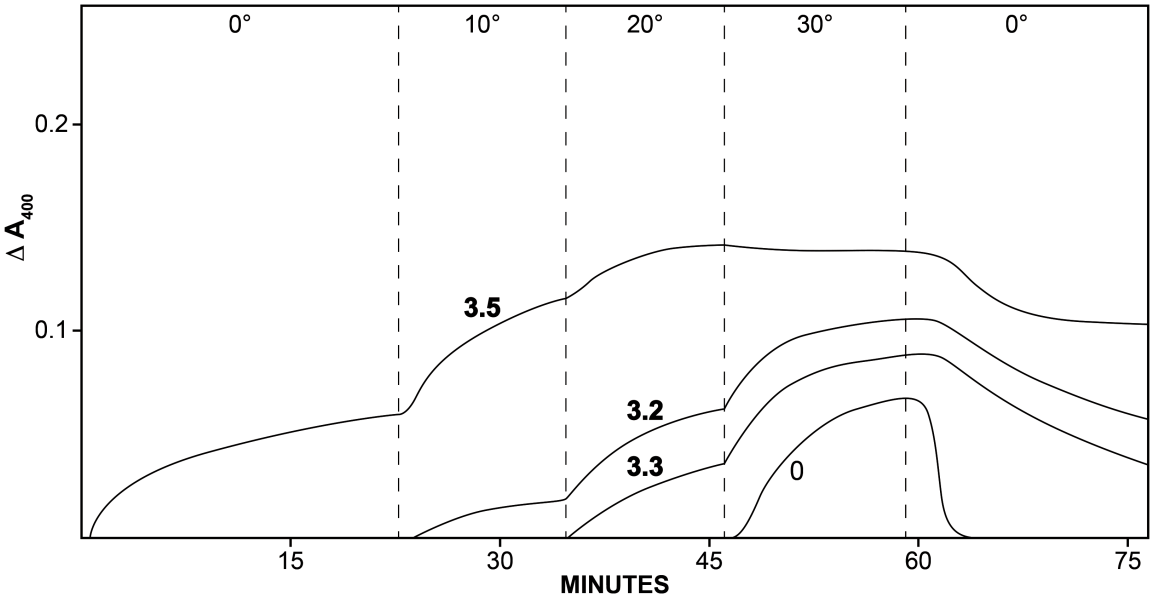

0 = No Drug Added
3.2 = Photoprobe **3.2**
3.3 = Photoprobe **3.3**
3.5 = Epothilone A (**3.5**)

Figure 3.13. Low Sensitivity Assay for Photoprobes **3.2** and **3.3**.

For this assay, mixtures of tubulin at (10 μM), heat-treated MAPs (0.75 mg/mL), 4-morpholineethane sulfonate (Mes) (0.1 M), $MgCl_2$ (0.5 mM), GTP (0.1 mM) at pH 6.9 with 4% DMSO, and the phototprobes (40 μM) were prepared. Turbidity at 400 nm was measured. The Gilford 250 spectrophotometer equipped with electronic temperature controller was used. This experiment showed strong assembly at low temperatures with epothilone A, and weak assembly at higher temperatures with the photoprobes **3.2** and **3.3**.

In the UV-Vis experiments, the diazo/triazolo photoprobe **3.1** showed the expected band at 300 nm whereas the photoprobes **3.2** and **3.3** showed the expected band at 350 nm.

3.6.2 Mass Spectrometric Studies

The results from the cytotoxicity studies, tubulin assembly assays and UV-Vis experiments suggested that photoillumination studies should be carried out with photoprobe **3.1**. Dr. Hamel, according to the protocol shown in Figure 3.14, carried out the photoaffinity labeling studies and our collaborator Dr. Higgins (University of Minnesota) performed the mass spectrometric studies.

The photoprobe **3.1** was incubated with preformed microtubules prepared from the electrophoretically homogenized bovine brain tubulin and illuminated with UV light at 300 nm. Two samples were created in this process. Sample A had a 10 min exposure to the UV light whereas sample B had a 60 min exposure. Rapid loss of epothilone binding ability was observed with exposures greater than 60 min due to denaturation of the protein. After irradiation, the microtubules were harvested by centrifugation and the

samples were frozen and sent to our collaborator Dr. Higgins at the University of Minnesota Proteomic Core Facility. Both samples (15 μg each) of the centrifuged mixture of microtubules were initially subjected to trypsin digestion.

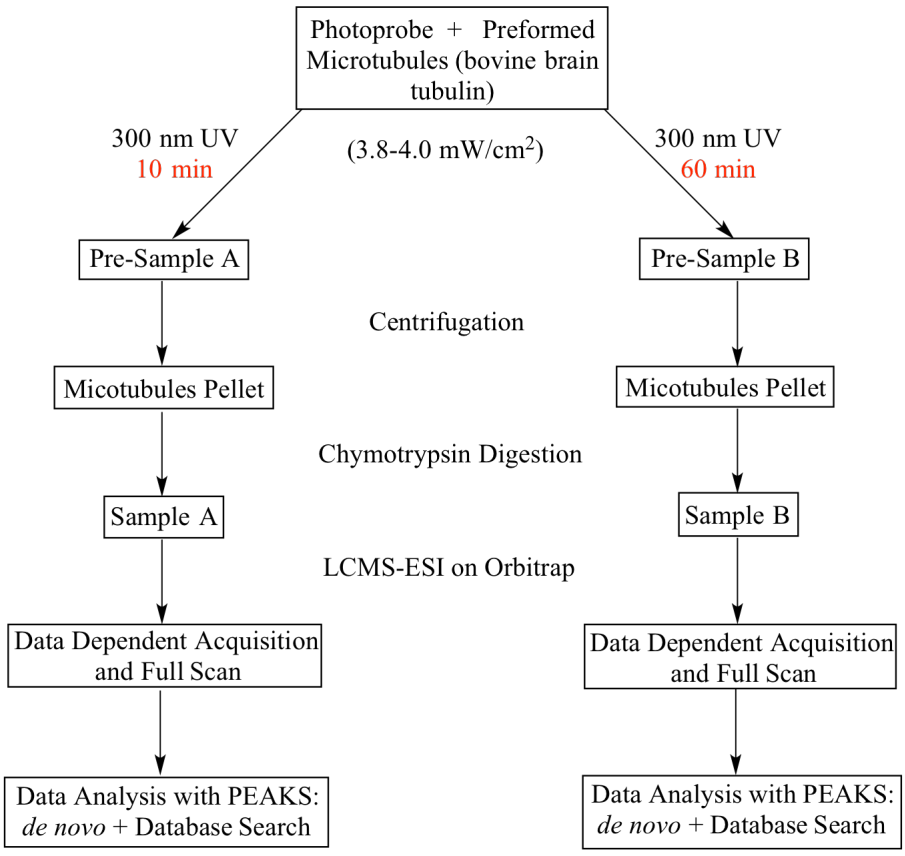

Figure 3.14. Photoillumination Protocol.

The peptide mixtures were analyzed by 2D LC-ESI-MS[330] on an "LTQ Orbitrap Velos" mass spectrometer[331] in two scan modes: data dependent acquisition (DDA) and full scan MS. In DDA mode, peptides are selected for MS/MS (or MS2) acquisition using higher energy collision induced dissociation (HCD) activation in an automated fashion from MS1 scans with an absolute intensitiy threshold and charge state restriction. In full scan mode MS1 data is acquired only. "PEAKS" software (Bioinformatics Solutions) was

used for peptide tandem MS data interpretation, which combines *de novo* peptide sequencing with mass-based database searching against a species-specific protein sequence dastabase (UniProt Bos taurus taxonomy ID 9913). Peaks results show peptide matches, partial peptide matches and protein groups for all detected proteins. Eleven alpha and beta tubulin isoforms were detected; amino acid coverage range was 59 – 77%. Trypsin digestion of the tubulin preparation yielded many peptides that were not amenable to efficient fragmentation by HCD and could not be sequenced. Alternatively, the microtubule samples (15 μg each) were subjected to chymotrypsin digestion and analyzed as described above for automated interpretation of peptide tandem MS data. Nine alpha and beta tubulin isoforms were detected; amino acid coverage range was 63 – 86%. Since probe reactivity is high and non-specific for amino acids and bond-types, the search for modified peptides using PEAKS (in the amino acid modification library) was not effective and manual interpretation of data was employed.

Because it was possible that probe-specific fragment ions could exist in the peptide tandem MS spectra, the neat probe compounds were subjected to tandem MS in order to identify peaks that could assist in manual data interpretation. Firstly, photoprobe **3.1** was infused into the Orbitrap Velos at 2 μL/min in 80:20, methanol:water at an approximate concentration of 2 micromolar and subjected to HCD activation. Probe fragmentation produced 135, 141, 164, 176, 178, 304, 316, 386, 404, 474 and 492 *m/z* values in the tandem MS (Figure 3.15). The probe-specific fragment ions were subserquently used as 'signature' ions in the pursuit of probe-modified peptides during the manual inspection of the chymotrypsin peptide data.

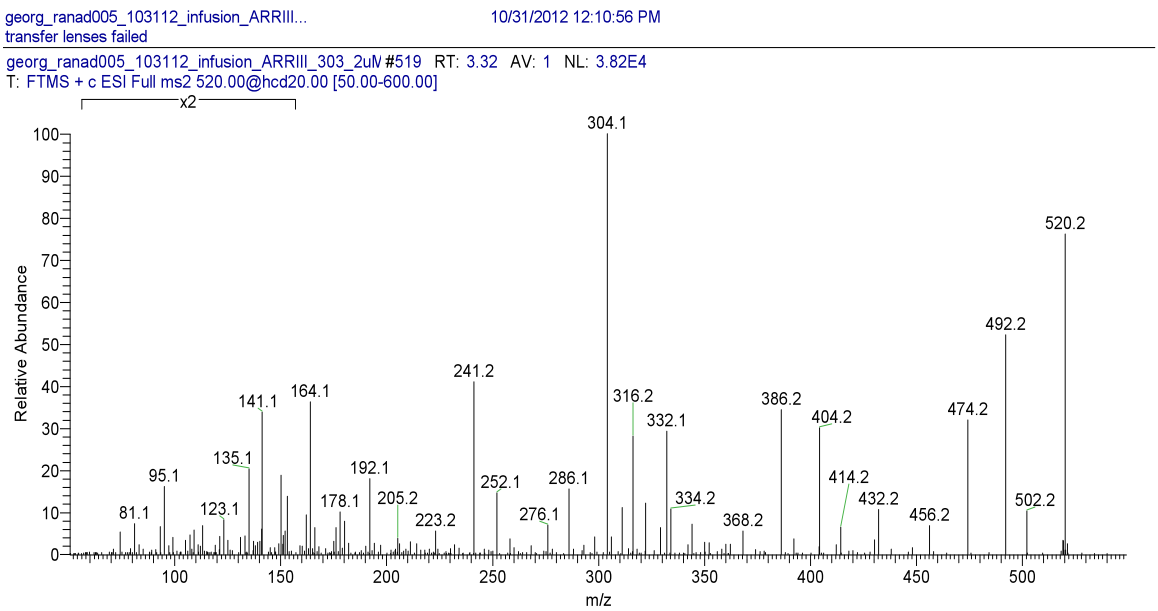

Figure 3.15. Neat Infusion of Photoprobe **3.1**.

Extracted ion chromatograms (XIC's) for probe-specific 'signature ion' peaks (*m/z* values 304, 241 and 164) were generated for every raw MS file; tandem MS that contained all the three fragment ions were visually inspected for the presence of additional probe specific fragment ions. Two spectra were identified as candidates for possible probe-modified peptides. Two spectra with doubly charged precursor ions **701.34** *m/z* from sample A and **709.34** *m/z* from sample B (Figure 3.16), showed numerous probe-related signature ions (135, 141, 164, 176, 178, 304, 316, 386, 404, 474, 492 *m/z*). The doubly charged precursor values were manually deconvoluted to neutral, monoisotopic peptide masses. The difference between the deconvoluted precursor mass 1416.66 (sample B) and 1400.66 (sample A) is 16 Da, which corresponds to a single oxidation. Sample A had light exposure for 10 min whereas sample B was exposed for 60 min. Therefore it is possible that the extra 50 min could oxidize an amino acid residue of a candidate peptide. Theoretical chymotrypsin neutral, monoisotopic peptide masses for

bovine brain beta-tubulin isoform 3 (Q2T9S0 (TBB_BOVIN) from UniProt) was generated using "Protein Prospector" with 1 missed cleave site and oxidized methionine as a variable modification and copied into Excel. The theoretical monoisotopic mass of the probe was added to all peptide masses and the list was compared to the experimental peptide masses calculated manually from the spectra with the probe-specific signature ions. The doubly charged experimental precursor 701.34 *m/z* matched the peptide TARGSQQY and the doubly charged experimental precursor 709.34 *m/z* matched the oxidized version of peptide TARGSQQY.

Further examination of the MS/MS with doubly charged ions 701.34 and 709.34 *m/z* showed **910.43** and **926.43** as singly charged ions respectively (Figures 3.17 and 3.18) as the base peaks. The base peaks in both MS/MS spectra represent intact peptide $[M + H]^{+1}$ values, which indicate that the probe (monoisotopic neutral mass 490.23) dissociated from the peptide with a neutral loss of 490.23 Da (Figures 3.17 and 3.18). Potential dissociation of labile amino acid modifications and loss of site specificity information is well documented for certain classes of modified peptides and certain forms of peptides. Classical examples include phosophorylated peptide dissociation in ion trap and triple quadrupole MS systems[332,333] and glycopeptide analysis.[334] Further inspection of all fragment ions in the tandem MS revealed that probe dissociation was very labile and no peptide b- or y-type fragment ions with the probe attached were present, and site localization of the probe (to a specific amino acid) was not possible. However, numerous peptide b- or y-type peptide fragment ions formed *after* probe dissociation, and the amino acid sequences were confirmed unambiguously. The observation that the probe easily falls off in the MS analysis probably points out that the probe formed a relatively labile

covalent bond with the amino acid residues at the binding site. It is highly unlikely for a carbene of the probe to form a C–C bond and fall off easiliy in the MS analysis. This could mean that the carbene of the probe inserted into an O–H bond of side chains of Thr (T), Ser (S) or Tyr (Y) residues forming a C–O bond, which is relatively weaker than the C–C bond and hence more prone to falling off during the MS analysis. Alternatively, the carbene of the probe could also have possibly inserted into an N–H bond of side chains of either Arg (R) or Gln (Q) residues forming a weak C–N bond, before falling off during MS analysis.

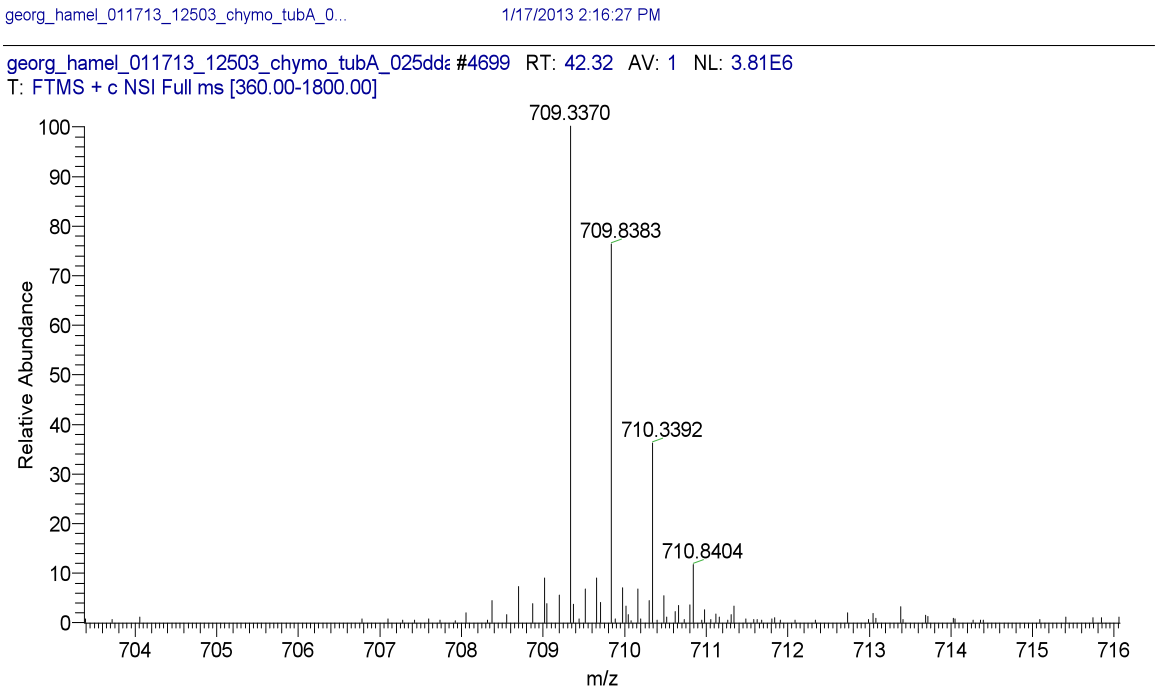

Figure 3.16. Doubly Charged Precursor Ion 709.34 (from Sample B).

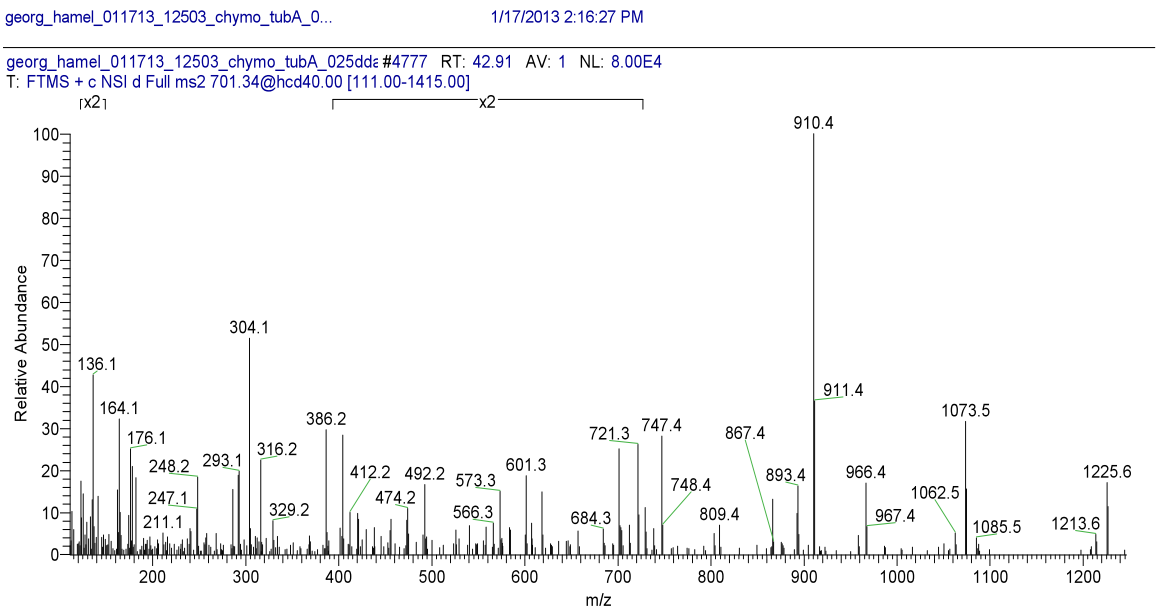

Figure 3.17. MS/MS of Sample A (Chymotrypsin Digestion) of Photoprobe **3.1**.

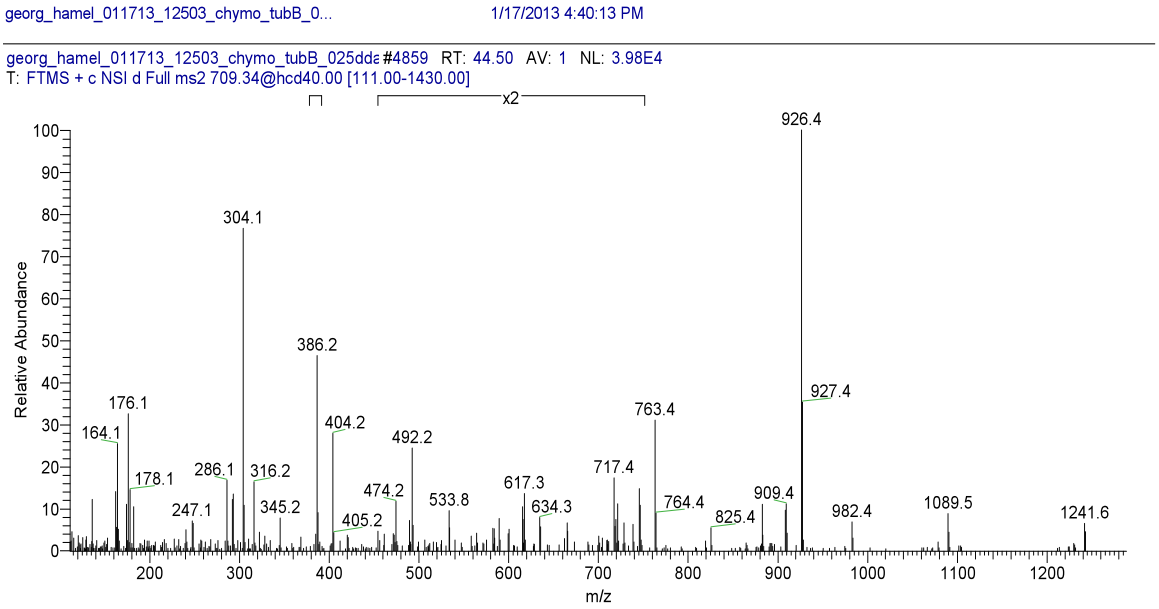

Figure 3.18. MS/MS of Sample B (Chymotrypsin Digestion) of Photoprobe **3.1**.

Comparison of the two experimental tandem MS that contained probe-specific ions to the peptide fragment "TARGSQQY" in the bovine TBB3 isoform (residues 274 to 281),

provided strong support for the peptide match. To address the issue of specificity another experiment was carried out. In this experiment the photoprobe **3.1** was incubated with preformed microtubules prepared from the electrophoretically homogenized bovine brain tubulin with and without a 20-fold excess epothilone B. The two samples were simultaneously illuminated with UV light at 300 nm for 5 min. Other than that, the same photoillumination protocol was followed as shown in Figure 3.14. The target peptide in the specimen "without added epothilone B" was identified. And as expected, the target peptide was not found in the specimen "with added epothilone B". This experiment demonstrated the specificity of binding of the analog to microtubules.

Similar to the photoprobe **3.1**, one sample each was prepared from photoprobes **3.2** and **3.3** by incubation and UV irradiation at 350 nm for 10 minutes. None of the samples showed any labeled peptide fragments. Studies were repeated by carrying out the UV irradiation at 365 and 300 nm as well to check for a possibility of labeling, but no labeling was observed. Finally, the α- and the β-strands of tubulin were isolated and the photoprobes **3.2** and **3.3** were exclusively incubated with β-tubulin, followed by UV irradiation at 300 nm for 10 min. These samples also failed to show any peptide labeling.

3.6.3 Docking Studies

Based on the electron crystallography[258] and NMR[259] models, it is already known that Thr274 and Arg276 are necessary for binding of epothilones in the taxol-binding cavity of β-tubulin. However, both the models predict a very different conformation of epothilone compared to what was found experimentally. The fact that the reactive carbene species generated from the photolysis of the photoprobe **3.1** binds to the peptide

sequence "TARGSQQY" from amino acids 274 to 281 in TBB3 indicates that the thiazole portion of the epothilones must be in vicinity to the aforementioned amino acid residues to facilitate the covalent binding upon photoactivation. In order to visualize this possibility, we carried out docking studies of the photoprobe **3.1** in a homology model of the bovine brain TBB3. Homology modeling was performed using Prime[335] and the docking simulations were performed using Glide.[336] Figure 3.19 shows a 2D model of photoprobe **3.1** docked in homology model of bovine brain tubulin TBB3. The C21 of the photoprobe **3.1** is within H-bond forming distance from the residue Gln280, making the probe possible to bind covalently with the residue upon photolysis.

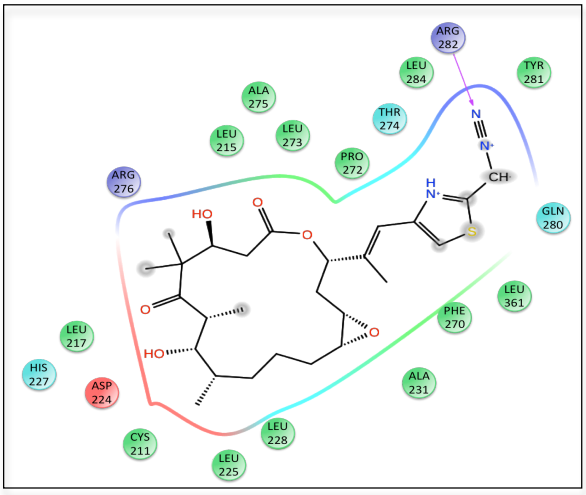

Green = Hydrophobic amino acids, Red = Negatively charged amino acids, Blue = Positively charged amino acids, Cyan = Amino acids with Coulombic interactions, Gray = Solvent exposed

Figure 3.19. 2D Model of Photoprobe **3.1** Docked in Homology Model of Bovine Brain Tubulin TBB3.

Figure 3.20 shows a comparison of the 3D conformations of epothilone A based on the electron-crystallography model (a), NMR model (b) and the conformation of our the photoprobe **3.1** docked in the homology model (c). It can be seen that epothilone still occupies the same binding cavity as predicted by the NMR and EC models, however with a completely different orientation. In both the EC and the NMR model, the thiazole ring is seen in the southwest corner of the binding pocket, whereas in the homology model, the thiazole ring of the photoprobe **3.1** is seen in the northeast corner of the binding pocket. This change in the orientation of the epothilone helps explain the vicinity of the thiazole portion with the region of amino acid residues 270 to 289.

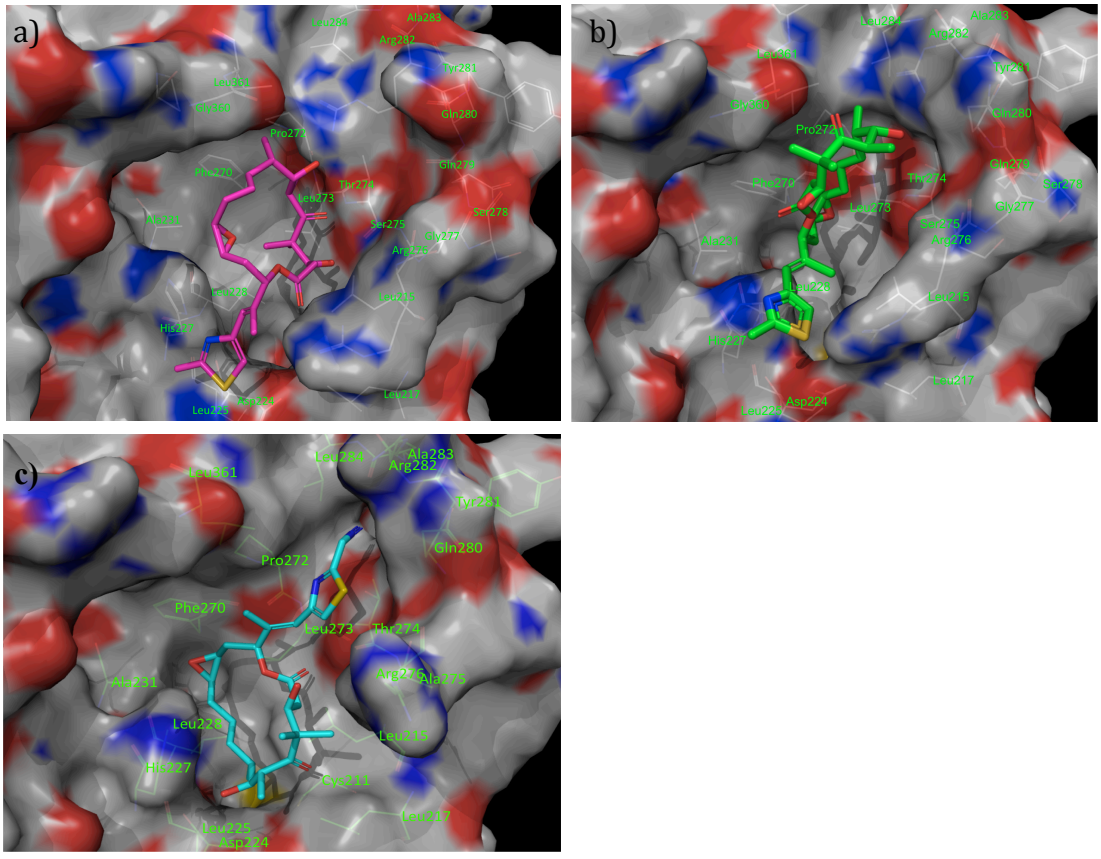

Red = oxygen, Blue = nitrogen, Yellow = sulfur, Gray = carbon, hydrogen

Figure 3.20. Comparison of Binding Poses of Epothilone A and Photoprobe **3.1**. a) Epothilone A in β-Tubulin from Electron Crystallography Model, b) Epothilone A in β-Tubulin from NMR Model, c) Photoprobe **3.1** Docked in Homology Model of Bovine Brain Tubulin TBB3.

3.7 Summary and Discussion

In conclusion, we designed and synthesized epothilone A photoaffinity probes **3.1**, **3.2** and **3.3** but were not able to achieve the synthesis of photoprobe **3.4**. Using photoprobe **3.1** the peptide fragment 'TARGSQQY' (from amino acid 274 to 281) in the β-tubulin isoform TBB3 was identified. This data represents the first labeling of β-tubulin by an epothilone photoaffinity label. The results from the photolabeling studies with the photoprobe **3.1** show a completely different binding mode of epothilones compared to what was predicted by both the electron-crystallography and the NMR models. However, since the photolabile group in the photoprobe **3.1** was situated on C21 of epothilone, we could only get information about the 270–289 region of the β-tubulin. If we had obtained any data from the labeling studies of photoprobes **3.2** and **3.3**, which have the photolabile group at C12–C13 aziridine, then that would have probably given us information about other regions of β-tubulin, thereby giving us a global picture of epothilone binding to the β-tubulin. Nevertheless, since the photoprobes **3.2** and **3.3** showed excellent cytotoxicity and also tubulin assembly activity, we hypothesized that the incorporation of these two photolabels into the tubulin protein may have taken place at such a low level that any labeled peptide fragments could not be detected in the MS studies. Therefore, additional studies are underway with photoprobes **3.2** and **3.3**. Very recently the photolabeling studies of HeLa and MCF-7 cell line tubulins with the photoprobes **3.2** and **3.3** were planned. For this study, our collaborator Dr. Hamel carried out a photoillumination

protocol where, he incubated 25 μM of the photoprobe (**3.2** and **3.3)** with 0.75 M glutamate, 100 μM ddGTP, and 2.5 μM of the tubulin. After a 30 min assembly phase at 37 °C, the samples were exposed to 365 nm UV light. After irradiation, the microtubules were harvested by centrifugation and the collected pellet was sent to our collaborator Dr. LeeAnn Higgins for further MS studies. We are currently awaiting the results from these studies. Additionally, the photolabeling studies with photoprobes **3.2** and **3.3** using chicken erythrocyte (CE) tubulin could also be done. The CE tubulin has only one α-1 and one β-VI isotype, therefore it is less complicated than the bovine brain tubulin and hence relatively easier for mass spectrometry analysis. Also, alternatively, the synthesis and use of radioactive photoprobes derived from compounds **3.2** and **3.3** is another possible approach to detect low levels of labeled peptide fragments that could be pursued in the future.

Chapter 4

Experimental Section

4.1 General Information

All starting materials, reagents and anhydrous solvents were purchased and directly used without further purification or drying unless otherwise specified. Flash column chromatography was carried out on silica gel (230–400 mesh). TLC was conducted on silica gel 250 micron, F_{254} plates. TLC visualization was performed by fluorescence quenching or by using stains such as $KMnO_4$, *p*-anisaldehyde, vanillin and iodine. ^1H NMR spectra were recorded on a 400 MHz NMR instrument. Chemical shifts are reported in ppm relative to chloroform (δ = 7.26 ppm) or with TMS as an internal standard (δ = 0.0 ppm). Data are reported as follows: chemical shift, multiplicity (s = singlet, d = doublet, t = triplet, q = quartet, p = pentet, br = broad, m = multiplet), integration and coupling constants (Hz). ^{13}C NMR spectra were recorded on a 100 MHz NMR spectrometer with complete proton decoupling. Chemical shifts are reported in ppm relative to chloroform (d = 77.2 ppm). High-resolution mass spectrometry was performed using an electrospray ionization (ESI) technique and analyzed by a time-of-flight (TOF) mass analyzer. IR spectra were recorded on a FT-IR spectrometer and are reported in terms of frequency of absorption (cm^{-1}).

4.2 Chapter 1

4.2.1 Synthesis of Cyclic Enaminones 1.7 to 1.11

General procedure: To a solution of 4-methoxypyridine (**1.6**) (0.50 g, 4.58 mmol, 1.00 equiv), in of anhydrous THF (70 mL) at –23 °C was added benzyloxycarbonyl chloride (0.82 g, 4.81 mmol, 1.05 equiv) dropwise. The mixture was stirred at –23 °C for 1.5 h. To this, an appropriate Grignard reagent solution (5.50 mmol, 1.20 equiv) was added

dropwise and the resulting mixture was stirred at –23 °C for 2 h. Then, a saturated oxalic acid solution (20 mL) was added to quench the reaction and the mixture was allowed to warm to rt and stirred for additional 2 h. After this, the aqueous layer was extracted with diethyl ether (3 X 50 mL). The combined ether extracts were washed with sat. aq. Na_2CO_3, brine, dried over K_2CO_3, filtered through Celitepad and concentrated *in vacuo*.

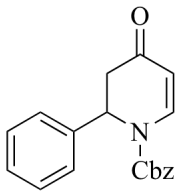

1.7

Benzyl 4-Oxo-2-phenyl-3,4-dihydropyridine-1(2*H*)-carboxylate (1.7). The residue was purified by silica gel flash chromatography (30% EtOAc/hexanes) to afford the title compound **1.7** as a colorless oil (1.41 g, 100%). ^{1}H NMR (400 MHz, $CDCl_3$) δ 2.80 (d, 1H, J = *16* Hz), 3.15 (dd, 1H, J_1 = 8 Hz, J_2 = 18 Hz), 5.19–5.27 (m, 2H), 5.39 (d, 1H, J = 8 Hz), 5.73 (d, 1H, J = 8 Hz), 7.19–7.34 (m, 10H), 7.98 (d, 1H, J = 8 Hz); ^{13}C NMR (100 MHz, $CDCl_3$) δ 41.8, 56.0, 69.2, 108.0, 125.9, 128.0, 128.3, 128.6, 128.7, 128.9, 134.8, 138.4, 142.3, 152.7, 191.1; HRMS calculated for ($C_{19}H_{17}NO_3$) requires *m/z* [M+Na] 330.1106, found *m/z* 330.1118.

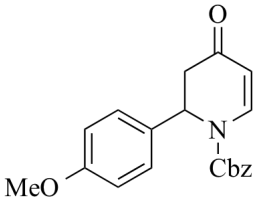

1.8

Benzyl 2-(4-Methoxyphenyl)-4-oxo-3,4-dihydropyridine-1(2*H*)-carboxylate (1.8). The residue was purified by silica gel flash chromatography (30% EtOAc/hexanes) to furnish the title compound **1.8** as colorless oil (1.16 g, 75%). ^{1}H NMR (400 MHz, $CDCl_3$) δ 2.73 (d, 1H, J = 16 Hz), 3.07 (dd, 1H, J_1 = 8 Hz, J_2 = 16 Hz), 3.72 (s, 3H), 5.17–5.26 (m, 2H), 5.35 (d, 1H, J = 8 Hz), 5.67 (d, 1H, J = 8 Hz), 6.78 (d, 2H, J = 8 Hz), 7.12 (d, 2H, J = 8 Hz), 7.26–7.31 (m, 5H), 7.92 (d, 1H, J = 8 Hz); ^{13}C NMR (100 MHz, $CDCl_3$) δ 41.8, 55.2, 55.4, 69.0, 107.8, 114.1, 127.3, 128.3, 128.4, 128.6, 130.6, 134.9, 142.2, 152.7, 159.2, 192.1; HRMS calculated for ($C_{20}H_{19}NO_4$) requires *m/z* [M+Na] 360.1212, found *m/z* 360.1222.

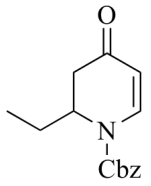

1.9

Benzyl 2-Ethyl-4-oxo-3,4-dihydropyridine-1(2*H*)-carboxylate (1.9). The residue was purified by silica gel flash chromatography (30% EtOAc/hexanes) to give the title compound **1.9** (0.75 g, 65%) as a pale yellow oil. ^{1}H NMR (400 MHz, $CDCl_3$) δ 0.84 (t, 3H, J = 6 Hz), 1.54–1.68 (m, 2H), 2.40 (d, 1H, J = 16 Hz), 2.72 (dd, 1H, J_1 = 8 Hz, J_2 = 12 Hz), 4.47–4.48 (m, 1H), 5.23–5.27 (m, 3H), 7.28–7.37 (m, 5H), 7.74 (d, 1H, J = 8 Hz); ^{13}C NMR (100 MHz, $CDCl_3$) δ 10.2, 23.6, 39.2, 54.6, 68.8, 107.0, 126.7, 128.3, 128.7, 135.1, 141.6, 152.5, 192.8; HRMS calculated for ($C_{15}H_{17}NO_3$) requires *m/z* [M+Na] 282.1106, found *m/z* 282.1089.

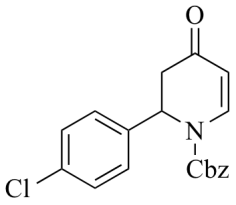

1.10

Benzyl 2-(4-Chlorophenyl)-4-oxo-3,4-dihydropyridine-1(2*H*)-carboxylate (1.10). The residue was purified by silica gel flash chromatography (30% EtOAc/hexanes) to get the title compound **1.10** (1.04 g, 66%) as a yellow oil. ^{1}H NMR (400 MHz, $CDCl_3$) δ 2.68 (d, 1H, J = 16 Hz), 3.05 (dd, 1H, J_1 = 8 Hz, J_2 = 16 Hz), 5.15–5.24 (m, 2H), 5.33 (d, 1H, J = 8 Hz), 5.65 (d, 1H, J = 4 Hz), 7.09 (d, 2H, J = 8 Hz), 7.18–7.29 (m, 7H), 7.92 (d, 1H, J = 8 Hz); ^{13}C NMR (100 MHz, $CDCl_3$) δ 41.5, 55.3, 69.1, 107.8, 127.3, 128.2, 128.6, 128.7, 128.9, 133.7, 134.7, 137.1, 142.1, 152.4, 191.2; HRMS calculated for ($C_{19}H_{16}ClNO_3$) requires *m/z* [M+Na] 364.0716, found *m/z* 364.0722.

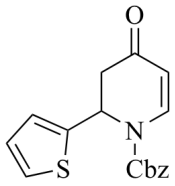

1.11

Benzyl 4-Oxo-2-(thiophen-2-yl)-3,4-dihydropyridine-1(2*H*)-carboxylate (1.11). The residue was purified by silica gel flash chromatography (30% EtOAc/hexanes) to yield the title compound **1.11** (0.96 g, 67%) as a yellow oil. ^{1}H NMR (400 MHz, $CDCl_3$) δ 2.79 (d, 1H, J = 16 Hz), 3.02 (dd, 1H, J_1 = 8 Hz, J_2 = 16 Hz), 5.23–5.29 (m, 2H), 5.35 (d, 1H, J = 8 Hz), 5.91 (d, 1H, J = 8 Hz), 6.81–6.84 (m, 1H), 6.91 (s, 1H), 7.13 (d, 1H, J = 8 Hz), 7.27–7.34 (m, 5H), 7.72 (d, 1H, J = 8 Hz); ^{13}C NMR (100 MHz, $CDCl_3$) δ 41.5,

52.0, 69.2, 107.7, 125.4, 126.1, 126.4, 128.4, 128.6, 128.7, 134.7, 140.9, 152.2, 191.6; HRMS calculated for ($C_{17}H_{15}NO_3S$) requires *m/z* [M+Na] 336.0670, found *m/z* 336.0684.

4.2.2 Synthesis of Piperidinones 1.13 to 1.18

General Procedure for the Synthesis of Piperidinones 1.13 to 1.18. Dihydropyridones **1.7** to **1.11** (1.00 equiv) were dissolved in MeOH (0.50 M). 10% Pd/C was added to the reaction mixture. The flask was evacuated and filled with hydrogen gas using a hydrogen balloon. The reaction mixture was stirred at rt for 12 h and then filtered over a short Celite pad and concentrated *in vacuo*. The crude products obtained were directly used in the next step without further purification. Compound **1.18**, piperidin-4-one was commercially available as a monohydrochloride monohydrate salt and was used directly as is.

4.2.3 Synthesis of Piperidinone Sulfonamides 1.19 to 1.36

General Procedure for the Synthesis of Piperidinone sulfonamides 1.19 to 1.36. To a MeCN (0.30 M) solution of piperidinone **1.13** to **1.18** (1.00 equiv), appropriate arylsulfonyl chloride (1.20 equiv) and K_2CO_3 (2.00 equiv) were added. The reaction mixture was stirred at rt for 24 h. After the reaction was complete as deemed by the TLC, the solvent was removed and EtOAc and water were added to the residue. After extraction, the organic layer was separated and dried over Na_2SO_4 and concentrated *in vacuo*. The crude product thus obtained was then purified by silica gel chromatography to furnish the title compound.

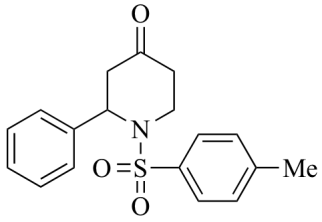

1.19

2-Phenyl-1-tosylpiperidin-4-one (1.19). The residue was purified by silica gel flash chromatography (30% EtOAc/hexanes) to afford the title compound **1.19** (338 mg, 64%) as a colorless film. ^{1}H NMR (400 MHz, $CDCl_3$) δ 2.20–2.26 (m, 1H), 2.38–2.47 (m, 1H), 2.68–2.73 (m, 1H), 2.89–2.94 (m, 1H), 3.10–3.18 (m, 1H), 3.97–4.03 (m, 1H), 5.62 (d, 1H, *J* = 4 Hz), 7.23–7.35 (m, 7H), 7.82 (d, 2H, *J* = 8 Hz); ^{13}C NMR (100 MHz, $CDCl_3$) δ 21.6, 40.3, 43.4, 56.4, 127.1, 127.3, 128.0, 128.8, 130.1, 137.4, 138.4, 144.0, 206.2; HRMS calculated for ($C_{18}H_{19}NO_3S$) requires *m/z* [M+Na] 352.0983, found *m/z* 352.0998.

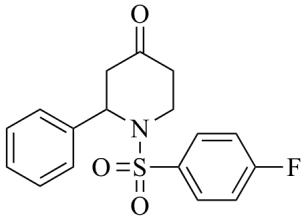

1.20

1-((4-Fluorophenyl)sulfonyl)-2-phenylpiperidin-4-one (1.20). The residue was purified by silica gel flash chromatography (30% EtOAc/hexanes) to furnish the title compound **1.20** (200 mg, 38%) as a film. ^{1}H NMR (400 MHz, $CDCl_3$) δ 2.28–2.33 (m, 1H), 2.45–2.52 (m, 1H), 2.75–2.81 (m, 1H), 2.92–2.97 (m, 1H), 3.14–3.22 (m, 1H), 3.97–4.03 (m, 1H), 5.61 (d, 1H, *J* = 8 Hz), 7.18–7.23 (m, 4H), 7.24–7.31 (m, 3H), 7.91–7.94 (m, 2H); ^{13}C NMR (100 MHz, $CDCl_3$) δ 40.4, 40.5, 43.8, 56.6, 116.8, 127.2, 128.2, 128.9, 129.9, 136.5, 138.1, 166.5, 205.8; HRMS calculated for ($C_{17}H_{16}ClNO_3S$) requires *m/z* [M+Na]

356.0773, found *m/z* 356.0779.

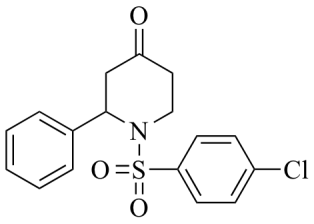

1.21

1-((4-Chlorophenyl)sulfonyl)-2-phenylpiperidin-4-one (1.21). The residue was purified by silica gel flash chromatography (30% EtOAc/hexanes) to yield the title compound **1.21** (190 mg, 34%) as a film. ^{1}H NMR (400 MHz, $CDCl_3$) δ 2.28–2.32 (m, 1H), 2.44–2.52 (m, 1H), 2.73–2.79 (m, 1H), 2.92–2.97 (m, 1H), 3.15–3.22 (m, 1H), 3.96–4.03 (m, 1H), 5.61 (d, 1H, *J = 8 Hz*), 7.18–7.20 (m, 2H), 7.26–7.32 (m, 3H), 7.50 (d, 2H, *J* = 8 Hz), 7.84 (d, 2H, *J* = 8 Hz); ^{13}C NMR (100 MHz, $CDCl_3$) δ 40.4, 40.5, 43.8, 56.6, 127.2, 128.2, 128.5, 128.9, 129.7, 138.0, 138.9, 139.5, 205.7; HRMS calculated for ($C_{17}H_{16}ClNO_3S$) requires *m/z* [M+Na] 372.0437, found *m/z* 372.0444.

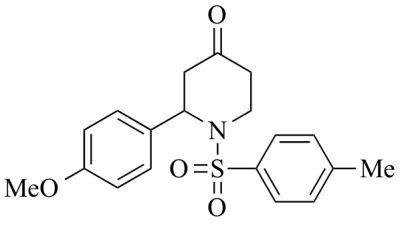

1.22

2-(4-Methoxyphenyl)-1-tosylpiperidin-4-one (1.22). The residue was purified by silica gel chromatography (30% EtOAc/hexanes) to get the title compound **1.22** (59 mg, 48%) as a film. ^{1}H NMR (400 MHz, $CDCl_3$) δ 2.21–2.25 (m, 1H), 2.38–2.47 (m, 4H), 2.66–

2.72 (m, 1H), 2.86–2.91 (m, 1H), 3.09–3.16 (m, 1H), 3.77 (s, 3H), 3.96–4.03 (m, 1H), 5.58 (d, 1H, J = 8 Hz), 6.81 (d, 2H, J = 8 Hz), 7.15 (d, 2H, J = 8 Hz), 7.34 (d, 2H, J = 8 Hz), 7.82 (d, 2H, J = 8 Hz); ^{13}C NMR (100 MHz, $CDCl_3$) δ 21.6, 40.1, 40.3, 43.6, 55.3, 56.0, 114.1, 127.1, 128.6, 130.1, 130.3, 137.6, 144.0, 159.3, 206.4; HRMS calculated for ($C_{19}H_{21}NO_4S$) requires *m/z* [M+Na] 382.1089, found *m/z* 382.1098.

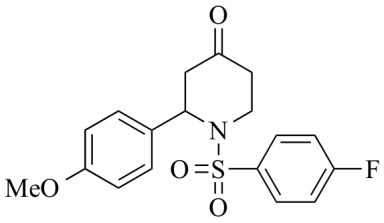

1.23

1-((4-Fluorophenyl)sulfonyl)-2-(4-methoxyphenyl)piperidin-4-one (1.23). The residue was purified by silica gel chromatography (gradient, 10–25% EtOAc/hexanes) to give the title compound **1.23** (41 mg, 23%) as a film. ^{1}H NMR (400 MHz, $CDCl_3$) δ 2.28–2.33 (m, 1H), 2.46–2.54 (m, 1H), 2.75–2.80 (m, 1H), 2.90–2.94 (m, 1H), 3.12–3.20 (m, 1H), 3.78 (s, 3H), 3.95–4.02 (m, 1H), 5.57 (d, 1H, J = 8 Hz), 6.81 (d, 2H, J = 8 Hz), 7.09 (d, 2H, J = 8 Hz), 7.20–7.24 (m, 2H), 7.91–7.94 (m, 2H); ^{13}C NMR (100 MHz, $CDCl_3$) δ 40.2, 40.6, 44.0, 55.3, 56.2, 114.2, 116.8, 128.6, 129.8, 136.6, 159.4, 163.9, 206.1; HRMS calculated for ($C_{18}H_{18}FNO_4S$) requires *m/z* [M+Na] 386.0838, found *m/z* 386.0852.

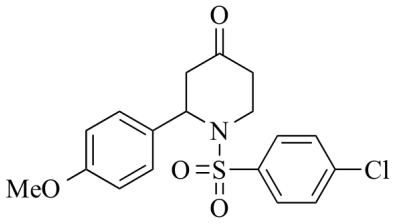

1.24

1-((4-Chlorophenyl)sulfonyl)-2-(4-methoxyphenyl)piperidin-4-one (1.24). The residue was purified by silica gel chromatography (gradient, 10–30% EtOAc/hexanes) to afford the title compound **1.24** (37 mg, 20%) as a film. ^{1}H NMR (400 MHz, $CDCl_3$) δ 2.24–2.28 (m, 1H), 2.40–2.49 (m, 1H), 2.69–2.74 (m, 1H), 2.88–2.92 (m, 1H), 3.10–3.18 (m, 1H), 3.77 (s, 3H), 3.99–4.04 (m, 1H), 5.60 (d, 1H, J = 8 Hz), 6.81 (d, 2H, *J* = 8 Hz), 7.12 (d, 2H, *J* = 8 Hz), 7.56 (d, 2H, *J* = 8 Hz), 7.93 (d, 2H, *J* = 8 Hz); ^{13}C NMR (100 MHz, $CDCl_3$) δ 40.1, 40.4, 43.7, 55.3, 56.1, 114.1, 127.1, 128.6, 129.5, 130.1, 133.1, 140.6, 159.3, 206.4; HRMS calculated for ($C_{18}H_{18}ClNO_4S$) requires *m/z* [M+Na] 402.0543, found *m/z* 402.0533.

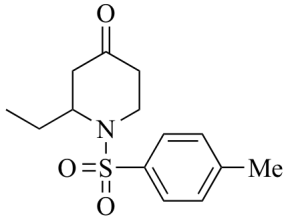

1.25

2-Ethyl-1-tosylpiperidin-4-one (1.25). The residue was purified by silica gel chromatography (gradient, 10–30% EtOAc/hexanes) to furnish the title compound **1.25** (388 mg, 44%) as a film. ^{1}H NMR (400 MHz, $CDCl_3$) δ 0.83 (t, 3H, *J* = 8 Hz), 1.40–1.48 (m, 2H), 2.20–2.27 (m, 2H), 2.34–2.39 (m, 1H), 2.43 (s, 3H), 2.50–2.55 (m, 1H), 3.23–

3.30 (m, 1H), 4.11–4.17 (m, 1H), 4.27–4.32 (m, 1H), 7.33 (d, 2H, J = 8 Hz), 7.78 (d, 2H, J = 8 Hz); ^{13}C NMR (100 MHz, $CDCl_3$) δ 10.5, 21.5, 25.4, 40.0, 40.3, 45.1, 56.1, 127.0, 130.0, 137.6, 143.8, 206.5; HRMS calculated for ($C_{14}H_{19}NO_3S$) requires *m/z* [M+Na] 304.0983, found *m/z* 304.0985.

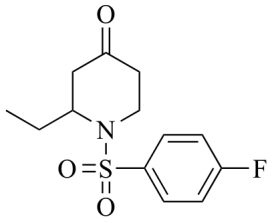

1.26

2-Ethyl-1-((4-fluorophenyl)sulfonyl)piperidin-4-one (1.26). The residue was purified by silica gel chromatography (gradient, 10–30% EtOAc/hexanes) to yield the title compound **1.26** (219 mg, 51%) as a film. ^{1}H NMR (400 MHz, $CDCl_3$) δ 0.80 (t, 3H, J = 8 Hz), 1.41–1.49 (m, 2H), 2.26–2.32 (m, 2H), 2.40–2.45 (m, 1H), 2.56–2.61 (m, 1H), 3.23–3.31 (m, 1H), 4.11–4.16 (m, 1H), 4.26–4.31 (m, 1H), 7.20–7.24 (m, 2H), 7.90–7.94 (m, 2H); ^{13}C NMR (100 MHz, $CDCl_3$) δ 10.5, 25.4, 40.0, 40.5, 45.3, 56.2, 116.7, 129.8, 136.6, 166.4, 206.2; HRMS calculated for ($C_{13}H_{16}FNO_3S$) requires *m/z* [M+Na] 308.0733, found *m/z* 308.0740.

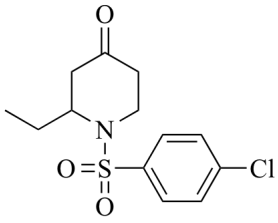

1.27

1-((4-Chlorophenyl)sulfonyl)-2-ethylpiperidin-4-one (1.27). The residue was purified by silica gel chromatography (gradient, 10–30% EtOAc/hexanes) to provide the title compound **1.27** (200 mg, 50%) as a film. ^{1}H NMR (400 MHz, $CDCl_3$) δ 0.80 (t, 3H, J = 8 Hz), 1.42–1.46 (m, 2H), 2.26–2.32 (m, 2H), 2.39–2.48 (m, 1H), 2.55–2.58 (m, 1H), 3.24–3.30 (m, 1H), 4.10–4.15 (m, 1H), 4.28–4.31 (m, 1H), 7.51 (d, 2H, J = 8 Hz), 7.84 (d, 2H, J = 8 Hz); ^{13}C NMR (100 MHz, $CDCl_3$) δ 10.5, 25.4, 40.0, 40.4, 45.3, 56.3, 128.5, 129.7, 139.3, 139.4, 206.3; HRMS calculated for ($C_{13}H_{16}ClNO_3S$) requires *m/z* [M+Na] 324.0437, found *m/z* 324.0444.

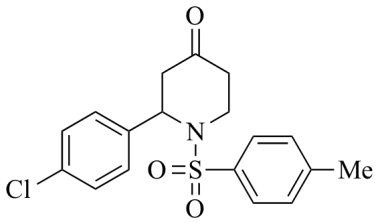

1.28

2-(4-Chlorophenyl)-1-tosylpiperidin-4-one (1.28). The residue was purified by silica gel chromatography (gradient, 10–30% EtOAc/hexanes) to afford the title compound **1.28** (39 mg, 30%) as a film. ^{1}H NMR (400 MHz, $CDCl_3$) δ 2.22–2.27 (m, 1H), 2.40–2.48 (m, 4H), 2.69–2.75 (m, 1H), 2.91–2.95 (m, 1H), 3.10–3.18 (m, 1H), 3.98–4.04 (m, 1H), 5.63 (d, 1H, J = 8 Hz), 7.23 (d, 2H, J = 8 Hz), 7.30 (d, 2H, J = 8 Hz), 7.35 (d, 2H, J = 8 Hz), 7.82 (d, 2H, J = 8 Hz); ^{13}C NMR (100 MHz, $CDCl_3$) δ 21.6, 40.3 (2C), 43.4, 56.4, 127.1, 127.3, 128.0, 128.8, 130.1, 137.5, 138.3, 144.0, 206.3; HRMS calculated for ($C_{18}H_{18}ClNO_3S$) requires *m/z* [M+Na] 386.0594, found *m/z* 386.0601.

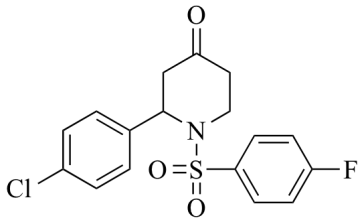

1.29

2-(4-Chlorophenyl)-1-((4-fluorophenyl)sulfonyl)piperidin-4-one (1.29). The residue was purified by silica gel chromatography (gradient, 10–30% EtOAc/hexanes) to furnish the title compound **1.29** (96 mg, 69%) as a film. ^{1}H NMR (400 MHz, $CDCl_3$) δ 2.30–2.33 (m, 1H), 2.49–2.50 (m, 1H), 2.78–2.80 (m, 1H), 2.94–2.97 (m, 1H), 3.16–3.21 (m, 1H), 3.99–4.01 (m, 1H), 5.61 (d, 1H, *J* = 8 Hz), 7.19 (m, 4H), 7.28 (m, 2H), 7.92 (m, 2H); ^{13}C NMR (100 MHz, $CDCl_3$) δ 40.4 (2C), 43.8, 56.6, 116.8, 127.2, 128.2, 128.9, 129.9, 136.4, 138.1, 166.5, 205.8; HRMS calculated for ($C_{17}H_{15}ClFNO_3S$) requires *m/z* [M+Na] 390.0343, found *m/z* 390.0339.

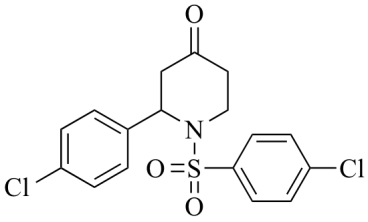

1.30

2-(4-Chlorophenyl)-1-((4-chlorophenyl)sulfonyl)piperidin-4-one (1.30). The residue was purified by silica gel chromatography (gradient, 10–30% EtOAc/hexanes) to give the title compound **1.30** (38 mg, 31%) as a film. ^{1}H NMR (400 MHz, $CDCl_3$) δ 2.30–2.34 (m, 1H), 2.47–2.55 (m, 1H), 2.76–2.79 (m, 1H), 2.95–2.98 (m, 1H), 3.15–3.21 (m, 1H), 3.98–4.01 (m, 1H), 5.61 (d, 1H, *J* = 8 Hz), 7.18 (m, 2H), 7.29 (m, 2H), 7.51 (m, 2H), 7.83

(m, 2H); ^{13}C NMR (100 MHz, $CDCl_3$) δ 40.5 (2C), 43.8, 56.6, 127.2, 128.2, 128.5, 128.9, 129.7, 138.0, 138.9, 139.6, 205.7; HRMS calculated for ($C_{17}H_{15}Cl_2NO_3S$) requires *m/z* [M+Na] 406.0047, found *m/z* 406.0039.

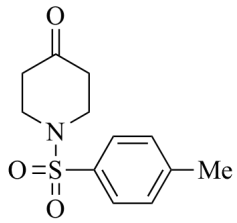

1.31

1-Tosylpiperidin-4-one (1.31). The residue was purified by silica gel chromatography (gradient, 10–30% EtOAc/hexanes) to get the title compound **1.31** (376 mg, 91%) as a film. ^{1}H NMR (400 MHz, $CDCl_3$) δ 2.39 (s, 3H), 2.47–2.50 (m, 4H), 3.32–3.35 (m, 4H), 7.30 (d, 2H, J = 8 Hz), 7.63 (d, 2H, J = 8 Hz); ^{13}C NMR (100 MHz, $CDCl_3$) δ 21.5, 40.6, 45.8, 127.5, 129.9, 133.3, 144.1, 205.6; HRMS calculated for ($C_{12}H_{15}NO_3S$) requires *m/z* [M+Na] 276.0670, found *m/z* 276.0673.

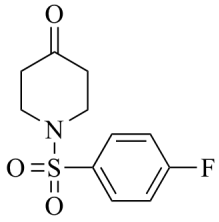

1.32

1-((4-Fluorophenyl)sulfonyl)piperidin-4-one (1.32). The residue was purified by silica gel chromatography (gradient, 10–30% EtOAc/hexanes) to afford the title compound **1.32** (389 mg, 93%) as a film. ^{1}H NMR (400 MHz, $CDCl_3$) δ 2.54–2.57 (m, 4H), 3.39–

3.42 (m, 4H), 7.22–7.27 (m, 2H), 7.81–7.85 (m, 2H); ^{13}C NMR (100 MHz, $CDCl_3$) δ 40.6, 45.8, 116.5, 116.8, 130.2, 130.3, 132.6, 166.6, 205.2; HRMS calculated for ($C_{11}H_{12}FNO_3S$) requires *m/z* [M+Na] 280.0420, found *m/z* 280.0422.

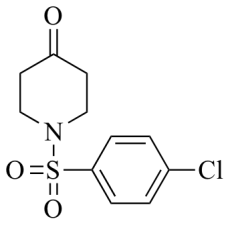

1.33

1-((4-Chlorophenyl)sulfonyl)piperidin-4-one (1.33). The residue was purified by silica gel chromatography (gradient, 10–30% EtOAc/hexanes) to provide the title compound **1.33** (760 mg, 85%) as a film. ^{1}H NMR (400 MHz, $CDCl_3$) δ 2.53–2.56 (m, 4H), 3.39–3.42 (m, 4H), 7.54 (d, 2H, *J* = 8 Hz), 7.75 (d, 2H, *J* = 8 Hz); ^{13}C NMR (100 MHz, $CDCl_3$) δ 40.5, 45.7, 128.9, 129.6, 135.0, 139.7, 205.1; HRMS calculated for ($C_{11}H_{12}ClNO_3S$) requires *m/z* [M+Na] 296.0124, found *m/z* 296.0126.

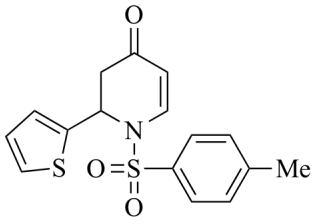

1.34

2-(Thiophen-2-yl)-1-tosyl-2,3-dihydropyridin-4(1*H*)-one (1.34). The residue was purified by silica gel chromatography (gradient, 10–30% EtOAc/hexanes) to furnish the title compound **1.34** (0.18 g, 52%) as a film. ^{1}H NMR (400 MHz, $CDCl_3$) δ 2.40 (s, 3H),

2.70 (dd, 1H, J_1 = 6.6 Hz, J_2 = 16.6 Hz), 2.83 (dd, 1H, J_1 = 6.6 Hz, J_2 = 16.6 Hz), 5.44 (d, 1H, J = 9.3 Hz), 5.79 (d, 1H, J = 6.6 Hz), 6.81 (dd, 1H, J_1 = 3.6 Hz, J_2 = 5.1 Hz), 6.90 (d, 1H, J = 3.5 Hz), 7.11 (dd, 1H, J_1 = 1.1 Hz, J_2 = 5.1 Hz), 7.25 (d, 2H, J = 8.2 Hz), 7.60–7.65 (m, 3H); ^{13}C NMR (100 MHz, $CDCl_3$) δ 21.6, 42.2, 54.3, 108.5, 125.9, 126.3, 126.9, 127.0, 130.1, 135.5, 139.9, 141.5, 145.0, 190.3; HRMS calculated for ($C_{16}H_{15}NO_3S_2$) requires *m/z* [M+Na] 356.0391, found *m/z* 356.0398.

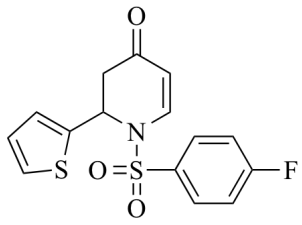

1.35

1-((4-Fluorophenyl)sulfonyl)-2-(thiophen-2-yl)-2,3-dihydropyridin-4(1*H*)-one (1.35)

The residue was purified by silica gel chromatography (gradient, 10–30% EtOAc/hexanes) to get the title compound **1.35** (0.15 g, 43%) as a film. ^{1}H NMR (400 MHz, $CDCl_3$) δ 2.71 (dd, 1H, J_1 = 6.8 Hz, J_2 = 16.5 Hz), 2.95 (dd, 1H, J_1 = 6.8 Hz, J_2 = 16.5 Hz), 5.49 (d, 1H, J = 8.4 Hz), 5.84 (d, 1H, J = 6.5 Hz), 6.80 (m, 1H), 6.89 (d, 1H, J = 3.1 Hz), 7.09 (m, 3H), 7.64 (d, 1H, J = 8.4 Hz), 7.69–7.72 (m, 2H); ^{13}C NMR (100 MHz, $CDCl_3$) δ 42.7, 54.6, 108.8, 116.6, 126.1, 126.3, 127.1, 129.9, 134.4, 139.5, 141.2, 166.8, 190.1; HRMS calculated for ($C_{15}H_{12}FNO_3S_2$) requires *m/z* [M+Na] 360.0140, found *m/z* 360.0145.

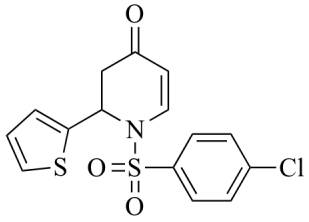

1.36

1-((4-Chlorophenyl)sulfonyl)-2-(thiophen-2-yl)-2,3-dihydropyridin-4(1*H*)-one (1.36). The residue was purified by silica gel chromatography (gradient, 10–30% EtOAc/hexanes) to give the title compound **1.36** (0.20 g, 55%) as a film. ^{1}H NMR (400 MHz, $CDCl_3$) δ 2.71 (dd, 1H, J_1 = 6.8 Hz, J_2 = 16.5 Hz), 2.94 (dd, 1H, J_1 = 6.8 Hz, J_2 = 16.5 Hz), 5.49 (d, 1H, J = 9.3 Hz), 5.83 (d, 1H, J = 6.7 Hz), 6.80 (dd, 1H, J_1 = 3.6 Hz, J_2 = 5.0 Hz), 6.89 (d, 1H, J = 3.4 Hz), 7.10 (dd, 1H, J_1 = 1.1 Hz, J_2 = 5.1 Hz). 7.38 (d, 2H, J = 8.7 Hz), 7.61–7.64 (m, 3H); ^{13}C NMR (100 MHz, $CDCl_3$) δ 42.6, 54.6, 108.9, 126.1, 126.3, 127.1, 128.4, 129.6, 136.8, 139.4, 140.5, 141.1, 190.0; HRMS calculated for ($C_{15}H_{12}ClNO_3S_2$) requires *m/z* [M+Na] 375.9845, found *m/z* 375.9847.

4.3 Chapter 2

For chapter 2 experiments, the ^{19}F NMR spectra for the optimization reactions were recorded at 376 MHz and were referenced based on the internal standard C_6F_6 (d = –161.7 ppm); all reactions were carried out in clear 2–dram vials used after drying; all the reported yields are averages of at least two experimental runs.

4.3.1 Synthesis of Starting Enaminones

Cyclic enaminones for preparing compounds **2.2**, **2.14**, **2.16–2.18** and 1,3,-dimethyluracil for the synthesis of compound **2.15**, were commercially available. The other cyclic

enaminones were prepared according to the reported procedures[6,8,10,96,337-339] by former group member Dr. Yiyun Yu.

4.3.2 Synthesis of 5-Trifluoromethylated Cyclic Enaminones

General Procedures for the C5–Trifluoromethylation of Cyclic Enaminones:

In a 2-dram PTFE sealed glass vial the enaminone (0.1 mmol) and $PhI(OAc)_2$ (64.4 mg, 0.2 mmol) were added. The glass vial was transferred to a glove box to add KF (23.5 mg, 0.4 mmol). The vial was then capped and taken out of the glove box. $TMSCF_3$ (59.7 µL, 0.4 mmol) and anhydrous MeCN (1.0 mL) were added by syringes. The reaction mixture was then stirred at rt for 24 h. After completion of the reaction, the mixture was diluted by addition of acetone, filtered over a pad of Celite and eluted with acetone. After the eluent was concentrated *in vacuo*, the residue was purified by silica gel chromatography (0-100% EtOAc/hexanes, gradient) using the Combiflash Rf system, to give the desired compounds **2.2–2.18**.

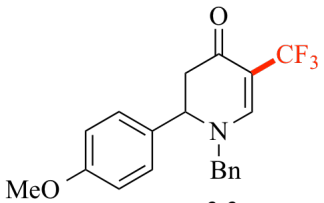

2.2

1-Benzyl-2-(4-methoxyphenyl)-5-(trifluoromethyl)-2,3-dihydropyridin-4(1*H*)-one (2.2). The title compound **2.2** was obtained as a yellow oil (21.3 mg, 59%). IR (thin film) 2925, 1658, 1618, 1513, 1394, 1357, 1326, 1253, 1122, 1030 cm^{-1}; ^1H NMR (400 MHz, $CDCl_3$) δ 2.69 (dd, 1H, J = 16.5, 6.6 Hz), 2.89 (dd, 1H, J = 16.5, 7.3), 3.81 (s, 3H), 4.25 (d, 1H, J = 15.0 Hz), 4.43 (d, 1H, J = 15.0 Hz), 4.51 (t, 1H, J = 7.0), 6.88 (d, 2H, J = 8.6

Hz), 7.10–7.14 (m, 4H) 7.35–7.42 (m, 3H), 7.73 (s, 1H); ^{13}C NMR (100 MHz, $CDCl_3$) δ 43.3, 55.4, 58.1, 59.7, 100.0 (q, *J* = 29.8 Hz), 114.7, 123.9 (d, *J* = 268.0 Hz), 127.7, 128.2, 128.8, 129.1, 130.4, 134.6, 152.5 (q, *J* = 5.4 Hz), 159.9, 185.2; ^{19}F NMR (376 MHz, $CDCl_3$) δ –60.9 (s, 3F); HRMS calculated for ($C_{20}H_{18}F_3NO_2$) requires *m/z* [M+Na] 384.1182, found *m/z* 384.1187.

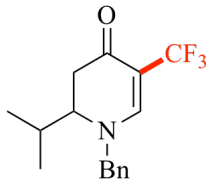

2.3

1-Benzyl-2-isopropyl-5-(trifluoromethyl)-2,3-dihydropyridin-4(1*H*)-one (2.3). The title compound **2.3** was obtained as a yellow oil (23.2 mg, 78%). IR (thin film) 2967, 1655, 1618, 1454, 1396, 1351, 1329, 1099, 1024, 700 cm^{-1}; ^{1}H NMR (400 MHz, $CDCl_3$) δ 0.97 (d, 3H, *J* = 6.8 Hz), 1.00 (d, 3H, *J* = 6.9 Hz), 2.21–2.31 (m, 1H), 2.48 (dd, 1H, *J* = 16.7, 7.7 Hz), 2.62 (dd, 1H, *J* = 16.7, 7.7 Hz), 3.29–3.32 (m, 1H), 4.49–4.61 (m, 2H), 7.28 (d, 2H, *J* = 7.3 Hz), 7.37–7.45 (m, 3H), 7.61 (s, 1H); ^{13}C NMR (100 MHz, $CDCl_3$) δ 17.8, 19.6, 29.2, 36.5, 59.6, 61.3, 99.5 (q, *J* = 30.1 Hz), 124.0 (q, *J* = 270.0 Hz), 127.4, 128.8, 129.3, 135.3, 151.8 (q, *J* = 5.4 Hz), 185.9; ^{19}F NMR (376 MHz, $CDCl_3$) δ –60.8 (s, 3F); HRMS calculated for ($C_{16}H_{18}F_3NO$) requires *m/z* [M+Na] 320.1233, found *m/z* 320.1238.

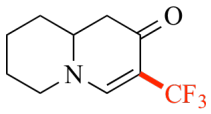

2.4

3-(Trifluoromethyl)-1,6,7,8,9,9a-hexahydro-2*H*-quinolizin-2-one (2.4). The title compound **2.4** was obtained as a pale yellow oil (14.5 mg, 66%). IR (thin film) 2943, 2862, 1655, 1620, 1450, 1397, 1372, 1346, 1214, 1184, 1139, 1102, 999 cm^{-1}; ^{1}H NMR (400 MHz, $CDCl_3$) δ 1.40–1.67 (m, 3H), 1.81–1.92 (m, 3H), 2.41 (dd, 1H, *J* = 16.6, 5.9 Hz), 2.60 (dd, 1H, *J* = 16.5, 12.1 Hz), 3.16–3.23 (m, 1H), 3.43–3.54 (m, 2H), 7.34 (s, 1H); ^{13}C NMR (100 MHz, $CDCl_3$) δ 22.9, 25.7, 31.6, 42.6, 53.9, 56.6, 100.5 (q, *J* = 29.8 Hz), 123.8 (q, *J* = 270.0 Hz), 152.7 (q, *J* = 5.5 Hz), 186.4; ^{19}F NMR (376 MHz, $CDCl_3$) δ –61.1 (s, 3F); HRMS calculated for ($C_{10}H_{12}F_3NO$) requires *m/z* [M+Na] 242.0763, found *m/z* 242.0763.

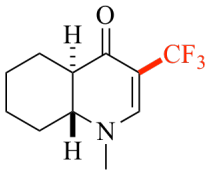

2.5

(4a*R,8a*R**)-1-Methyl-3-(trifluoromethyl)-4a,5,6,7,8,8a-hexahydroquinolin-4(1*H*)-one (2.5)**. The title compound **2.5** was obtained as a colorless oil (14.2 mg, 61%). IR (thin film) 3046, 2946, 2867, 1641, 1618, 1441, 1388, 1355, 1319, 1311, 1179, 1119, 1096, 1073 cm^{-1}; ^{1}H NMR (400 MHz, $CDCl_3$) δ 1.03–1.20 (m, 2H), 1.26–1.33 (m, 1H), 1.37–1.46 (m, 1H), 1.83 (d, 1H, *J* = 12.5 Hz), 1.89 (d, 1H, *J* = 12.6 Hz), 2.08–2.14 (m, 1H), 2.23–2.27 (m, 1H), 2.43 (d, 1H, *J* = 12.8 Hz), 3.09 (s, 3H), 3.12–3.19 (m, 1H), 7.44

(s, 1H); ^{13}C NMR (100 MHz, $CDCl_3$) δ 24.3, 24.4, 24.5, 30.0, 40.0, 48.0, 61.2, 100.0 (q, J = 29.5 Hz), 124.0 (q, J = 269.8 Hz), 153.4 (q, J = 5.5 Hz), 188.4; ^{19}F NMR (376 MHz, $CDCl_3$) δ –60.9 (s, 3F); HRMS calculated for ($C_{11}H_{14}F_3NO$) requires *m/z* [M+Na] 256.0920, found *m/z* 256.0919.

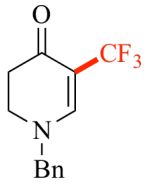

2.6

1-Benzyl-5-(trifluoromethyl)-2,3-dihydropyridin-4(1*H*)-one (2.6). The title compound **2.6** was obtained as a pale yellow oil (17.1 mg, 67%). IR (thin film) 3033, 1655, 1619, 1453, 1399, 1361, 1334, 1253, 1148, 1121, 1098, 1017 cm^{-1}; ^{1}H NMR (400 MHz, $CDCl_3$) δ 2.51 (t, 2H, J = 7.8 Hz), 3.47 (t, 2H, J = 7.8 Hz), 4.50 (s, 2H), 7.28 (d, 2H, J = 7.0 Hz), 7.37–7.45 (m, 3H), 7.65 (s, 1H); ^{13}C NMR (100 MHz, $CDCl_3$) δ 35.1, 46.0, 60.6, 100.3 (q, J = 29.8 Hz), 124.0 (q, J = 270.0 Hz), 127.7, 128.9, 129.3, 134.3, 152.6 (q, J = 5.5 Hz), 186.0; ^{19}F NMR (376 MHz, $CDCl_3$) δ –60.9 (s, 3F); HRMS calculated for ($C_{13}H_{12}F_3NO$) requires *m/z* [M+Na] 278.0763, found *m/z* 278.0774.

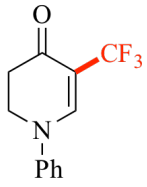

2.7

1-Phenyl-5-(trifluoromethyl)-2,3-dihydropyridin-4(1*H*)-one (2.7). The title compound

2.7 was obtained as a pale yellow oil (19.5 mg, 81%). IR (thin film) 1666, 1619, 1590, 1497, 1396, 1354, 1324, 1267, 1127, 1045, 1012, 755, 695, 605 cm^{-1}; ^{1}H NMR (400 MHz, $CDCl_3$) δ 2.67 (t, 2H, *J* = 7.6 Hz), 4.04 (t, 2H, *J* = 7.6 Hz), 7.14 (d, 2H, *J* = 8.2 Hz), 7.23 (t, 1H, *J* = 6.9 Hz), 7.39 (t, 2H, *J* = 7.8 Hz), 7.80 (s, 1H); ^{13}C NMR (100 MHz, $CDCl_3$) δ 35.6, 47.9, 103.6 (q, *J* = 30.0 Hz), 119.5, 123.5 (q, *J* = 270.0 Hz), 126.3, 129.9, 144.4, 149.4 (q, *J* = 5.7 Hz), 186.3; ^{19}F NMR (376 MHz, $CDCl_3$) δ –61.4 (s, 3F); HRMS calculated for ($C_{12}H_{10}F_3NO$) requires *m/z* [M+Na] 264.0607, found *m/z* 264.0608.

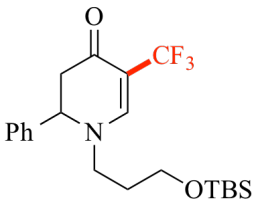

2.8

1-(3-((tert-Butyldimethylsilyl)oxy)propyl)-2-phenyl-5-(trifluoromethyl)-2,3-dihydropyridin-4(1*H*)-one (2.8). The title compound **2.8** was obtained as a yellow oil (16.5 mg, 40%). IR (thin film) 2954, 2930, 2858, 1661, 1619, 1452, 1396, 1346, 1326, 1258, 1154, 1102, 972, 837, 777, 699 cm^{-1}; ^{1}H NMR (400 MHz, $CDCl_3$) δ 0.00 (s, 6H), 0.84 (s, 9H), 1.66–1.72 (p, 2H, *J* = 6.6, 6.2 Hz), 2.69 (dd, 1H, *J* = 16.5, 6.2 Hz), 2.94 (dd, 1H, *J* = 16.5, 7.4 Hz), 3.28 (dt, 1H, *J* = 13.6, 6.1 Hz), 3.41 (dt, 1H, *J* = 14.6, 7.5 Hz), 3.60 (qt, 2H, *J* = 10.8, 5.4 Hz), 4.66 (t, 1H, *J* = 6.8 Hz), 7.21 (d, 2H, *J* = 6.9 Hz), 7.30–7.35 (m, 3H), 7.63 (s, 1H); ^{13}C NMR (100 MHz, $CDCl_3$) δ –5.5, 18.1, 25.8, 31.2, 43.2, 51.1, 58.7, 60.6, 100.0 (q, *J* = 30.0 Hz), 123.9 (q, *J* = 270.0 Hz), 126.6, 128.8, 129.3, 137.4, 152.9 (q, *J* = 5.4 Hz), 184.7; ^{19}F NMR (376 MHz, $CDCl_3$) δ –60.8 (s, 3F); HRMS calculated for ($C_{21}H_{30}F_3NO_2Si$) requires *m/z* [M+Na] 436.1896, found *m/z* 436.1903.

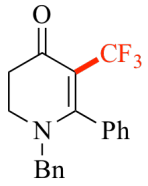

2.9

1-Benzyl-6-phenyl-5-(trifluoromethyl)-2,3-dihydropyridin-4(1*H*)-one (2.9). The title compound **2.9** was obtained as a pale yellow oil (24.8 mg, 75%). IR (thin film) 3031, 2918, 1652, 1533, 1463, 1439, 1383, 1322, 1255, 1240, 1119, 1092, 766, 701 cm^{-1}; ^{1}H NMR (400 MHz, $CDCl_3$) δ 2.45 (t, 2H, J = 7.2 Hz), 3.67 (t, 2H, J = 7.2 Hz), 4.28 (s, 2H), 7.14 (d, 2H, J = 7.1 Hz), 7.31–7.36 (m, 5H), 7.42–7.51 (m, 3H); ^{13}C NMR (100 MHz, $CDCl_3$) δ 36.0, 46.9, 55.6, 102.9 (q, J = 27.8 Hz), 124.4 (q, J = 270.0 Hz), 127.2, 127.9, 128.4, 128.8, 129.1, 130.2, 133.2, 135.9, 165.0, 187.9; ^{19}F NMR (376 MHz, $CDCl_3$) δ –52.3 (s, 3F); HRMS calculated for ($C_{19}H_{16}F_3NO$) requires *m/z* [M+Na] 354.1076, found *m/z* 354.1083.

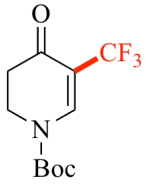

2.10

***tert*-Butyl 4-oxo-5-(trifluoromethyl)-3,4-dihydropyridine-1(2*H*)-carboxylate (2.10)**. The title compound **2.10** was obtained as a yellow oil (17.5 mg, 66%). IR (thin film) 2983, 1741, 1687, 1625, 1387, 1372, 1322, 1279, 1261, 1248, 1124, 1049, 1012, 883, 842, 759, 735, 684 cm^{-1}; ^{1}H NMR (400 MHz, $CDCl_3$) δ 1.56 (s, 9H), 2.62 (t, 2H, J = 7.4 Hz), 4.01 (t, 2H, J = 7.4 Hz), 8.31 (s, 1H); ^{13}C NMR (100 MHz, $CDCl_3$) δ 27.9, 35.4,

42.2, 85.3, 107.9 (q, J = 30.4 Hz), 122.5 (q, J = 271.3 Hz), 144.9 (q, J = 6.3 Hz), 150.5, 187.7; ^{19}F NMR (376 MHz, $CDCl_3$) δ –62.9 (s, 3F); HRMS calculated for ($C_{11}H_{14}F_3NO_3$) requires *m/z* [M+Na] 288.0818, found *m/z* 288.0820.

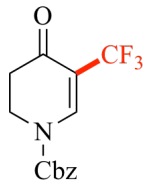

2.11

Benzyl 4-Oxo-5-(trifluoromethyl)-3,4-dihydropyridine-1(2*H*)-carboxylate (2.11). The title compound **2.11** was obtained as a colorless to pale yellow oil (18.3 mg, 61%). IR (thin film) 2984, 1742, 1687, 1627, 1388, 1322, 1270, 1238, 1206, 1135, 1049, 1002, 952, 756, 699 cm^{-1}; ^{1}H NMR (400 MHz, $CDCl_3$) δ 2.64 (t, 2H, J = 7.4 Hz), 4.09 (t, 2H, J = 7.4 Hz), 5.32 (s, 2H), 7.41 (s, 5H), 8.36 (s, 1H); ^{13}C NMR (100 MHz, $CDCl_3$) δ 35.4, 42.5, 70.1, 109.0 (q, J = 30.1 Hz), 122.3 (q, J = 271.5 Hz), 128.8, 128.9, 129.2, 134.2, 144.4 (q, J = 5.9 Hz), 152.0, 187.4; ^{19}F NMR (376 MHz, $CDCl_3$) δ –63.0 (s, 3F); HRMS calculated for ($C_{14}H_{12}F_3NO_3$) requires *m/z* [M+Na] 322.0661, found *m/z* 322.0668.

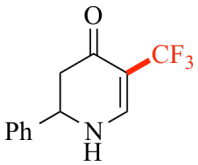

2.12

2-Phenyl-5-(trifluoromethyl)-2,3-dihydropyridin-4(1*H*)-one (2.12). The title compound **2.12** was obtained as a colorless flaky semi-solid to sticky oil (5.5 mg, 23%). IR (thin film) 3219, 1640, 1599, 1539, 1388, 1358, 1322, 1271, 1246, 1197, 1106, 1021,

746, 699, 606, 543 cm^{-1}; ^{1}H NMR (400 MHz, $CDCl_3$) δ 2.61 (dd, 1H, *J* = 16.4, 5.1 Hz), 2.78 (dd, 1H, *J* = 16.3, 5.1 Hz), 4.82 (dd, 1H, *J* = 14.1, 5.0 Hz), 5.80 (br s, 1H), 7.34–7.44 (m, 5H), 7.72 (d, 1H, *J* = 7.2 Hz); ^{13}C NMR (100 MHz, $CDCl_3$) δ 43.8, 57.9, 102.0 (q, *J* = 30.2 Hz), 123.7 (q, *J* = 268.0 Hz), 126.5, 129.1, 129.3, 138.4, 150.2 (q, *J* = 5.5 Hz), 186.7; ^{19}F NMR (376 MHz, $CDCl_3$) δ –61.4 (s, 3F); HRMS calculated for ($C_{12}H_{10}F_3NO$) requires *m/z* [M+Na] 264.0607, found *m/z* 264.0600.

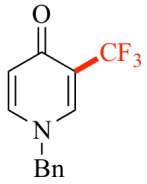

2.13

1-Benzyl-3-(trifluoromethyl)pyridin-4(1*H*)-one (2.13). The title compound **2.13** was obtained as a colorless to pale yellow oil (11.5 mg, 45%). IR (thin film) 1662, 1593, 1490, 1456, 1335, 1208, 1161, 1123, 1054, 838, 733, 700 cm^{-1}; ^{1}H NMR (400 MHz, $CDCl_3$) δ 5.02 (s, 2H), 6.52 (d, *J* = 7.7 Hz, 1H), 7.21–7.23 (m, 2H), 7.38–7.46 (m, 4H), 7.79 (s, 1H); ^{13}C NMR (100 MHz, $CDCl_3$) 60.8, 119.1 (q, *J* = 29.5 Hz), 121.4, 125.6 (q, *J* = 270.8 Hz), 127.6, 129.5, 129.6, 133.7, 139.8 (q, *J* = 6.4 Hz), 140.5, 174.0; ^{19}F NMR (376 MHz, $CDCl_3$) δ –65.2 (s, 3F); HRMS calculated for ($C_{13}H_{10}F_3NO$) requires *m/z* [M+Na] 276.0607, found *m/z* 276.0615.

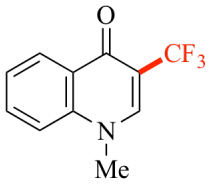

2.14

1-Methyl-3-(trifluoromethyl)quinolin-4(1*H*)-one (2.14). The title compound **2.14** was obtained as a white to very pale yellow oil (10.0 mg, 44%). IR (thin film) 1644, 1596, 1508, 1477, 1367, 1251, 1228, 1175, 1112, 1081, 879, 760, 704 cm^{-1}; ^{1}H NMR (400 MHz, $CDCl_3$) δ 3.88 (s, 3H), 7.46 (m, 2H), 7.74 (m, 1H), 7.93 (s, 1H), 8.48 (d, 1H, J = 8.0 Hz); ^{13}C NMR (100 MHz, $CDCl_3$) δ 41.3, 100.0, 110.9 (q, J = 29.5 Hz), 115.6, 120.8 (q, J = 270.2 Hz), 125.1, 127.2, 127.6, 133.2, 140.3, 142.9 (q, J = 6.1 Hz), 173.8; ^{19}F NMR (376 MHz, $CDCl_3$) δ –63.6 (s, 3F); HRMS calculated for ($C_{11}H_8F_3NO$) requires *m/z* [M+Na] 250.0450, found *m/z* 250.0457.

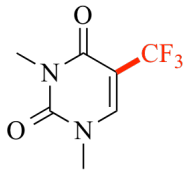

2.15

1,3-Dimethyl-5-(trifluoromethyl)pyrimidine-2,4(1*H*,3*H*)-dione (2.15). The title compound **2.15** was obtained as a colorless oil (9.6 mg, 46%) (61% bsrm). The spectral data of the title compound was in agreement with those found in the literature.[164] IR (thin film) 3082, 1720, 1674, 1492, 1459, 1385, 1326, 1212, 1127, 1019, 782, 759, 699 cm^{-1}; ^{1}H NMR (400 MHz, $CDCl_3$) δ 3.36 (s, 3H), 3.48 (s, 3H), 7.67 (s, 1H); ^{13}C NMR (100 MHz, $CDCl_3$) δ 28.0, 37.7, 104.1 (q, J = 33.0 Hz), 122.0 (q, J = 270.0 Hz), 143.5 (q, J =

5.8 Hz), 150.9, 158.7; ^{19}F NMR (376 MHz, $CDCl_3$) δ –63.8 (s, 3F); HRMS calculated for ($C_7H_7F_3N_2O_2$) requires *m/z* [M+Na] 231.0352, found *m/z* 231.0357.

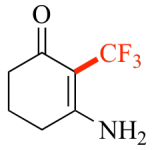

2.16

3-Amino-2-(trifluoromethyl)cyclohex-2-en-1-one (2.16). The title compound **2.16** was obtained as a yellow ochre oil (4.7 mg, 26%). IR (thin film) 3212, 1663, 1601, 1552, 1443, 1102 cm^{-1}; ^{1}H NMR (400 MHz, $CDCl_3$) δ 1.62 (br s, 2H), 1.97 (p, 2H, *J* = 6.4 Hz), 2.39 (t, 2H, *J* = 6.5 Hz), 2.51 (t, 2H, *J* = 6.2 Hz); ^{13}C NMR (100 MHz, $CDCl_3$) δ 20.3, 31.8, 37.1, 104.1 (q, *J* = 34.7 Hz), 125.6 (d, *J* = 270.0 Hz), 163.2, 192.5; ^{19}F NMR (376 MHz, $CDCl_3$) δ –55.4 (s, 3F); HRMS calculated for ($C_7H_8F_3NO$) requires *m/z* [M+Na] 202.0450, found *m/z* 202.0451.

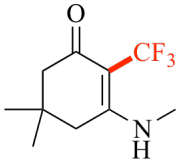

2.17

5,5-Dimethyl-3-(methylamino)-2-(trifluoromethyl)cyclohex-2-en-1-one (2.17). The title compound **2.17** was obtained as a yellow oil (5.8 mg, 26%). IR (thin film) 3216, 2960, 1636, 1575, 1470, 1411, 1338, 1240, 1095 cm^{-1}; ^{1}H NMR (400 MHz, $CDCl_3$) δ 1.09 (s, 6H), 1.65 (br s, 1H), 2.23 (s, 2H), 2.38 (s, 2H), 2.99 (d, 3H, *J* = 5.0 Hz); ^{13}C NMR (100 MHz, $CDCl_3$) δ 28.3, 30.6, 30.8, 50.3, 98.9 (d, *J* = 25.1 Hz), 125.8 (d, *J* =

274.0 Hz), 164.1, 191.4; ^{19}F NMR (376 MHz, $CDCl_3$) δ –54.1 (s, 3F); HRMS calculated for ($C_{10}H_{14}F_3NO$) requires *m/z* [M+Na] 244.0920, found *m/z* 244.0921.

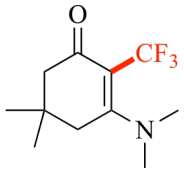

2.18

3-(Dimethylamino)-5,5-dimethyl-2-(trifluoromethyl)cyclohex-2-en-1-one (2.18). The title compound **2.18** was obtained as a yellow oil (8.5 mg, 36%). IR (thin film) 2958, 1634, 1558, 1415, 1330, 1252, 1217, 1157, 1080, 1006 cm^{-1}; ^{1}H NMR (400 MHz, $CDCl_3$) δ 1.07 (s, 6H), 2.17 (s, 2H), 2.41 (s, 2H), 3.08 (s, 6H); ^{13}C NMR (100 MHz, $CDCl_3$) δ 28.4, 29.8, 43.5, 44.0, 49.9, 100.1 (q, *J* = 28.3 Hz), 125.8 (d, *J* = 272.0 Hz), 164.1, 191.4; ^{19}F NMR (376 MHz, $CDCl_3$) δ –53.9 (s, 3F); HRMS calculated for ($C_{11}H_{16}F_3NO$) requires *m/z* [M+Na] 258.1076, found *m/z* 258.1077.

4.3.3 General Procedure for a Radical Clock Experiment

Diethyl diallylmalonate (24.0 mg, 0.1 mmol), $PhI(OAc)_2$ (64.4 mg, 0.2 mmol) and KF (23.2 mg, 0.4 mmol) were added into a 2-dram PTFE sealed glass vial, followed by anhydrous MeCN (1.0 mL) and $TMSCF_3$ (59.3 μL, 0.4 mmol) through syringes. The reaction mixture was stirred at room temperature for 24 h. The mixture was then diluted with acetone, filtered over a pad of Celite and eluted with acetone. The eluent was concentrated *in vacuo*. To the residue were added anisole (10.9 μL, 0.1 mmol) and monofluorobenzene (9.4 μL, 0.1 mmol) as ^{1}H and ^{19}F NMR internal standards

respectively. The crude mixture was analyzed by ^{1}H and ^{19}F NMR and LC-MS, and purified by silica gel chromatography (0-20% ethyl acetate/hexanes) to furnish two major products **2.19** (5.5 mg, 17%) and **2.20** (13.8 mg, 36%). Other trifluoromethylated byproducts were also observed in the crude ^{19}F NMR spectrum (present in 1–5% yield), but could not be isolated.

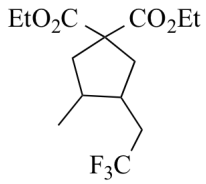

2.19

Diethyl 3-methyl-4-(2,2,2-trifluoroethyl)cyclopentane-1,1-dicarboxylate (2.19).[212] ^{1}H NMR (500 MHz, $CDCl_3$) δ 0.86 (d, *J* = 6.8 Hz, 3H), 1.24 (t, *J* = 7.0 Hz, 6H), 1.96–2.23 (m, 4H), 2.29 (td, *J* = 14.6, 11.9, 7.4 Hz, 2H), 2.46 (ddd, *J* = 13.8, 10.5, 6.7 Hz, 2H), 4.18 (q, *J* = 7.1 Hz, 4H); ^{13}C NMR (126 MHz, $CDCl_3$) δ 14.2, 15.0, 33.9 (q, *J* = 27.2 Hz), 36.1, 36.6, 38.1, 41.3, 58.8, 61.7, 61.7, 127.3 (q, *J* = 274.6 Hz), 172.7, 172.7; ^{19}F NMR (376 MHz, $CDCl_3$) δ –64.9 (s, 3F); LCMS (ESI) calculated for ($C_{14}H_{22}F_3O_4$) requires *m/z* [M+H] 311.2, found 311.3.

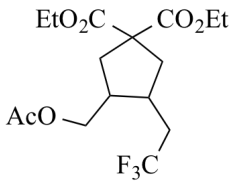

2.20

Diethyl 3-(acetoxymethyl)-4-(2,2,2-trifluoroethyl)cyclopentane-1,1-dicarboxylate (2.20). ^{1}H NMR (400 MHz, $CDCl_3$) δ 1.24 (t, *J* = 7.0 Hz, 6H), 2.04 (s, 3H), 2.10–2.21

(m, 2H), 2.22–2.40 (m, 2H), 2.40–2.57 (m, 4H), 3.92–4.11 (m, 2H), 4.18 (q, J = 7.1 Hz, 4H); ^{13}C NMR (126 MHz, $CDCl_3$) δ 14.1, 21.0, 33.9 (q, J = 28.5 Hz), 35.2, 36.4, 39.1, 40.4, 58.8, 61.8, 61.9, 63.9, 128.8 (q, J = 271.3 Hz), 170.9, 172.0, 172.3; ^{19}F NMR (376 MHz, $CDCl_3$) δ –64.9 (s, 3F); LCMS (ESI) calculated for ($C_{16}H_{24}F_3O_6$) requires *m/z* [M+H] 369.2, found 369.3.

4.3.4 Utility of 5-Trifluoromethylated Cyclic Enaminones

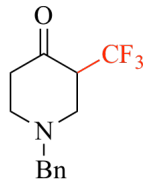

2.23

1-Benzyl-3-(trifluoromethyl)piperidin-4-one (2.23). L-Selectride (1.0 M solution in THF, 0.056 mL, 0.056 mmol) was added dropwise to a stirred solution compound **2.6** (14.2 mg, 0.056 mmol) in THF (1.50 mL) at –78 °C. The resulting mixture was stirred at this temperature for 1 h, quenched by a sat. aq. NH_4Cl solution (1.50 mL) and then extracted with diethyl ether (3 X 5 mL). The combined organic extracts were washed with brine (5 mL), dried over Na_2SO_4, filtered and concentrated *in vacuo*. Silica gel flash chromatography (15% EtOAc/hexanes) furnished the title compound **2.23** (9.30 mg, 65%) as a colorless oil. IR (thin film) 2907, 2791, 1731, 1360, 1267, 1244, 1151, 1116, 1093, 1023, 756, 721 cm^{-1}; ^{1}H NMR (400 MHz, $CDCl_3$) δ 2.45–2.65 (m, 4H), 3.06–3.08 (m, 1H), 3.29–3.38 (m, 2H), 3.68 (q, 2H, J = 13.2 Hz), 7.30–7.38 (m, 5H); ^{13}C NMR (100 MHz, $CDCl_3$) δ 37.7, 48.9, 49.2, 49.4, 57.9, 123.9, 124.8, 125.0, 125.6 (q, J = 270 Hz), 133.6, 196.9; ^{19}F NMR (376 MHz, $CDCl_3$) δ –70.9 (s, 3F); HRMS calculated for

($C_6H_8F_3NO$) requires *m/z* [M+H] 258.1100, found *m/z* 258.1101.

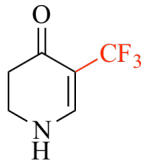

2.24

5-(Trifluoromethyl)-2,3-dihydropyridin-4(1*H*)-one (2.24). Compound **2.11** (26.1 mg, 0.087 mmol) was dissolved in MeOH (2.00 mL). 10% Pd/C (20.0 mg) was added to reaction mixture and was hydrogenated under atmospheric pressure at rt. After stirring overnight, the reaction mixture was filtered through a pad of Celite, followed by a short plug of silica gel, and the solvent was evaporated to obtain the title compound **2.24** as a pale yellow oil (11.9 mg, 83%). IR (thin film) 3331, 2927, 1611, 1513, 1455, 1255, 1167, 1136, 1030, 833, 735, 699, 474 cm^{-1}; ^1H NMR (400 MHz, $CDCl_3$) δ 2.56 (t, 2H, *J* = 7.8 Hz), 3.65–3.69 (m, 2H), 6.16 (br s, 1H), 7.66 (d, 1H, *J* = 7.1 Hz); ^{13}C NMR (100 MHz, $CDCl_3$) δ 35.3, 41.3, 101.5 (q, *J* = 30.0 Hz), 122.5 (q, *J* = 265 Hz), 150.9 (q, *J* = 5.5 Hz), 187.4; ^{19}F NMR (376 MHz, $CDCl_3$) δ –61.3 (s, 3F); HRMS calculated for ($C_6H_6F_3NO$) requires *m/z* [M+Na] 188.0294, found *m/z* 188.0290.

4.4 Chapter 3

4.4.1 Synthesis of Photoprobe 3.1

Epothilone A (**3.5**) and epothilone E (**3.8**) were provided to us by Dr. Höfle. Intermediates **3.6** and **3.7** for the synthesis of compound **3.8** were synthesized in Dr. Höfle's laboratory.

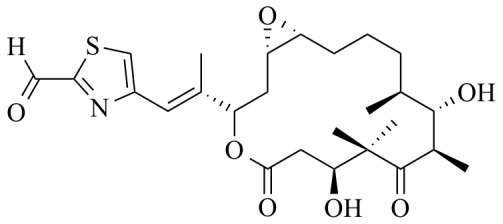

3.9

4-((*E*)-2-((1*S*,3*S*,7*S*,10*R*,11*S*,12*S*,16*R*)-7,11-Dihydroxy-8,8,10,12-tetramethyl-5,9-dioxo-4,17-dioxabicyclo[14.1.0]heptadecan-3-yl)prop-1-en-1-yl)thiazole-2-carbaldehyde (3.9). Epothilone E (**3.8**, 30.0 mg, 58.9 μmol) was dissolved in CH_2Cl_2 (2.00 mL) at rt under N_2. To the reaction mixture was added MnO_2 (8 X 55.0 mg) after 10 min each. After that, Celite was added and the mixture filtered. The pellet was washed two times with a 8:2 mixture of CH_2Cl_2/MeOH. After the reaction was complete as deemed by the TLC, the solvent was evaporated and the residue was purified by silica gel chromatography (0–5% MeOH/CH_2Cl_2 gradient elution) to furnish the title compound **3.9** as a colorless oily substance (29.0 mg, 97%). ^{1}H NMR (400 MHz, $CDCl_3$) δ 1.01 (d, 3H, *J* = 8 Hz), 1.11 (s, 3H), 1.19 (d, 3H, *J* = 8 Hz), 1.38 (s, 3H), 1.53–1.76 (m, 7H), 1.97–2.00 (m, 1H), 2.08–2.10 (m, 1H), 2.20 (s, 3H), 2.50–2.57 (m, 2H), 2.91–2.95 (m, 1H), 3.03–3.07 (m, 1H), 3.22–3.29 (m, 1H), 3.80–3.82 (m, 1H), 4.12–4.15 (m, 1H), 5.48–5.51 (m, 1H), 6.68 (s, 1H), 7.55 (s, 1H), 9.99 (s, 1H); ^{13}C NMR (100 MHz, $CDCl_3$) δ 14.6, 15.5, 17.3, 21.0, 21.6, 23.9, 26.8, 30.2, 31.2, 36.1, 38.7, 44.0, 52.5, 54.2, 57.5, 73.9, 75.2, 76.5, 118.8, 124.1, 139.4, 155.6, 164.9, 170.5, 183.7, 220.1; HRMS calculated for ($C_{26}H_{37}NO_7S$) requires *m/z* [M+H] 508.2369, found *m/z* 508.2375.

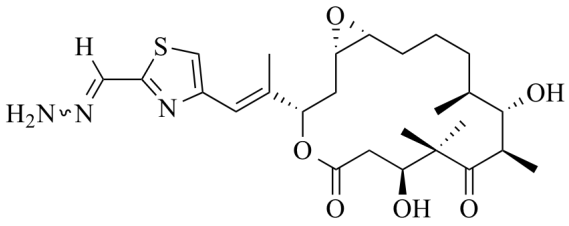

3.10

(1*S*,3*S*,7*S*,10*R*,11*S*,12*S*,16*R*)-3-((*E*)-1-(2-((*E/Z*)-Hydrazonomethyl)thiazol-4-yl)prop-1-en-2-yl)-7,11-dihydroxy-8,8,10,12-tetramethyl-4,17-dioxabicyclo[14.1.0]heptadecane-5,9-dione (3.10). Aldehyde **3.9** (14.0 mg, 27.6 mmol) was dissolved in MeOH (1.00 mL). To this solution, with stirring, 4 portions of hydrazine monohydrate (1.75 mL each, total 148 mmol) were added at rt. After stirring for 10 more min, a sat. Na_2CO_3 solution (0.50 mL) was added to the reaction mixture and extracted with EtOAc (3 X 3 mL). The organic layers were combined, dried over Na_2SO_4, and concentrated *in vacuo*. The crude residue obtained was a mixture of *E*- and *Z*-hydrazones the title compound **3.10** as glassy oil (9.8 mg, 64%), which was used directly for the next step without further purification.

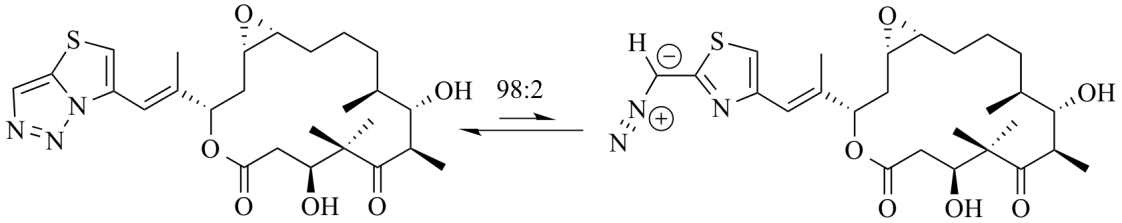

3.1 **3.1**

(1*S*,3*S*,7*S*,10*R*,11*S*,12*S*,16*R*)-7,11-Dihydroxy-8,8,10,12-tetramethyl-3-((*E*)-1-(thiazolo[3,2-*c*][1,2,3]triazol-6-yl)prop-1-en-2-yl)-4,17-dioxabicyclo[14.1.0]heptadecane-5,9-dione (3.1). The mixture of *E*- and *Z*-hydrazones

3.10 (9.8 mg, 18.8 mmol) was dissolved in CH_2Cl_2 (2.00 mL). With stirring, three portions of nickel peroxide monohydrate ($NiO_2.H_2O$) (8.59 mg X 3 times, total 284 mmol) were added each 15 min. After 15 more min, the reaction mixture was filtered over Celite, washed with CH_2Cl_2 and the filtrates were evaporated. The residue was purified by silica gel chromatography (2–5% MeOH/CH_2Cl_2 gradient elution) to afford the title compound **3.1** as a colorless oil (4.00 mg, 41%). ^{1}H NMR (400 MHz, $CDCl_3$) δ 0.98 (d, 3H, *J* = 4 Hz), 1.09 (s, 3H), 1.19 (d, 3H, *J* = 4 Hz), 1.32–1.34 (m, 2H), 1.66–1.93 (m, 7H), 2.16 (s, 3H), 2.22–2.35 (m, 3H), 2.56–2.62 (m, 1H), 2.95–3.04 (m, 2H), 3.24–3.27 (m, 1H), 3.72–3.74 (m, 1H), 4.63–4.68 (m, 1H), 5.08–5.09 (m, 1H), 5.53–5.56 (m, 1H), 6.94 (s, 1H), 7.08 (s, 1H), 7.86 (s, 1H); ^{13}C NMR (100 MHz, $CDCl_3$) δ 14.1, 15.8, 16.5, 18.1, 22.1, 22.7, 23.3, 28.0, 31.4, 32.0, 36.6, 39.5, 41.2, 54.7, 55.2, 57.7, 72.9, 74.9, 109.1, 115.5, 124.8, 129.1, 136.4, 145.1, 169.9, 220.1; HRMS calculated for ($C_{26}H_{37}N_3O_6S$) requires *m/z* [M+H] 520.2481, found *m/z* 520.2484.

4.4.2 Synthesis of Photoprobes 3.2 and 3.3

4.4.2.1 Synthesis of the Epothilone A Aziridine Fragment 3.11

Intermediates **3.14–3.19** and **3.11** were synthesized according to the literature procedure.[272] The spectral data of these compounds was in agreement with that found in the literature.[272]

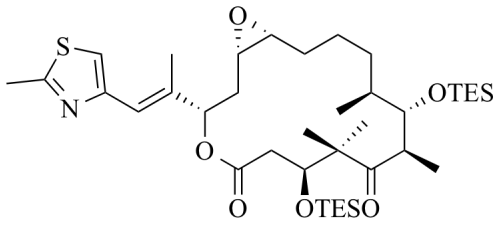

3.14

(1*S*,3*S*,7*S*,10*R*,11*S*,12*S*,16*R*)-8,8,10,12-Tetramethyl-3-((*E*)-1-(2-methylthiazol-4-yl)prop-1-en-2-yl)-7,11-bis((triethylsilyl)oxy)-4,17-dioxabicyclo[14.1.0]heptadecane-5,9-dione (3.14). To a DMF (14.5 mL) solution of epothilone A (**3.5**) (2.00 g, 4.05 mmol) at 25 °C, *N,N*-diisopropylethylamine (55.0 mL**,** 315 mmol), imidazole (7.15 g, 105 mmol) and Et_3SiCl (4.88 mL, 28.8 mmol) were added sequentially. Then, the reaction mixture was heated to 55 °C for 6.5 h, solvent was evaporated and the reaction mixture was concentrated *in vacuo*. The residue was then diluted with CH_2Cl_2 (20.0 mL) and the organic extracts were washed with aq. $NaHCO_3$ (6.00 mL), dried over Na_2SO_4 and concentrated *in vacuo*. The residue was then purified by silica gel flash chromatography (100% hexanes to 15% EtOAc/hexanes gradient elution) to afford the title compound **3.14** as a white foam (2.70 g, 92%). ^{1}H NMR (400 MHz, $CDCl_3$) δ 0.43–0.59 (m, 12H), 0.78–0.91 (m, 24H), 0.97–0.99 (d, 3H, *J* = 8 Hz), 1.03 (s, 3H), 1.06 (s, 3H), 1.32–1.59 (m, 4H), 1.65–1.74 (m, 2H), 2.00 (s, 3H), 2.10–2.14 (m, 1H), 2.58 (s, 3H), 2.66 (br s, 1H), 2.70–2.73 (m, 1H), 2.88–2.93 (m, 2H), 3.81–3.84 (d, 1H, *J* = 12 Hz), 3.92–3.95 (d, 1H, *J* = 12 Hz), 5.13–5.15 (d, 1H, *J* = 8 Hz), 6.45 (s, 1H), 6.87 (s, 1H); ^{13}C NMR (100 MHz, $CDCl_3$) δ 5.1, 5.5, 5.8, 6.6, 6.8, 7.1, 14.6, 17.5, 19.0, 19.4, 23.5, 25.1, 25.2, 27.0, 33.0, 38.9, 48.4, 53.2, 55.2, 57.8, 76.5, 80.1, 116.5, 120.2, 137.4, 152.2, 164.5, 170.8, 214.6; HRMS calculated for ($C_{38}H_{67}NO_6SSi_2$) requires *m/z* [M+H] 722.4306, found *m/z* 722.4293.

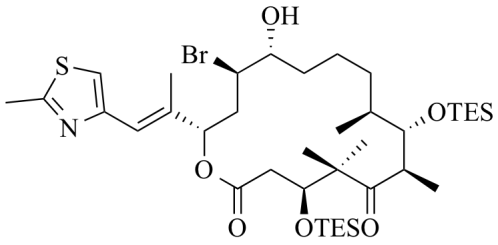

3.15

(4*S*,7*R*,8*S*,9*S*,13*R*,14*R*,16*S*)-14-Bromo-13-hydroxy-5,5,7,9-tetramethyl-16-((*E*)-1-(2-methylthiazol-4-yl)prop-1-en-2-yl)-4,8-bis((triethylsilyl)oxy)oxacyclohexadecane-2,6-dione (3.15). To a CH_2Cl_2 (28.5 mL) solution of bis-TES-epothilone A **3.14** (2.7 g, 3.74 mmol) at –20 °C under Ar, $MgBr_2$•OEt_2 (3 x 1.49 g, 16.0 mmol total) was added in three portions every two h while maintaining an internal temperature between –15 and –5 °C. After 7 h, the reaction mixture was quenched with pH 7 aqueous phosphate buffer (54 mL) and brine (54 mL), carefully extracted with EtOAc (3 x 133 mL), dried over Na_2SO_4, and concentrated *in vacuo*. The residue was purified by silica gel flash chromatography (10–20% EtOAc/hexanes gradient elution) to provide the title compound **3.15** as a white foam [1.11 g, 37 % (57% based on 0.8 g of recovered starting material)]. ^{1}H NMR (400 MHz, $CDCl_3$) δ 0.59–0.68 (m, 12H), 0.92–0.97 (m, 22H), 1.08 (d, 3H, J = 8 Hz), 1.13 (s, 3H), 1.19 (s, 3H), 1.23–1.30 (m, 2H), 1.58–1.72 (m, 4H), 2.10 (s, 3H), 2.40–2.46 (m, 1H), 2.51–2.61 (m, 2H), 2.66–2.71 (m, 4H), 2.93–3.00 (m, 1H), 3.63–3.64 (m, 1H), 3.85–3.87 (m, 1H), 4.23–4.26 (m, 1H), 4.32–4.36 (m, 1H), 5.40–5.42 (m, 1H), 6.51 (s, 1H), 6.93 (s, 1H); ^{13}C NMR (100 MHz, $CDCl_3$) δ 5.3, 5.4, 7.0, 7.1, 15.0, 17.4, 17.8, 19.2, 22.4, 23.5, 25.2, 32.6, 35.2, 38.8, 39.9, 40.6, 46.2, 53.7, 61.7, 73.6, 74.8, 76.5, 78.1, 116.5, 119.5, 137.5, 152.3, 164.7, 170.0, 216.2; HRMS calculated for ($C_{38}H_{68}BrNO_6SSi_2$) requires *m/z* [M+H] 802.3568, found *m/z* 802.3535.

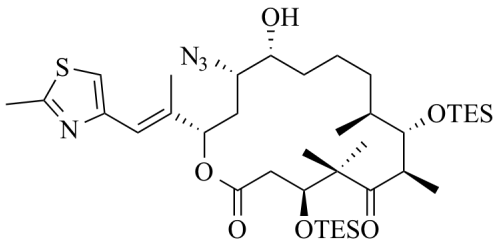

3.16

(4*S*,7*R*,8*S*,9*S*,13*R*,14*S*,16*S*)-14-Azido-13-hydroxy-5,5,7,9-tetramethyl-16-((*E*)-1-(2-methylthiazol-4-yl)prop-1-en-2-yl)-4,8-bis((triethylsilyl)oxy)oxacyclohexadecane-2,6-dione (3.16). To a solution of bromohydrin **3.15** (1.11 g, 1.38 mmol) in DMF (13.1 mL) under Ar was added sodium azide (0.897 g, 13.8 mmol) and the resulting suspension was warmed to 43 °C. After 36–48 h, the solvent was removed *in vacuo* and the residue was directly purified by silica gel flash chromatography (10–20% EtOAc/hexanes gradient elution) to give the title compound **3.16** as a white foam (0.634 g, 62%). ^{1}H NMR (400 MHz, $CDCl_3$) δ 0.58–0.67 (m, 12H), 0.90–0.99 (m, 21 H), 1.06–1.14 (m, 8H), 1.19 (s, 3H), 1.36–1.44 (m, 2H), 1.57–1.61 (m, 3H), 1.67–1.72 (m, 1H), 2.09 (s, 3H), 2.24–2.31 (m, 1H), 2.55–2.62 (m, 1H), 2.70 (s, 3H), 2.80–2.84 (m, 1H), 2.93–3.00 (m, 1H), 3.46–3.48 (m, 1H), 3.81–3.84 (m, 1H), 3.96–3.98 (m, 1H), 4.02–4.05 (m, 1H), 5.28–5.31 (m, 1H), 6.57 (s, 1H), 6.97 (s, 1H); ^{13}C NMR (100 MHz, $CDCl_3$) δ 5.4, 5.5, 7.0, 7.1, 14.9, 17.6, 19.0, 19.1, 23.6, 24.3, 25.0, 31.1, 33.1, 34.2, 37.1, 39.3, 48.0, 53.3, 62.5, 74.2, 76.2, 78.3, 79.6, 116.6, 120.5, 137.2, 152.1, 164.8, 170.7, 214.8; HRMS calculated for ($C_{38}H_{68}N_4O_6SSi_2$) requires *m/z* [M+H] 765.4476, found *m/z* 765.4437.

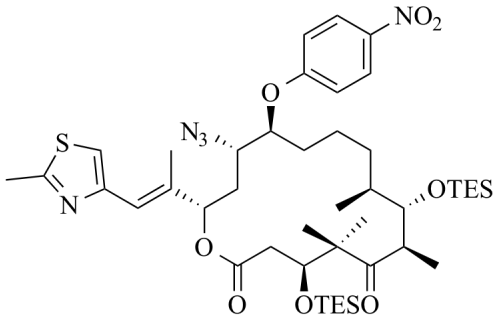

3.17

(2*S*,4*S*,5*S*,9*S*,10*S*,11*R*,14*S*)-4-Azido-9,11,13,13-tetramethyl-2-((*E*)-1-(2-methylthiazol-4-yl)prop-1-en-2-yl)-12,16-dioxo-10,14-bis((triethylsilyl)oxy)oxacyclohexadecan-5-yl 4-Nitrobenzoate (3.17). To a solution of *cis*-azido alcohol **3.16** (0.634 g, 0.829 mmol) in THF (9.05 mL) under Ar was sequentially added 4-nitrobenzoic acid (0.346 g, 2.07 mmol), triphenylphosphine (0.543 mg, 2.07 mmol), and diethyl azodicarboxylate (40 wt% solution in toluene, 0.901 mL**,** 2.07 mmol). The reaction mixture was stirred at 25 °C for 4 h, concentrated *in vacuo* and the residue was purified by silica gel flash chromatography (10–20% EtOAc/hexanes gradient elution) to provide the title compound **3.17** as a white foam (0.584 g, 77%). ^{1}H NMR (400 MHz, $CDCl_3$) δ 0.61–0.69 (m, 12H), 0.94–0.99 (m, 22 H), 1.04–1.09 (m, 1H), 1.12–1.14 (m, 6H), 1.21 (s, 3H), 1.51–1.60 (m, 3H), 1.73–1.79 (m, 1H), 1.91–1.97 (m, 1H), 2.02–2.05 (m, 1H), 2.08–2.14 (m, 4H), 2.52–2.57 (m, 1H), 2.65–2.71 (m, 4H), 2.99–3.06 (m, 1H), 3.91–3.96 (m, 2H), 4.44–4.47 (m, 1H), 5.24–5.28 (m, 1H), 5.61–5.64 (m, 1H), 6.58 (s, 1H), 6.95 (s, 1H), 8.21 (d, 2H, J = 8 Hz), 8.29 (d, 2H, J = 8 Hz); ^{13}C NMR (100 MHz, $CDCl_3$) δ 5.4, 5.4, 7.0, 7.1, 14.9, 17.7, 19.2, 22.4, 30.5, 30.7, 36.3, 39.0, 41.6, 45.6, 54.4, 59.0, 73.5, 76.8, 77.2, 117.0, 121.0, 123.7, 130.9, 135.0, 136.7, 150.7, 152.1, 163.8, 164.9, 170.2, 216.5; HRMS calculated for ($C_{45}H_{71}N_5O_9SSi_2$) requires *m/z* [M+H]

914.4589, found *m/z* 914.4581.

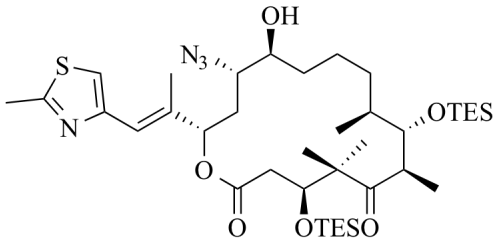

3.18

(4*S*,5*R*,7*R*,8*S*,9*S*,13*S*,14*S*,16*S*)-14-Azido-13-hydroxy-5,7,9-trimethyl-16-((*E*)-1-(2-methylthiazol-4-yl)prop-1-en-2-yl)-4,8-bis((triethylsilyl)oxy)oxacyclohexadecane-2,6-dione (3.18). The intermediate **3.17** (0.584 g, 0.639 mmol) was treated with 2.0 M ammonia in methanol (5.81 mL) at 25 °C under Ar overnight. The solvent was removed *in vacuo* and the residue was directly purified by silica gel flash chromatography (10-30% EtOAc/hexanes gradient elution) to afford the title compound **3.18** as a white foam (0.488 g, 100%). ^{1}H NMR (400 MHz, $CDCl_3$) δ 0.60–0.67 (m, 12H), 0.92–0.99 (m, 21H), 1.02–1.11 (m, 7H), 1.16 (s, 3H), 1.31–1.33 (m, 1H), 1.50–1.67 (m, 4H), 1.81–1.84 (m, 1H), 2.02–2.03 (m, 2H), 2.12 (s, 3H), 2.54–2.60 (m, 1H), 2.70–2.73 (m, 4H), 2.98–3.05 (m, 1H), 3.60–3.68 (m, 2H), 3.92–3.95 (m, 1H), 4.40 (br s, 1H), 5.52–5.53 (m, 1H), 6.59 (s, 1H), 6.96 (s, 1H); ^{13}C NMR (100 MHz, $CDCl_3$) δ 5.4, 5.5, 7.0, 7.1, 14.9, 17.6, 18.3, 19.2, 21.6, 21.9, 22.1, 29.7, 33.4, 37.0, 38.1, 41.0, 45.9, 54.2, 61.6, 73.0, 74.0, 77.6, 78.6, 116.7, 120.7, 137.0, 152.2, 164.8, 170.3, 215.9 ppm; HRMS calculated for ($C_{38}H_{69}N_4O_6SSi_2$) requires *m/z* [M+H] 765.4476, found *m/z* 765.4514.

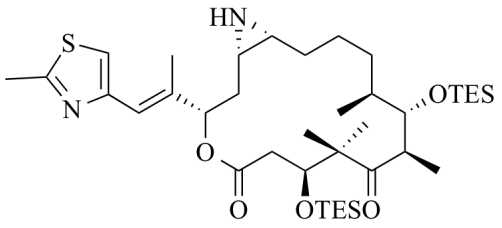

3.19

(1*S*,3*S*,7*S*,10*R*,11*S*,12*S*,16*R*)-8,8,10,12-Tetramethyl-3-((*E*)-1-(2-methylthiazol-4-yl)prop-1-en-2-yl)-7,11-bis((triethylsilyl)oxy)-4-oxa-17-azabicyclo[14.1.0]heptadecane-5,9-dione (3.19). A solution of *trans*-azido alcohol **3.18** (0.171 g, 0.224 mmol) in CH_2Cl_2 (4.00 mL) was cooled to 0 °C. To this, triethylamine (0.125 mL, 0.896 mmol) was added. After stirring for 5 min, methanesulfonyl chloride (52.0 mL, 0.672 mmol) was added slowly over a period of 5 min. After 15 min, the reaction mixture was removed from the ice bath and stirred for 3 h at rt. After 3 h, sat. aq. $NaHCO_3$ (15 mL) was added to the reaction mixture, extracted with CH_2Cl_2 (3 times X 5 mL), dried over Na_2SO_4, concentrated *in vacuo*. The residue was taken to next step without further purification. The crude mesylate was dissolved in a 10:1 mixture of THF:Water (6.60 mL). Triethylamine (94.1 mL, 0.672 mmol) and trimethylphosphine (0.448 mL, 0.448 mmol of 1.0 M solution in THF) were added and the reaction mixture was stirred at rt. After 3 h, the reaction mixture was heated at 45 °C for 12 h and then the solvent was removed under a constant flow of nitrogen. Then the residue was purified by silica gel flash chromatography (0–6% MeOH/CH_2Cl_2 gradient elution) to furnish the title compound **3.19** as a film (137 mg, 85%). ^{1}H NMR (400 MHz, $CDCl_3$) δ 0.57–0.67 (m, 12H), 0.87–0.99 (m, 24H), 1.05–1.07 (d, 3H, J = 8 Hz), 1.12 (s, 3H), 1.15 (s, 3H), 1.47–1.70 (m, 5H), 1.91–1.95 (m, 1H), 2.07–2.10 (m, 4H), 2.14–2.18 (m, 1H), 2.68–2.76 (m, 5H), 2.95–3.02 (m, 1H), 3.89–3.91 (m, 1H), 4.01–4.03 (m, 1H), 5.19–5.21 (m, 1H),

6.53 (s, 1H), 6.94 (s, 1H); ^{13}C NMR (100 MHz, $CDCl_3$) δ 5.2, 5.6, 7.0, 7.2, 14.6, 17.6, 19.2, 19.6, 23.7, 27.0, 28.1, 31.0, 36.5, 39.0, 48.5, 53.3, 76.5, 78.6, 80.2, 116.4, 120.2, 138.1, 152.4, 164.6, 171.2, 215.1 ppm; HRMS calculated for ($C_{38}H_{69}N_2O_5SSi_2$) requires *m/z* [M+H] 721.4466, found *m/z* 721.4439.

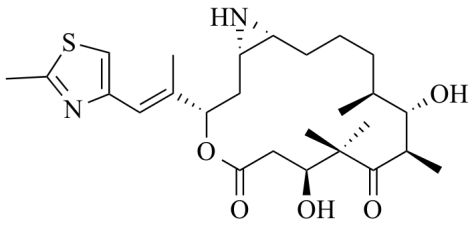

3.11

(1*S*,3*S*,7*S*,10*R*,11*S*,12*S*,16*R*)-7,11-dihydroxy-8,8,10,12-tetramethyl-3-((*E*)-1-(2-methylthiazol-4-yl)prop-1-en-2-yl)-5,9-dioxo-4-oxa-17-azabicyclo[14.1.0]heptadecan-17-ium 2,2,2-Trifluoroacetate (3.11). Compound **3.19** (49.0 mg, 68.0 μmol) was treated with 20% trifluoroacetic acid in CH_2Cl_2 (1.50 mL) at 0 °C under N_2 for 10 min. The reaction mixture was concentrated under a constant stream of nitrogen at 0 °C and the residue was purified by silica gel chromatography (2–10% MeOH/CH_2Cl_2 gradient elution) to obtain the title compound **3.11** as a white film (37.4 mg, 91%). ^{1}H NMR (400 MHz, $CDCl_3$) δ 0.98 (d, 3H, *J* = 8 Hz), 1.10 (s, 3H), 1.15 (d, 3H, *J* = 8 Hz), 1.37 (s, 3H), 1.43–1.59 (m, 4H), 1.67–1.84 (m, 3H), 2.07 (s, 3H), 2.13–2.29 (m, 2H), 2.41–2.45 (m, 1H), 2.53–2.59 (m, 1H), 2.70 (s, 3H), 2.83–2.95 (m, 2H), 3.22–3.28 (m, 1H), 3.75–3.78 (m, 1H), 4.09–4.12 (m, 1H), 5.39–5.42 (m, 1H), 6.60 (s, 1H), 7.02 (s, 1H); ^{13}C NMR (100 MHz, $CDCl_3$) δ 13.8, 15.3, 17.2, 18.9, 21.0, 21.4, 23.7, 24.1, 27.9, 29.9, 35.5, 36.9, 39.9, 44.1, 52.8, 74.0, 74.6, 117.0, 117.9, 120.5, 136.2, 151.1, 162.3, 165.5, 170.7, 220.1; HRMS calculated for ($C_{28}H_{42}F_3N_2O_7S$) requires *m/z* [M+H]

607.2665, found *m/z* 607.2662.

4.4.2.2 Synthesis of the *meta*– and the *para*–Acids 3.12 and 3.13

The *m*-trifluoromethyldiazirino benzoic acid **3.12** was synthesized in Dr. Höfle's lab and was sent to us for our experiments. The *p*-trifluoromethyldiazirino benzoic acid **3.13** was commercially available. It was purchased from Chem-Impex International Inc., and used directly without any further purification.

4.4.2.3 General Procedure for the Synthesis of Photoprobes 3.2 and 3.3.

Solution of the aziridine **3.11** (14.0 mg, 23.0 mmol) in CH_2Cl_2 (2.00 mL) was stirred with Hunig's base (4.90 mL, 28.0 mmol) at rt. In a separate flask, to a solution of the trifluoromethyldiazirino benzoic acid (**3.12** or **3.13**, 6.65 mg, 28.0 mmol) in CH_2Cl_2 (3.00 mL), Hünig's base (10.5 mL, 60.0 mmol) and benzotriazol-1-yloxy)tris(dimethylamino)phosphonium hexafluorophosphate (BOP) (12.8 mg, 28.0 mmol) were added sequentially. After stirring for 10 min, the solution of aziridine **3.11** was added to the acid solution. The reaction mixture was allowed to react for 16 h in the dark at rt. After 16 h, the reaction mixture was diluted with CH_2Cl_2 (3.00 mL) and then washed with pH 3 buffer (citric acid, 3 X 10 mL), sat. aq. $NaHCO_3$ (3 X 10 mL) and water (1 X 10 mL). The organic layer was dried over Na_2SO_4, and concentrated *in vacuo*. The residue was purified by silica gel chromatography (2–5% MeOH/CH_2Cl_2 gradient elution) to afford the desired compound **3.2** or **3.3**.

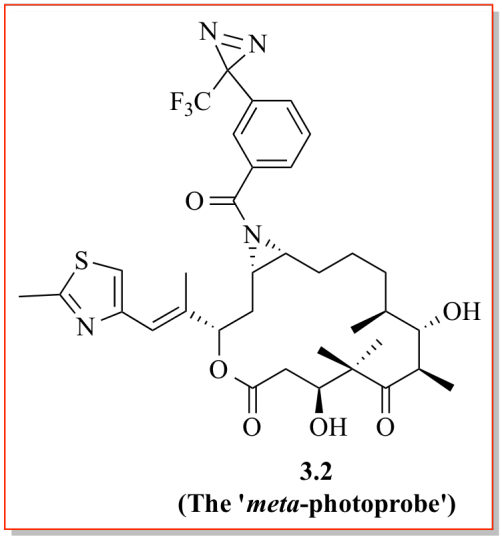

3.2
(The '*meta*-photoprobe')

(1*S*,3*S*,7*S*,10*R*,11*S*,12*S*,16*R*)-7,11-Dihydroxy-8,8,10,12-tetramethyl-3-((*E*)-1-(2-methylthiazol-4-yl)prop-1-en-2-yl)-17-(3-(3-(trifluoromethyl)-3*H*-diazirin-3-yl)benzoyl)-4-oxa-17-azabicyclo[14.1.0]heptadecane-5,9-dione (3.2). The title compound **3.2** was obtained as a colorless oil (13.1 mg, 81%). ^{1}H NMR (400 MHz, $CDCl_3$) δ 1.03 (d, 3H, *J* = 8 Hz), 1.15 (s, 3H), 1.19 (d, 3H, *J* = 8 Hz), 1.37 (s, 3H), 1.51–1.57 (m, 3H), 1.71–1.75 (m, 2H), 1.93–1.99 (m, 2H), 2.11 (s, 3H), 2.35–2.56 (m, 5H), 2.65–2.70 (m, 4H), 3.15–3.22 (m, 1H), 3.80–3.82 (m, 1H), 4.12–4.15 (m, 1H), 5.34–5.38 (m, 1H), 6.58 (s, 1H), 6.98 (s, 1H), 7.39 (d, 2H, *J* = 8 Hz), 7.51 (t, 3H, *J* = 8 Hz), 7.77 (s, 1H), 7.99 (d, 2H, *J* = 8 Hz); ^{13}C NMR (100 MHz, $CDCl_3$) δ 13.6, 15.3, 17.3, 19.0, 20.2, 22.8, 24.0, 28.3 (q, *J* = 40.5 Hz), 31.2, 31.8, 36.3, 39.2, 40.1, 43.2, 43.6, 52.8, 73.1, 73.6, 78.1, 116.3, 120.3, 122.0 (q, *J* = 273.1 Hz), 127.1, 129.2, 129.6, 130.2, 130.4, 134.1, 138.1, 151.7, 165.2, 170.8, 178.7, 220.1; ^{19}F NMR (376 MHz, $CDCl_3$) δ –65.0 (s, 3F); HRMS calculated for ($C_{35}H_{44}F_3N_4O_6S$) requires *m/z* [M+Na] 727.2753, found *m/z* 727.2777.

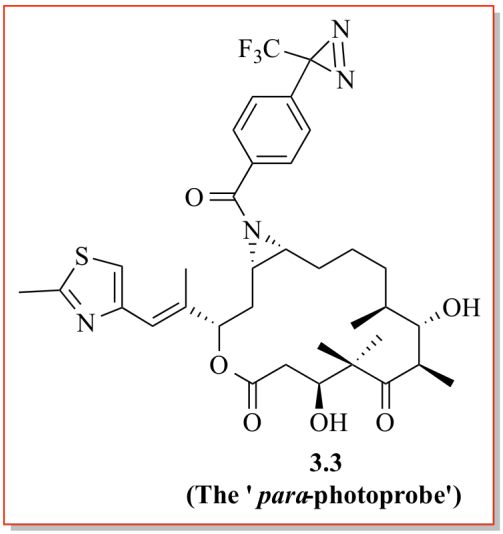

3.3
(The '*para*-photoprobe')

(1*S*,3*S*,7*S*,10*R*,11*S*,12*S*,16*R*)-7,11-Dihydroxy-8,8,10,12-tetramethyl-3-((*E*)-1-(2-methylthiazol-4-yl)prop-1-en-2-yl)-17-(4-(3-(trifluoromethyl)-3*H*-diazirin-3-yl)benzoyl)-4-oxa-17-azabicyclo[14.1.0]heptadecane-5,9-dione (3.3). The title compound **3.3** was obtained as a colorless oil (14.7 mg, 91%). ^{1}H NMR (400 MHz, $CDCl_3$) δ 1.03 (d, 3H, *J* = 8 Hz), 1.15 (s, 3H), 1.19 (d, 3H, *J* = 8 Hz), 1.37 (s, 3H), 1.50–1.57 (m, 3H), 1.67–1.75 (m, 2H), 1.90–1.99 (m, 2H), 2.11 (s, 3H), 2.33–2.56 (m, 5H), 2.65–2.71 (m, 4H), 3.15–3.21 (m, 1H), 3.80–3.82 (m, 1H), 4.12–4.14 (m, 1H), 5.34–5.37 (m, 1H), 6.58 (s, 1H), 6.99 (s, 1H), 7.25–7.27 (m, 2H), 7.94–7.97 (m, 2H); ^{13}C NMR (100 MHz, $CDCl_3$) δ 13.7, 15.3, 17.4, 19.1, 20.3, 22.8, 24.0, 25.6, 28.4 (q, *J* = 40.5 Hz), 31.2, 31.9, 36.3, 39.2, 40.1, 43.3, 52.8, 68.0, 73.3, 73.8, 78.3, 116.4, 120.5, 121.8 (q, *J* = 273.1 Hz), 126.5, 129.4, 133.6, 134.3, 138.1, 151.7, 165.2, 170.7, 178.8, 220.0; ^{19}F NMR (376 MHz, $CDCl_3$) δ –64.9 (s, 3F); HRMS calculated for ($C_{35}H_{44}F_3N_4O_6S$) requires *m/z* [M+Na] 727.2753, found *m/z* 727.2777.

4.4.3 Attempts at Synthesizing the Photoprobe 3.4

4.4.3.1 Suzuki Coupling Strategy

4.4.3.1.1 Synthesis of Fragment 3.26

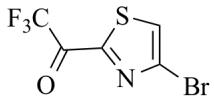

3.29

1-(4-Bromothiazol-2-yl)-2,2,2-trifluoroethan-1-one (3.29). 2,4-Dibromothiazole (**3.28**, 2.00 g, 8.23 mmol, 1.00 equiv) was dissolved in diethyl ether (35.0 mL), cooled to –78 °C and with stirring *n*-butyllithium (3.50 mL, 8.73 mmol, 1.06 equiv, diluted with 3.00 ml of diethyl ether) was added dropwise. After 1 h, *N*,*N*-diethyl trifluoroacetamide (1.52 mL, 10.7 mmol, 1.30 equiv) was added to the above mixture over a period of 30 min and the reaction mixture was stirred –78 °C. After 1 h, the reaction mixture was warmed to –10 °C and kept for 4 h. Then the reaction was quenched with sat. aq. NH_4Cl solution. The organic phase was separated from the aqueous phase, dried over Na_2SO_4, and concentrated *in vacuo* to get the crude trifluoromethyl ketone **3.29** (2.14 g) This intermediate was used directly for the next step without further purification.

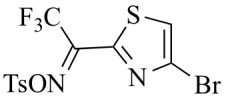

3.30

(*Z*)-1-(4-Bromothiazol-2-yl)-2,2,2-trifluoroethan-1-one *O*-Tosyl Oxime (3.30). The crude trifluoromethyl ketone **3.29** (2.14 g, 8.23 mmol, 1.00 equiv) obtained from the earlier step was dissolved in ethanol (18.0 mL) and hydroxylammonium chloride (2.00 g, 28.8 mmol, 3.50 equiv) and pyridine (4.35 mL, 53.8 mmol, 6.53 equiv) were added and

the mixture was refluxed for 4 h. After 4 h, the mixture was evaporated and the residue was distributed between water and diethyl ether. The ether phase was evaporated, and the pyridine was removed *in vacuo* with toluene to furnish the crude oxime (2.26 g). The crude oxime (2.26 g, 8.22 mmol, 1.00 equiv), triethylamine (2.30 mL, 16.4 mmol, 2.00 equiv), DMAP (0.101 g, 0.822 mol, 0.10 equiv) and tosyl chloride (2.39 g, 12.4 mmol, 1.51 equiv) were dissolved in dichloromethane (25 mL) and stirred at rt for 1 h. The reaction mixture was washed with water (1 X 25 mL) and the organic phase was separated. The organic phase was dried over Na_2SO_4, evaporated and purified by flash chromatography on silica gel (10:1 to 5:1 EtOAc/petroleum ether gradient elution) to yield the title compound **3.30** as a yellow solid (2.63 g, 37% over 3 steps), and 1.15 g of impure **3.30**. ^{1}H NMR (400 MHz, $CDCl_3$) δ 2.48 (s, 3H), 7.41 (d, 2H, J = 8.1 Hz), 7.74 (s, 1H), 7.94 (d, 2H, J = 8.4 Hz); ^{13}C NMR (100 MHz, $CDCl_3$) δ 21.8, 119.0 (q, J = 278.5 Hz), 125.3, 127.0, 128.3, 129.5, 130.2, 144.9 (q, J = 33.5 Hz), 147.1, 149.1; ^{19}F NMR (376 MHz, $CDCl_3$) –64.8; HRMS calculated for ($C_{12}H_8BrF_3N_2O_3S_2$) requires *m/z* [M+H] 428.9190, found *m/z* 428.9195.

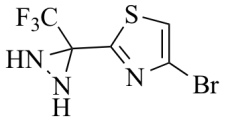

3.31

4-Bromo-2-(3-(trifluoromethyl)diaziridin-3-yl)thiazole (3.31). In a flask, *O*-tosyloxime **3.30** (1.23 g, 2.87 mmol, 1.00 equiv) was dissolved in abs. diethyl ether (17.0 mL) and cooled to –78 °C. Then, ammonia gas (ca. 12.3 mL) was condensed to the reaction flask. After 2 h stirring, the temperature was slowly raised to rt. The reaction

mixture was quenched with water (15 mL) and the aq. phase was extracted with diethyl ether (1 X 20 mL). The separated organic phase was dried over Na_2SO_4, evaporated, and the residue purified by flash chromatography (8–16% EtOAc/petroleum ether gradient elution) to furnish the title compound **3.31** (0.623 g, 79%). ^{1}H NMR (400 MHz, $CDCl_3$) δ 3.07 (s, 2H), 7.38 (s, 1H); ^{13}C NMR (100 MHz, $CDCl_3$) δ 55.4 (q, *J* = 38.1 Hz), 120.1, 122.2 (q, *J* = 276 Hz), 126.1, 161.3; ^{19}F NMR (376 MHz, $CDCl_3$) –74.5; HRMS calculated for ($C_5H_3BrF_3N_3S$) requires *m/z* [M+H] 273.9261, found *m/z* 273.9262.

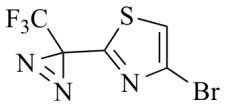

3.26

4-Bromo-2-(3-(trifluoromethyl)-3*H*-diazirin-3-yl)thiazole (3.26). Diaziridine **3.31** (0.104 g, 0.379 mmol, 1.00 equiv) was dissolved in dry CH_2Cl_2 (2.50 mL) and Ag(I) oxide (0.704 g, 3.04 mmol, 8.00 equiv) was added. The resulting suspension was stirred for 24 h in the dark. After stirring, the slurry was applied to a silica gel column, soaked in and eluted with low boiling petroleum ether/diethyl ether (20:1). The solvents were evaporated from the eluent at 40 °C under a slight vacuum to get the title compound **3.26** (0.077 g, 75%). ^{1}H NMR (400 MHz, $CDCl_3$) δ 7.39 (s, 1H); ^{13}C NMR (100 MHz, $CDCl_3$) δ 28.7 (q, *J* = 43.3 Hz), 119.3, 120.9 (q, *J* = 276.6 Hz), 126.8, 158.8; ^{19}F NMR (376 MHz, $CDCl_3$) –66.5; HRMS calculated for ($C_5HBrF_3N_3S$) requires *m/z* [M+H] 271.9105, found *m/z* 271.9112.

4.4.3.1.2 Synthesis of Fragment 3.32

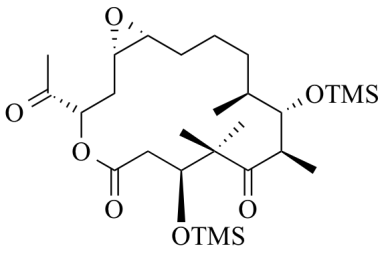

3.32

(1*S*,3*S*,7*S*,10*R*,11*S*,12*S*,16*R*)-3-Acetyl-8,8,10,12-tetramethyl-7,11-bis((trimethylsilyl)oxy)-4,17-dioxabicyclo[14.1.0]heptadecane-5,9-dione (3.32). Compound **3.32** was synthesized in Dr. Höfle's lab and was shipped to us for use in the further experiments.

4.4.3.1.3 Synthesis of Fragment 3.33

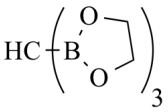

3.33

Tris(ethylenedioxyboryl)methane (3.33). In a dry round bottom flask, boron trichloride **3.35** (1.0 M in hexanes) (100 mL, 100 mmol, 1.00 equiv) was added under nitrogen and the flask cooled to –50 °C. Trimethyl borate **3.36** (22.3 mL, 200 mmol, 2.00 equiv) was then added with stirring at this temperature over a period of 5 min to form dimethoxyboron chloride **3.37**. After slowly warming to rt, chloroform (8.05 mL, 100 mmol, 1.00 equiv) was added to the above mixture to get the 'mixture A', which was transferred to a 250 mL dropping funnel. In a dry 1000 mL three–necked flask, lithium metal chunks (3.75 g, 540 mmol, 5.4 equiv) were added under nitrogen and the flask was fitted with an internal thermometer and the dropping funnel with 'mixture A' in it. Dry

THF (156 mL) was then added to the lithium and the flask was cooled to –40 °C. Then slowly 'mixture A' was added over a period of 2 h. The temperature was kept between –40 to –30 °C and vigorous stirring was maintained during the addition. Then the mixture was allowed to warm up to rt over 2 h and stirred overnight at that temperature. The next day, the reaction mixture was filtered under a stream of nitrogen through a Büchner funnel and the residue was washed with dry THF (15 mL). The filtrate was concentrated *in vacuo* to ~60 mL and mixed with dry hexanes (30 mL). The resulting precipitate was removed by filtration. The filtrate was evaporated and the residue was shaken vigorously with diethyl ether (20 mL). The slurry was filtered and the filtrate was concentrated to dryness *in vacuo* to yield 15.4 g of crude tris(dimethoxyboryl)methane (**3.39**). Compound **3.39** (15.4 g, 66.4 mmol, 1.00 equiv) was dissolved in dry THF (36 mL), cooled to 0 °C and then ethylene glycol (9.00 mL, 161 mmol, 2.43 equiv) was added. After stirring for 30 min at this temperature, the solvent was evaporated. The residue was heated at 70 °C under reduced pressure to remove excess ethylene glycol and volatile by-products to yield the crude product tris(ethylenedioxyboryl)methane (**3.33**). This was dissolved in 30 mL of boiling THF, filtered and cooled down to 5 °C. After one to three days at 5 °C, 2.05 g of colorless crystals of pure solid product **3.33** were collected (mp = 170–172 °C). The mother liquor was concentrated to about half of the volume and kept again at 5 °C for several days to yield a second batch of 0.573 g of **3.3**. The total yield was 2.62 g (18%). The spectroscopic data of product **3.33** agreed with those reported in literature.[327] ^{1}H NMR (400 MHz, $CDCl_3$) δ 0.78 (br s, 1H), 4.21 (s, 12H); ^{13}C NMR (100 MHz, $CDCl_3$) δ 47.4, 65.7; HRMS calculated for ($C_7H_{13}B_3O_6$) requires *m/z* [M+H] 227.1070, found *m/z* 227.1075.

4.4.3.2 Cross Metathesis Strategy

4.4.3.2.1 Synthesis of Fragment 3.40

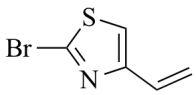

3.43

2-Bromo-4-vinylthiazole (3.43). In a round bottom flask 2-bromothiazole-4-carbaldehyde (**3.42**, 2.00 g, 8.23 mmol, 1.00 equiv) was dissolved in THF (30.0 mL) and stirred at rt. In a separate flask, potassium *tert*-butoxide (1.84 g, 15.6 mmol, 1.50 equiv) was dissolved in dry THF (20.0 mL) under nitrogen and stirred for 15 min. Simultaneously in another flask, methyl triphenylphosphonium bromide salt (7.59 g, 20.8 mmol, 2.00 equiv) was dissolved in dry THF (70.0 mL) at rt and then cooled to 0 °C. The THF solution of potassium *tert*-butoxide was added to the Wittig salt solution slowly over 5 min. The mixture was then refluxed for 1 h, then removed from the oil bath and cooled to rt within 30 min. To this, the aldehyde solution was slowly added over 5 min at rt. The reaction mixture was then stirred at rt untill the reaction was completed as monitored by the TLC. At this point, water (120 mL) was added to the reaction mixture and the aq. layer was extracted with diethyl ether (3 X 100 mL). The separated organic layer was washed once with brine (100 mL), dried over Na_2SO_4, evaporated and purified by flash chromatography on silica gel (10–15% diethyl ether/petroleum ether gradient elution) to afford the title compound **3.43** (1.57 g, 79%). ^{1}H NMR (400 MHz, $CDCl_3$) δ 5.35 (d, 1H, J = 10.8 Hz), 6.02 (d, 1H, J = 17.2 Hz), 6.58 (dd, 1H, J_1 = 10.8 Hz, J_2 = 17.2 Hz), 6.99 (s, 1H); ^{13}C NMR (100 MHz, $CDCl_3$) δ 117.7, 118.6, 128.6, 136.0, 154.5; HRMS calculated for (C_5H_4BrNS) requires *m/z* [M+Na] 211.9146, found *m/z* 211.9152.

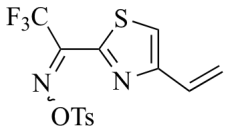

3.44

2,2,2-Trifluoro-1-(4-vinylthiazol-2-yl)ethan-1-one *O*-Tosyl Oxime (3.44). 2-Bromo-4-vinylthiazole (**3.43**, 1.99 g, 10.5 mmol, 1.00 equiv) was dissolved in diethyl ether (45.0 mL), cooled to –78 °C and with stirring *n*-butyllithium (6.96 mL, 11.1 mmol, 1.06 equiv, diluted with 3.76 mL of diethyl ether) was added dropwise. After 1 h, *N*,*N*-diethyl trifluoroacetamide (1.94 mL, 13.7 mmol, 1.30 equiv) was added to the above mixture over a period of 30 min and the reaction mixture was stirred –78 °C. After 1 h, the reaction mixture was warmed to –10 °C and kept for 4 h. Then the reaction was quenched with sat. aq. NH_4Cl solution. The organic phase was separated from the aqueous phase, dried over Na_2SO_4, and concentrated *in vacuo* to obtain the crude trifluoromethyl ketone (2.18 g). The crude trifluoromethyl ketone (2.18 g, 10.5 mmol, 1.00 equiv) was dissolved in ethanol (22.5 mL) and hydroxylammonium chloride (2.55 g, 36.7 mmol, 3.50 equiv) and pyridine (5.55 mL, 68.6 mmol, 6.53 equiv) were added and the mixture was refluxed for 4 h. After 4 h, the mixture was evaporated and the residue was distributed between water and diethyl ether. The ether phase was evaporated, and the pyridine was removed *in vacuo* with toluene to afford the crude oxime (2.33 g). The crude oxime (2.33 g, 10.5 mmol, 1.00 equiv), triethylamine (2.94 mL, 21.0 mmol, 2.00 equiv), DMAP (0.130 g, 1.05 mol, 0.100 equiv) and tosyl chloride (3.03 g, 15.8 mmol, 1.51 equiv) were dissolved in dichloromethane (29 mL) and stirred at rt for 1 h. The reaction mixture was washed with water (1 X 25 mL) and the organic phase was separated. The organic phase was dried over Na_2SO_4, evaporated and purified by flash chromatography on silica gel (5–

20% diethyl ether/petroleum ether gradient elution) to give the title compound **3.44** as a pale yellow solid (mp = 113–114 °C) (2.47 g, 62% over 3 steps). ^{1}H NMR (400 MHz, $CDCl_3$) δ 2.48 (s, 3H), 5.49 (d, 1H, J = 10.8 Hz), 6.16 (d, 1H, J = 18.5 Hz), 6.78 (dd, 1H, J_1 = 10.8 Hz, J_2 = 17.3 Hz), 7.40 (d, 2H, J = 8.2 Hz), 7.58 (s, 1H), 7.96 (d, 2H, J = 8.4 Hz); ^{13}C NMR (100 MHz, $CDCl_3$) δ 21.8, 119.2, 119.3 (q, J = 276.7 Hz), 121.9, 128.6, 129.4, 130.0, 130.6, 146.0 (q, J = 36.7 Hz), 146.7, 148.1, 155.4; ^{19}F NMR (376 MHz, $CDCl_3$) –64.8, –61.4; HRMS calculated for ($C_{14}H_{11}F_3N_2O_3S_2$) requires *m/z* [M+Na] 399.0061, found *m/z* 399.0068.

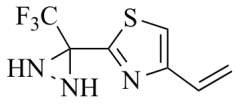

3.45

2-(3-(Trifluoromethyl)diaziridin-3-yl)-4-vinylthiazole (3.45). In a flask, *O*-tosyloxime **3.44** (1.38 g, 3.24 mmol, 1.00 equiv) was dissolved in abs. diethyl ether (17.0 mL) and cooled to –78 °C. Then, ammonia gas (ca. 13.8 mL) was condensed to the reaction flask. After 2 h stirring, the temperature was slowly raised to rt. The reaction mixture was quenched with water (15 mL) and the aq. phase was extracted with diethyl ether (1 X 20 mL). The separated organic phase was dried over Na_2SO_4, evaporated, and the residue purified by flash chromatography (6–16% diethyl ether/petroleum ether gradient elution) to furnish the title compound **3.45** (0.752 g, 93%). ^{1}H NMR (400 MHz, $CDCl_3$) δ 3.09 (d, 1H, J = 8.9 Hz), 3.27 (d, 1H, J = 9.0 Hz), 5.41 (d, 1H, J = 10.9 Hz), 6.08 (d, 1H, J = 17.3 Hz), 6.69 (dd, 1H, J_1 = 10.9 Hz, J_2 = 17.3 Hz), 7.20 (s, 1H); ^{13}C NMR (100 MHz, $CDCl_3$) δ 55.4 (q, J = 38.1 Hz), 117.2, 118.0, 120.5 (q, J = 273.3 Hz), 128.9, 154.9, 159.9; ^{19}F

NMR (376 MHz, $CDCl_3$) –74.7; HRMS calculated for ($C_7H_6F_3N_3S$) requires *m/z* [M+H] 244.0132, found *m/z* 244.0142.

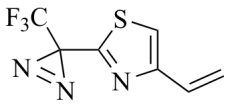

3.40

2-(3-(Trifluoromethyl)-3*H*-diazirin-3-yl)-4-vinylthiazole (3.40). Diaziridine **3.45** (0.104 g, 0.379 mmol, 1.00 equiv) was dissolved in dry CH_2Cl_2 (2.50 mL) and Ag(I) oxide (0.704 g, 3.04 mmol, 8.00 equiv) was added. The resulting suspension was stirred for 24 h in the dark. After this, the slurry was applied on a silica gel column, soaked in and eluted with low boiling petroleum ether/diethyl ether (20:1). The solvents were evaporated from the eluent at 40°C under a slight vacuum to yield the title compound **3.26** (0.077 g, 75%). ^{1}H NMR (400 MHz, $CDCl_3$) δ 5.43 (d, 1H, J = 10.8 Hz), 6.08 (d, 1H, J = 17.3 Hz), 6.68 (dd, 1H, J_1 = 10.8 Hz, J_2 = 17.3 Hz), 7.17 (s, 1H); ^{13}C NMR (100 MHz, $CDCl_3$) δ 28.9 (q, J = 42.4 Hz), 116.3, 118.6, 121.1 (q, J = 273.3 Hz), 128.6, 155.4, 157.6; ^{19}F NMR (376 MHz, $CDCl_3$) –66.4; HRMS calculated for ($C_7H_4F_3N_3S$) requires *m/z* [M+Na] 241.9976, found *m/z* 241.9982.

4.4.3.2.2 Synthesis of Fragment 3.46

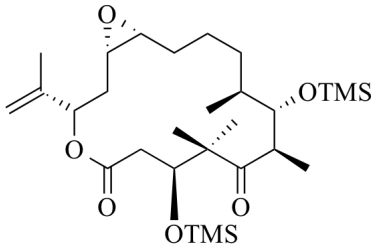

3.46

(1*S*,3*S*,7*S*,10*R*,11*S*,12*S*,16*R*)-8,8,10,12-Tetramethyl-3-(prop-1-en-2-yl)-7,11-bis((trimethylsilyl)oxy)-4,17-dioxabicyclo[14.1.0]heptadecane-5,9-dione (3.46). The bis-TMS epothilone A ketone **3.32** (0.022 g, 0.041 mmol, 1.00 equiv) was charged into an oven dried flask and dry THF (1.50 mL) was added to it under nitrogen. The flask was cooled to 0 °C. Then, the Tebbe reagent (0.5M in toluene, 0.130 mL, 0.065 mmol, 1.60 equiv) was added dropwise to the ketone solution and the reaction mixture was stirred at 0 °C for 30 min. After the reaction was complete as deemed by TLC, it was quenched with 0.1 M NaOH (1 mL), stirred and diluted with diethyl ether (10 mL). Then the slurry was filtered over a short pad of silica gel. The filtrate was concentrated and the residue was purified by flash chromatography (6–12% diethyl ether/petroleum ether gradient elution) to obtain the title compound **3.46** as colourless foam (0.012 g, 53%). ^{1}H NMR (400 MHz, $CDCl_3$) δ 0.05 (s, 19H), 0.15 (s, 9H), 0.97 (d, 3H, J = 8 Hz), 1.07 (d, 3H, J = 8 Hz), 1.13 (s, 3H), 1.18 (s, 3H), 1.20–1.24 (m, 1H), 1.39–1.49 (m, 3H), 1.53–1.58 (m, 1H), 1.62–1.71 (m, 2H), 1.74–1.82 (m, 4H), 2.19 (dd, 1H, J_1 = 3.3 Hz, J_2 = 14.8 Hz), 2.69–2.78 (m, 2H), 2.81–2.84 (m, 1H), 2.95–3.02 (m, 2H), 3.89 (d, 1H, J = 9.9 Hz), 4.04 (dd, 1H, J_1 = 3.1 Hz, J_2 = 9.7 Hz), 4.90 (s, 1H), 4.98 (s, 1H), 5.21 (d, 1H, J = 10.7 Hz); ^{13}C NMR (100 MHz, $CDCl_3$) δ 0.0, 0.5, 17.6, 17.8, 19.1, 23.0, 24.7, 25.1, 26.7, 30.0, 30.7, 32.6, 35.5, 38.5, 48.1, 52.9, 55.2, 57.6, 74.4, 80.6, 112.3, 143.1, 171.1, 214.4; HRMS calculated for ($C_{28}H_{52}O_6Si_2$) requires *m/z* [M+Na] 563.3200, found *m/z* 563.3214.

Bibliography

1. Bohacek, R. S.; McMartin, C.; Guida, W. C. The art and practice of structure-based drug design: a molecular modeling perspective. *Med. Res. Rev.* **1996**, *16*, 3-50.
2. Dobson, C. M. Chemical space and biology. *Nature* **2004**, *432*, 824-828.
3. Newman, D. J.; Cragg, G. M.; Snader, K. M. Natural products as sources of new drugs over the period 1981-2002. *J. Nat. Prod.* **2003**, *66*, 1022-1037.
4. Feher, M.; Schmidt, J. M. Property distributions: differences between drugs, natural products, and molecules from combinatorial chemistry. *J. Chem. Inf. Comput. Sci.* **2003**, *43*, 218-227.
5. Ranade, A. R.; Georg, G. I. Enantioselective synthesis of 3,4-dihydro-1,2-oxazepin-5(2*H*)-ones and 2,3-dihydropyridin-4(1*H*)-ones from β-substituted β-hydroxyaminoaldehydes. *J. Org. Chem.* **2014**, *79*, 984-992.
6. Bi, L.; Georg, G. I. Direct Hiyama cross-coupling of enaminones with triethoxy(aryl)silanes and dimethylphenylsilanol. *Org. Lett.* **2011**, *13*, 5413-5415.
7. Ge, H.; Niphakis, M. J.; Georg, G. I. Palladium(II)-catalyzed direct arylation of enaminones using organotrifluoroborates. *J. Am. Chem. Soc.* **2008**, *130*, 3708-3709.
8. Kim, Y. W.; Niphakis, M. J.; Georg, G. I. Copper-assisted palladium(II)-catalyzed direct arylation of cyclic enaminones with arylboronic acids. *J. Org. Chem.* **2012**, *77*, 9496-9503.
9. Yu, Y.-Y.; Bi, L.; Georg, G. I. Palladium-catalyzed direct C-H arylation of cyclic enaminones with aryl iodides. *J. Org. Chem.* **2013**, *78*, 6163-6169.
10. Yu, Y.-Y.; Niphakis, M. J.; Georg, G. I. Palladium(II)-catalyzed dehydrogenative alkenylation of cyclic enaminones via the Fujiwara-Moritani reaction. *Org. Lett.* **2011**, *13*, 5932-5935.
11. Ye, X. M.; Konradi, A. W.; Smith, J.; Xu, Y.-Z.; Dressen, D.; Garofalo, A. W.; Marugg, J.; Sham, H. L.; Truong, A. P.; Jagodzinski, J.; Pleiss, M.; Zhang, H.; Goldbach, E.; Sauer, J.-M.; Brigham, E.; Bova, M.; Basi, G. S. Discovery of a novel sulfonamide-pyrazolopiperidine series as potent and efficacious γ-secretase inhibitors. *Bioorg. Med. Chem. Lett.* **2010**, *20*, 2195-2199.
12. Garofalo, A. W.; Jagodzinski, J. J.; Konradi, A. W.; Semko, C. M.; Smith, J. L.; Xu, Y.-Z.; Ye, X. M. 5-(Arylsulfonyl)pyrazolopiperidines useful for treating cognitive disorders, their preparation, their methods of use, and pharmaceutical compositions containing them. WO2007064914A2, 2007.
13. Neitzel, M. L.; Marugg, J. L. Preparation of *N*-cyclic benzenesulfonamido compounds as inhibitors of gamma-secretase. WO2005113542A2, 2005.
14. Halazy, S. Pharmaceutically active benzsulfonamides as inhibitors of JNK proteins. EP1193256A1, 2002.
15. Xie, X.; Gu, Y.; Fox, T.; Coll, J. T.; Fleming, M. A.; Markland, W.; Caron, P. R.; Wilson, K. P.; Su, M. S. S. Crystal structure of JNK3: a kinase implicated in neuronal apoptosis. *Structure* **1998**, *6*, 983-991.
16. Yang, D. D.; Conze, D.; Whitmarsh, A. J.; Barrett, T.; Davis, R. J.; Rincon, M.; Flavell, R. A. Differentiation of CD4+ T cells to Th1 cells requires MAP kinase JNK2. *Immunity* **1998**, *9*, 575-585.

17. Almstead, N. G.; De, B.; Bradley, R. S.; Garrett, G. S.; Marlin, J. E., II; McIver, J. M.; Wang, Z.; Taiwo, Y. O. Preparation of nitrogen heterocycles as bidentate metalloprotease inhibitors. WO9808814A1, 1998.
18. Xie, Y. F.; Sircar, I.; Lake, K.; Komandla, M.; Ligsay, K.; Li, J.; Xu, K.; Parise, J.; Schneider, L.; Huang, D.; Liu, J.; Sakurai, N.; Barbosa, M.; Jack, R. Identification of novel series of human CCR1 antagonists. *Bioorg. Med. Chem. Lett.* **2008**, *18*, 2215-2221.
19. Proudfoot, A. E. I. Chemokine receptors: multifaceted therapeutic targets. *Nat. Rev. Immunol.* **2002**, *2*, 106-115.
20. Godessart, N.; Kunkel, S. L. Chemokines in autoimmune disease. *Curr. Opin. Immunol.* **2001**, *13*, 670-675.
21. Loetscher, P.; Moser, B. Homing chemokines in rheumatoid arthritis. *Arthritis Res.* **2002**, *4*, 233-236.
22. Haringman, J. J.; Kraan, M. C.; Smeets, T. J. M.; Zwinderman, K. H.; Tak, P. P. Chemokine blockade and chronic inflammatory disease: Proof of concept in patients with rheumatoid arthritis. *Ann. Rheum. Dis.* **2003**, *62*, 715-721.
23. Baliah, V.; Jeyaraman, R.; Chandrasekaran, L. Synthesis of 2,6-disubstituted piperidines, oxanes, and thianes. *Chem. Rev.* **1983**, *83*, 379-423.
24. Weintraub, P. M.; Sabol, J. S.; Kane, J. M.; Borcherding, D. R. Recent advances in the synthesis of piperidones and piperidines. *Tetrahedron* **2003**, *59*, 2953-2989.
25. Numata, A.; Ibuka, T. Alkaloids from ants and other insects. *Alkaloids (Academic Press)* **1987**, *31*, 193-315.
26. Edwards, M. W.; Daly, J. W. Alkaloids from a Panamanian poison frog, Dendrobates speciosus: identification of pumiliotoxin A and allopumiliotoxin class alkaloids, 3,5-disubstituted indolizidines, 5-substituted 8-methylindolizidines, and a 2-methyl-6-nonyl-4-hydroxypiperidine. *J. Nat. Prod.* **1988**, *51*, 1188-1197.
27. Davis, F. A.; Chao, B.; Rao, A. Intramolecular Mannich reaction in the asymmetric synthesis of polysubstituted piperidines: concise synthesis of the dendrobate alkaloid (+)-241D and its C-4 epimer. *Org. Lett.* **2001**, *3*, 3169-3171.
28. Rameshkumar, N.; Veena, A.; Ilavarasan, R.; Adiraj, M.; Shanmugapandiyan, P.; Sridhar, S. K. Synthesis and biological activities of 2,6-diaryl-3-methyl-4-piperidone derivatives. *Biol. Pharm. Bull.* **2003**, *26*, 188-193.
29. Ramalingan, C.; Balasubramanian, S.; Kabilan, S.; Vasudevan, M. Synthesis and study of antibacterial and antifungal activities of novel 1-[2-(benzoxazol-2-yl)ethoxy]-2,6-diarylpiperidin-4-ones. *Eur. J. Med. Chem.* **2004**, *39*, 527-533.
30. Struntz, G. M.; Findlay, J. A. Pyridine and piperidine alkaloids. In *The Alkaloids (Academic Press)*, Brossi, A., Ed. Elsevier: New York, 1985; Vol. 26, pp 89-183.
31. Ishimaru, K.; Kojima, T. Stereoselective synthesis of trans-2,6-diaryl-4-piperidones by using benzaldiminetricarbonylchromium derivatives. *J. Chem. Soc., Perkin Trans. 1* **2000**, 2105-2108.
32. El-Subbagh, H. I.; Abu-Zaid, S. M.; Mahran, M. A.; Badria, F. A.; Al-Obaid, A. M. Synthesis and biological evaluation of certain α,β-unsaturated ketones and their corresponding fused pyridines as antiviral and cytotoxic agents. *J. Med. Chem.* **2000**, *43*, 2915-2921.

33. Watson, A. A.; Fleet, G. W. J.; Asano, N.; Molyneux, R. J.; Nash, R. J. Polyhydroxylated alkaloids: Natural occurrence and therapeutic applications. *Phytochemistry* **2001**, *56*, 265-295.
34. Bagley, J. R.; Spencer, K. H. Preparation and testing of 4-(heterocyclylacylamino)piperidines as narcotic antagonists and analgesics. EP277794A2, 1988.
35. Venkatesa Perumal, R.; Adiraj, M.; Shanmuga Pandiyan, P. Synthesis, analgesic, and anti-inflammatory evaluation of substituted 4-piperidones. *Indian Drugs* **2001**, *38*, 156-159.
36. Ganellin, C. R.; Spickett, R. G. W. Compounds affecting the central nervous system. I. 4 Piperidones and related compounds. *J. Med. Chem.* **1965**, *8*, 619-625.
37. Nikolova, M.; Stefanova, D.; Chavdarov, D. Influence of tempidon on the EEG [electroencephalogram] of cats at a single and repeated application. *Act. Nerv. Super.* **1974**, *16*, 264-268.
38. Hagenbach, R. E.; Gysin, H. Some heterocyclic thiosemicarbazones. *Experientia* **1952**, *8*, 184-185.
39. Baracu, I.; Dobre, V.; Niculescu-Duvaz, I. Potential anticancer agents. XXVI. Spin labeled nitrosoureas. *J. Prakt. Chem.* **1985**, *327*, 667-674.
40. Basic substituted alkylbenzenes and pharmaceutical compositions containing them. FR2437405A1, 1980.
41. Nakanishi, M.; Shiraki, M.; Kobayakawa, T.; Kobayashi, R. Heterocyclic compounds. JP49003987B, 1974.
42. Sanczuk, S.; Hermans, H. K. F. *N*-Aryl-*N*-(4-piperidinyl)arylacetamides. DE2642856A1, 1977.
43. Meyers, A. I.; Shawe, T. T.; Gottlieb, L. Stereoselective nucleophilic addition to conformationally constrained piperidines. An efficient route to 2-axial-6-equatorial disubstituted piperidines. *Tetrahedron Lett.* **1992**, *33*, 867-870.
44. Tawara, J. N.; Lorenz, P.; Stermitz, F. R. 4-Hydroxylated piperidines and *N*-methyleuphococcinine (1-methyl-3-granatanone) from Picea (spruce) species. Identification and synthesis. *J. Nat. Prod.* **1999**, *62*, 321-323.
45. Watson, P. S.; Jiang, B.; Scott, B. A diastereoselective synthesis of 2,4-disubstituted piperidines: Scaffolds for drug discovery. *Org. Lett.* **2000**, *2*, 3679-3681.
46. Brooks, C. A.; Comins, D. L. Asymmetric synthesis of (2*S*,4*R*)-hydroxypipecolic acid. *Tetrahedron Lett.* **2000**, *41*, 3551-3553.
47. Buffat, M. G. P. Synthesis of piperidines. *Tetrahedron* **2004**, *60*, 1701-1729.
48. Murty, M. S. R.; Ram, K. R.; Yadav, J. S. $BiCl_3$ promoted aza-Prins type cyclization: a rapid and efficient synthesis of 2,4-disubstituted piperidines. *Tetrahedron Lett.* **2008**, *49*, 1141-1145.
49. Howard, N.; Abell, C.; Blakemore, W.; Chessari, G.; Congreve, M.; Howard, S.; Jhoti, H.; Murray, C. W.; Seavers, L. C. A.; Van Montfort, R. L. M. Application of fragment screening and fragment linking to the discovery of novel thrombin inhibitors. *J. Med. Chem.* **2006**, *49*, 1346-1355.
50. Wright, J. L.; Gregory, T. F.; Kesten, S. R.; Boxer, P. A.; Serpa, K. A.; Meltzer, L. T.; Wise, L. D.; Espitia, S. A.; Konkoy, C. S.; Whittemore, E. R.; Woodward, R. M. Subtype-selective *N*-methyl-D-aspartate receptor antagonists: Synthesis and biological

evaluation of 1-(heteroarylalkynyl)-4-benzylpiperidines. *J. Med. Chem.* **2000**, *43*, 3408-3419.
51. Dimmock, J. R.; Kumar, P. Anticancer and cytotoxic properties of Mannich bases. *Curr. Med. Chem.* **1997**, *4*, 1-22.
52. Kubota, H.; Kakefuda, A.; Okamoto, Y.; Fujii, M.; Yamamoto, O.; Yamagiwa, Y.; Orita, M.; Ikeda, K.; Takeuchi, M.; Shibanuma, T.; Isomura, Y. Spiro-substituted piperidines as neurokinin receptor antagonists. III. Synthesis of (±)-N-[2-(3,4-Dichlorophenyl)-4-(spiro-substituted piperidin-1'-yl)butyl]-N-methylbenzamides and evaluation of NK1-NK2 dual antagonistic activities. *Chem. Pharm. Bull.* **1998**, *46*, 1538-1544.
53. Prostakov, N. S.; Gaivoronskaya, L. A. γ-Piperidinones in organic synthesis. *Russ. Chem. Rev.* **1978**, *47*, 447-469.
54. Hohenlohe-Oehringen, N. K. 3-Phenyl-4-aminopiperidine and its derivatives alkylated at the ring. *Monatsh. Chem.* **1965**, *96*, 262-265.
55. Ott, H.; Suess, R. *cis*-1,2,3,4,4a,10b-Hexahydro-2-methyl-6-phenylbenzo[c][1,6]naphthyridines against thrombocyte aggregation. DE2123328A, 1971.
56. Ott, H.; Suess, R. *cis*-6-[(Acylamino)phenyl]-1,2,3,4,4a,10b-hexahydro-8,9-dimethoxy-2-methylbenzo[c][1,6]naphthyridines. DE2352909A1, 1974.
57. Flockerzi, D.; Klemm, K.; Amschler, H.; Figala, V.; Beume, R.; Haefner, D.; Hanauer, G.; Eltze, M.; Schudt, C.; Kilian, U. Preparation of 6-(sulfonamidophenyl) benzo[c][1,6]naphthyridines as bronchodilators. WO9117991A1, 1991.
58. Engelstaetter, R.; Beume, R.; Kilian, U.; Schudt, C.; Riedel, R.; Amschler, H.; Flockerzi, D. Use of sulfonamides for treatment of rhinitis, sinusitis, and related diseases. DE4310050A1, 1993.
59. Riley, T. N.; Hale, D. B.; Wilson, M. C. 4-Anilidopiperidine analgesics. I. Synthesis and analgesic activity of certain ring-methylated, 1-substituted 4-propananilidopiperidines. *J. Pharm. Sci.* **1973**, *62*, 983-986.
60. Lednicer, D.; Mitscher, L. A. *The Organic Chemistry of Drug Synthesis*. John Wiley & Sons: New York, 1977; Vol. 1.
61. Angle, S. R.; Breitenbucher, J. G. Recent progress in the synthesis of piperidine and indolizidine alkaloids. In *Stereoselective Synthesis*, Atta-ur-Rahman, Ed. Elsevier: New York, 1995; Vol. 16, pp 453-502.
62. Schneider, M. J. Pyridine and piperidine alkaloids: An update In *Alkaloids: Chemical and Biological Perspectives*, Pelletier, S. W., Ed. Elsevier: New York, 1996; Vol. 10, pp 155-299.
63. Katritzky, A. R.; Fan, W. The chemistry of benzotriazole. A novel and versatile synthesis of 1-alkyl-, 1-aryl-, 1-(alkylamino)-, or 1-amido-substituted and of 1,2,6-trisubstituted piperidines from glutaraldehyde and primary amines or monosubstituted hydrazines. *J. Org. Chem.* **1990**, *55*, 3205-3209.
64. O'Hagan, D. Pyrrole, pyrrolidine, pyridine, piperidine and tropane alkaloids. *Nat. Prod. Rep.* **2000**, *17*, 435-446.
65. Liu, Q.-F.; Wang, J.-D.; Wang, X.-J.; Liu, C.-X.; Zhang, J.; Pang, Y.-W.; Yu, C.; Xiang, W.-S. Two new piperidine alkaloids from Streptomyces sp. NEAU-Z4. *J. Asian Nat. Prod. Res.* **2013**, *15*, 221-224.

66. Radha Krishna, P.; Reddy, B. K. Total synthesis of the 2,6-disubstituted piperidine alkaloid (-)-andrachcinidine. *Tetrahedron: Asymmetry* **2013**, *24*, 758-763.
67. Gross, D. Occurrence, structure, and biosynthesis of natural piperidine compounds. *Fortschr. Chem. Org. Naturst.* **1971**, *29*, 1-59.
68. Heringa, M. Review on raloxifene: profile of a selective estrogen receptor modulator. *Int. J. Clin. Pharmacol. Ther.* **2003**, *41*, 331-345.
69. Traub, Y. M.; Redmond, D. P.; Rosenfeld, J. B.; McDonald, R. H., Jr.; Shapiro, A. P. Treatment of severe hypertension with minoxidil. *Isr. J. Med. Sci.* **1975**, *11*, 991-998.
70. Martin-Islan, A. P.; Martin-Ramos, D.; Sainz-Diaz, C. I. Crystal structure of minoxidil at low temperature and polymorph prediction. *J. Pharm. Sci.* **2007**, *97*, 815-830.
71. Bovill, J. G.; Sebel, P. S.; Stanley, T. H. Opioid analgesics in anesthesia: with special reference to their use in cardiovascular anesthesia. *Anesthesiology* **1984**, *61*, 731-755.
72. Stanley, T. H. Opiate anaesthesia. *Anaesth. Intens. Care* **1987**, *15*, 38-59.
73. Brocks, D. R. Anticholinergic drugs used in Parkinson's disease: An overlooked class of drugs from a pharmacokinetic perspective. *J. Pharm. Pharm. Sci.* **1999**, *2*, 39-46.
74. Nishiyama, K.; Mizuno, T.; Sakuta, M.; Kurisaki, H. Chronic dementia in Parkinson's disease treated by anticholinergic agents. Neuropsychological and neuroradiological examination. *Adv. Neurol.* **1993**, *60*, 479-483.
75. Sahu, S. K.; Dubey, B. K.; Tripathi, A. C.; Koshy, M.; Saraf, S. K. Piperidin-4-one: the potential pharmacophore. *Mini-Rev. Med. Chem.* **2013**, *13*, 565-583.
76. Petrenko-Kritchenko, P. Condensation of acetonedicarboxylic ester with aldehydes, ammonia and amines. *J. Prakt. Chem.* **1912**, *85*, 1-37.
77. Noller, C. R.; Baliah, V. Preparation of some piperidine derivatives by the Mannich reaction. *J. Am. Chem. Soc.* **1948**, *70*, 3853-3855.
78. Edwards, M. W.; Garraffo, H. M.; Daly, J. W. Facile synthesis of 4-piperidones by condensation of an α,β-unsaturated ketone, an aldehyde and ammonia: synthesis of the Dendrobatid frog alkaloid 241D. *Synthesis* **1994**, 1167-1170.
79. Rastogi, S.; Rastogi, H. An efficient synthesis of some substituted piperidin-4-one thiosemicarbazone derivatives as potential anticonvulsant under microwave irradiation. *Indian J. Chem., Sect. B: Org. Chem. Incl. Med. Chem.* **2010**, *49B*, 547-553.
80. Feng, L.-C.; Sun, Y.-W.; Tang, W.-J.; Xu, L.-J.; Lam, K.-L.; Zhou, Z.; Chan, A. S. C. Highly efficient chemoselective construction of 2,2-dimethyl-6-substituted 4-piperidones via multi-component tandem Mannich reaction in ionic liquids. *Green Chem.* **2010**, *12*, 949-952.
81. Soundarrajan, C.; Saraswathi, K.; Asiyaparvin, A. Piperidone synthesis using amino acid: A promising scope for green chemistry. *Microchem. J.* **2011**, *98*, 204-206.
82. Chan, Y.; Guthmann, H.; Brimble, M. A.; Barker, D. Diastereoselective synthesis of substituted 4-piperidones and 4-piperidols using a double Mannich reaction. *Synlett* **2008**, 2601-2604.
83. Jia, X.-D.; Wang, X.-E.; Yang, C.-X.; Huo, C.-D.; Wang, W.-J.; Ren, Y.; Wang, X.-C. Synthesis of β-aminoketones and construction of highly substituted 4-piperidones

by Mannich reaction induced by persistent radical cation salts. *Org. Lett.* **2010**, *12*, 732-735.
84. Jia, X.-D.; Chen, X.-N.; Wang, X.-E.; Huo, C.-D.; Wang, W.-J.; Ren, Y.; Wang, X.-C. I_2-induced stereospecific synthesis of 4-piperidones through double Mannich reaction and tandem cyclization. *Eur. J. Org. Chem.* **2011**, *2011*, 1627-1631.
85. Jia, X.-D.; Wang, W.-J.; Huo, C.-D.; Ren, Y.; Chen, X.-N.; Xu, X.-L.; Wang, X.-C. Double Mannich reaction and tandem cyclization of imines with ketones catalyzed by indium(III) chloride tetrahydrate: stereoselective synthesis of highly substituted 4-piperidones. *Adv. Synth. Catal.* **2011**, *353*, 315-319.
86. Harmata, M.; Lee, D. R. A synthesis of 2,3-dihydro-4-pyridones. *ARKIVOC* **2007**, 91-103.
87. Burke, M. D.; Schreiber, S. L. A planning strategy for diversity-oriented synthesis. *Angew. Chem. Int. Ed.* **2004**, *43*, 46-58.
88. Ali, M.; Ansari, S. H.; Qadry, J. S. Rare phenanthroindolizidine alkaloids and a substituted phenanthrene, tyloindane, from Tylophora indica. *J. Nat. Prod.* **1991**, *54*, 1271-1278.
89. Comins, D. L. Asymmetric synthesis and synthetic utility of 2,3-dihydro-4-pyridones. *J. Heterocycl. Chem.* **1999**, *36*, 1491-1500.
90. Wagman, A. S.; Wentland, M. P. Quinolone antibacterial agents. In *Comprehensive Medicinal Chemistry II*, Taylor, J. B.; Triggle, D. J., Eds. Elsevier: New York, 2006; Vol. 7, pp 567-596.
91. Xia, Y.; Yang, Z.-Y.; Xia, P.; Bastow, K. F.; Tachibana, Y.; Kuo, S.-C.; Hamel, E.; Hackl, T.; Lee, K.-H. Antitumor agents. 181. Synthesis and biological evaluation of 6,7,2',3',4'-substituted-1,2,3,4-tetrahydro-2-phenyl-4-quinolones as a new class of antimitotic antitumor agents. *J. Med. Chem.* **1998**, *41*, 1155-1162.
92. Matsuo, J.-i.; Okado, R.; Ishibashi, H. A new synthesis of 2,3-di- or 2,3,3-trisubstituted 2,3-dihydro-4-pyridones by reaction of 3-ethoxycyclobutanones and N-*p*-toluenesulfonyl imines using titanium(IV) chloride: synthesis of (±)-bremazocine. *Org. Lett.* **2010**, *12*, 3266-3268.
93. Xu, Q.; Zhang, R.; Zhang, T.; Shi, M. Asymmetric 1,4-addition of arylboronic acids to 2,3-dihydro-4-pyridones catalyzed by axially chiral NHC-Pd(II) complexes. *J. Org. Chem.* **2010**, *75*, 3935-3937.
94. Comins, D. L.; Brooks, C. A.; Ingalls, C. L. Reduction of N-acyl-2,3-dihydro-4-pyridones to N-acyl-4-piperidones using zinc/acetic acid. *J. Org. Chem.* **2001**, *66*, 2181-2182.
95. Shintani, R.; Tokunaga, N.; Doi, H.; Hayashi, T. A new entry of nucleophiles in rhodium-catalyzed asymmetric 1,4-addition reactions: addition of organozinc reagents for the synthesis of 2-aryl-4-piperidones. *J. Am. Chem. Soc.* **2004**, *126*, 6240-6241.
96. Sebesta, R.; Pizzuti, M. G.; Boersma, A. J.; Minnaard, A. J.; Feringa, B. L. Catalytic enantioselective conjugate addition of dialkylzinc reagents to *N*-substituted-2,3-dehydro-4-piperidones. *Chem. Commun.* **2005**, 1711-1713.
97. Shintani, R.; Hayashi, T. Preparation of arylzinc reagents and their use in the rhodium-catalyzed asymmetric 1,4-addition for the synthesis of 2-aryl-4-piperidones. *Nat. Protoc.* **2007**, *2*, 2903-2909.

98. Endo, K.; Ogawa, M.; Shibata, T. Multinuclear catalyst for copper-catalyzed asymmetric conjugate addition of organozinc reagents. *Angew. Chem. Int. Ed.* **2010**, *49*, 2410-2413.
99. Jagt, R. B. C.; De Vries, J. G.; Feringa, B. L.; Minnaard, A. J. Enantioselective synthesis of 2-aryl-4-piperidones via rhodium/phosphoramidite-catalyzed conjugate addition of arylboroxines. *Org. Lett.* **2005**, *7*, 2433-2435.
100. Thaler, T.; Guo, L.-N.; Steib, A. K.; Raducan, M.; Karaghiosoff, K.; Mayer, P.; Knochel, P. Sulfoxide-alkene hybrids: A new class of chiral ligands for the Hayashi-Miyaura reaction. *Org. Lett.* **2011**, *13*, 3182-3185.
101. Zhang, X.; Chen, J.; Han, F.; Cun, L.; Liao, J. Rhodium-catalyzed enantioselective conjugate addition of sodium tetraarylborates to 2,3-dihydro-4-pyridones and 4-quinolones by using (*R*,*R*)-1,2-bis(*tert*-butylsulfinyl)benzene as a ligand. *Eur. J. Org. Chem.* **2011**, *2011*, 1443-1446.
102. Nakao, Y.; Chen, J.; Imanaka, H.; Hiyama, T.; Ichikawa, Y.; Duan, W.-L.; Shintani, R.; Hayashi, T. Organo[2-(hydroxymethyl)phenyl]dimethylsilanes as mild and reproducible agents for rhodium-catalyzed 1,4-addition reactions. *J. Am. Chem. Soc.* **2007**, *129*, 9137-9143.
103. Pizzuti, M. G.; Minnaard, A. J.; Feringa, B. L. Catalytic asymmetric synthesis of the alkaloid (+)-myrtine. *Org. Biomol. Chem.* **2008**, *6*, 3464-3466.
104. Muller, D.; Alexakis, A. Copper-catalyzed asymmetric 1,4-addition of alkenyl alanes to *N*-substituted-2-3-dehydro-4-piperidones. *Org. Lett.* **2012**, *14*, 1842-1845.
105. Akiba, K.; Motoshima, T.; Ishimaru, K.; Yabuta, K.; Hirota, H.; Yamamoto, Y. [4+2]Type cycloaddition of aldimines bearing α-hydrogens with 2-siloxy-1,3-butadienes catalyzed by trimethylsilyl triflate. *Synlett* **1993**, 657-659.
106. Aznar, F.; Garcia, A.-B.; Cabal, M.-P. Proline-catalyzed imino-Diels-Alder reactions: synthesis of meso-2,6-diaryl-4-piperidones. *Adv. Synth. Catal.* **2006**, *348*, 2443-2448.
107. Norman, B. H.; Gareau, Y.; Padwa, A. Tandem addition-cycloaddition reaction of oximes with 2,3-bis(phenylsulfonyl)-1,3-butadiene as a method for 4-piperidone synthesis. *J. Org. Chem.* **1991**, *56*, 2154-2161.
108. Padwa, A.; Norman, B. H. Intramolecular cycloaddition reactions of oximes with vinyl sulfones. *Tetrahedron Lett.* **1988**, *29*, 2417-2420.
109. Flick, A. C.; Padwa, A. A new route to heterocyclic compounds by the mercuric acetate oxidation of *N*-alkyl substituted 4-piperidones. *Tetrahedron Lett.* **2008**, *49*, 5739-5741.
110. Selvaraj, S.; Maragathasundaram, S.; Perumal, S.; Arumugam, N. Synthesis of *cis*-1-methyl-2,6-diaryl-4-piperidones. *Indian J. Chem., Sect. B* **1987**, *26B*, 1104-1105.
111. Padmavathi, V.; Reddy, T. V. R.; Reddy, K. A.; Reddy, D. B. Synthesis of some novel annelated 1,2,3-selena/thiadiazoles and 2*H*-diazaphospholes. *J. Heterocycl. Chem.* **2003**, *40*, 149-153.
112. Doerrenbaecher, S.; Kazmaier, U.; Ruf, S. A straightforward approach towards piperidines via Stille coupling and subsequent 1,4-addition of amines. *Synlett* **2006**, 547-550.
113. Sun, C.-W.; Wang, H.-F.; Zhu, J.; Yang, D.-R.; Xing, J.; Jin, J. Novel symmetrical trans-bis-Schiff bases of *N*-substituted-4-piperidones: Synthesis,

characterization, and preliminary antileukemia activity mensurations. *J. Heterocycl. Chem.* **2013**, *50*, 1374-1380.
114. Chen, B.-L.; Wang, B.; Lin, G.-Q. A novel and concise synthetic access to chiral 2-substituted-4-piperidones. *Sci. China Chem.* **2014**, Ahead of Print. DOI: 10.1007/s11426-014-5065-3.
115. Comins, D. L.; Brown, J. D. Addition of Grignard reagents to 1-acyl-4-methoxypyridinium salts. An approach to the synthesis of quinolizidinones. *Tetrahedron Lett.* **1986**, *27*, 4549-4552.
116. Comins, D. L.; Joseph, S. P. Alkaloid synthesis using 1-acylpyridinium salts as intermediates. *Adv. Nitrogen Heterocycl.* **1996**, *2*, 251-294.
117. Williams, A. L.; Abad Grillo, T.; Comins, D. L. A novel free-radical ring contraction of a cyclic carbamate. *J. Org. Chem.* **2002**, *67*, 1972-1973.
118. Angle, S. R.; Arnaiz, D. O. Stereoselective synthesis of substituted pipecolic acids. *Tetrahedron Lett.* **1989**, *30*, 515-518.
119. Avenoza, A.; Busto, J. H.; Cativiela, C.; Corzana, F.; Peregrina, J. M.; Zurbano, M. M. Asymmetric hetero Diels-Alder as an access to carbacephams. *J. Org. Chem.* **2002**, *67*, 598-601.
120. Perrio-Huard, C.; Ducandas, c.; Lasne, M. C.; Moreau, B. Syntheses of piperidine and perhydroazepine derivatives, precursors of two selective antagonists of muscarinic M2 receptors: AF-DX 384 and its perhydroazepine isomer. *J. Chem. Soc., Perkin Trans. 1* **1996**, 2925-2932.
121. Oberboersch, S.; Reich, M.; Schunk, S.; Engels, M. F.-M.; Jostock, R.; Germann, T.; De Vry, J.; Schiene, K.; Hees, S. Preparation of sulfonamides as bradykinin B1 receptor antagonists. US20090264400A1, 2009.
122. Arnott, G.; Brice, H.; Clayden, J.; Blaney, E. Electrophile-induced dearomatizing spirocyclization of *N*-arylisonicotinamides: a route to spirocyclic piperidines. *Org. Lett.* **2008**, *10*, 3089-3092.
123. Ellis, G. L.; Amewu, R.; Sabbani, S.; Stocks, P. A.; Shone, A.; Stanford, D.; Gibbons, P.; Davies, J.; Vivas, L.; Charnaud, S.; Bongard, E.; Hall, C.; Rimmer, K.; Lozanom, S.; Jesus, M.; Gargallo, D.; Ward, S. A.; O'Neill, P. M. Two-step synthesis of achiral dispiro-1,2,4,5-tetraoxanes with outstanding antimalarial activity, low toxicity, and high-stability profiles. *J. Med. Chem.* **2008**, *51*, 2170-2177.
124. Yoo, K. H.; Choi, H. S.; Kim, D. C.; Shin, K. J.; Kim, D. J.; Song, Y. S.; Jin, C. Synthesis of hetero-aryl-piperazines and hetero-aryl-bipiperidines with a restricted side chain and their affinities for 5-HT1A receptor. *Arch. Pharm. (Weinheim, Ger.)* **2003**, *336*, 208-215.
125. https://pubchem.ncbi.nlm.nih.gov/assay/assay.cgi?aid=488862 (accessed Jun 20, 2014).
126. Anderson, J. L. Lipoprotein-associated phospholipase A2: An independent predictor of coronary artery disease events in primary and secondary prevention. *Am. J. Cardiol.* **2008**, *101*, 23-33.
127. Sudhir, K. Clinical review: Lipoprotein-associated phospholipase A2, a novel inflammatory biomarker and independent risk predictor for cardiovascular disease. *J. Clin. Endocrinol. Metab.* **2005**, *90*, 3100-3105.

128. https://pubchem.ncbi.nlm.nih.gov/assay/assay.cgi?aid=492953 (accessed Jun 20, 2014).
129. Grushin, V. V. The organometallic fluorine chemistry of palladium and rhodium: studies toward aromatic fluorination. *Accounts Chem. Res.* **2009**, *43*, 160-171.
130. Müller, K.; Faeh, C.; Diederich, F. Fluorine in pharmaceuticals: looking beyond intuition. *Science* **2007**, *317*, 1881-1886.
131. Purser, S.; Moore, P. R.; Swallow, S.; Gouverneur, V. Fluorine in medicinal chemistry. *Chem. Soc. Rev.* **2008**, *37*, 320-330.
132. Jeschke, P. The unique role of fluorine in the design of active ingredients for modern crop protection. *ChemBioChem* **2004**, *5*, 571-589.
133. Simons, J. H.; Lewis, C. J. The preparation of benzotrifluoride. *J. Am. Chem. Soc.* **1938**, *60*, 492-492.
134. Wu, X. F.; Neumann, H.; Beller, M. Recent developments on the trifluoromethylation of (hetero)arenes. *Chem. Asian J.* **2012**, *7*, 1744-1754.
135. Studer, A. A "renaissance" in radical trifluoromethylation. *Angew. Chem. Int. Ed.* **2012**, *51*, 8950-8958.
136. Qing, F.-L. Recent advances of trifluoromethylation. *Chinese J. Org. Chem.* **2012**, *32*, 815-824.
137. Lu, C. P.; Shen, Q. L.; Liu, D. Transition metal-catalyzed arene trifluoromethylation. *Chinese J. Org. Chem.* **2012**, *32*, 1380-1387.
138. Garcia-Monforte, M. A.; Martinez-Salvador, S.; Menjon, B. The trifluoromethyl group in transition metal chemistry. *Eur. J. Inorg. Chem.* **2012**, *2012*, 4945-4966.
139. Tomashenko, O. A.; Grushin, V. V. Aromatic trifluoromethylation with metal complexes. *Chem. Rev.* **2011**, *111*, 4475-4521.
140. Furuya, T.; Kamlet, A. S.; Ritter, T. Catalysis for fluorination and trifluoromethylation. *Nature* **2011**, *473*, 470-477.
141. Liu, H.; Gu, Z. H.; Jiang, X. F. Direct trifluoromethylation of the C-H bond. *Adv. Synth. Catal.* **2013**, *355*, 617-626.
142. Kamei, T. Metal-catalyzed/mediated aromatic C-H bond trifluoromethylation. *J. Syn. Org. Chem. Jpn.* **2012**, *70*, 756-757.
143. Besset, T.; Schneider, C.; Cahard, D. Tamed arene and heteroarene trifluoromethylation. *Angew. Chem. Int. Ed.* **2012**, *51*, 5048-5050.
144. Chu, L.; Qing, F.-L. Copper-mediated aerobic oxidative trifluoromethylation of terminal alkynes with Me_3SiCF_3. *J. Am. Chem. Soc.* **2010**, *132*, 7262-7263.
145. Jiang, X.; Chu, L.; Qing, F.-L. Copper-catalyzed oxidative trifluoromethylation of terminal alkynes and aryl boronic acids using (trifluoromethyl)trimethylsilane. *J. Org. Chem.* **2012**, *77*, 1251-1257.
146. Ke, Z.; Xiao-Long, Q.; Yangen, H.; Feng-Ling, Q. An improved copper-mediated oxidative trifluoromethylation of terminal alkynes. *Eur. J. Org. Chem.* **2012**, *2012*, 58-61.
147. Jun-An, M.; Dominique, C. Strategies for nucleophilic, electrophilic, and radical trifluoromethylations. *J. Fluorine Chem.* **2007**, *128*, 975-996.
148. Wang, X.; Truesdale, L.; Yu, J.-Q. Pd(II)-catalyzed ortho-trifluoromethylation of arenes using TFA as a promoter. *J. Am. Chem. Soc.* **2010**, *132*, 3648-3649.

149. Zhang, X.-G.; Dai, H.-X.; Wasa, M.; Yu, J.-Q. Pd(II)-catalyzed ortho trifluoromethylation of arenes and insights into the coordination mode of acidic amide directing groups. *J. Am. Chem. Soc.* **2012**, *134*, 11948-11951.
150. Zhang, L.-S.; Chen, K.; Chen, G.; Li, B.-J.; Luo, S.; Guo, Q.-Y.; Wei, J.-B.; Shi, Z.-J. Palladium-catalyzed trifluoromethylation of aromatic C-H bond directed by an acetamino group. *Org. Lett.* **2013**, *15*, 10-13.
151. Ye, Y.; Ball, N. D.; Kampf, J. W.; Sanford, M. S. Oxidation of a cyclometalated Pd(II) dimer with "CF_3^+": Formation and reactivity of a catalytically competent monomeric Pd(IV) aquo complex. *J. Am. Chem. Soc.* **2010**, *132*, 14682-14687.
152. Besset, T.; Cahard, D.; Pannecoucke, X. Regio- and diastereoselective Cu-mediated trifluoromethylation of functionalized alkenes. *J. Org. Chem.* **2014**, *79*, 413-418.
153. Wiehn, M. S.; Vinogradova, E. V.; Togni, A. Electrophilic trifluoromethylation of arenes and *N*-heteroarenes using hypervalent iodine reagents. *J. Fluorine Chem.* **2010**, *131*, 951-957.
154. Shimizu, R.; Egami, H.; Nagi, T.; Chae, J.; Hamashima, Y.; Sodeoka, M. Direct C2-trifluoromethylation of indole derivatives catalyzed by copper acetate. *Tetrahedron Lett.* **2010**, *51*, 5947-5949.
155. Egami, H.; Shimizu, R.; Kawamura, S.; Sodeoka, M. Alkene trifluoromethylation coupled with C–C bond formation: construction of trifluoromethylated carbocycles and heterocycles. *Angew. Chem. Int. Ed.* **2013**, *52*, 4000–4003.
156. Chao, F.; Teck-Peng, L. Copper-catalyzed olefinic trifluoromethylation of enamides at room temperature. *Chem. Sci.* **2012**, *3*, 3458-3462.
157. Mu, X.; Chen, S.; Zhen, X.; Liu, G. Palladium-catalyzed oxidative trifluoromethylation of indoles at room temperature. *Chem. Eur. J.* **2011**, *17*, 6039-6042.
158. Mu, X.; Wu, T.; Wang, H.-Y.; Guo, Y.-L.; Liu, G. Palladium-catalyzed oxidative aryltrifluoromethylation of activated alkenes at room temperature. *J. Am. Chem. Soc.* **2012**, *134*, 878-881.
159. Chu, L.; Qing, F.-L. Copper-catalyzed direct C-H oxidative trifluoromethylation of heteroarenes. *J. Am. Chem. Soc.* **2012**, *134*, 1298-1304.
160. Kino, T.; Nagase, Y.; Ohtsuka, Y.; Yamamoto, K.; Uraguchi, D.; Tokuhisa, K.; Yamakawa, T. Trifluoromethylation of various aromatic compounds by CF_3I in the presence of Fe(II) compound, H_2O_2 and dimethylsulfoxide. *J. Fluorine Chem.* **2010**, *131*, 98-105.
161. Ye, Y.; Lee, S. H.; Sanford, M. S. Silver-mediated trifluoromethylation of arenes using $TMSCF_3$. *Org. Lett.* **2011**, *13*, 5464-5467.
162. Hafner, A.; Bräse, S. Ortho-trifluoromethylation of functionalized aromatic triazenes. *Angew. Chem. Int. Ed.* **2012**, *51*, 3713-3715.
163. Parsons, A. T.; Buchwald, S. L. Organic chemistry: A radical approach to diversity. *Nature* **2011**, *480*, 184-185.
164. Nagib, D. A.; MacMillan, D. W. C. Trifluoromethylation of arenes and heteroarenes by means of photoredox catalysis. *Nature* **2011**, *480*, 224-228.
165. Iqbal, N.; Choi, S.; Ko, E.; Cho, E. J. Trifluoromethylation of heterocycles via visible light photoredox catalysis. *Tetrahedron Lett.* **2012**, *53*, 2005-2008.

166. Ji, Y.; Brueckl, T.; Baxter, R. D.; Fujiwara, Y.; Seiple, I. B.; Su, S.; Blackmond, D. G.; Baran, P. S. Innate C-H trifluoromethylation of heterocycles. *Proc. Natl. Acad. Sci. U.S.A.* **2011**, *108*, 14411-14415.
167. Shi, L.; Yang, X.; Wang, Y.; Yang, H.; Fu, H. Metal-free trifluoromethylation and arylation of alkenes: Domino synthesis of oxindole derivatives. *Adv. Synth. Catal.* **2014**, *356*, 1021-1028.
168. Pan, Y.; Wang, S.; Kee, C. W.; Dubuisson, E.; Yang, Y.; Loh, K. P.; Tan, C.-H. Graphene oxide and Rose Bengal: oxidative C–H functionalisation of tertiary amines using visible light. *Green Chemistry* **2011**, *13*, 3341-3344.
169. Chu, L.; Qing, F.-L. Copper-mediated oxidative trifluoromethylation of boronic acids. *Org. Lett.* **2010**, *12*, 5060-5063.
170. Mitsudera, H.; Li, C.-J. Copper-catalyzed oxidative trifluoromethylation of benzylic sp^3 C–H bond adjacent to nitrogen in amines. *Tetrahedron Lett.* **2011**, *52*, 1898-1900.
171. Xu, J.; Fu, Y.; Luo, D.-F.; Jiang, Y.-Y.; Xiao, B.; Liu, Z.-J.; Gong, T.-J.; Liu, L. Copper-catalyzed trifluoromethylation of terminal alkenes through allylic C-H bond activation. *J. Am. Chem. Soc.* **2011**, *133*, 15300-15303.
172. Parsons, A. T.; Buchwald, S. L. Copper-catalyzed trifluoromethylation of unactivated olefins. *Angew. Chem. Int. Ed.* **2011**, *50*, 9120-9123.
173. Wang, X.; Ye, Y.; Zhang, S.; Feng, J.; Xu, Y.; Zhang, Y.; Wang, J. Copper-catalyzed $C(sp^3)$-$C(sp^3)$ bond formation using a hypervalent iodine reagent: An efficient allylic trifluoromethylation. *J. Am. Chem. Soc.* **2011**, *133*, 16410-16413.
174. Chu, L.; Qing, F.-L. Copper-catalyzed oxidative trifluoromethylation of terminal alkenes using nucleophilic CF_3SiMe_3: efficient $C(sp^3)$-CF_3 bond formation. *Org. Lett.* **2012**, *14*, 2106-2109.
175. Nagib, D. A.; Scott, M. E.; MacMillan, D. W. C. Enantioselective alpha-trifluoromethylation of aldehydes via photoredox organocatalysis. *J. Am. Chem. Soc.* **2009**, *131*, 10875-10877.
176. Allen, A. E.; MacMillan, D. W. C. The productive merger of iodonium salts and organocatalysis: a non-photolytic approach to the enantioselective alpha-trifluoromethylation of aldehydes. *J. Am. Chem. Soc.* **2010**, *132*, 4986-4987.
177. Pham, P. V.; Nagib, D. A.; MacMillan, D. W. C. Photoredox catalysis: a mild, operationally simple approach to the synthesis of α-trifluoromethyl carbonyl compounds. *Angew. Chem. Int. Ed.* **2011**, *50*, 6119-6122.
178. Mao, Z.; Huang, F.; Yu, H.; Chen, J.; Yu, Z.; Xu, Z. Copper-catalyzed trifluoromethylation of internal olefinic C –H bonds: efficient routes to trifluoromethylated tetrasubstituted olefins and *N*-heterocycles. *Chem. Eur. J.* **2014**, *20*, 3439-3445.
179. Khan, P. M.; El-Gendy, B. E.-D. M.; Kumar, N.; Garcia-Ordonez, R.; Lin, L.; Ruiz, C. H.; Cameron, M. D.; Griffin, P. R.; Kamenecka, T. M. Small molecule amides as potent ROR-γ selective modulators. *Bioorg. Med. Chem. Lett.* **2013**, *23*, 532-536.
180. Jiang, R.; Song, X.; Bali, P.; Smith, A.; Bayona, C. R.; Lin, L.; Cameron, M. D.; McDonald, P. H.; Kenny, P. J.; Kamenecka, T. M. Disubstituted piperidines as potent orexin (hypocretin) receptor antagonists. *Bioorg. Med. Chem. Lett.* **2012**, *22*, 3890-3894.

181. D'Amico, D. C.; Herberich, B. J.; Jackson, C. L. M.; Pettus, L. H.; Tasker, A.; Wang, H.-L.; Wu, B.; Wurz, R. Preparation of imidazo[1,5-b]pyridazine derivatives as Pim kinase inhibitors. WO2012148775A1, 2012.
182. Priepke, H.; Doods, H.; Heim-Riether, A.; Kuelzer, R.; Pfau, R.; Rudolf, K.; Stenkamp, D. Preparation of aminophenylaminobenzimidazolecarboxamide derivatives for use as microsomal prostaglandin E2 synthase-1 inhibitors. WO2012076673A1, 2012.
183. Sun, C.; Ewing, W. R.; Bolton, S. A.; Gu, Z.; Huang, Y.; Murugesan, N.; Zhu, Y. Preparation of adipic acid amides derivatives as modulators of NPY4 (neuropeptide Y4) receptor. WO2012125622A1, 2012.
184. Woods, J. R.; Mo, H.; Bieberich, A. A.; Alavanja, T.; Colby, D. A. Fluorinated amino-derivatives of the sesquiterpene lactone, parthenolide, as ^{19}F NMR probes in deuterium-free environments. *J. Med. Chem.* **2011**, *54*, 7934-7941.
185. Apodaca, R. L.; Jablonowski, J. A.; Ly, K. S.; Shah, C. R.; Swanson, D. M.; Xiao, W. Preparation of piperazinyl and diazepanyl benzamides and benzothioamides as inhibitors of histamine H3 receptor. WO2004037801A1, 2004.
186. Pan, F.; Shi, Z. Transition metal-catalyzed C–H trifluoromethylation. *Acta Chim. Sinica* **2012**, *70*, 1679-1681.
187. Tsukanov, S. V.; Comins, D. L. Concise total synthesis of the frog alkaloid (–)-205 B. *Angew. Chem. Int. Ed.* **2011**, *50*, 8626-8628.
188. Wolfe, B. H.; Libby, A. H.; Al-Awar, R. S.; Foti, C. J.; Comins, D. L. Asymmetric synthesis of all the known phlegmarine alkaloids. *J. Org. Chem.* **2010**, *75*, 8564-8570.
189. Wilson, M. S.; Padwa, A. A stereoselective approach to the azaspiro[5.5] undecane ring system using a conjugate addition/dipolar cycloaddition cascade: Application to the total synthesis of (±)-2,7,8-epi-perhydrohistrionicotoxin. *J. Org. Chem.* **2008**, *73*, 9601-9609.
190. Niphakis, M. J.; Georg, G. I. Synthesis of tylocrebrine and related phenanthroindolizidines by VOF_3-mediated oxidative aryl-alkene coupling. *Org. Lett.* **2011**, *13*, 196-199.
191. Joseph, S.; Comins, D. L. Synthetic applications of chiral 2,3-dihydro-4-pyridones. *Curr. Opin. Drug Discov. Dev.* **2002**, *5*, 870-880.
192. Kim, Y. W.; Georg, G. I. Boron-Heck reaction of cyclic enaminones: regioselective direct arylation via oxidative palladium(II) catalysis. *Org. Lett.* **2014**, *16*, 1574-1577.
193. Yu, Y.-Y.; Georg, G. I. Biomimetic aerobic C–H olefination of cyclic enaminones at room temperature: Development toward the synthesis of 1,3,5-trisubstituted benzenes. *Adv. Synth. Catal.* **2014**, *356*, 1359-1369.
194. Leighty, M. W.; Georg, G. I. Total syntheses and cytotoxicity of (*R*)- and (*S*)-boehmeriasin A. *ACS Med. Chem. Lett.* **2011**, *2*, 313-315.
195. Niphakis, M. J.; Georg, G. I. Total syntheses of arylindolizidine alkaloids (+)-ipalbidine and (+)-antofine. *J. Org. Chem.* **2010**, *75*, 6019-6022.
196. Yasu, Y.; Koike, T.; Akita, M. Intermolecular aminotrifluoromethylation of alkenes by visible-light-driven photoredox catalysis. *Org. Lett.* **2013**, *15*, 2136-2139.

197. Kong, W. Q.; Casimiro, M.; Fuentes, N.; Merino, E.; Nevado, C. Metal-free aryltrifluoromethylation of activated alkenes. *Angew. Chem. Int. Ed.* **2013**, *52*, 13086-13090.
198. Feng, C.; Loh, T.-P. Directing-group-assisted copper-catalyzed olefinic trifluoromethylation of electron-deficient alkenes. *Angew. Chem. Int. Ed.* **2013**, *52*, 12414-12417.
199. Besset, T.; Cahard, D.; Pannecoucke, X. Regio- and diastereoselective Cu-mediated trifluoromethylation of functionalized alkenes. *J. Org. Chem.* **2013**, *79*, 413-418.
200. Feng, C.; Loh, T.-P. Copper-catalyzed olefinic trifluoromethylation of enamides at room temperature. *Chem. Sci.* **2012**, *3*, 3458-3462.
201. Xu, C.; Liu, J.; Ming, W.; Liu, Y.; Liu, J.; Wang, M.; Liu, Q. In situ generation of PhI(+)CF_3 and transition-metal-free oxidative sp^2 C-H trifluoromethylation. *Chem. Eur. J.* **2013**, *19*, 9104-9109.
202. Wang, X.; Ye, Y.; Ji, G.; Xu, Y.; Zhang, S.; Feng, J.; Zhang, Y.; Wang, J. Copper-catalyzed direct C-H trifluoromethylation of quinones. *Org. Lett.* **2013**, *15*, 3730-3733.
203. Ilchenko, N. O.; Janson, P. G.; Szabo, K. J. Copper-mediated cyanotrifluoromethylation of styrenes using the Togni reagent. *J. Org. Chem.* **2013**, *78*, 11087-11091.
204. Wu, X.; Chu, L.; Qing, F.-L. $PhI(OAc)_2$-mediated oxidative trifluoromethylation of arenes with CF_3SiMe_3 under metal-free conditions. *Tetrahedron Lett.* **2013**, *54*, 249–251.
205. Facchinetti, V.; Gomes, C. R. B.; De Souza, M. V. N.; Vasconcelos, T. R. A. Perspectives on the development of novel potentially active quinolones against tuberculosis and cancer. *Mini-Rev. Med. Chem.* **2012**, *12*, 866-874.
206. Ahmed, A.; Daneshtalab, M. Nonclassical biological activities of quinolone derivatives. *J. Pharm. Pharm. Sci.* **2012**, *15*, 52-72.
207. Heeb, S.; Fletcher, M. P.; Chhabra, S. R.; Diggle, S. P.; Williams, P.; Camara, M. Quinolones: from antibiotics to autoinducers. *Fems Microbiol. Rev.* **2011**, *35*, 247-274.
208. Wicke, L.; Engels, J. W. Postsynthetic on column RNA labeling via Stille coupling. *Bioconjugate Chem.* **2012**, *23*, 627-642.
209. Medda, F.; Russell, R. J. M.; Higgins, M.; McCarthy, A. R.; Campbell, J.; Slawin, A. M. Z.; Lane, D. P.; Lain, S.; Westwood, N. J. Novel cambinol analogs as sirtuin Inhibitors: synthesis, biological evaluation, and rationalization of activity. *J. Med. Chem.* **2009**, *52*, 2673-2682.
210. Cahova, H.; Havran, L.; Brazdilova, P.; Pivonkova, H.; Pohl, R.; Fojta, M.; Hocek, M. Aminophenyl- and nitrophenyl-labeled nucleoside triphosphates: Synthesis, enzymatic incorporation, and electrochemical detection. *Angew. Chem. Int. Ed.* **2008**, *47*, 2059-2062.
211. De Mico, A.; Margarita, R.; Parlanti, L.; Vescovi, A.; Piancatelli, G. A versatile and highly selective hypervalent iodine(III)/2,2,6,6-tetramethyl-1-piperidinyloxyl-mediated oxidation of alcohols to carbonyl compounds. *J. Org. Chem.* **1997**, *62*, 6974-6977.

212. Mizuta, S.; Verhoog, S.; Engle, K. M.; Khotavivattana, T.; O'Duill, M.; Wheelhouse, K.; Rassias, G.; Medebielle, M.; Gouverneur, V. Catalytic hydrotrifluoromethylation of unactivated alkenes. *J. Am. Chem. Soc.* **2013**, *135*, 2505-2508.
213. Wang, Q.; Dong, X.; Xiao, T.; Zhou, L. $PhI(OAc)_2$-mediated synthesis of 6-(trifluoromethyl)phenanthridines by oxidative cyclization of 2-isocyanobiphenyls with CF_3SiMe_3 under metal-free conditions. *Org. Lett.* **2013**, *15*, 4846-4849.
214. Li, L.; Deng, M.; Zheng, S.-C.; Xiong, Y.-P.; Tan, B.; Liu, X.-Y. Metal-free direct intramolecular carbotrifluoromethylation of alkenes to functionalized trifluoromethyl azaheterocycles. *Org. Lett.* **2014**, *16*, 504-507.
215. Huang, J.; He, Y.; Wang, Y.; Zhu, Q. Synthesis of benzimidazoles by PIDA-promoted direct $C(sp^2)$–H imidation of *N*-arylamidines. *Chem. Eur. J.* **2012**, *18*, 13964-13967.
216. Kitazume, T.; Murata, K.; Okabe, A.; Takahashi, Y.; Yamazaki, T. A highly stereocontrolled synthetic approach to 1,6-dideoxy-6,6-difluoroaza sugar derivatives. *Tetrahedron: Asymmetry* **1994**, *5*, 1029-1040.
217. Creswell, M. W.; Bolton, G. L.; Hodges, J. C.; Meppen, M. Combinatorial synthesis of dihydropyridone libraries and their derivatives. *Tetrahedron* **1998**, *54*, 3983-3998.
218. Sahn, J. J.; Comins, D. L. [2 + 2] Photochemical cycloaddition/ring opening of 6-alkenyl-2,3-dihydro-4-pyridones. *J. Org. Chem.* **2010**, *75*, 6728-6731.
219. Padmavathi, V.; Reddy, T. V. R.; Reddy, K. A. 4-Piperidone - a synthon for spiro-heterocycles. *Indian J. Chem., Sect. B: Org. Chem. Incl. Med. Chem.* **2007**, *46B*, 818-822.
220. Ege, M.; Wanner, K. T. Synthesis of β-amino acids based on oxidative cleavage of dihydropyridone derivatives. *Org. Lett.* **2004**, *6*, 3553-3556.
221. Garcia Mancheno, O.; Gomez Arrayas, R.; Adrio, J.; Carretero, J. C. Catalytic enantioselective approach to the stereodivergent synthesis of (+)-lasubines I and II. *J. Org. Chem.* **2007**, *72*, 10294-10297.
222. Gerth, K.; Bedorf, N.; Höfle, G.; Irschik, H.; Reichenbach, H. Antibiotics from gliding bacteria. 74. Epothilons A and B: antifungal and cytotoxic compounds from Sorangium cellulosum (Myxobacteria): production, physico-chemical and biological properties. *J. Antibiot.* **1996**, *49*, 560-563.
223. Höfle, G.; Bedorf, N.; Gerth, K.; Reichenbach, H. Epothilone derivatives. DE4138042A1, 1993.
224. Brunden, K. R.; Zhang, B.; Carroll, J.; Yao, Y.; Potuzak, J. S.; Hogan, A.-M. L.; Iba, M.; James, M. J.; Xie, S. X.; Ballatore, C.; Smith, A. B., III; Lee, V. M. Y.; Trojanowski, J. Q. Epothilone D improves microtubule density, axonal integrity, and cognition in a transgenic mouse model of tauopathy. *J. Neurosci.* **2010**, *30*, 13861-13866.
225. Lee, V. M.-Y.; Daughenbaugh, R.; Trojanowski, J. Q. Microtubule stabilizing drugs for the treatment of Alzheimer's disease. *Neurobiol. Aging* **1994**, *15*, S87-S89.
226. Michaelis, M. L.; Chen, Y.; Hill, S.; Reiff, E.; Georg, G. I.; Rice, A.; Audus, K. Amyloid peptide toxicity and microtubule-stabilizing drugs. *J. Mol. Neurosci.* **2002**, *19*, 101-105.

227. Bollag, D. M.; McQueney, P. A.; Zhu, J.; Hensens, O.; Koupal, L.; Liesch, J.; Goetz, M.; Lazarides, E.; Woods, C. M. Epothilones, a new class of microtubule-stabilizing agents with a taxol-like mechanism of action. *Cancer Res.* **1995**, *55*, 2325-2333.
228. Höfle, G.; Reichenbach, H. Epothilone, a myxobacterial metabolite with promising antitumor activity. In *Anticancer Agents from Natural Products*, 2nd ed.; Cragg, G. M.; Kingston, D. G. I.; Newman, D. J., Eds. CRC Press: Boca Raton, 2012; pp 513-573.
229. Lee, F. Y. F.; Borzilleri, R.; Fairchild, C. R.; Kim, S.-H.; Long, B. H.; Reventos-Suarez, C.; Vite, G. D.; Rose, W. C.; Kramer, R. A. BMS-247550: A novel epothilone analog with a mode of action similar to paclitaxel but possessing superior antitumor efficacy. *Clin. Cancer Res.* **2001**, *7*, 1429-1437.
230. Kowalski, R. J.; Giannakakou, P.; Hamel, E. Activities of the microtubule-stabilizing agents epothilones A and B with purified tubulin and in cells resistant to paclitaxel (Taxol). *J. Biol. Chem.* **1997**, *272*, 2534-2541.
231. Kamath, K.; Jordan, M. A. Suppression of microtubule dynamics by epothilone B is associated with mitotic arrest. *Cancer Res.* **2003**, *63*, 6026-6031.
232. Li, H.; DeRosier, D. J.; Nicholson, W. V.; Nogales, E.; Downing, K. H. Microtubule structure at 8 Å resolution. *Structure* **2002**, *10*, 1317-1328.
233. Vale, R. D. The molecular motor toolbox for intracellular transport. *Cell* **2003**, *112*, 467-480.
234. Weisenberg, R. C. Microtubule formation in vitro in solutions containing low calcium concentrations. *Science* **1972**, *177*, 1104-1105.
235. Walker, R. A.; O'Brien, E. T.; Pryer, N. K.; Soboeiro, M. F.; Voter, W. A.; Erickson, H. P.; Salmon, E. D. Dynamic instability of individual microtubules analyzed by video light microscopy: rate constants and transition frequencies. *J. Cell Biol.* **1988**, *107*, 1437-1448.
236. Karp, G. *Cell and Molecular Biology: Concepts and Experiments*. 4th ed.; John Wiley & Sons: New York, 2004; p 355.
237. Weisenberg, R. C.; Deery, W. J.; Dickinson, P. J. Tubulin-nucleotide interactions during the polymerization and depolymerization of microtubules. *Biochemistry* **1976**, *15*, 4248-4254.
238. Mitchison, T.; Kirschner, M. Dynamic instability of microtubule growth. *Nature* **1984**, *312*, 237-242.
239. Ojima, I.; Chakravarty, S.; Inoue, T.; Lin, S.; He, L.; Horwitz, S. B.; Kuduk, S. D.; Danishefsky, S. J. A common pharmacophore for cytotoxic natural products that stabilize microtubules. *Proc. Natl. Acad. Sci. U.S.A.* **1999**, *96*, 4256-4261.
240. Giannakakou, P.; Gussio, R.; Nogales, E.; Downing, K. H.; Zaharevitz, D.; Bollbuck, B.; Poy, G.; Sackett, D.; Nicolaou, K. C.; Fojo, T. A common pharmacophore for epothilone and taxanes: molecular basis for drug resistance conferred by tubulin mutations in human cancer cells. *Proc. Natl. Acad. Sci. U.S.A.* **2000**, *97*, 2904-2909.
241. Gupta, M. L., Jr.; Bode, C. J.; Georg, G. I.; Himes, R. H. Understanding tubulin-taxol interactions: Mutations that impart taxol binding to yeast tubulin. *Proc. Natl. Acad. Sci. U.S.A.* **2003**, *100*, 6394-6397.

242. Bode, C. J.; Gupta, M. L., Jr.; Reiff, E. A.; Suprenant, K. A.; Georg, G. I.; Himes, R. H. Epothilone and paclitaxel: unexpected differences in promoting the assembly and stabilization of yeast microtubules. *Biochemistry* **2002**, *41*, 3870-3874.
243. Snyder, J. P.; Nettles, J. H.; Cornett, B.; Downing, K. H.; Nogales, E. The binding conformation of Taxol in beta-tubulin: a model based on electron crystallographic density. *Proc. Natl. Acad. Sci. U.S.A.* **2001**, *98*, 5312-5316.
244. Rao, S.; He, L.; Chakravarty, S.; Ojima, I.; Orr, G. A.; Horwitz, S. B. Characterization of the Taxol binding site on the microtubule: Identification of Arg282 in β-tubulin as the site of photoincorporation of a 7-benzophenone analogue of taxol. *J. Biol. Chem.* **1999**, *274*, 37990-37994.
245. Rao, S.; Krauss, N. E.; Heerding, J. M.; Swindell, C. S.; Ringel, I.; Orr, G. A.; Horwitz, S. B. 3'-(*p*-Azidobenzamido)taxol photolabels the *N*-terminal 31 amino acids of β-tubulin. *J. Biol. Chem.* **1994**, *269*, 3132-3134.
246. Rao, S.; Orr, G. A.; Chaudhary, A. G.; Kingston, D. G. I.; Horwitz, S. B. Characterization of the taxol binding site on the microtubule. 2-(*m*-Azidobenzoyl)taxol photolabels a peptide (amino acids 217-231) of β-tubulin. *J. Biol. Chem.* **1995**, *270*, 20235-20238.
247. Wartmann, M.; Altmann, K. H. The biology and medicinal chemistry of epothilones. *Curr. Med. Chem.: Anti-Cancer Agents* **2002**, *2*, 123-148.
248. Nicolaou, K. C.; Winssinger, N.; Pastor, J.; Ninkovic, S.; Sarabia, F.; He, Y.; Vourloumis, D.; Yang, Z.; Li, T.; Giannakakou, P.; Hamel, E. Synthesis of epothilones A and B in solid and solution phase. *Nature* **1997**, *387*, 268-272.
249. Nicolaou, K. C.; He, Y.; Roschangar, F.; King, N. P.; Vourloumis, D.; Li, T. Total synthesis of epothilone E and analogs with modified side chains through the Stille coupling reaction. *Angew. Chem. Int. Ed.* **1998**, *37*, 84-87.
250. Nicolaou, K. C.; Sarabia, F.; Ninkovic, S.; Finlay, M. R.; Boddy, C. N. C. Probing the ring size of epothilones: total synthesis of [14]-, [15]-, [17]-, and [18]Epothilones A. *Angew. Chem. Int. Ed.* **1998**, *37*, 81-84.
251. Rivkin, A.; Njardarson, J. T.; Biswas, K.; Chou, T.-C.; Danishefsky, S. J. Total syntheses of [17]- and [18]-dehydrodesoxyepothilones B via a concise ring-closing metathesis-based strategy: correlation of ring size with biological activity in the epothilone series. *J. Org. Chem.* **2002**, *67*, 7737-7740.
252. Borzilleri, R. M.; Zheng, X.; Schmidt, R. J.; Johnson, J. A.; Kim, S.-H.; DiMarco, J. D.; Fairchild, C. R.; Gougoutas, J. Z.; Lee, F. Y. F.; Long, B. H.; Vite, G. D. A novel application of a Pd(0)-catalyzed nucleophilic substitution reaction to the regio- and stereoselective synthesis of lactam analogues of the epothilone natural products. *J. Am. Chem. Soc.* **2000**, *122*, 8890-8897.
253. Regueiro-Ren, A.; Leavitt, K.; Kim, S.-H.; Hoefle, G.; Kiffe, M.; Gougoutas, J. Z.; DiMarco, J. D.; Lee, F. Y. F.; Fairchild, C. R.; Long, B. H.; Vite, G. D. SAR and pH stability of cyano-substituted epothilones. *Org. Lett.* **2002**, *4*, 3815-3818.
254. Hardt, I. H.; Steinmetz, H.; Gerth, K.; Sasse, F.; Reichenbach, H.; Höfle, G. New Natural Epothilones from *Sorangium cellulosum*, Strains So ce90/B2 and So ce90/D13: Isolation, Structure Elucidation, and SAR Studies. *J. Nat. Prod.* **2001**, *64*, 847-856.

255. Nicolaou, K. C.; Vallberg, H.; King, N. P.; Roschangar, F.; He, Y.; Vourloumis, D.; Nicolaou, C. G. Total synthesis of oxazole- and cyclopropane-containing epothilone A analogs by the olefin metathesis approach. *Chem. Eur. J.* **1997**, *3*, 1957-1970.
256. Nicolaou, K. C.; Sarabia, F.; Finlay, M. R. V.; Ninkovic, S.; King, N. P.; Vourloumis, D.; He, Y. Total synthesis of oxazole- and cyclopropane-containing epothilone B analogs by the macrolactonization approach. *Chem. Eur. J.* **1997**, *3*, 1971-1986.
257. Klar, U.; Skuballa, W.; Buchmann, B.; Schwede, W.; Bunte, T.; Hoffmann, J.; Lichtner, R. B. Synthesis and biological activity of epothilones. In *Anticancer Agents*, Ojima, I.; Vite, G. D.; Altmann, K. H., Eds. American Chemical Society: Washington, 2001; Vol. 796, pp 131-147.
258. Nettles, J. H.; Li, H.; Cornett, B.; Krahn, J. M.; Snyder, J. P.; Downing, K. H. The binding mode of epothilone A on alpha, beta-tubulin by electron crystallography. *Science (Washington, DC, U. S.)* **2004**, *305*, 866-869.
259. Reese, M.; Sanchez-Pedregal, V. M.; Kubicek, K.; Meiler, J.; Blommers, M. J. J.; Griesinger, C.; Carlomagno, T. Structural basis of the activity of the microtubule-stabilizing agent epothilone a studied by NMR spectroscopy in solution. *Angew. Chem. Int. Ed.* **2007**, *46*, 1864-1868.
260. Sun, J.; Sinha, S. C. Stereoselective total synthesis of epothilones by the metathesis approach involving C9-C10 bond formation. *Angew. Chem. Int. Ed.* **2002**, *41*, 1381-1383.
261. Rivkin, A.; Yoshimura, F.; Gabarda, A. E.; Chou, T.-C.; Dong, H.; Tong, W. P.; Danishefsky, S. J. Complex target-oriented total synthesis in the drug discovery process: the discovery of a highly promising family of second generation epothilones. *J. Am. Chem. Soc.* **2003**, *125*, 2899-2901.
262. Rivkin, A.; Biswas, K.; Chou, T.-C.; Danishefsky, S. J. On the introduction of a trifluoromethyl substituent in the epothilone setting: chemical issues related to ring forming olefin metathesis and earliest biological findings. *Org. Lett.* **2002**, *4*, 4081-4084.
263. Yoshimura, F.; Rivkin, A.; Gabarda, A. E.; Chou, T.-C.; Dong, H.; Sukenick, G.; Morel, F. F.; Taylor, R. E.; Danishefsky, S. J. Synthesis and conformational analysis of (*E*)-9,10-dehydroepothilone B: A suggestive link between the chemistry and biology of epothilones. *Angew. Chem. Int. Ed.* **2003**, *42*, 2518-2521.
264. Biswas, K.; Lin, H.; Njardarson, J. T.; Chappell, M. D.; Chou, T.-C.; Guan, Y.; Tong, W. P.; He, L.; Horwitz, S. B.; Danishefsky, S. J. Highly concise routes to epothilones: the total synthesis and evaluation of epothilone 490. *J. Am. Chem. Soc.* **2002**, *124*, 9825-9832.
265. Yamamoto, K.; Biswas, K.; Gaul, C.; Danishefsky, S. J. Effects of temperature and concentration in some ring closing metathesis reactions. *Tetrahedron Lett.* **2003**, *44*, 3297-3299.
266. White, J. D.; Sundermann, K. F.; Wartmann, M. Synthesis, conformational analysis, and bioassay of 9,10-didehydroepothilone D. *Org. Lett.* **2002**, *4*, 995-997.
267. Quintard, D.; Bertrand, P.; Bachmann, C.; Gesson, J.-P. Synthesis and conformational analysis of macrocycles related to 10-oxa-epothilone. *Eur. J. Org. Chem.* **2004**, 4762-4770.

268. Nicolaou, K. C.; Ritzen, A.; Namoto, K.; Buey, R. M.; Diaz, J. F.; Andreu, J. M.; Wartmann, M.; Altmann, K.-H.; O'Brate, A.; Giannakakou, P. Chemical synthesis and biological evaluation of novel epothilone B and *trans*-12,13-cyclopropyl epothilone B analogues. *Tetrahedron* **2002**, *58*, 6413-6432.
269. Johnson, J.; Kim, S.-H.; Bifano, M.; DiMarco, J.; Fairchild, C.; Gougoutas, J.; Lee, F.; Long, B.; Tokarski, J.; Vite, G. Synthesis, structure proof, and biological activity of epothilone cyclopropanes. *Org. Lett.* **2000**, *2*, 1537-1540.
270. Nicolaou, K. C.; Namoto, K.; Ritzen, A.; Ulven, T.; Shoji, M.; Li, J.; D'Amico, G.; Liotta, D.; French, C. T.; Wartmann, M.; Altmann, K.-H.; Giannakakou, P. Chemical synthesis and biological evaluation of cis- and trans-12,13-cyclopropyl and 12,13-cyclobutyl epothilones and related pyridine side chain analogues. *J. Am. Chem. Soc.* **2001**, *123*, 9313-9323.
271. Pfeiffer, B.; Hauenstein, K.; Merz, P.; Gertsch, J.; Altmann, K.-H. Synthesis and SAR of C12-C13-oxazoline derivatives of epothilone A. *Bioorg. Med. Chem. Lett.* **2009**, *19*, 3760-3763.
272. Regueiro-Ren, A.; Borzilleri, R. M.; Zheng, X.; Kim, S.-H.; Johnson, J. A.; Fairchild, C. R.; Lee, F. Y. F.; Long, B. H.; Vite, G. D. Synthesis and biological activity of novel epothilone aziridines. *Org. Lett.* **2001**, *3*, 2693-2696.
273. Gaich, T.; Karig, G.; Martin, H. J.; Mulzer, J. New solutions to the C-12,13 stereo-problem of epothilones B and D; synthesis of a 12,13-diol-acetonide epothilone B analog. *Eur. J. Org. Chem.* **2006**, 3372-3394.
274. Glunz, P. W.; He, L.; Horwitz, S. B.; Chakravarty, S.; Ojima, I.; Chou, T.-C.; Danishefsky, S. J. The synthesis and evaluation of 12,13-benzodesoxyepothilone B: a highly convergent route. *Tetrahedron Lett.* **1999**, *40*, 6895-6898.
275. Su, D.-S.; Balog, A.; Meng, D.; Bertinato, P.; Danishefsky, S. J.; Zheng, Y.-H.; Chou, T.-C.; He, L.; Horwitz, S. B. Structure-activity relationships of the epothilones and the first in vivo comparison with paclitaxel. *Angew. Chem. Int. Ed.* **1997**, *36*, 2093-2096.
276. Meng, D.; Su, D.-S.; Balog, A.; Bertinato, P.; Sorensen, E. J.; Danishefsky, S. J.; Zheng, Y.-H.; Chou, T.-C.; He, L.; Horwitz, S. B. Remote effects in macrolide formation through ring-forming olefin metathesis: An application to the synthesis of fully active epothilone congeners. *J. Am. Chem. Soc.* **1997**, *119*, 2733-2734.
277. Nicolaou, K. C.; Vourloumis, D.; Li, T.; Pastor, J.; Winssinger, N.; He, Y.; Ninkovic, S.; Sarabia, F.; Vallberg, H.; Roschangar, F.; King, N. P.; Finlay, M. R. V.; Giannakakou, P.; Verdier-Pinard, P.; Hamel, E. Designed epothilones: combinatorial synthesis, tubulin assembly properties, and cytotoxic action against taxol-resistant tumor cells. *Angew. Chem. Int. Ed.* **1997**, *36*, 2097-2103.
278. Su, D.-S.; Meng, D.; Bertinato, P.; Balog, A.; Sorensen, E. J.; Danishefsky, S. J.; Zheng, Y.-H.; Chou, T.-C.; He, L.; Horwitz, S. B. Total synthesis of (-)-epothilone B: an extension of the Suzuki coupling method and insights into structure-activity relationships of the epothilones. *Angew. Chem. Int. Ed.* **1997**, *36*, 757-759.
279. Altmann, K.-H.; Bold, G.; Caravatti, G.; Denni, D.; Florsheimer, A.; Schmidt, A.; Rihs, G.; Wartmann, M. The total synthesis and biological assessment of trans-epothilone A. *Helv. Chim. Acta* **2002**, *85*, 4086-4110.

280. Ganesh, T.; Schilling, J. K.; Palakodety, R. K.; Ravindra, R.; Shanker, N.; Bane, S.; Kingston, D. G. I. Synthesis and biological evaluation of fluorescently labeled epothilone analogs for tubulin binding studies. *Tetrahedron* **2003**, *59*, 9979-9984.
281. Taylor, R. E.; Chen, Y.; Galvin, G. M.; Pabba, P. K. Conformation-activity relationships in polyketide natural products. Towards the biologically active conformation of epothilone. *Org. Biomol. Chem.* **2004**, *2*, 127-132.
282. Karama, U.; Hofle, G. Synthesis of epothilone 16,17-alkyne analogs by replacement of the C13-C15(*O*)-ring segment of natural epothilone C. *Eur. J. Org. Chem.* **2003**, 1042-1049.
283. Nicolaou, K. C.; Hepworth, D.; King, N. P.; Finlay, M. R. V.; Scarpelli, R.; Pereira, M. M. A.; Bollbuck, B.; Bigot, A.; Werschkun, B.; Winssinger, N. Total synthesis of 16-desmethylepothilone B, epothilone B10, epothilone F, and related side chain modified epothilone B analogues. *Chem. Eur. J.* **2000**, *6*, 2783-2800.
284. Hearn, B. R.; Zhang, D.; Li, Y.; Myles, D. C. C-15 thiazol-4-yl analogues of (*E*)-9,10-didehydroepothilone D: synthesis and cytotoxicity. *Org. Lett.* **2006**, *8*, 3057-3059.
285. Höfle, G.; Glaser, N.; Leibold, T.; Sefkow, M. Epothilone A-D and their thiazole-modified analogs as novel anticancer agents. *Pure Appl. Chem.* **1999**, *71*, 2019-2024.
286. Sefkow, M.; Kiffe, M.; Schummer, D.; Hofle, G. Oxidative and reductive transformations of epothilone A. *Bioorg. Med. Chem. Lett.* **1998**, *8*, 3025-3030.
287. Nicolaou, K. C.; King, N. P.; Finlay, M. R. V.; He, Y.; Roschangar, F.; Vourloumis, D.; Vallberg, H.; Sarabia, F.; Ninkovic, S.; Hepworth, D. Total synthesis of epothilone E and related side-chain modified analogues via a Stille coupling based strategy. *Bioorg. Med. Chem.* **1999**, *7*, 665-697.
288. Nicolaou, K. C.; Scarpelli, R.; Bollbuck, B.; Werschkun, B.; Pereira, M. M. A.; Wartmann, M.; Altmann, K. H.; Zaharevitz, D.; Gussio, R.; Giannakakou, P. Chemical synthesis and biological properties of pyridine epothilones. *Chem. Biol.* **2000**, *7*, 593-599.
289. Glaser, N. Semisynthese Seitenketten-modifizierter epothilone, Doctoral Thesis. Technical University of Braunschweig, 2001.
290. Sefkow, M.; Höfle, G. Substitutions at the thiazole moiety of epothilone. *Heterocycles* **1998**, *48*, 2485-2488.
291. Altmann, K. H.; Bold, G.; Caravatti, G.; Florsheimer, A.; Guagnano, V.; Wartmann, M. Synthesis and biological evaluation of highly potent analogues of epothilones B and D. *Bioorg. Med. Chem. Lett.* **2000**, *10*, 2765-2768.
292. Cachoux, F.; Isarno, T.; Wartmann, M.; Altmann, K.-H. Scaffolds for microtubule inhibition through extensive modification of the epothilone template. *Angew. Chem. Int. Ed.* **2005**, *44*, 7469-7473.
293. Cachoux, F.; Isarno, T.; Wartmann, M.; Altmann, K.-H. Total synthesis and biological assessment of benzimidazole-based analogs of epothilone A: Ambivalent effects on cancer cell growth inhibition. *ChemBioChem* **2006**, *7*, 54-57.
294. Dietrich, S. A.; Lindauer, R.; Stierlin, C.; Gertsch, J.; Matesanz, R.; Notararigo, S.; Diaz, J. F.; Altmann, K.-H. Epothilone analogues with benzimidazole and quinoline side chains: chemical synthesis, antiproliferative activity, and interactions with tubulin. *Chem. Eur. J.* **2009**, *15*, 10144-10157.
295. Bold, G.; Wojeik, S.; Caravatti, G.; Lindauer, R.; Stierlin, C.; Gertsch, J.; Wartmann, M.; Altmann, K.-H. Structure-activity relationships in side-chain-modified

epothilone analogues. How important is the position of the nitrogen atom? *ChemMedChem* **2006**, *1*, 37-40.
296. Heinz, D. W.; Schubert, W.-D.; Höfle, G. Much anticipated - The bioactive conformation of epothilone and its binding to tubulin. *Angew. Chem. Int. Ed.* **2005**, *44*, 1298-1301.
297. Verrills, N. M.; Flemming, C. L.; Liu, M.; Ivery, M. T.; Cobon, G. S.; Norris, M. D.; Haber, M.; Kavallaris, M. Microtubule alterations and mutations induced by desoxyepothilone B. Implications for drug-target interactions. *Chem. Biol.* **2003**, *10*, 597-607.
298. He, L.; Jagtap, P. G.; Kingston, D. G. I.; Shen, H.-J.; Orr, G. A.; Horwitz, S. B. A common pharmacophore for taxol and the epothilones based on the biological activity of a taxane molecule lacking a C-13 side chain. *Biochemistry* **2000**, *39*, 3972-3978.
299. Day, B. W. Mutants yield a pharmacophore model for the tubulin-paclitaxel binding site. Comments. *Trends Pharmacol. Sci.* **2000**, *21*, 321-323.
300. Lee, K. W.; Briggs, J. M. Comparative molecular field analysis (CoMFA) study of epothilones - tubulin depolymerization inhibitors: pharmacophore development using 3D QSAR methods. *J. Comput.-Aided Mol. Des.* **2001**, *15*, 41-55.
301. Jimenez-Barbero, J.; Amat-Guerri, F.; Snyder, J. P. The solid state, solution and tubulin-bound conformations of agents that promote microtubule stabilization. *Curr. Med. Chem.: Anti-Cancer Agents* **2002**, *2*, 91-122.
302. Wang, M.; Xia, X.; Kim, Y.; Hwang, D.; Jansen, J. M.; Botta, M.; Liotta, D. C.; Snyder, J. P. A unified and quantitative receptor model for the microtubule binding of paclitaxel and epothilone. *Org. Lett.* **1999**, *1*, 43-46.
303. Winkler, J. D.; Axelsen, P. H. A model for the taxol (paclitaxel)/epothilone pharmacophore. *Bioorg. Med. Chem. Lett.* **1996**, *6*, 2963-2966.
304. Erdelyi, M.; Navarro-Vazquez, A.; Pfeiffer, B.; Kuzniewski, C. N.; Felser, A.; Widmer, T.; Gertsch, J.; Pera, B.; Diaz, J. F.; Altmann, K.-H.; Carlomagno, T. The binding mode of side chain- and C3-modified epothilones to tubulin. *ChemMedChem* **2010**, *5*, 911-920.
305. Barasoain, I.; Garcia-Carril, A. M.; Matesanz, R.; Maccari, G.; Trigili, C.; Mori, M.; Shi, J.-Z.; Fang, W.-S.; Andreu, J. M.; Botta, M.; Diaz, J. F. Probing the pore drug binding site of microtubules with fluorescent taxanes: evidence of two binding poses. *Chem. Biol.* **2010**, *17*, 243-253.
306. Kubicek, K.; Grimm, S. K.; Orts, J.; Sasse, F.; Carlomagno, T. The tubulin-bound structure of the antimitotic drug tubulysin. *Angew. Chem. Int. Ed.* **2010**, *49*, 4809-4812.
307. Shafer, J.; Barnowsky, P.; Laursen, R.; Finn, F.; Westheimer, F. H. Products from the photolysis of diazoacetyl chymotrypsin. *J. Biol. Chem.* **1966**, *241*, 421-427.
308. Singh, A.; Thornton, E. R.; Westheimer, F. H. Photolysis of diazoacetylchymotrypsin. *J. Biol. Chem.* **1962**, *237*, 3006-3008.
309. Lekostaj, J. K.; Natarajan, J. K.; Paguio, M. F.; Wolf, C.; Roepe, P. D. Photoaffinity labeling of the Plasmodium falciparum chloroquine resistance transporter with a novel perfluorophenylazido chloroquine. *Biochemistry* **2008**, *47*, 10394-10406.
310. Knowles, J. R. Photogenerated reagents for biological receptor-site labeling. *Accounts Chem. Res.* **1972**, *5*, 155-160.

311. Galardy, R. E.; Craig, L. C.; Printz, M. P. Benzophenone triplet. New photochemical probe of biological ligand-receptor interactions. *Nature* **1973**, *242*, 127-128.
312. Fleet, G. W. J.; Porter, R. R.; Knowles, J. R. Affinity labeling of antibodies with aryl nitrene as reactive group. *Nature* **1969**, *224*, 511-512.
313. Chapman, O. L. Photochemistry of diazo compounds and azides in argon. *Pure Appl. Chem.* **1979**, *51*, 331-339.
314. Iddon, B.; Meth-Cohn, O.; Scriven, E. F. V.; Suschitzky, H.; Gallagher, P. T. New synthetic methods. 31. Developments in aryl nitrene chemistry: syntheses and mechanisms. *Angew. Chem.* **1979**, *91*, 965-982.
315. Colman, R.; Scriven, E. F. V.; Suschitzky, H.; Thomas, D. R. Photolysis of phenyl azide in the presence of 'naked' anions. *Chem. Ind.* **1981**, *7*, 249-250.
316. Takeuchi, H.; Koyama, K. Photolysis and thermolysis of phenyl azide in acetic acid. *J. Chem. Soc., Chem. Commun.* **1981**, 202-204.
317. Nielsen, P. E.; Buchardt, O. Aryl azides as photoaffinity labels. A photochemical study of some 4-substituted aryl azides. *Photochem. Photobiol.* **1982**, *35*, 317-323.
318. Chowdhry, V.; Vaughan, R.; Westheimer, F. H. 2-Diazo-3,3,3-trifluoropropionyl chloride: reagent for photoaffinity labeling. *Proc. Natl. Acad. Sci. U.S.A.* **1976**, *73*, 1406-8.
319. Chowdhry, V.; Westheimer, F. H. p-Toluenesulfonyldiazoacetates as photoaffinity labeling reagents. *J. Am. Chem. Soc.* **1978**, *100*, 309-310.
320. Smith, R. A. G.; Knowles, J. R. Aryldiazirines. Potential reagents for photolabeling of biological receptor sites. *J. Am. Chem. Soc.* **1973**, *95*, 5072-5073.
321. Smith, R. A. G.; Knowles, J. R. Preparation and photolysis of 3-aryl-3*H*-diazirines. *J. Chem. Soc., Perkin Trans. 2* **1975**, 686-694.
322. Bradley, G. F.; Evans, W. B. L.; Stevens, I. D. R. Thermal and photochemical decomposition of cycloalkanespirodiazirines. *J. Chem. Soc., Perkin Trans. 2* **1977**, 1214-1220.
323. Brunner, J.; Senn, H.; Richards, F. M. 3-Trifluoromethyl-3-phenyldiazirine. A new carbene generating group for photolabeling reagents. *J. Biol. Chem.* **1980**, *255*, 3313-3318.
324. Hutt, O. E.; Inagaki, J.; Reddy, B. S.; Nair, S. K.; Reiff, E. A.; Henri, J. T.; Greiner, J. F.; Vander Velde, D. G.; Chiu, T.-L.; Amin, E. A.; Himes, R. H.; Georg, G. I. Total synthesis and evaluation of 22-(3-azidobenzoyloxy)methyl epothilone C for photoaffinity labeling of beta-tubulin. *Bioorg. Med. Chem. Lett.* **2009**, *19*, 3293-3296.
325. Reiff, E. A.; Nair, S. K.; Henri, J. T.; Greiner, J. F.; Reddy, B. S.; Chakrasali, R.; David, S. A.; Chiu, T.-L.; Amin, E. A.; Himes, R. H.; Vander Velde, D. G.; Georg, G. I. Total synthesis and evaluation of C26-hydroxyepothilone D derivatives for photoaffinity labeling of beta-tubulin. *J. Org. Chem.* **2010**, *75*, 86-94.
326. Hutt, O. E.; Reddy, B. S.; Nair, S. K.; Reiff, E. A.; Henri, J. T.; Greiner, J. F.; Chiu, T.-L.; VanderVelde, D. G.; Amin, E. A.; Himes, R. H.; Georg, G. I. Total synthesis and evaluation of C25-benzyloxyepothilone C for tubulin assembly and cytotoxicity against MCF-7 breast cancer cells. *Bioorg. Med. Chem. Lett.* **2008**, *18*, 4904-4906.

327. Schummer, D.; Höfle, G. An improved preparation of tris(ethylenedioxyboryl)methane, a reagent for the homologation of aldehydes and ketones. *Tetrahedron* **1995**, *51*, 11219-11222.
328. Stewart, I. C.; Douglas, C. J.; Grubbs, R. H. Increased efficiency in cross-metathesis reactions of sterically hindered olefins. *Org. Lett.* **2008**, *10*, 441-444.
329. Lowry, O. H.; Rosebrough, N. J.; Farr, A. L.; Randall, R. J. Protein measurement with the Folin phenol reagent. *J. Biol. Chem.* **1951**, *193*, 265-275.
330. Tran, P. V.; Dakoji, S.; Reise, K. H.; Storey, K. K.; Georgieff, M. K. Fetal iron deficiency alters the proteome of adult rat hippocampal synaptosomes. *Am J Physiol Regul Integr Comp Physiol* **2013**, *305*, R1297-306.
331. Lin-Moshier, Y.; Sebastian, P. J.; Higgins, L.; Sampson, N. D.; Hewitt, J. E.; Marchant, J. S. Re-evaluation of the role of calcium homeostasis endoplasmic reticulum protein (CHERP) in cellular calcium signaling. *J. Biol. Chem.* **2013**, *288*, 355-367.
332. DeGnore, J. P.; Qin, J. Fragmentation of phosphopeptides in an ion trap mass spectrometer. *J. Am. Soc. Mass Spectrom.* **1998**, *9*, 1175-1188.
333. Tholey, A.; Reed, J.; Lehmann, W. D. Electrospray tandem mass spectrometric studies of phosphopeptides and phosphopeptide analogues. *J. Mass Spectrom.* **1999**, *34*, 117-123.
334. Mechref, Y. Use of CID/ETD mass spectrometry to analyze glycopeptides. In *Current Protocols in Protein Science*, Coligan, J. E.; Dunn, B. M.; Speicher, D. W.; Wingfield, P. T., Eds. John Wiley & Sons: New York, 2012; Vol. 68, pp 12.11.1-12.11.11.
335. *Prime*, Version 3.1; Schrödinger, LLC: New York, 2012.
336. *Glide*, Version 5.6; Schrödinger, LLC: New York, 2012.
337. Turunen, B. J.; Georg, G. I. Amino acid-derived enaminones: A study in ring formation providing valuable asymmetric synthons. *J. Am. Chem. Soc.* **2006**, *128*, 8702-8703.
338. Niphakis, M. J.; Turunen, B. J.; Georg, G. I. Synthesis of 6- and 7-membered cyclic enaminones: scope and mechanism. *J. Org. Chem.* **2010**, *75*, 6793-6805.
339. Yamada, H.; Aoyagi, S.; Kibayashi, C. Exploitation of palladium-catalyzed reductive enyne cyclization in the synthesis of (-)-4a,5-dihydrostreptazolin. *Tetrahedron Lett.* **1996**, *37*, 8787-8790.